Flavour Model Building in the Framework of Grand Unification and Supergravity

Inauguraldissertation
zur
Erlangung der Würde eines Doktors der Philosophie
vorgelegt der
Philosophisch-Naturwissenschaftlichen Fakultät
der Universität Basel

von

Christian Hohl

2020

Genehmigt von der Philosophisch-Naturwissenschaftlichen Fakultät

auf Antrag von

Prof. Dr. Stefan Antusch, Prof. Dr. Bernd Krusche, Prof. Dr. Borut Bajc

Basel, den 23. Juni 2020

Prof. Dr. Martin Spiess
Dekan

Acknowledgements

First of all, I would like to thank my supervisor, Stefan Antusch, for the guidance and the professional support during the four years of my doctoral studies. Moreover, I thank Borut Bajc for his work as co-referee.

Special thanks goes to Vasja Susič for the collaboration in various projects, and the interesting and "horizon-expanding" discussions concerning topics of all kinds. Furthermore, I give thanks to Johannes Rosskopp for his IT support, and to Kenneth Marschall, Ahmed Hammad, Francisco Torrenti, Eros Cazzato and Francesco Cefalà for the pleasant chats during the lunch breaks.

Finally, I would like to thank my parents for all the support during my education, and my brother for the numerous joint running trainings in the Jura Mountains during these years.

Abstract

In this thesis, we study new aspects of flavour model building in the context of supersymmetric Grand Unified Theories, where the focus lies on models with an SU(5) or SO(10) gauge group.

In the framework of supergravity, we discuss how a typical flavon sector of a flavour model with spontaneously broken family symmetry can be combined with a SUSY breaking sector in a consistent manner. To demonstrate the predictive power of such an implementation, an example calculation for a flavour GUT model, which is based on an SU(5) gauge group, an A_4 family symmetry and a $\mathbb{Z}_4^R$ R-symmetry, is performed. Assuming hidden sector SUSY breaking, we determine the structure of the soft SUSY breaking terms at the GUT scale and investigate the predictions for observables at low energy scales, such as the sparticle spectrum, the dark matter relic density and flavour violating processes.

Next, we carry out a systematic analysis of a class of predictive SU(5) flavour GUT models with the CSD2 setup in the neutrino sector, and where the ratios of the Yukawa couplings in the down-quark and charged lepton sector are fixed by Clebsch-Gordan coefficients at the GUT scale, following the principle of single operator dominance. Alongside the identification of viable model candidates by performing a fit to experimental data for different combinations of CG coefficients, we calculate, among others, the predictions for the 2-3 mixing angle $\theta_{23}^{\text{PMNS}}$ and the CP violating phase δ^{PMNS} in the lepton sector.

In the context of SO(10) Grand Unification, a class of non-renormalizable Yukawa operators of the schematic form $\mathbf{16}_I \cdot \mathbf{16}_J \cdot \mathbf{H} \cdot \mathbf{45}^n \cdot \mathbf{210}^m$ is investigated, where $\mathbf{H} \in \{\mathbf{10}, \mathbf{120}, \overline{\mathbf{126}}\}$ contains $\text{SU}(2)_\text{L}$ doublet and antidoublet states, and $\mathbf{16}_{I,J}$ the SM fermions. Moreover, the representations **45** and **210** acquire SM singlet vevs at the GUT scale. We provide general formulas to compute the resulting Yukawa couplings in the different fermion sectors of the MSSM, and discuss the construction of such operators from renormalizable interactions by using heavy mediators. In addition, we show that the alignment of the MSSM Higgs (anti)doublets H_u and H_d in the space of all $\text{SU}(2)_\text{L}$ (anti)doublets of a concrete model is a central aspect for the prediction of Yukawa ratios at the GUT scale.

Finally, we specify the numerical procedure to quantitatively calculate nucleon decay from dimension 5 operators in SUSY models, and apply the analysis to an example model with an SU(5) GUT symmetry.

Contents

PART I

Introduction

Introduction

The Standard Model (SM) of particle physics forms the foundation for the current understanding of the phenomena at the quantum level and is one of the great achievements in theoretical physics of the 20th century. It successfully describes the electromagnetic and the nuclear forces, as well as the properties of nearly all known fundamental particles. The predictions of the SM are tested by experimental measurements to a remarkable precision, and with the discovery of the Higgs boson in 2012 by the ATLAS and CMS experiment at CERN, the last missing component has experimentally been verified.

Despite the great predictive power, there are shortcomings in the SM whose solution requires new physics. First of all, the neutrinos are described as massless particles in the SM, however the experimentally observed flavour oscillation implies that the masses of the neutrinos are different from zero. Furthermore, observations in astronomy give strong hints for the existence of dark matter (DM), which can not be explained within the SM. From a theoretical point of view, an unsatisfactory feature of the SM is, that the masses of the particles, as well as the mixing angles and CP violating phases are simply fitted to the experimental data, without explaining the origin of this flavour structure. Moreover, the SM is plagued by the so called hierarchy problem, namely the instability of the Higgs mass under quantum corrections. Thus, if there is physics beyond the SM at high energy scales, which after all is present when gravity is considered at the quantum level at the Planck scale, the mass of the Higgs boson is naturally expected to be at this energy scale too, and not at the electroweak (EW) scale as measured by experiments.

An appropriate framework to address the shortcomings of the SM are Grand Unified Theories (GUTs), where the gauge couplings of the SM are unified into one single gauge coupling at high energies, i.e. at the GUT scale, and the SM particles are embedded into bigger representations of the GUT gauge group. This embedding leads to relations between the Yukawa couplings in the different fermion sectors at the GUT scale, and thus also to relations between the fermion masses, mixing angles and complex phases at low energies. Furthermore, certain Grand Unified Theories also predict the existence of SM singlet states, namely right-handed neutrinos, with which the small masses of the SM neutrinos can be explained. Due to the presence of heavy particles in GUTs which induce baryon and lepton violating processes, a general prediction of such models is proton decay, which, however, has not been observed in experiments. A further step towards an explanation of the observed flavour structure is made in GUTs with an additional flavour symmetry, which is either implemented as an exact or a spontaneously broken symmetry.

A resolution for the hierarchy problem of the Higgs mass is given by supersymmetry (SUSY), which is a symmetry between bosonic and fermionic states, i.e. all quantum numbers of superpartners are the same except the spin, and hence the loop corrections to the Higgs mass cancel. If SUSY is indeed realized, it can not be an exact symmetry since no superpartners of the SM particles have been observed. However, even if the masses of the supersymmetric particles are somewhat above the EW scale, the remaining hierarchy is still

small compared to the hierarchy between the GUT or the Planck scale and the EW scale. In the minimal supersymmetric Standard Model (MSSM) the lightest supersymmetric particle is a viable candidate for DM. Moreover, the additional supersymmetric particles in the MSSM modify the renormalization group (RG) running of the three gauge couplings of the SM gauge group in such a way, that they meet exactly at one energy scale, namely the GUT scale, which is not the case in the SM and which is a necessary condition to formulate a Grand Unified Theory.

Supersymmetry can either be realized as a global or a local (gauge) symmetry. Since the local formulation of SUSY incorporates the description of general coordinate transformations, it is also called supergravity (SUGRA). Supergravity is the preferred framework to implement spontaneous supersymmetry breaking which leads to soft supersymmetry breaking terms, such that there is still a systematic cancellation of the quantum corrections to the Higgs mass.

The above discussion illustrates, that supersymmetric flavour GUT models provide a promising framework to address several shortcomings of the SM. The purpose of this thesis is to investigate new aspects of flavour model building in the context of supersymmetric Grand Unified Theories with an SU(5) or an SO(10) gauge group, and to make statements about the predictive power of such models. Furthermore, the thesis shows how flavour models can be combined with spontaneous supersymmetry breaking in a consistent and predictive manner in the framework of supergravity.

To this end, the thesis is organized as follows: in Part II the theoretical framework, which is used in Part III, is discussed, and conventions and notations are fixed. In Chapter 1 a short summary of the SM is given. Supersymmetry, and especially supergravity, is discussed in Chapter 2. Based on the general Lagrangian in SUGRA, spontaneous supersymmetry breaking is discussed, and in particular gravity mediated SUSY breaking from a hidden sector. Part II is completed by the consideration of Grand Unification in Chapter 3. Specifically, an overview of the implementation of irreducible representations and the construction of invariants in SU(5) and SO(10) is given, and in addition proton decay is discussed. Part III focusses on different aspects of flavour model building in supersymmetric Grand Unified Theories. In Chapter 4 the combination of a flavon sector with a SUSY breaking sector in the context of flavour GUT models is discussed. The predictive power of such an implementation is demonstrated by applying the general considerations to an example model. A systematic analysis of a class of SU(5) flavour GUT models with the "Constrained Sequential Dominance 2" (CSD2) setup in the neutrino sector is performed in Chapter 5, where the focus is on predictions for quantities in the lepton sector which are not accurately measured by experiments. In Chapter 6 the predictions for Yukawa ratios at the GUT scale from a class of non-renormalizable operators in SO(10) are worked out, which serves as a starting point for future model building. The numerical procedure for the quantitative calculation of proton decay from dimension 5 operators in SUSY models is specified in Chapter 7, where the calculation is demonstrated by means of an example model. Finally, in Part IV the results are summarized and a conclusion is drawn.

The thesis is partially based on the publications [1], [2] and [3], and on not yet published work. Further work which is not considered in this thesis are the publications [4, 5] and the notes [6].

PART II

Theoretical Framework

CHAPTER 1

The Standard Model

1.1 The Standard Model Lagrangian

The Standard Model of particle physics [7–12] is formulated as a chiral, renormalizable field theory with the gauge group $\mathrm{SU(3)_C} \times \mathrm{SU(2)_L} \times \mathrm{U(1)_Y}$ (labelled as $\mathrm{G_{321}}$), which is spontaneously broken to $\mathrm{SU(3)_C} \times \mathrm{U(1)_{EM}}$ by a non-zero vacuum expectation value (vev) of the electroweak Higgs field, called electroweak symmetry breaking (EWSB). The different components of the gauge group are referred to as strong interaction $\mathrm{SU(3)_C}$, electroweak interaction $\mathrm{SU(2)}_L \times \mathrm{U(1)_Y}$ and electromagnetic interaction $\mathrm{U(1)_{EM}}$. Chiral means, that for each fermion there exists no other fermion, such that the corresponding representations concerning the SM gauge group are mutually conjugated. Thus, the fermions are naturally massless and the mass terms are generated by the vev of the EW Higgs field (see Section 1.2). In Table 1.1 a list of the scalar and fermion fields, which are present in the SM, is given. Furthermore, the SM contains gauge bosons, which are associated with the three components of the gauge group, namely

- gluons $G_\mu{}^{(r)}$: gauge bosons of $\mathrm{SU(3)}_C$, where $(r) \in \{1, ..., 8\}$,
- W bosons $W_\mu{}^{(s)}$: gauge bosons of $\mathrm{SU(2)}_L$, where $(s) \in \{1, 2, 3\}$,
- B boson B_μ: gauge boson of $\mathrm{U(1)}_Y$.

The adjoint indices (r) and (s) are defined with respect to a set of Hermitian generators $\mathbf{T}^3_{(r)}$ and $\mathbf{T}^2_{(s)}$ of $\mathrm{SU(3)_C}$ and $\mathrm{SU(2)_L}$, respectively, with the corresponding real structure constants $c^3_{(p)(q)}{}^{(r)}$ and $c^2_{(p)(q)}{}^{(s)}$. Moreover, the real gauge couplings of the three components of the gauge group are labelled by g_3, g_2 and g_1.

The part of the SM Lagrangian which contains the kinetic terms of the gauge fields is given by [1]

$$\mathcal{L}_{\text{gauge}} = -\frac{1}{4}\sum_{(r)=1}^{8} G_{\mu\nu}{}^{(r)} G^{\mu\nu(r)} - \frac{1}{4}\sum_{(s)=1}^{3} W_{\mu\nu}{}^{(s)} W^{\mu\nu(s)} - \frac{1}{4} B_{\mu\nu} B^{\mu\nu}\,, \tag{1.1}$$

[1] There is an other term which contains only gauge fields, namely the CP-violating term $\mathcal{L}_\theta^{\mathrm{QCD}} = \theta_{\mathrm{QCD}} \frac{g_3^2}{64\pi^2} \epsilon_{\mu\nu\rho\tau} G^{\mu\nu(r)} G^{\rho\tau(r)}$. However, this term is often neglected, because experiments set a stringent bound for the QCD vacuum angle: $|\theta_{\mathrm{QCD}}| \leq 10^{-10}$ [13].

Table 1.1: List of the fields in the SM, where the fermions are written as left-handed Weyl spinors. For a particular field the representation with respect to the SM gauge group and the spin is specified. Futhermore, for each fermion there exist three copies with the same quantum numbers, forming three families.

Fields	$\mathrm{SU(3)_C} \times \mathrm{SU(2)_L} \times \mathrm{U(1)_Y}$	Spin
$Q = \begin{pmatrix} u_L \\ d_L \end{pmatrix}$	$(\mathbf{3}, \mathbf{2})(+\frac{1}{6})$	$\frac{1}{2}$
$u_R^\dagger$	$(\overline{\mathbf{3}}, \mathbf{1})(-\frac{2}{3})$	$\frac{1}{2}$
$d_R^\dagger$	$(\overline{\mathbf{3}}, \mathbf{1})(+\frac{1}{3})$	$\frac{1}{2}$
$L = \begin{pmatrix} \nu_L \\ e_L \end{pmatrix}$	$(\mathbf{1}, \mathbf{2})(-\frac{1}{2})$	$\frac{1}{2}$
$e_R^\dagger$	$(\mathbf{1}, \mathbf{1})(+1)$	$\frac{1}{2}$
$H = \begin{pmatrix} H^+ \\ H^0 \end{pmatrix}$	$(\mathbf{1}, \mathbf{2})(+\frac{1}{2})$	0

where the field strength tensors are defined as

$$G_{\mu\nu}{}^{(r)} = \partial_\mu G_\nu{}^{(r)} - \partial_\nu G_\mu{}^{(r)} + c^3_{(p)(q)}{}^{(r)} G_\mu{}^{(p)} G_\nu{}^{(q)} \,, \tag{1.2}$$

$$W_{\mu\nu}{}^{(r)} = \partial_\mu W_\nu{}^{(r)} - \partial_\nu W_\mu{}^{(r)} + c^2_{(p)(q)}{}^{(r)} W_\mu{}^{(p)} W_\nu{}^{(q)} \,, \tag{1.3}$$

$$B_{\mu\nu}{}^{(r)} = \partial_\mu B_\nu{}^{(r)} - \partial_\nu B_\mu{}^{(r)} \,. \tag{1.4}$$

The kinetic terms of the scalar and fermion fields are formulated by using the covariant derivative [14] with respect to the SM gauge group, which has the form

$$\mathcal{D}_\mu = \partial_\mu - i g_3 \, G_\mu{}^{(r)} \mathbf{T}^3_{(r)} - i g_2 \, W_\mu{}^{(s)} \mathbf{T}^2_{(s)} - i g_1 \, q_\mathrm{Y} B_\mu \,, \tag{1.5}$$

where for a particular field the generators are written in the corresponding representation. Using Weyl spinor notation and the mostly plus convention for the Minkowski metric, the kinetic terms of the fermions have the following form:

$$\begin{aligned} \mathcal{L}_\mathrm{kin} = -\frac{i}{2} \sum_{I=1}^{3} \big[& Q_I \sigma^\mu \mathcal{D}_\mu \overline{Q}_I + u^\dagger_{R_I} \sigma^\mu \mathcal{D}_\mu \overline{u}^\dagger_{R_I} + d^\dagger_{R_I} \sigma^\mu \mathcal{D}_\mu \overline{d}^\dagger_{R_I} \\ & + L_I \sigma^\mu \mathcal{D}_\mu \overline{L}_I + e^\dagger_{R_I} \sigma^\mu \mathcal{D}_\mu \overline{e}^\dagger_{R_I} + c.c. \big] \,, \end{aligned} \tag{1.6}$$

with the family index $I \in \{1, 2, 3\}$. For the sake of readability, $\mathrm{SU(3)_C}$ and $\mathrm{SU(2)_L}$ indices are suppressed. Furthermore, the couplings of the fermions to the EW Higgs field are specified by 3×3-dimensional complex Yukawa matrices $\mathbf{Y}$ in family space. In left-right notation the Yukawa terms are written as

$$\mathcal{L}_\mathrm{Yukawa} = -(\mathbf{Y}_u)_{IJ} \, Q_I \cdot H \, u^\dagger_{R_J} - (\mathbf{Y}_d)_{IJ} \, Q_I \, \overline{H} \, d^\dagger_{R_J} - (\mathbf{Y}_e)_{IJ} \, L_I \, \overline{H} \, e^\dagger_{R_J} + c.c. \,, \tag{1.7}$$

with the antisymmetric product $Q_J \cdot H = u_{L_J} H^0 - d_{L_J} H^+$ in the $\mathrm{SU(2)_L}$ indices. Finally, the part of the Lagrangian which only contains the EW Higgs field is given by

$$\mathcal{L}_{\text{Higgs}} = -\mathcal{D}_\mu H \, \mathcal{D}^\mu \overline{H} + \mu_H^2 \, \overline{H} \, H - \frac{1}{4} \lambda_H (\overline{H} \, H)^2 \,, \tag{1.8}$$

where the couplings μ_H^2 and λ_H are real.

The last two terms in Eq. (1.8) form (up to an overall minus sign) the scalar potential of the SM. If the parameters $\mu_H^2, \lambda_H > 0$, the scalar potential has a non-trivial minimum and the vev $\langle H \rangle$ of the EW Higgs field (at tree-level) is given by

$$\langle H \rangle = \begin{pmatrix} 0 \\ v \end{pmatrix}, \quad \text{with} \quad v = \sqrt{\frac{2\mu_H^2}{\lambda_H}} \,. \tag{1.9}$$

The experimental value of the vev is $v \approx 174\,\mathrm{GeV}$ [13], which defines the EW scale. The SM gauge group is spontaneously broken by the non-vanishing $\langle H \rangle$, namely

$$\mathrm{SU(3)_C} \times \mathrm{SU(2)_L} \times \mathrm{U(1)_Y} \quad \xrightarrow{\text{EWSB}} \quad \mathrm{SU(3)_C} \times \mathrm{U(1)_{EM}} \,. \tag{1.10}$$

Moreover, the charge of the electromagnetic interaction is computed as $q_{\text{EM}} = I_3 + q_{\text{Y}}$, where I_3 is the third component of the weak isospin and q_{Y} is the weak hypercharge. According to the Higgs mechanism [15–18], the three massless Goldstone bosons are absorbed by a suitable gauge transformation into the gauge bosons which correspond to the broken generators, and which acquired a mass. The four mass eigenstates of the electroweak theory are then called W bosons $W^\pm$, Z boson Z^0 and photon γ, with the corresponding masses

$$M_W = \frac{1}{\sqrt{2}} g_2 v \,, \qquad M_Z = \frac{1}{\sqrt{2}} \frac{g_2 v}{\cos\theta_{\text{W}}} \,, \qquad M_\gamma = 0 \,, \tag{1.11}$$

where $\theta_{\text{W}} = \arctan(g_1/g_2)$ is the weak angle. Furthermore, the remaining degree of freedom of the EW Higgs field is the Higgs boson h^0, which has the mass

$$m_h^2 = \lambda_H v^2 \,. \tag{1.12}$$

1.2 Fermion masses and the CKM matrix

The masses of the fermions in the SM originate from the Yukawa coupling terms in Eq. (1.7), if the EW Higgs field is substituted with its vev given in Eq. (1.9). The Dirac mass terms are then given by

$$\mathcal{L}_{\text{Mass}} = -(\mathbf{M}_u)_{IJ} \, u_{L_J} \, u_{R_J}^\dagger - (\mathbf{M}_d)_{IJ} \, d_{L_I} \, d_{R_J}^\dagger - (\mathbf{M}_e)_{IJ} \, e_{L_I} \, e_{R_J}^\dagger + c.c. \,, \tag{1.13}$$

where the 3×3-dimensional mass matrices have the form

$$\mathbf{M}_u = \frac{1}{\sqrt{2}} \, v \, \mathbf{Y}_u \,, \qquad \mathbf{M}_d = \frac{1}{\sqrt{2}} \, v \, \mathbf{Y}_d \,, \qquad \mathbf{M}_e = \frac{1}{\sqrt{2}} \, v \, \mathbf{Y}_e \,. \tag{1.14}$$

Each mass matrix $\mathbf{M}_f$ ($f \in \{u, d, e\}$) can be rotated into a diagonal matrix $\mathbf{M}_f^{\text{diag}}$ with real and positive entries, namely the mass eigenbasis, by a singular value decomposition:

$$\mathbf{M}_f^{\text{diag}} = (\mathbf{U}_f^L)^* \, \mathbf{M}_f \, (\mathbf{U}_f^R)^\mathsf{T} \,, \tag{1.15}$$

where $\mathbf{U}_f^R$ and $\mathbf{U}_f^L$ are unitary matrices. Since u_L and d_L are components of the same doublet Q, they can not be rotated independently, which implies that the two mass matrices $\mathbf{M}_u$ and $\mathbf{M}_d$ can not be diagonal at the same time. The mass eigenbases of the up- and down-type quarks are then connected via the Cabibbo-Kobayashi-Maskawa (CKM) matrix [19, 20], which is defined by

$$\mathbf{U}^{\text{CKM}} := \mathbf{U}_u^L \, \mathbf{U}_d^{L\dagger} \,. \tag{1.16}$$

The CKM matrix is a unitary 3×3-dimensional matrix, which, in the standard parametrization, is determined by three angles θ_{23}^{CKM}, θ_{13}^{CKM} and θ_{12}^{CKM}, and the complex phase δ^{CKM}:

$$\begin{aligned} \mathbf{U}^{\text{CKM}} &= \begin{pmatrix} 1 & 0 & 0 \\ 0 & c_{23} & s_{23} \\ 0 & -s_{23} & c_{23} \end{pmatrix} \begin{pmatrix} c_{13} & 0 & s_{13}e^{-i\delta} \\ 0 & 1 & 0 \\ -s_{13}e^{i\delta} & 0 & c_{13} \end{pmatrix} \begin{pmatrix} c_{12} & s_{12} & 0 \\ -s_{12} & c_{12} & 0 \\ 0 & 0 & 1 \end{pmatrix} \\ &= \begin{pmatrix} c_{12}c_{13} & s_{12}c_{13} & s_{13}e^{-i\delta} \\ -s_{12}c_{23} - c_{12}s_{23}s_{13}e^{i\delta} & c_{12}c_{23} - s_{12}s_{23}s_{13}e^{i\delta} & s_{23}c_{13} \\ s_{12}s_{23} - c_{12}c_{23}s_{13}e^{i\delta} & -c_{12}s_{23} - s_{12}c_{23}s_{13}e^{i\delta} & c_{23}c_{13} \end{pmatrix} , \end{aligned} \tag{1.17}$$

where the notations $c_{ij} \equiv \cos\theta_{ij}^{\text{CKM}}$, $s_{ij} \equiv \sin\theta_{ij}^{\text{CKM}}$ and $\delta \equiv \delta^{\text{CKM}}$ are used. The five additional (unphysical) phases, which are present in a general U(3) matrix, are absorbed into the fields. Moreover, the angle θ_{12}^{CKM} is also referred to as Cabibbo angle θ_{C}, and δ^{CKM} is called Dirac CP-violating phase.

1.3 Open questions

Although the SM successfully describes the weak, strong and electromagnetic interaction, as well as the properties of most of the known fundamental particles at the EW scale, there are observed phenomena and issues of a theoretical kind that are not explained. These shortcomings indicate that the SM is not the final theory and that it has to be extended. Some of these open questions are discussed in the following.

- **Neutrino masses:**
  In the SM, as defined in Section 1.1, neutrinos are described as massless particles. However, the observed neutrino flavour oscillation in experiments [21–29] implies that the mass and the flavour eigenbases of the neutrinos do not match. Thus, neutrinos have to carry a mass, which requires an extension of the SM. A brief discussion about this topic is given in Section 1.4.

- **Dark matter:**
  Strong evidence for dark matter is given, among others, by unexpectedly high velocities of galaxies within clusters [30, 31], flat rotation curves of galaxies [32, 33],

lensing effects of distant galaxies and quasars [34, 35], and by the so-called bullet cluster [36, 37]. Furthermore, the well established ΛCDM-model in cosmology postulates the existence of (cold) DM as well. There are numerous candidates for dark matter, whose masses can range from 10^{-22} eV up to five times the solar mass [13]. A promising candidate for a weakly interacting massive particle (WIMP) appears in supersymmetric extensions of the SM, where a neutralino is the lightest supersymmetric particle (LSP), which implies that it is completely stable (see Section 2.4).[2] The neutralino forms so-called cold DM, which means that the freeze out temperature, where the DM particle decouples from the thermal bath, is smaller than the mass of the particle.

- **Flavour puzzle & Grand Unification:**
  The SM without neutrino masses contains 18 parameters,[3] namely three gauge couplings, nine fermion masses, four CKM parameters and two Higgs parameters. This shows that most of the parameters are present in the flavour and in the gauge sector, where these parameters are simply fitted to the experimental data, without providing any explanation for an underlying structure. A strategy towards resolving this shortcoming of the SM is given by Grand Unified Theories, where the SM gauge group is embedded into a simple Lie Group; hence, there is only one gauge coupling at high energy scales, namely above the GUT scale. In such a theory, the representations of fermions of different sectors, but of the same generation, are embedded into bigger representations of the GUT gauge group, which relates the individual Yukawa matrices, as discussed in Chapter 3. Moreover, the introduction of a discrete symmetry in family space, a so-called flavour symmetry, can be used to make relations between the Yukawa couplings of different generations, which may lead to a better understanding of mass hierarchies and mixing angles.

- **Hierarchy Problem:**
  The fundamental energy scale in the SM is the EW scale at around 174 GeV, which is determined by the vev of the EW Higgs field as discussed in Section 1.1. Experimentally it was found that the Higgs boson mass is of the same order of magnitude, namely at about 125 GeV. This is also the order of magnitude that is expected by calculating the Higgs mass without including any quantum corrections. However, the Higgs mass is sensitive to quantum corrections which arise from direct or indirect couplings of particles to the Higgs boson and which are proportional to the masses of these particles in the loop diagrams. Thus, it is expected that if there exists physics at energy scales much above the EW scale, the Higgs boson mass is determined by these energy scales as well; this is called the hierarchy problem [38–43]. Strong hints for physics beyond the SM are given by Grand Unified Theories, or by theories which combine concepts from quantum field theory and general relativity, like supergravity (see Chapter 2), whose fundamental energy scales are the GUT and the Planck scale at roughly 10^{16} GeV and 10^{19} GeV, respectively. To keep the Higgs mass at the electroweak scale, an unpleasant fine-tuning of counter terms has to be performed, so that the different loop corrections cancel.

[2] In the context of the WIMP, the word "weakly" does not refer to the electroweak interaction.
[3] Neglecting the QCD vacuum angle θ_{QCD}.

A way out of this is to introduce supersymmetry, which is a symmetry between bosons and fermions as discussed in Chapter 2. If supersymmetry is realised, for every loop diagram of a fermion which contributes to the Higgs boson mass there is also a loop diagram of a boson, namely of the corresponding superpartner, which gives the same contribution up to a different sign, and vice versa. Thus, an exact cancellation takes place.

Since no superpartners of the SM particles have been detected, supersymmetry must be either explicitly or spontaneously broken, such that these particles are heavier than the ones of the SM. In order that there is still a systematic, although not exact cancellation of the contributions to the Higgs mass from loop diagrams, the supersymmetry breaking terms must be "soft" [44], i.e. the mass dimensions of the corresponding operators in the Lagrangian are smaller or equal to three.[4] In that case, the quadratically divergent terms of the loop diagrams are still cancelled, and even if the masses of superpartners are somewhat above the EW scale, the hierarchy is small compared to the big hierarchy between the GUT or Planck scale and the EW scale.

1.4 Neutrino masses and the PMNS matrix

An obvious way to generate masses for the neutrinos is to introduce right-handed neutrinos $\nu_R^\dagger$ which are singlets under the SM gauge group, namely $\nu_R^\dagger \sim (\mathbf{1},\mathbf{1})(0)$. This allows to write the Yukawa term

$$\mathcal{L}_{\text{Yukawa}} \supset -(\mathbf{Y}_\nu)_{IJ}\, L_I \cdot H\, \nu_{R_J}^\dagger + c.c.\,, \tag{1.18}$$

such that the neutrinos get a Dirac mass after EWSB like the other fermions, as described in Section 1.2. An upper limit for the neutrino masses follows from β decay experiments and is given by $m_\nu < 2\,\text{eV}$ [13]. This translates to an upper limit of about 10^{-11} for the neutrino Yukawa couplings, which looks unusually small even compared to the electron Yukawa coupling $y_e \approx 10^{-6}$.

A different way to make the left-handed neutrinos massive is to allow for non-renormalizable operators in the Lagrangian, in particular the dimension five Weinberg operator [46] which generates neutrino masses after EWSB:

$$\mathcal{L} \supset -\frac{1}{4}\boldsymbol{\kappa}_{IJ}(L_I \cdot H)(L_J \cdot H) + c.c. \quad \xrightarrow{\text{EWSB}} \quad -\frac{1}{2}(\mathbf{M}_\nu)_{IJ}\,\nu_{L_I}\,\nu_{L_J} + c.c.\,, \tag{1.19}$$

where $\mathbf{M}_\nu = \frac{1}{4}v^2\boldsymbol{\kappa}$. Since the term is a Majorana mass term, no additional fields have to be introduced. The Majorana mass term is consistent with gauge symmetries, because the neutrino is a singlet under $\mathrm{SU}(3)_\mathrm{C} \times \mathrm{U}(1)_\mathrm{EM}$.

An elegant solution to generate the Weinberg operator from renormalizable operators and to explain the smallness of the neutrino masses is given by the seesaw mechanism [47–50]. There are three different realizations of this mechanism, however only the type I seesaw mechanism is considered in the following, which is formulated by introducing right-handed

[4] Strictly speaking, non-holomorphic operators of scalar fields of dimension three are soft only in certain cases, see e.g. [45].

neutrinos $\nu_R^\dagger$, as discussed above.[5] Since the $\nu_R^\dagger$ are singlets under the SM gauge group, they can form a Majorana mass term

$$\mathcal{L} \supset -\frac{1}{2}(\mathbf{M}_R)_{IJ}\, \nu_{R_I}^\dagger\, \nu_{R_J}^\dagger + c.c.\,, \tag{1.20}$$

in addition to the Yukawa term in Eq. (1.18). If the mass $\mathbf{M}_R$ is much bigger than the EW scale, the right-handed neutrinos are integrated out at this energy scale and a Weinberg operator as in Eq. (1.19) is generated, where

$$\boldsymbol{\kappa} = -2\mathbf{Y}_\nu\, \mathbf{M}_R^{-1}\, \mathbf{Y}_\nu^\mathsf{T}\,. \tag{1.21}$$

The Majorana mass matrix $\mathbf{M}_\nu$ of the left-handed neutrinos, as defined in Eq. (1.19), is symmetric and can therefore be diagonalized by a Takagi decomposition:

$$\mathbf{M}_\nu^{\text{diag}} = \mathbf{U}_\nu^\mathsf{T}\, \mathbf{M}_\nu\, \mathbf{U}_\nu\,, \tag{1.22}$$

where $\mathbf{U}_\nu$ is unitary. Because ν_L and e_L are both contained in the same doublet L, the mass matrices $\mathbf{M}_e$ and $\mathbf{M}_\nu$ can not be diagonalized simultaneously. Similar to the CKM matrix in the case of the quarks, the Pontecorvo-Maki-Nakagawa-Sakata (PMNS) matrix [51–53]

$$\mathbf{U}^{\text{PMNS}} := \mathbf{U}_e^L\, \mathbf{U}_\nu\,, \tag{1.23}$$

is introduced, which connects the mass eigenbases of the electrons and neutrinos. The PMNS matrix is a unitary 3×3-dimensional matrix, which, in the standard parametrization, is determined by three angles $\theta_{23}^{\text{PMNS}}$, $\theta_{13}^{\text{PMNS}}$ and $\theta_{12}^{\text{PMNS}}$, and three complex phases δ^{PMNS}, φ_1^{PMNS} and φ_2^{PMNS}:

$$\begin{aligned}
\mathbf{U}^{\text{PMNS}} &= \begin{pmatrix} 1 & 0 & 0 \\ 0 & c_{23} & s_{23} \\ 0 & -s_{23} & c_{23} \end{pmatrix} \begin{pmatrix} c_{13} & 0 & s_{13}e^{-i\delta} \\ 0 & 1 & 0 \\ -s_{13}e^{i\delta} & 0 & c_{13} \end{pmatrix} \begin{pmatrix} c_{12} & s_{12} & 0 \\ -s_{12} & c_{12} & 0 \\ 0 & 0 & 1 \end{pmatrix} \begin{pmatrix} e^{i\varphi_1/2} & 0 & 0 \\ 0 & e^{i\varphi_2/2} & 0 \\ 0 & 0 & 1 \end{pmatrix} \\
&= \begin{pmatrix} c_{12}c_{13} & s_{12}c_{13} & s_{13}e^{-i\delta} \\ -s_{12}c_{23} - c_{12}s_{23}s_{13}e^{i\delta} & c_{12}c_{23} - s_{12}s_{23}s_{13}e^{i\delta} & s_{23}c_{13} \\ s_{12}s_{23} - c_{12}c_{23}s_{13}e^{i\delta} & -c_{12}s_{23} - s_{12}c_{23}s_{13}e^{i\delta} & c_{23}c_{13} \end{pmatrix} \begin{pmatrix} e^{i\varphi_1/2} & 0 & 0 \\ 0 & e^{i\varphi_2/2} & 0 \\ 0 & 0 & 1 \end{pmatrix},
\end{aligned} \tag{1.24}$$

where the notations $c_{ij} \equiv \cos\theta_{ij}^{\text{PMNS}}$, $s_{ij} \equiv \sin\theta_{ij}^{\text{PMNS}}$, $\delta \equiv \delta^{\text{PMNS}}$ and $\varphi_{1,2} \equiv \varphi_{1,2}^{\text{PMNS}}$ are used. In contrast to the CKM matrix, the two Majorana phases φ_1^{PMNS} and φ_2^{PMNS} in the PMNS matrix are physical, since the left-handed neutrinos have a Majorana mass term. Experimentally measured are the three angles $\theta_{23}^{\text{PMNS}}$, $\theta_{13}^{\text{PMNS}}$ and $\theta_{12}^{\text{PMNS}}$, as well as the Dirac CP-violating phase δ^{PMNS}, for which, however, there is still a big uncertainty [54].

The three mass eigenstates of the neutrinos are labelled as m_{ν_i} ($i \in \{1,2,3\}$), using the convention that

$$0 < \Delta m_{21}^2\,, \qquad \Delta m_{21}^2 < |\Delta m_{31}^2|\,, \qquad m_{21}^2 < |\Delta m_{32}^2|\,, \tag{1.25}$$

[5] Strictly speaking, only two right-handed neutrinos are necessary, leaving one left-handed neutrino massless, in order to explain the neutrino oscillation data, because only mass-squared differences are measured.

where the mass-squared differences are defined as $\Delta m_{ij}^2 = m_{\nu_i}^2 - m_{\nu_j}^2$. There are two possible orderings of the neutrino masses which fulfil these requirements:

$$m_{\nu_1} < m_{\nu_2} < m_{\nu_3} : \quad \text{normal ordering (NO)}\,, \tag{1.26}$$

$$m_{\nu_3} < m_{\nu_1} < m_{\nu_2} : \quad \text{inverse ordering (IO)}\,. \tag{1.27}$$

Both scenarios are still compatible with the data from neutrino oscillation experiments, which provide values for two mass-squared differences, namely

- $\Delta m_{21}^2,\ \Delta m_{31}^2$ in case of NO,
- $\Delta m_{21}^2,\ \Delta m_{32}^2$ in case of IO,

where $\Delta m_{21}^2 \ll |m_{3i}^2|$ ($i \in \{1, 2\}$) in the respective case [54].

CHAPTER 2

Supersymmetry

In contrast to ordinary spacetime and gauge symmetries, supersymmetry [55–58] is a symmetry which maps bosonic states onto fermionic states and and vice versa. Because of this property, the corresponding generator $\mathbf{Q}$ and its conjugate $\overline{\mathbf{Q}}$ are fermionic objects and they fulfil the schematic anticommutation relation

$$\{\mathbf{Q}, \overline{\mathbf{Q}}\} = \mathbf{P}_\mu \,, \tag{2.1}$$

where $\mathbf{P}_\mu$ is the generator of spacetime translations. Supersymmetry is parametrized by an anticommuting spinor and it is either a global or a local symmetry, depending on whether the spinor is spacetime-dependent or not. Global SUSY is also referred to as rigid supersymmetry. As illustrated in Eq. (2.1), the anticommutation of the two supersymmetry generators induces a spacetime translation. In the case of local SUSY these translations vary from point to point, which corresponds to general coordinate transformation. Thus, local supersymmetry describes a field theory which combines concepts from supersymmetry and general relativity, and is called supergravity [59–61]. As for any covariant formulation of a local symmetry, there exists a gauge field, namely the gravitino, which is related to local supersymmetry transformations. Under SUSY transformations the gravitino transitions into the graviton, which mediates the gravitational interactions.

2.1 Structural aspects

2.1.1 Notations

Throughout this chapter the mostly plus convention for the Minkowski metric η_{ab}, namely

$$\eta_{ab} = \eta^{ab} = \mathrm{diag}(-1, +1, +1, +1) \,, \tag{2.2}$$

is used, with the Lorentz vector indices $a, b \in \{0, 1, 2, 3\}$. The matrix η^{ab} is the inverse of η_{ab}, and the two matrices are employed to raise and lower Lorentz vector indices.

The totally antisymmetric Levi-Civita tensor ϵ_{abcd} with four Lorentz vector indices is defined as

$$\epsilon_{0123} = +1 \,, \qquad\qquad \epsilon^{0123} = -1 \,, \tag{2.3}$$

such that

$$\epsilon_{abcd} = \eta_{ae}\eta_{bf}\eta_{cg}\eta_{dh}\epsilon^{efgh} \,, \qquad\qquad \epsilon^{abcd} = \eta^{ae}\eta^{bf}\eta^{cg}\eta^{dh}\epsilon_{efgh} \,. \tag{2.4}$$

Furthermore, the totally antisymmetric Levi-Civita tensor $\epsilon^{\alpha\beta}$ ($\epsilon^{\dot\alpha\dot\beta}$) with two (Lorentz) Weyl spinor indices $\alpha,\beta\in\{1,2\}$ ($\dot\alpha,\dot\beta\in\{1,2\}$) is defined as follows:

$$\epsilon^{12}=\epsilon_{21}\,(=\epsilon^{\dot1\dot2}=\epsilon_{\dot2\dot1})=+1\,. \tag{2.5}$$

Thus, $\epsilon^{\alpha\beta}$ and $\epsilon_{\alpha\beta}$ are the inverses of each other, namely

$$\epsilon^{\alpha\gamma}\epsilon_{\gamma\beta}=\epsilon_{\beta\gamma}\epsilon^{\gamma\alpha}=\delta^\alpha_\beta\,, \tag{2.6}$$

and they are used to raise and lower spinor indices.

The Pauli matrices $\sigma^a_{\beta\dot\gamma}$ and $\bar\sigma^{a\dot\beta\gamma}$ carry a vector and two spinor indices, and are given by

$$\begin{aligned}
\sigma^0&=+\bar\sigma^0=\begin{pmatrix}1&0\\0&1\end{pmatrix}, & \sigma^1&=-\bar\sigma^1=\begin{pmatrix}0&1\\1&0\end{pmatrix},\\
\sigma^2&=-\bar\sigma^2=\begin{pmatrix}0&-i\\i&0\end{pmatrix}, & \sigma^3&=-\bar\sigma^3=\begin{pmatrix}1&0\\0&-1\end{pmatrix}.
\end{aligned} \tag{2.7}$$

It is convenient to use the following notations for Pauli matrices with one upper and one lower spinor index:

$$(\epsilon\sigma^a)^\beta{}_{\dot\alpha}=\epsilon^{\beta\alpha}\sigma_{\alpha\dot\alpha}\,, \qquad (\epsilon\bar\sigma^a)_{\dot\beta}{}^\alpha=\epsilon_{\dot\beta\dot\alpha}\bar\sigma^{a\dot\alpha\alpha}\,, \tag{2.8}$$

$$(\sigma^a\epsilon)_\alpha{}^{\dot\beta}=\sigma^a_{\alpha\dot\alpha}\epsilon^{\dot\alpha\dot\beta}\,, \qquad (\bar\sigma^a\epsilon)^{\dot\alpha}{}_\beta=\bar\sigma^{a\dot\alpha\alpha}\epsilon_{\alpha\beta}\,. \tag{2.9}$$

In addition, the matrices σ^{ab} and $\bar\sigma^{ab}$ are defined as

$$(\sigma^{ab})_\alpha{}^\beta=\frac14(\sigma^a\bar\sigma^b-\sigma^b\bar\sigma^a)_\alpha{}^\beta\,, \qquad (\bar\sigma^{ab})^{\dot\alpha}{}_{\dot\beta}=\frac14(\bar\sigma^a\sigma^b-\bar\sigma^b\sigma^a)^{\dot\alpha}{}_{\dot\beta}\,, \tag{2.10}$$

implying that they are antisymmetric in the indices a,b.

Weyl spinors with an undotted and a dotted spinor index, namely χ_α and $\bar\chi^{\dot\alpha}$, transform in the representations $(\frac12,0)$ and $(0,\frac12)$, respectively, under Lorentz transformations, and are also referred to as left- and right-handed spinors. In particular, $\bar\chi^{\dot\alpha}$ with an upper index transforms in the dual conjugate representation of χ_α with a lower index. The two types of Weyl spinors are related via conjugation, by taking the Grassmann parity into account:

$$(\chi_\alpha)^*=\bar\chi_{\dot\alpha}\,, \tag{2.11}$$

$$(\chi_\alpha\psi_\beta)^*=-\bar\chi_{\dot\alpha}\bar\psi_{\dot\beta}\,. \tag{2.12}$$

If spinor indices are suppressed, it is always assumed that they contract in the following way: ${}^\alpha{}_\alpha$ and ${}_{\dot\alpha}{}^{\dot\alpha}$.

Finally, spacetime indices are represented by indices $\mu,\nu,...$, and adjoint indices of internal gauge symmetries are written as $(r),(s),...$.

2.1.2 Super-Poincaré algebra

The super-Poincaré algebra $\mathfrak{siso}(1,3)$ is the supersymmetric extension of the Poincaré algebra and, from a group theory point of view, the super-Lie algebra of the super-Poincaré group sISO(1, 3). The word "super" indicates that the algebra has a $\mathbb{Z}_2$-grading, which means that the corresponding vector space decomposes into a direct sum of a Grassmann even and a Grassmann odd subspace. Furthermore, the binary operation $(\ ,\ )$ respects the grading of the algebra and is called super-Lie bracket or supercommutator. In particular, if $\mathbf{X}, \mathbf{Y} \in \mathfrak{siso}(1,3)$ have definite Grassmann parity, the supercommutator is written as

$$\begin{aligned} (\mathbf{X}, \mathbf{Y}) &= [\mathbf{X}, \mathbf{Y}]\,, \quad \text{if } \mathbf{X} \text{ or } \mathbf{Y} \text{ is even}\,, \\ (\mathbf{X}, \mathbf{Y}) &= \{\mathbf{X}, \mathbf{Y}\}\,, \quad \text{if } \mathbf{X} \text{ and } \mathbf{Y} \text{ are odd}\,, \end{aligned} \tag{2.13}$$

where $[\ ,\ ]$ and $\{\ ,\ \}$ represent the common commutator and anticommutator, respectively. In addition to the generators of the Poincaré algebra, the super-Poincaré algebra contains pairs of generators $\mathbf{Q}^I$, $\overline{\mathbf{Q}}^I$ $(I \in \{1, ..., N\})$, which generate supersymmetry transformations. The number N specifies the number of supersymmetries. In the following, only the case $N = 1$ is considered and the label I is neglected. In that case, a complete set of generators of the super-Poincaré algebra, including the respective Grassmann parity, is given by [1]

- $\mathbf{J}_{ab}$ Lorentz generators (even), with $a, b \in \{0, 1, 2, 3\}$ and $\mathbf{J}_{ba} = -\mathbf{J}_{ab}$,
- $\mathbf{P}_a$ translation/momentum generators (even), with $a \in \{0, 1, 2, 3\}$,
- $\mathbf{Q}_\alpha$, $\overline{\mathbf{Q}}_{\dot\alpha}$ supersymmetry generators (odd), with $\alpha, \dot\alpha \in \{1, 2\}$ and $(\mathbf{Q}_\alpha)^* = -\overline{\mathbf{Q}}_{\dot\alpha}$.

The definitions of the generators are chosen such, that $i\mathbf{J}_{ab}, i\mathbf{P}_a, i\mathbf{Q}_\alpha, i\overline{\mathbf{Q}}_{\dot\alpha} \in \mathfrak{siso}(1,3)$. With respect to this set of generators, the super-Lie bracket is defined as follows (cf. e.g. [62]):

$$[\mathbf{J}_{ab}, \mathbf{J}_{cd}] = +i(\eta_{ac}\mathbf{J}_{bd} - \eta_{ad}\mathbf{J}_{bc} - \eta_{bc}\mathbf{J}_{ad} + \eta_{bd}\mathbf{J}_{ac})\,, \tag{2.14a}$$
$$[\mathbf{J}_{ab}, \mathbf{P}_c] = +i(\eta_{ac}\mathbf{P}_b - \eta_{bc}\mathbf{P}_a)\,, \tag{2.14b}$$
$$[\mathbf{P}_a, \mathbf{P}_c] = 0\,, \tag{2.14c}$$
$$\{\mathbf{Q}_\alpha, \overline{\mathbf{Q}}_{\dot\gamma}\} = +2\sigma^b_{\alpha\dot\gamma}\mathbf{P}_b\,, \tag{2.14d}$$
$$\{\mathbf{Q}_\alpha, \mathbf{Q}_\gamma\} = \{\overline{\mathbf{Q}}_{\dot\alpha}, \overline{\mathbf{Q}}_{\dot\gamma}\} = 0\,, \tag{2.14e}$$
$$[\mathbf{J}_{ab}, \mathbf{Q}_\gamma] = -i(\sigma_{ab})_\gamma{}^\delta\mathbf{Q}_\delta\,, \tag{2.14f}$$
$$[\mathbf{J}_{ab}, \overline{\mathbf{Q}}_{\dot\gamma}] = +i(\bar\sigma_{ab})^{\dot\delta}{}_{\dot\gamma}\overline{\mathbf{Q}}_{\dot\delta}\,, \tag{2.14g}$$
$$[\mathbf{P}_a, \mathbf{Q}_\gamma] = [\mathbf{P}_a, \overline{\mathbf{Q}}_{\dot\gamma}] = 0\,. \tag{2.14h}$$

The three commutation relations in Eqs. (2.14a)–(2.14c) just represent the Poincaré algebra. In particular, the second equation indicates that the translation generator $\mathbf{P}_a$ transforms as a Lorentz vector. Furthermore, Eq. (2.14f) and (2.14g) show, that the

[1] In Minkowski spacetime, the Lorentz vector indices $a, b, ...$ are in one to one correspondence with the spacetime indices $\mu, \nu, ...$. Thus, in that context the Lorentz vector indices, which appear in the following definitions and identities, can simply be replaced by spacetime indices.

supersymmetry generators $\mathbf{Q}_\alpha$ and $\overline{\mathbf{Q}}_{\dot\alpha}$ are in the 2-dimensional representations $(\frac{1}{2},0)$ and $(0,\frac{1}{2})$, respectively, with respect to the Lorentz algebra, and can therefore be treated as Weyl spinors. This implies that the anticommutator of $\mathbf{Q}_\alpha$ and $\overline{\mathbf{Q}}_{\dot\alpha}$ transforms in the vector representation $(\frac{1}{2},\frac{1}{2})$ of the Lorentz group like the generator $\mathbf{P}_a$, which is taken account of in Eq. (2.14d). A similar consideration leads to the trivial (anti-)commutation relations in Eq. (2.14e) and (2.14h), because there are no generators in the appropriate representations.

The super-Poincaré algebra can be extended by adding an internal symmetry, which is represented by the Lie algebra $\mathfrak{g}$ of some Lie group G. The generators $\mathbf{T}$ of the internal symmetry, where $i\mathbf{T} \in \mathfrak{g}$, commute with all generators of the Poincaré algebra, but they can have non-trivial commutation relations with the supersymmetry generators. Such a symmetry is then called R-symmetry. For $N = 1$ supersymmetry, the most general form of an R-symmetry is a U(1) symmetry and is labelled by $\mathrm{U}(1)_\mathrm{R}$. In principle, the internal symmetry may contain multiple $\mathrm{U}(1)_\mathrm{R}$ factors. Hence, the Lie algebra has the form $\mathfrak{g} = \tilde{\mathfrak{g}} \oplus \mathfrak{u}(1)_\mathrm{R} \oplus ... \oplus \mathfrak{u}(1)_\mathrm{R}$ and the generators are written as

- $\mathbf{T}_{(r)}$ internal generators (even), with $(r) \in \{1, ..., \dim \mathfrak{g}\}$,
  - $\tilde{\mathbf{T}}_{(r)}$ generator of $\tilde{\mathfrak{g}}$,
  - $\mathbf{T}^\mathrm{R}_{(r)}$ generator of $\mathrm{U}(1)_\mathrm{R}$,

where it is distinguished whether a generator represents a $\mathrm{U}(1)_\mathrm{R}$ symmetry or not. The additional commutation relations of the extended super-Poincaré algebra are defined as

$$[\mathbf{T}_{(r)}, \mathbf{T}_{(s)}] = ic_{(r)(s)}{}^{(t)}\mathbf{T}_{(t)}\,, \tag{2.15a}$$
$$[\mathbf{T}_{(r)}, \mathbf{J}_{cd}] = [\mathbf{T}_{(r)}, \mathbf{P}_c] = 0\,, \tag{2.15b}$$
$$[\tilde{\mathbf{T}}_{(r)}, \mathbf{Q}_\gamma] = [\tilde{\mathbf{T}}_{(r)}, \overline{\mathbf{Q}}_{\dot\gamma}] = 0\,, \tag{2.15c}$$
$$[\mathbf{T}^\mathrm{R}_{(r)}, \mathbf{Q}_\gamma] = -\mathbf{Q}_\gamma\,, \tag{2.15d}$$
$$[\mathbf{T}^\mathrm{R}_{(r)}, \overline{\mathbf{Q}}_{\dot\gamma}] = +\overline{\mathbf{Q}}_{\dot\gamma}\,. \tag{2.15e}$$

If the generators $\mathbf{T}_{(r)}$ are chosen Hermitian, the structure constants $c_{(r)(s)}{}^{(t)}$ of the Lie algebra $\mathfrak{g}$, as defined in Eq. (2.15a), are real. The trivial commutation relations between internal and Poincaré generators is taken account of in Eq. (2.15b). This holds true for the supersymmetry generators, if an internal generator does not represent an R-symmetry, as stated in Eq. (2.15c). Finally, Eq. (2.15d) and (2.15e) show, that $\mathbf{Q}_\alpha$ and $\overline{\mathbf{Q}}_{\dot\alpha}$ have by definition charge -1 and $+1$, respectively, with respect to any $\mathrm{U}(1)_\mathrm{R}$ symmetry.

2.1.3 Supermultiplets

Supermultiplets are irreducible representations with respect to the super-Poincaré algebra given in Eq. (2.14). Because the Poincaré algebra is a subalgebra and the supersymmetry generators transform as Weyl spinors under the Lorentz group, a supermultiplet basically consists of a bunch of particles with different spin. Since the momentum generator $\mathbf{P}_a$ commutes with the supersymmetry generators, the squared-mass operator $-\mathbf{P}^2 \equiv -\mathbf{P}^a\mathbf{P}_a$ is a Casimir operator of the super-Poincaré algebra. Thus, all particles in a supermultiplet have the same mass. Furthermore, a supermultiplet with a finite number of particles

contains the same number of bosonic (Grassmann odd) and fermionic (Grassmann even) degrees of freedom. In order to show this, the operator $(-1)^{n_F}$ is introduced, which has the property that bosonic and fermionic states have the eigenvalues $+1$ and -1, respectively. Hence, the relations

$$\begin{aligned} (-1)^{n_F}\mathbf{Q}_\alpha &= -\mathbf{Q}_\alpha(-1)^{n_F}\,, \\ (-1)^{n_F}\overline{\mathbf{Q}}_{\dot\beta} &= -\overline{\mathbf{Q}}_{\dot\beta}(-1)^{n_F}\,, \end{aligned} \tag{2.16}$$

apply for the fermionic supersymmetry generators. Because it is assumed that the supermultiplet contains a finite number of particles, the generators can be written as finite dimensional matrices with respect to that basis. The identities from Eq. (2.16), as well as the cyclic property of the trace and the fact that $\mathbf{Q}_\alpha$ and $\overline{\mathbf{Q}}_{\dot\beta}$ are Grassmann odd, are then used in the calculation

$$\begin{aligned} 2\sigma^c_{\alpha\dot\beta}\,\mathrm{tr}\left[(-1)^{n_F}\mathbf{P}_c\right] &= \mathrm{tr}\left[(-1)^{n_F}\{\mathbf{Q}_\alpha,\overline{\mathbf{Q}}_{\dot\beta}\}\right] \\ &= \mathrm{tr}\left[(-1)^{n_F}\mathbf{Q}_\alpha\overline{\mathbf{Q}}_{\dot\beta}\right] + \mathrm{tr}\left[(-1)^{n_F}\overline{\mathbf{Q}}_{\dot\beta}\mathbf{Q}_\alpha)\right] \\ &= \mathrm{tr}\left[\mathbf{Q}_\alpha(-1)^{n_F}\overline{\mathbf{Q}}_{\dot\beta}\right] - \mathrm{tr}\left[\mathbf{Q}_\alpha(-1)^{n_F}\overline{\mathbf{Q}}_{\dot\beta}\right] \\ &= 0\,. \end{aligned} \tag{2.17}$$

Since the momentum generator maps a particle onto itself, Eq. (2.17) implies that the trace of $(-1)^{n_F}$ vanishes. Thus, the number of bosonic and fermionic degrees of freedom in a supermultiplet match. If the super-Poincaré algebra is extended by an internal symmetry which does not represent an R-symmetry, Eq. (2.15c) implies that all particles within a supermultiplet have the same transformation properties concerning this symmetry. A complete classification of the irreducible representations of the super-Poincaré algebra can be found in the standard literature, e.g. [62].

In the context of field theory, particles are described as fields in spacetime. Depending on whether a field fulfils the corresponding equation of motion or not, it is called on-shell or off-shell. Ordinary particles are the ones which are on-shell. However, in order that supersymmetry represents a symmetry of a quantum field theory, where virtual particles appear, it must be formulated off-shell, i.e. in a manifestly covariant manner.[2] In either case, the conclusion from Eq. (2.17), that a supermultiplet contains the same number of bosonic and fermionic degrees of freedom, applies. On the other hand, the equations of motion eliminate a different number of degrees of freedom for fields with different spin. Hence, an off-shell supermultiplet contains not only the physical fields which are present in the on-shell formulation of the supermultiplet, but also additional fields, so-called auxiliary fields. The equations of motion of these fields are purely algebraic, i.e. they have no kinetic term, such that the corresponding degrees of freedom vanish on-shell.

The most commonly used supermultiplets in supersymmetric theories are the chiral multiplet and the gauge multiplet. Furthermore, in supergravity, where supersymmetry is a local symmetry, the supergravity multiplet is present. These are the three kinds of supermultiplets which are considered in this chapter, and an overview of these supermultiplets is given below. They are written in the form $\left(\,\textit{physical}\;\middle|\;\textit{auxiliary}\,\right)$, where on the left-hand side of the bar the physical fields are listed, and on the right-hand side

[2] Strictly speaking, it is enough to ensure that in principle an off-shell formulation exists, because the auxiliary fields, as discussed below, have algebraic equations of motion and may be integrated out.

the auxiliary fields are specified. Furthermore, **b** and **f** stand for bosonic and fermionic off-shell real degrees of freedom, respectively.

- **Supergravity multiplet:**
  The physical fields in the supergravity multiplet are the spin 2 graviton ${e_\mu}^a$, the spin $\frac{3}{2}$ gravitino ${\psi_\mu}^\alpha$ and its conjugate $\bar{\psi}_{\mu\dot{\alpha}}$. The gravitino is the gauge field of local supersymmetry transformations and the graviton mediates gravitational interactions. In $N = 1$ supersymmetry there are three different known (off-shell) realisations of the supergravity multiplet, namely the minimal, the new-minimal and the non-minimal multiplet. In the following, only the minimal supergravity multiplet is considered, which, in addition to the physical fields, contains the auxiliary fields M, its conjugate $\overline{M}$, and b_a (see e.g. [63]):

$$\left({e_\mu}^a\,,\ {\psi_\mu}^\alpha\,(\bar{\psi}_{\mu\dot{\alpha}})\,\middle|\,M\,(\overline{M})\,,\ b_a\right) \quad \begin{cases} {e_\mu}^a & 6\,\mathbf{b} & \text{graviton} \\ {\psi_\mu}^\alpha\,(\bar{\psi}_{\mu\dot{\alpha}}) & 12\,\mathbf{f} & \text{gravitino} \\ M\,(\overline{M}) & 2\,\mathbf{b} & \text{complex scalar} \\ b_a & 4\,\mathbf{b} & \text{real vector} \end{cases} \tag{2.18}$$

  Six degrees of freedom of the graviton are removed by local Lorentz transformations and four are removed by spacetime diffeomorphism transformations. In the case of the gravitino, four degrees of freedom are removed by local supersymmetry transformations. The component fields have the following mass dimensions:

$$[{e_\mu}^a] = 0\,, \qquad [{\psi_\mu}^\alpha] = [\psi_{\mu\dot{\alpha}}] = \tfrac{3}{2}\,, \qquad [M] = [\overline{M}] = 2\,, \qquad [b_a] = 2\,. \tag{2.19}$$

  Furthermore, the supergravity multiplet is real.

- **Chiral multiplet:**
  The chiral multiplet is also called matter multiplet. The physical fields are a complex scalar φ and a Weyl fermion χ_α. Thus, this multiplet is usually used to describe a chiral fermion with the corresponding scalar superpartner, or a Higgs boson with a fermionic superpartner in a supersymmetric theory. In addition, the (off-shell) chiral multiplet contains the auxiliary field F:

$$\left(\varphi\,,\ \chi_\alpha\,\middle|\,F\right) \quad \begin{cases} \varphi & 2\,\mathbf{b} & \text{complex scalar} \\ \chi_\alpha & 4\,\mathbf{f} & \text{Weyl spinor} \\ F & 2\,\mathbf{b} & \text{complex scalar} \end{cases} \tag{2.20}$$

  Since the chiral multiplet is complex, there exists a conjugate multiplet $\left(\bar{\varphi}\,,\ \bar{\chi}^{\dot{\alpha}}\,\middle|\,\overline{F}\right)$, which contains the conjugated component fields. The mass dimensions of the individual fields are given by

$$[\varphi] = [\bar{\varphi}] = 1\,, \qquad [\chi_\alpha] = [\bar{\chi}^{\dot{\alpha}}] = \tfrac{3}{2}\,, \qquad [F] = [\overline{F}] = 2\,. \tag{2.21}$$

- **Gauge multiplet:**
  The (off-shell) gauge multiplet is used to formulate gauge interactions in a

supersymmetric framework. It is a vector multiplet in the so-called Wess-Zumino gauge. In either case, the multiplet contains a gauge boson A_μ, a Weyl fermion ${\lambda_\alpha}^{(r)}$ and its conjugate $\bar{\lambda}^{\dot{\alpha}(r)}$ as the physical fields, where the Weyl fermion is called gaugino. However, the gauge multiplet contains less auxiliary fields than the general vector multiplet, which are removed by a suitable chiral gauge transformation. These transformations are parametrized by a chiral multiplet and are fixed by this condition up to the real part of the corresponding scalar field φ, representing an ordinary gauge transformation. Thus, the gauge multiplet is only present in the context of gauge theories. Apart from the physical fields, it contains the auxiliary field D:

$$\left(A_\mu\,,\ \lambda_\alpha\,(\bar{\lambda}^{\dot{\alpha}})\,\middle|\,D\right) \quad \begin{cases} A_\mu & 3\,\mathbf{b} & \text{vector boson} \\ \lambda_\alpha\,(\bar{\lambda}^{\dot{\alpha}}) & 4\,\mathbf{f} & \text{Weyl spinor} \\ D & 1\,\mathbf{b} & \text{real scalar} \end{cases} \tag{2.22}$$

One degree of freedom of the vector boson is removed by gauge transformations. The individual fields have the mass dimensions

$$[A_\mu] = 1\,, \qquad [\lambda_\alpha] = [\bar{\lambda}^{\dot{\alpha}}] = \tfrac{3}{2}\,, \qquad [D] = 2\,. \tag{2.23}$$

Moreover, the gauge multiplet is real.

2.2 The Supergravity/matter/Yang-Mills system

The supergravity/matter/Yang-Mills system describes matter fields and gauge interactions in the context of local SUSY, which implies that the supergravity multiplet is present. In Section 2.2.1, supersymmetry in the context of the sigma model is discussed. The general off-shell supersymmetric Lagrangian of the supergravity/matter/Yang-Mills system is then presented in Section 2.2.2, and the corresponding supergravity transformations, namely local supersymmetry transformations adapted to the Wess-Zumino gauge, are given in Section 2.2.3. Finally, R-symmetries within supergravity are discussed in Section 2.2.4.

2.2.1 Supergravity within the sigma model

In the context of field theory, matter is described by the sigma model, that is a diffeomorphism Φ which goes from spacetime to a target manifold. Scalar fields $\varphi^k(x)$, with spacetime coordinates x^μ, are then given by the pullback of the coordinate functions z^k on the target manifold via Φ, i.e. $\varphi^k = z^k \circ \Phi$ (see e.g. [64–66]). It is often convenient to view the fields φ^k simply as coordinates of the target manifold. The kinetic terms of the scalar fields, which must be positive definite, are formed by (the pullback of) the metric on the target manifold; thus the target manifold is Riemannian. The sigma model is called linear, if the Riemannian metric is constant, and it is called non-linear, if the metric is coordinate dependent, i.e. a function of the scalar fields. For supersymmetric theories the target manifold is complex; thus the complex coordinates are represented by the complex scalar fields $\varphi^k(x)$ and $\bar{\varphi}^{\bar{k}}(x)$ and the metric $g_{k\bar{k}}$ is Hermitian. Furthermore, it turns out that for $N = 1$ supersymmetry in $d = 4$ dimensions the target manifold is Kähler, hence the Hermitian metric is locally specified by the Kähler potential $K(\varphi^k, \bar{\varphi}^{\bar{k}})$ (see e.g. [67]).

The superpotential $W(\varphi^k)$ is used, among others, to specify the scalar potential of the supersymmetric theory. In particular, the superpotential is a holomorphic section of a holomorphic line bundle over the target manifold, which carries locally the Hermitian metric e^K, where both quantities are locally defined with respect to some holomorphic section σ which forms a basis of the line bundle. Thus, the target manifold is a Kähler-Hodge manifold, which is also referred to as Kähler manifold of restricted type (see e.g. [68, 69]). Since the line bundle is 1-dimensional, the norm of the superpotential is just given by

$$||W(\varphi^k)||^2 = e^{K(\varphi^k,\bar{\varphi}^{\bar{k}})} W(\varphi^k)\overline{W}(\bar{\varphi}^{\bar{k}})\,. \tag{2.24}$$

Under a Kähler transformation, parametrized by a holomorphic function $F(\varphi^k)$, the Kähler potential transforms as

$$K(\varphi^k,\bar{\varphi}^{\bar{k}}) \mapsto K(\varphi^k,\bar{\varphi}^{\bar{k}}) + F(\varphi^k) + \overline{F}(\bar{\varphi}^{\bar{k}})\,, \tag{2.25}$$

which does not affect the Kähler metric. Since the metric on the line bundle is invariant under Kähler transformations as well, Eq. (2.25) implies the basis change $\sigma \mapsto \sigma e^F$. Hence, the transformations of $W(\varphi^k)$ and its conjugate $\overline{W}(\bar{\varphi}^{\bar{k}})$ are given by:

$$W(\varphi^k) \mapsto W(\varphi^k) e^{-F(\varphi^k)}\,, \qquad \overline{W}(\bar{\varphi}^{\bar{k}}) \mapsto \overline{W}(\bar{\varphi}^{\bar{k}}) e^{-\overline{F}(\bar{\varphi}^{\bar{k}})}\,. \tag{2.26}$$

There is a unique connection, namely the Chern connection, on the line bundle associated with the Hermitian metric e^K and the holomorphic structure $\bar{\partial}$. The corresponding connection 1-form with respect to the section σ and its conjugate are given by ∂K and $\bar{\partial} K$, where $\partial \equiv \mathrm{d}\varphi^k \frac{\partial}{\partial \varphi^k}$ and $\bar{\partial} \equiv \mathrm{d}\bar{\varphi}^{\bar{k}} \frac{\partial}{\partial \bar{\varphi}^{\bar{k}}}$. Under Kähler transformations, the two 1-forms transform as

$$\partial K \mapsto \partial K + \partial F\,, \qquad \bar{\partial} K \mapsto \bar{\partial} K + \bar{\partial}\overline{F}\,. \tag{2.27}$$

Moreover, the covariant derivatives of W and $\overline{W}$ with respect to Kähler transformations are thus given by

$$DW = \mathrm{d}W + W\partial K\,, \qquad D\overline{W} = \mathrm{d}\overline{W} + \overline{W}\bar{\partial} K\,, \tag{2.28}$$

which, in terms of components, take the form

$$D_k W = W_k + W K_k\,, \qquad D_{\bar{k}}\overline{W} = \overline{W}_{\bar{k}} + \overline{W} K_{\bar{k}}\,. \tag{2.29}$$

The line bundle is mapped to a U(1) bundle by the multiplication with $e^{K/2}$, and the corresponding U(1) connection $\tilde{A}$ has the form

$$\tilde{A} = \frac{1}{4}(\partial K - \bar{\partial} K)\,. \tag{2.30}$$

In particular, under Kähler transformations $\tilde{A}$, $e^{K/2}W$ and $e^{K/2}\overline{W}$ transform as

$$\tilde{A} \mapsto \tilde{A} + \frac{i}{2}\mathrm{d}\,\mathrm{Im}\,F\,, \tag{2.31}$$

$$e^{K/2}W \mapsto e^{-i\,\mathrm{Im}\,F} e^{K/2} W\,, \qquad e^{K/2}\overline{W} \mapsto e^{+i\,\mathrm{Im}\,F} e^{K/2}\overline{W}\,, \tag{2.32}$$

showing that the corresponding U(1) transformation is given by $-\frac{i}{2}\,\mathrm{Im}\,F$, and that $e^{K/2}W$ and $e^{K/2}\overline{W}$ have weights $+2$ and -2, respectively. This consideration is applied in Section 2.2.4, where R-symmetries are discussed.

The fermionic superpartners of the scalar fields are described by the section χ of a bundle over spacetime, which is the tensor product of the spinor bundle concerning a spin structure, and the pullback via Φ of the holomorphic tangent bundle of the complex target manifold.[3] In particular, χ_α is a Weyl spinor with spinor index α, and with respect to the canonical basis $\partial_k \equiv \frac{\partial}{\partial\varphi^k}$ of the holomorphic tangent bundle it is written as $\chi_\alpha = \chi^k{}_\alpha \partial_k$. The field $\chi^k{}_\alpha$ is then the fermionic superpartner of the scalar field φ^k. Similarly, the components $\bar\chi^{\bar k}{}_{\dot\alpha}$ of the conjugated section $\bar\chi_{\dot\alpha}$ with respect to the basis $\partial_{\bar k} \equiv \frac{\partial}{\partial\bar\varphi^{\bar k}}$ are the superpartners of $\bar\varphi^{\bar k}$. Moreover, the tangent bundle of the target manifold is equipped with the Levi-Civita connection of the Kähler metric $g_{k\bar k}$, which is used below to define covariant derivatives of the fermions.

A model is invariant under a compact Lie group G, which is associated to a principal G-bundle over spacetime, if the group elements act as isometries on the target manifold, i.e. G represents an internal symmetry.[4] The action is parametrized by the (real holomorphic) Killing vector field $-\alpha^{(r)}(\mathcal{K}_{(r)} + \bar{\mathcal{K}}_{(r)})$ concerning the Kähler metric, where $\alpha^{(r)}(x)$ are real functions on spacetime, and $\mathcal{K}_{(r)} = \mathcal{K}^k_{(r)}(\varphi)\partial_k$ and $\bar{\mathcal{K}}_{(r)} = \bar{\mathcal{K}}^{\bar k}_{(r)}(\bar\varphi)\partial_{\bar k}$ are holomorphic and antiholomorphic vector fields, respectively, which obey the commutation relations

$$[\mathcal{K}_{(p)}, \mathcal{K}_{(q)}] = c_{(p)(q)}{}^{(r)}\mathcal{K}_{(r)}\,, \qquad [\bar{\mathcal{K}}_{(p)}, \bar{\mathcal{K}}_{(q)}] = c_{(p)(q)}{}^{(r)}\bar{\mathcal{K}}_{(r)}\,, \qquad [\mathcal{K}_{(p)}, \bar{\mathcal{K}}_{(q)}] = 0\,. \tag{2.33}$$

The factors $c_{(p)(q)}{}^{(r)}$ are the real structure constants with respect to a set of Hermitian generators $\mathbf{T}_{(r)}$ of G. For infinitesimal $\alpha^{(r)}$, the changes of the scalars and the fermions under the group action read [5]

$$\delta\varphi^k = -\alpha^{(r)}\mathcal{K}^k_{(r)}\,, \qquad \delta\bar\varphi^{\bar k} = -\alpha^{(r)}\bar{\mathcal{K}}^{\bar k}_{(r)}\,, \tag{2.34}$$

$$\delta\chi^k = -\alpha^{(r)}(\partial_j\mathcal{K}^k_{(r)})\chi^j\,, \qquad \delta\bar\chi^{\bar k} = -\alpha^{(r)}(\partial_{\bar j}\bar{\mathcal{K}}^{\bar k}_{(r)})\bar\chi^{\bar j}\,. \tag{2.35}$$

Since the parameter $\alpha^{(r)}$ is spacetime-dependent, these transformations are called gauged isometries. In order to formulate covariant derivatives, a connection 1-form $A = A^{(r)}\mathbf{T}_{(r)} = \mathrm{d}x^\mu A^{(r)}_\mu \mathbf{T}_{(r)}$ with values in the Lie algebra $\mathfrak{g}$ of G is introduced. Under the infinitesimal group action $A^{(r)}$ transforms as

$$\delta A^{(r)} = \alpha^{(p)} A^{(q)} c_{(p)(q)}{}^{(r)} - \mathrm{d}\alpha^{(r)}\,. \tag{2.36}$$

Thus, the covariant derivatives of the scalar and the fermion fields have the form

$$\begin{aligned} \mathcal{D}_\mu\varphi^k &= \partial_\mu\varphi^k - A_\mu{}^{(r)}\mathcal{K}^k_{(r)}\,, \\ \mathcal{D}_\mu\bar\varphi^{\bar k} &= \partial_\mu\bar\varphi^{\bar k} - A_\mu{}^{(r)}\bar{\mathcal{K}}^{\bar k}_{(r)}\,, \end{aligned} \tag{2.37}$$

[3] The Grassmann property of the fermions can be accounted for by considering the exterior algebra of the tensor product bundle.

[4] The transformations are restricted to isometries in order that the kinetic terms in Eq. (2.41) are invariant under the action of G.

[5] The infinitesimal change of a tensor T on the target manifold under the induced diffeomorphisms of the Killing vector fields is calculated by using the Lie derivative, namely $\delta T = -\alpha^{(r)}(L_{\mathcal{K}_{(r)}}T + L_{\bar{\mathcal{K}}_{(r)}}T)$. On the other hand, χ and $\bar\chi$ are sections of a bundle over spacetime, thus $\delta(\chi^k\partial_k) = 0$, $\delta(\bar\chi^{\bar k}\partial_{\bar k}) = 0$. These transformation rules imply Eq. (2.34) and Eq. (2.35), which basically represent infinitesimal coordinate transformations.

$$\begin{aligned}\mathcal{D}_\mu\chi^k{}_\alpha &= \partial_\mu\chi^k{}_\alpha - \omega_\mu{}^\beta\chi^k{}_\beta - A_\mu{}^{(r)}(\partial_j\mathcal{K}^k_{(r)})\chi^j{}_\alpha + \Gamma^k{}_{ij}\chi^i{}_\alpha\mathcal{D}_\mu\varphi^j\,,\\ \mathcal{D}_\mu\bar\chi^{\bar k\dot\alpha} &= \partial_\mu\bar\chi^{\bar k\dot\alpha} - \omega_\mu{}^{\dot\alpha}{}_{\dot\beta}\bar\chi^{\bar k\dot\beta} - A_\mu{}^{(r)}(\partial_{\bar j}\bar{\mathcal{K}}^{\bar k}_{(r)})\chi^{\bar j\dot\alpha} + \Gamma^{\bar k}{}_{\bar i\bar j}\bar\chi^{\bar i\dot\alpha}\mathcal{D}_\mu\bar\varphi^{\bar j}\,,\end{aligned} \tag{2.38}$$

where ω is the spin connection 1-form associated with local Lorentz transformations on the spinor bundle. Furthermore, $\Gamma^k{}_{ij}$ and $\Gamma^{\bar k}{}_{\bar i\bar j}$ are the non-vanishing Christoffel symbols of the Levi-Civita connection with respect to $g_{k\bar k}$. The derivatives in Eq. (2.37) and (2.38) transform covariantly under local transformations of the group G and under local Lorentz transformations. Moreover, the covariant derivatives of the fermions are covariant with respect to ungauged isometries of the Kähler metric, which basically represent coordinate transformations on the target manifold. In particular, with respect to the gauge group G the covariant derivatives in Eq. (2.37) and (2.38) transform as

$$\delta\mathcal{D}_\mu\varphi^k = -\alpha^{(r)}(\partial_j\mathcal{K}^k_{(r)})\mathcal{D}_\mu\varphi^j\,, \qquad \delta\mathcal{D}_\mu\bar\varphi^{\bar k} = -\alpha^{(r)}(\partial_{\bar j}\bar{\mathcal{K}}^{\bar k}_{(r)})\mathcal{D}_\mu\bar\varphi^{\bar j}\,, \tag{2.39}$$

$$\delta\mathcal{D}_\mu\chi^k = -\alpha^{(r)}(\partial_j\mathcal{K}^k_{(r)})\mathcal{D}_\mu\chi^j\,, \qquad \delta\mathcal{D}_\mu\bar\chi^{\bar k} = -\alpha^{(r)}(\partial_{\bar j}\bar{\mathcal{K}}^{\bar k}_{(r)})\mathcal{D}_\mu\bar\chi^{\bar j}\,. \tag{2.40}$$

The kinetic terms of the scalar fields and their fermionic superpartners are then written as

$$\mathcal{L}_{\text{kin}} \supset -g_{k\bar k}\,g^{\mu\nu}\mathcal{D}_\mu\varphi^k\mathcal{D}_\nu\bar\varphi^{\bar k} - \frac{i}{2}g_{k\bar k}(\chi^k\sigma^\mu\mathcal{D}_\mu\bar\chi^{\bar k} + \bar\chi^{\bar k}\bar\sigma^\mu\mathcal{D}_\mu\chi^k)\,, \tag{2.41}$$

where $g^{\mu\nu}$ is the inverse spacetime metric.

Gauginos are described by the section λ of a bundle over spacetime, which is the tensor product of the spinor bundle and the adjoint bundle concerning the G-principal bundle, i.e. λ takes values in the Lie algebra $\mathfrak{g}$. In particular, the gaugino is a Weyl spinor, and with respect to the basis $i\mathbf{T}_{(r)}$ of $\mathfrak{g}$ it is written as $\lambda_\alpha = i\lambda_\alpha{}^{(r)}\mathbf{T}_{(r)}$. Similarly, the conjugated section has the form $\bar\lambda^{\dot\alpha} = i\bar\lambda^{\dot\alpha(r)}\mathbf{T}_{(r)}$. The field $\lambda_\alpha{}^{(r)}$ ($\bar\lambda^{\dot\alpha(r)}$) is then the superpartner of the gauge boson $A_\mu{}^{(r)}$. Since the gaugino is Lie algebra-valued, it transforms in the adjoint representation of the gauge group

$$\delta\lambda^{(r)} = \alpha^{(p)}\lambda^{(q)}c_{(p)(q)}{}^{(r)}\,, \qquad \delta\bar\lambda^{(r)} = \alpha^{(p)}\bar\lambda^{(q)}c_{(p)(q)}{}^{(r)}\,, \tag{2.42}$$

and the covariant derivative is given by

$$\begin{aligned}\mathcal{D}_\mu\lambda_\alpha{}^{(r)} &= \partial_\mu\lambda_\alpha{}^{(r)} - \omega_{\mu\alpha}{}^\beta\lambda_\beta{}^{(r)} + A_\mu{}^{(p)}c_{(p)(q)}{}^{(r)}\lambda_\alpha{}^{(q)}\,,\\ \mathcal{D}_\mu\bar\lambda^{\dot\alpha(r)} &= \partial_\mu\bar\lambda^{\dot\alpha(r)} - \omega_\mu{}^{\dot\alpha}{}_{\dot\beta}\bar\lambda^{\dot\beta(r)} + A_\mu{}^{(p)}c_{(p)(q)}{}^{(r)}\bar\lambda^{\dot\alpha(q)}\,.\end{aligned} \tag{2.43}$$

An ad($\mathfrak{g}$)-invariant metric on the Lie algebra $\mathfrak{g}$ is used to formulate kinetic terms of the gauge bosons and gauginos. In supersymmetric theories, it turns out that in general such a metric is a function of the scalar fields φ^k and $\bar\varphi^{\bar k}$. The metric has the form $\operatorname{Re} f_{(r)(s)}$ with respect to the basis $i\mathbf{T}_{(r)}$, where the function $f_{(r)(s)}(\varphi^k)$ is holomorphic in the fields φ^k and is called gauge kinetic function. The kinetic terms of the gauge bosons and the gauginos are then given by

$$\mathcal{L}_{\text{kin}} \supset -\frac{1}{4}\operatorname{Re} f_{(r)(s)}F^{\mu\nu(r)}F_{\mu\nu}{}^{(s)} - \frac{i}{2}\operatorname{Re} f_{(r)(s)}\Big(\lambda^{(r)}\sigma^\mu\mathcal{D}_\mu\bar\lambda^{(s)} + \bar\lambda^{(r)}\bar\sigma^\mu\mathcal{D}_\mu\lambda^{(s)}\Big)\,, \tag{2.44}$$

where the field strength tensor is defined as

$$F_{\mu\nu}{}^{(r)} = \partial_\mu A_\nu{}^{(r)} - \partial_\nu A_\mu{}^{(r)} + c_{(p)(q)}{}^{(r)}A_\mu{}^{(p)}A_\nu{}^{(q)}\,. \tag{2.45}$$

The graviton ${e_\mu}^a$ represents the components of the 1-form e^a on the spacetime manifold, called vielbein, concerning the coordinate patch x^μ. The vielbein is a section of the vector bundle associated to the spin structure with respect to the vector representation. The spacetime metric $g_{\mu\nu}$ is then given by

$$g_{\mu\nu} = {e_\mu}^a {e_\nu}^b \eta_{ab} \,, \tag{2.46}$$

where the Minkowski metric η_{ab} is the metric on the vector bundle. Moreover, the gravitino ${\psi_\mu}^\alpha$ (${\bar\psi_{\mu\dot\alpha}}$) represents the components of a 1-form, which is furthermore a section of the spinor bundle concerning the spin structure. Thus, the gravitino forms a Weyl spinor. The covariant derivatives of the graviton and the gravitino read

$$\mathcal{D}_\nu {e_\mu}^a = \partial_\nu {e_\mu}^a + {\Gamma^\rho}_{\nu\mu} {e_\rho}^a + {e_\mu}^b {\omega_{\nu b}}^a \,, \tag{2.47}$$

$$\mathcal{D}_\nu {\psi_\mu}^\alpha = \partial_\nu {\psi_\mu}^\alpha + {\Gamma^\rho}_{\nu\mu} {\psi_\rho}^\alpha + {\psi_\mu}^\beta {\omega_{\nu\beta}}^\alpha \,, \tag{2.48}$$

$$\mathcal{D}_\nu \bar\psi_{\mu\dot\alpha} = \partial_\nu \bar\psi_{\mu\dot\alpha} + {\Gamma^\rho}_{\nu\mu} \bar\psi_{\rho\dot\alpha} + \bar\psi_{\mu\dot\beta} {\omega_\nu}^{\dot\beta}{}_{\dot\alpha} \,, \tag{2.49}$$

with the Christoffel symbols ${\Gamma^\rho}_{\nu\mu}$ of the Levi-Civita connection with respect to $g_{\mu\nu}$. It turns out, that in supergravity the (Levi-Civita) spin connection ω is determined by the graviton and the gravitino (see Eq. (2.69)).

Ordinary Yang-Mills transformations are specified, if G acts via a linear representation on the scalar fields, i.e. the Killing vector fields have the following form: $\mathcal{K}_{(r)} = +i(\mathbf{T}_{(r)}\varphi)^k \partial_k$ and $\bar{\mathcal{K}}_{(r)} = -i(\bar\varphi \mathbf{T}_{(r)})^{\bar k} \partial_{\bar k}$, where the commutation relations of the Hermitian generators are $[\mathbf{T}_{(p)}, \mathbf{T}_{(q)}] = i {c_{(p)(q)}}^{(r)} \mathbf{T}_{(r)}$. In this case, Eq. (2.34) and (2.35) read

$$\delta\varphi^k = -i\alpha^{(r)} (\mathbf{T}_{(r)}\varphi)^k \,, \qquad \delta\bar\varphi^{\bar k} = +i\alpha^{(r)} (\bar\varphi \mathbf{T}_{(r)})^{\bar k} \,, \tag{2.50}$$

$$\delta\chi^k = -i\alpha^{(r)} (\mathbf{T}_{(r)}\chi)^k \,, \qquad \delta\bar\chi^{\bar k} = +i\alpha^{(r)} (\bar\chi \mathbf{T}_{(r)})^{\bar k} \,. \tag{2.51}$$

Since the Kähler potential and the superpotential are invariant under gauge transformations, the identities

$$K_k (\mathbf{T}_{(r)}\varphi)^k = K_{\bar k} (\bar\varphi \mathbf{T}_{(r)})^{\bar k} \,, \tag{2.52}$$

$$W_k (\mathbf{T}_{(r)}\varphi)^k = 0 \,, \qquad \overline{W}_{\bar k} (\bar\varphi \mathbf{T}_{(r)})^{\bar k} = 0 \,, \tag{2.53}$$

apply in the Yang-Mills case. Moreover, since $f_{(r)(s)}$ transforms as a tensor with two adjoint indices under gauge transformations and the corresponding metric is $\mathrm{ad}(\mathfrak{g})$-invariant, the identities

$$+i \frac{\partial f_{(r)(s)}}{\partial\varphi^k} (\mathbf{T}_{(q)}\varphi)^k = {c_{(q)(r)}}^{(p)} f_{(p)(s)} + {c_{(q)(s)}}^{(p)} f_{(r)(p)} \,, \tag{2.54}$$

$$-i \frac{\partial \bar f_{(r)(s)}}{\partial\bar\varphi^{\bar k}} (\bar\varphi \mathbf{T}_{(q)})^{\bar k} = {c_{(q)(r)}}^{(p)} \bar f_{(p)(s)} + {c_{(q)(s)}}^{(p)} \bar f_{(r)(p)} \,, \tag{2.55}$$

are valid. The gauge kinetic function is invariant under Kähler transformations. The mass dimensions of the scalar functions are the following:

$$[K] = 2 \,, \tag{2.56}$$

$$[W] = [\overline{W}] = 3 \,, \tag{2.57}$$

$$[f_{(r)(s)}] = [\bar f_{(r)(s)}] = 0 \,. \tag{2.58}$$

2.2.2 General Lagrangian

In this section the general off-shell supersymmetric Lagrangian of supergravity coupled to chiral and gauge multiplets (cf. Section 2.1.3) is presented. The gauge transformations of the internal symmetry are restricted to Yang-Mills transformations, i.e. the gauge group acts via a linear representation on the matter fields. The derivation of the supersymmetric Lagrangian is most conveniently done by using superspace techniques. The appropriate framework to describe the coupling of supergravity to matter is Kähler superspace, and the component fields of the supermultiplets are defined as lowest superspace components of superfields. However, the calculations are quite laborious, and therefore only the result is presented in the following. The full derivation can be found in the notes [6] or in the standard literature, e.g. [62, 63, 68, 70].

The general off-shell supersymmetric Lagrangian of the supergravity/matter/Yang-Mills system is completely specified by the quantities

- G Yang-Mills (internal) gauge group,
- $K(\varphi, \bar{\varphi})$ Kähler potential,
- $W(\varphi)\,,\ \overline{W}(\bar{\varphi})$ superpotential,
- $f_{(r)(s)}(\varphi)\,,\ \bar{f}_{(r)(s)}(\bar{\varphi})$ gauge kinetic function.

The Lagrangian is invariant under local Lorentz transformations, Yang-Mills gauge transformations, local supersymmetry transformations and under Kähler transformations. The transformation properties of the Kähler potential, the superpotential and the gauge kinetic function under Kähler transformations are stated in Section 2.2.1. Moreover, the Kähler transformation induces a U(1) transformation at the level of the component fields. For an arbitrary component field ϑ with the corresponding weight $w_F(\vartheta)$, the transformation is given by

$$\vartheta \mapsto e^{-\frac{i}{2} w_F(\vartheta)\,\mathrm{Im}\,F}\vartheta\,. \tag{2.59}$$

The specific weights with respect to Kähler transformations are listed in the following:

- **Supergravity multiplet:**

$$\begin{aligned} w_F(e_\mu{}^a) &= 0\,, & w_F(\psi_\mu{}^\alpha) &= +1\,, & w_F(\bar{\psi}_{\mu\dot{\alpha}}) &= -1\,, \\ w_F(M) &= +2\,, & w_F(\overline{M}) &= -2\,, & w_F(b_a) &= 0\,. \end{aligned} \tag{2.60}$$

- **Chiral multiplet:**

$$w_F(\varphi^k) = 0\,, \qquad w_F(\chi^k{}_\alpha) = -1\,, \qquad w_F(F^k) = -2\,, \tag{2.61}$$

$$w_F(\bar{\varphi}^{\bar{k}}) = 0\,, \qquad w_F(\bar{\chi}^{\bar{k}\dot{\alpha}}) = +1\,, \qquad w_F(\overline{F}^{\bar{k}}) = +2\,. \tag{2.62}$$

- **Gauge multiplet:**

$$w_F(A_\mu{}^{(r)}) = 0\,, \quad w_F(\lambda_\alpha{}^{(r)}) = +1\,, \quad w_F(\bar{\lambda}^{\dot{\alpha}(r)}) = -1 \quad w_F(D^{(r)}) = 0\,. \tag{2.63}$$

Finally, the general Lagrangian $\mathcal{L}$ of the supergravity/matter/Yang-Mills system reads

$$
\begin{aligned}
e^{-1}\mathcal{L} = &-\frac{1}{2}\mathcal{R} + \frac{1}{2}\epsilon^{\mu\nu\rho\tau}(\bar\psi_\mu\bar\sigma_\nu\nabla_\rho\psi_\tau - \psi_\mu\sigma_\nu\nabla_\rho\bar\psi_\tau)\\
&- g_{k\bar k}\, g^{\mu\nu}\mathcal{D}_\mu\varphi^k\mathcal{D}_\nu\bar\varphi^{\bar k} - \frac{i}{2}g_{k\bar k}(\chi^k\sigma^\mu\nabla_\mu\bar\chi^{\bar k} + \bar\chi^{\bar k}\bar\sigma^\mu\nabla_\mu\chi^k)\\
&- \frac{1}{4}\operatorname{Re} f_{(r)(s)}F^{\mu\nu(r)}F_{\mu\nu}{}^{(s)} + \frac{1}{8}\operatorname{Im} f_{(r)(s)}\epsilon_{\mu\nu\rho\tau}F^{\mu\nu(r)}F^{\rho\tau(s)}\\
&- \frac{i}{2}\Big(f_{(r)(s)}\lambda^{(r)}\sigma^\mu\nabla_\mu\bar\lambda^{(s)} + \bar f_{(r)(s)}\bar\lambda^{(r)}\bar\sigma^\mu\nabla_\mu\lambda^{(s)}\Big)\\
&+ e^K\Big(3W\overline{W} - g^{\bar k k}D_kW\,D_{\bar k}\overline{W}\Big) - \frac{1}{2}e^{K/2}\Big(\tilde D_jD_kW(\chi^j\chi^k) + \tilde D_{\bar j}D_{\bar k}\overline{W}(\bar\chi^{\bar j}\bar\chi^{\bar k})\Big)\\
&+ \frac{1}{4}\Big(R_{k\bar kj\bar j} + \frac{3}{2}g_{k\bar k}g_{j\bar j}\Big)(\chi^k\chi^j)(\bar\chi^{\bar k}\bar\chi^{\bar j}) - \frac{3}{4}g_{k\bar k}\operatorname{Re} f_{(r)(s)}(\chi^k\lambda^{(r)})(\bar\chi^{\bar k}\bar\lambda^{(s)})\\
&- i\sqrt{2}g_{k\bar k}(\chi^k\lambda^{(r)})(\bar\varphi\mathbf{T}_{(r)})^{\bar k} + i\sqrt{2}g_{k\bar k}(\bar\chi^{\bar k}\bar\lambda^{(r)})(\mathbf{T}_{(r)}\varphi)^k\\
&- \frac{1}{2\sqrt{2}}\Big(\partial_k f_{(r)(s)}(\chi^k\sigma^{\mu\nu}\lambda^{(r)}) + \partial_{\bar k}\bar f_{(r)(s)}(\bar\chi^{\bar k}\bar\sigma^{\mu\nu}\bar\lambda^{(r)})\Big)F_{\mu\nu}{}^{(s)}\\
&+ \frac{1}{8}\Big(\tilde\partial_j\partial_k f_{(r)(s)}(\chi^j\chi^k) + 2g^{\bar kk}e^{K/2}\partial_k f_{(r)(s)}D_{\bar k}\overline{W}\Big)(\lambda^{(r)}\lambda^{(s)})\\
&+ \frac{1}{8}\Big(\tilde\partial_{\bar j}\partial_{\bar k}\bar f_{(r)(s)}(\bar\chi^{\bar j}\bar\chi^{\bar k}) + 2g^{\bar kk}e^{K/2}\partial_{\bar k}\bar f_{(r)(s)}D_kW\Big)(\bar\lambda^{(r)}\bar\lambda^{(s)})\\
&+ \frac{1}{16}\Big(6\operatorname{Re} f_{(r)(p)}\operatorname{Re} f_{(s)(q)} - g^{\bar kk}\partial_k f_{(r)(s)}\partial_{\bar k}\bar f_{(p)(q)}\Big)(\lambda^{(r)}\lambda^{(s)})(\bar\lambda^{(p)}\bar\lambda^{(q)})\\
&- \frac{1}{2}\big(\operatorname{Re} f_{(r)(s)}\big)^{-1}\Big(K_k(\mathbf{T}_{(r)}\varphi)^k - \frac{i}{2\sqrt{2}}\partial_k f_{(r)(p)}(\chi^k\lambda^{(p)}) + \frac{i}{2\sqrt{2}}\partial_{\bar k}\bar f_{(r)(p)}(\bar\chi^{\bar k}\bar\lambda^{(p)})\Big)\\
&\qquad\qquad\times\Big(K_{\bar j}(\bar\varphi\mathbf{T}_{(s)})^{\bar j} - \frac{i}{2\sqrt{2}}\partial_j f_{(s)(q)}(\chi^j\lambda^{(q)}) + \frac{i}{2\sqrt{2}}\partial_{\bar j}\bar f_{(s)(q)}(\bar\chi^{\bar j}\bar\lambda^{(q)})\Big)\\
&- \frac{1}{\sqrt{2}}\Big(g_{k\bar k}(\bar\psi_\mu\bar\sigma^\nu\sigma^\mu\bar\chi^{\bar k})\mathcal{D}_\nu\varphi^k + g_{k\bar k}(\psi_\mu\sigma^\nu\bar\sigma^\mu\chi^k)\mathcal{D}_\nu\bar\varphi^{\bar k}\Big)\\
&- \frac{1}{4}\Big(\bar\psi_\mu\bar\sigma^\mu\lambda^{(r)} - \psi_\mu\sigma^\mu\bar\lambda^{(r)}\Big)\Big(K_k(\mathbf{T}_{(r)}\varphi)^k + K_{\bar k}(\bar\varphi\mathbf{T}_{(r)})^{\bar k}\Big)\\
&+ \frac{i}{8\sqrt{2}}\Big(\partial_k f_{(r)(s)}(\lambda^{(r)}\lambda^{(s)})(\bar\psi_\mu\bar\sigma^\mu\chi^k) + \partial_{\bar k}\bar f_{(r)(s)}(\bar\lambda^{(r)}\bar\lambda^{(s)})(\psi_\mu\sigma^\mu\bar\chi^{\bar k})\Big)\\
&+ \frac{i}{2\sqrt{2}}\Big(\partial_k f_{(r)(s)}(\psi_\mu\sigma_\nu\bar\lambda^{(r)})(\chi^k\sigma^{\mu\nu}\lambda^{(s)}) + \partial_{\bar k}\bar f_{(r)(s)}(\bar\psi_\mu\bar\sigma_\nu\lambda^{(r)})(\bar\chi^{\bar k}\bar\sigma^{\mu\nu}\bar\lambda^{(s)})\Big)\\
&+ \frac{i}{2}\operatorname{Re} f_{(r)(s)}F^{\mu\nu(r)}\Big((\psi_\mu\sigma_\nu\bar\lambda^{(s)} + \bar\psi_\mu\bar\sigma_\nu\lambda^{(s)}) + \frac{i}{2}\epsilon_{\mu\nu\rho\tau}(\psi^\rho\sigma^\tau\bar\lambda^{(s)} - \bar\psi^\rho\bar\sigma^\tau\lambda^{(s)})\Big)\\
&+ e^{K/2}\Big(\frac{i}{\sqrt{2}}(\bar\psi_\mu\bar\sigma^\mu\chi^k)D_kW + \frac{i}{\sqrt{2}}(\psi_\mu\sigma^\mu\bar\chi^{\bar k})D_{\bar k}\overline{W} - (\bar\psi_\mu\bar\sigma^{\mu\nu}\bar\psi_\nu)W - (\psi_\mu\sigma^{\mu\nu}\psi_\nu)\overline{W}\Big)\\
&- \frac{i}{2}g_{k\bar k}\epsilon^{\mu\nu\rho\tau}(\chi^k\sigma_\mu\bar\chi^{\bar k})(\psi_\nu\sigma_\rho\bar\psi_\tau) - \frac{1}{2}g_{k\bar k}\,g^{\mu\nu}(\psi_\mu\chi^k)(\bar\psi_\nu\bar\chi^{\bar k})\\
&- \frac{1}{16}\operatorname{Re} f_{(r)(s)}\Big((\lambda^{(r)}\lambda^{(s)})(3g^{\mu\nu} + 2\bar\sigma^{\mu\nu})(\bar\psi_\mu\bar\psi_\nu) + (\bar\lambda^{(r)}\bar\lambda^{(s)})(3g^{\mu\nu} + 2\sigma^{\mu\nu})(\psi_\mu\psi_\nu)\Big)\\
&+ \frac{1}{4}\Big(\operatorname{Re} f_{(r)(s)}(g^{\mu\rho}g^{\nu\tau} - g^{\mu\tau}g^{\nu\rho}) + \operatorname{Im} f_{(r)(s)}\epsilon^{\mu\nu\rho\tau}\Big)(\bar\psi_\mu\bar\sigma_\nu\lambda^{(r)})(\psi_\rho\sigma_\tau\bar\lambda^{(s)})\\
&- \frac{1}{3}\boldsymbol{M}\overline{\boldsymbol{M}} + \frac{1}{3}\boldsymbol{b}^a\boldsymbol{b}_a + g_{k\bar k}\boldsymbol{F}^k\overline{\boldsymbol{F}}^{\bar k} + \frac{1}{2}\operatorname{Re} f_{(r)(s)}\boldsymbol{D}^{(r)}\boldsymbol{D}^{(s)}\,, \qquad (2.64)
\end{aligned}
$$

where the diagonalized auxiliary fields are used, which are defined as

$$\boldsymbol{M} := M + 3e^{K/2}W\,, \tag{2.65a}$$

$$\overline{\boldsymbol{M}} := \overline{M} + 3e^{K/2}\overline{W}\,, \tag{2.65b}$$

$$\boldsymbol{b}_a := b_a - \frac{3}{4}g_{k\bar{k}}(\chi^k\sigma_a\bar{\chi}^{\bar{k}}) + \frac{3}{4}\,\mathrm{Re}\,f_{(r)(s)}(\lambda^{(r)}\sigma_a\bar{\lambda}^{(s)})\,, \tag{2.65c}$$

$$\boldsymbol{F}^k := F^k + g^{\bar{k}k}e^{K/2}D_{\bar{k}}\overline{W} - \frac{1}{4}g^{\bar{k}k}\partial_{\bar{k}}\bar{f}_{(r)(s)}(\bar{\lambda}^{(r)}\bar{\lambda}^{(s)})\,, \tag{2.65d}$$

$$\overline{\boldsymbol{F}}^{\bar{k}} := \overline{F}^{\bar{k}} + g^{\bar{k}k}e^{K/2}D_kW - \frac{1}{4}g^{\bar{k}k}\partial_k f_{(r)(s)}(\lambda^{(r)}\lambda^{(s)})\,, \tag{2.65e}$$

$$\begin{aligned}\boldsymbol{D}^{(r)} := D^{(r)} - \frac{1}{2}\big(\,\mathrm{Re}\,f_{(r)(s)}\big)^{-1}\Big(&K_k(\mathbf{T}_{(s)}\varphi)^k + K_{\bar{k}}(\bar{\varphi}\mathbf{T}_{(s)})^{\bar{k}}\\ &- \frac{i}{\sqrt{2}}\partial_k f_{(s)(p)}(\chi^k\lambda^{(p)}) + \frac{i}{\sqrt{2}}\partial_{\bar{k}}\bar{f}_{(s)(p)}(\bar{\chi}^{\bar{k}}\bar{\lambda}^{(p)})\Big)\,.\end{aligned} \tag{2.65f}$$

It is convenient to write the Lagrangian in terms of the diagonalized auxiliary fields, since they have trivial equations of motion. Hence, Eq. (2.64) without the last line represents the Lagrangian after integrating out the auxiliary fields, i.e. the on-shell supersymmetric Lagrangian. If the auxiliary fields are integrated out, the scalar part of the Lagrangian, namely the scalar potential (up to a minus sign), is given by

$$e^{-1}\mathcal{L}_{\text{scalar}} = -e^K\Big(g^{\bar{k}k}D_kW\,D_{\bar{k}}\overline{W} - 3W\overline{W}\Big) - \frac{1}{2}\big(\,\mathrm{Re}\,f_{(r)(s)}\big)^{-1}\Big(K_k(\mathbf{T}_{(r)}\varphi)^kK_{\bar{k}}(\bar{\varphi}\mathbf{T}_{(s)})^{\bar{k}}\Big)\,. \tag{2.66}$$

In the following, the quantities and expressions which are used in Eq. (2.64) and (2.65) are summarized.

- **Supergravity sector:**
  The spacetime metric is written as

$$g_{\mu\nu} = e_\mu{}^b e_\nu{}^a\eta_{ba}\,, \tag{2.67}$$

  and the corresponding curvature scalar is given by

$$\mathcal{R} = e_a{}^\nu e^{b\mu}\big(\partial_\nu\omega_{\mu b}{}^a - \partial_\mu\omega_{\nu b}{}^a + [\omega_\mu,\omega_\nu]_b{}^a\big)\,, \tag{2.68}$$

  where the spin connection has the form

$$\begin{aligned}e_\nu{}^b e_{\rho a}\omega_{\mu b}{}^a = \omega_{\mu\nu\rho} = &+\frac{1}{2}(e_\mu{}^a\partial_\nu e_{\rho a} - e_\rho{}^a\partial_\mu e_{\nu a} - e_\nu{}^a\partial_\rho e_{\mu a})\\ &-\frac{1}{2}(e_\mu{}^a\partial_\rho e_{\nu a} - e_\nu{}^a\partial_\mu e_{\rho a} - e_\rho{}^a\partial_\nu e_{\mu a})\\ &+\frac{i}{4}(\psi_\rho\sigma_\mu\bar{\psi}_\nu - \psi_\mu\sigma_\nu\bar{\psi}_\rho - \psi_\nu\sigma_\rho\bar{\psi}_\mu)\\ &-\frac{i}{4}(\psi_\nu\sigma_\mu\bar{\psi}_\rho - \psi_\mu\sigma_\rho\bar{\psi}_\nu - \psi_\rho\sigma_\nu\bar{\psi}_\mu)\,.\end{aligned} \tag{2.69}$$

Written in terms of spinor indices, the spin connection reads [6]

$$\omega_{\mu\underbrace{\beta\alpha}} = +\frac{1}{2}(\sigma^{ba}\epsilon)_{\beta\alpha}\omega_{\mu ba}\,, \qquad \omega_{\mu\underbrace{\dot\beta\dot\alpha}} = +\frac{1}{2}(\epsilon\bar\sigma^{ba})_{\dot\beta\dot\alpha}\omega_{\mu ba}\,, \tag{2.70}$$

$$\omega_{\mu ba} = -(\epsilon\sigma_{ba})^{\beta\alpha}\omega_{\mu\underbrace{\beta\alpha}} + (\bar\sigma_{ba}\epsilon)^{\dot\beta\dot\alpha}\omega_{\mu\underbrace{\dot\beta\dot\alpha}}\,. \tag{2.71}$$

Furthermore, the Pauli matrices with a spacetime index are defined as

$$\sigma^\mu = \sigma^a e_a{}^\mu\,, \qquad \bar\sigma^\mu = \bar\sigma^a e_a{}^\mu\,, \tag{2.72}$$

where $e_a{}^\mu$ is the inverse of $e_\mu{}^a$, and the Levi-Civita symbol with spacetime indices is specified by

$$\epsilon_{\mu\nu\rho\tau} = e_\mu{}^a e_\nu{}^b e_\rho{}^c e_\tau{}^d \epsilon_{abcd}\,, \qquad \epsilon^{\mu\nu\rho\tau} = e_a{}^\mu e_b{}^\nu e_c{}^\rho e_d{}^\tau \epsilon^{abcd}\,. \tag{2.73}$$

The canonical density of spacetime is given by

$$e = \det(e_\mu{}^a)\,. \tag{2.74}$$

- **Matter sector:**
  In terms of the Kähler potential, the Kähler metric is written as

$$g_{k\bar k} = K_{k\bar k}\,, \tag{2.75}$$

and the inverse matrix is labelled as $g^{\bar k k}$. The (non-vanishing) Christoffel symbols of the corresponding Levi-Civita connection are then given by

$$\Gamma^k{}_{ij} = g^{\bar k k} g_{i\bar k,j}\,, \qquad \Gamma^{\bar k}{}_{\bar i\bar j} = g^{\bar k k} g_{k\bar i,\bar j}\,, \tag{2.76}$$

and the Riemann tensor has the form

$$R_{k\bar k j\bar j} = g_{k\bar k,j\bar j} - g^{\bar l l}\, g_{k\bar l,j}\, g_{l\bar k,\bar j}\,. \tag{2.77}$$

Using the notation

$$\partial_k \equiv \frac{\partial}{\partial\varphi^k}\,, \qquad \partial_{\bar k} \equiv \frac{\partial}{\partial\bar\varphi^{\bar k}}\,, \tag{2.78}$$

the covariant derivative with respect to the Levi-Civita connection reads

$$\tilde\partial_j\partial_k = \partial_j\partial_k - \Gamma^i{}_{jk}\partial_i\,, \qquad \tilde\partial_{\bar j}\partial_{\bar k} = \partial_{\bar j}\partial_{\bar k} - \Gamma^{\bar i}{}_{\bar j\bar k}\partial_{\bar i}\,. \tag{2.79}$$

Furthermore, for the superpotential the covariant derivatives

$$D_k W = W_k + W K_k\,, \qquad D_{\bar k}\overline{W} = \overline{W}_{\bar k} + \overline{W} K_{\bar k}\,, \tag{2.80}$$

and

$$\tilde D_j D_k W = (\partial_j + K_j) D_k W - \Gamma^i{}_{jk} D_i W\,, \quad \tilde D_{\bar j} D_{\bar k}\overline{W} = (\partial_{\bar j} + K_{\bar j}) D_{\bar k}\overline{W} - \Gamma^{\bar i}{}_{\bar j\bar k} D_{\bar i}\overline{W}\,, \tag{2.81}$$

are defined.

[6] The horizontal parenthesis below the two spinor indices in $\omega_{\mu\underbrace{\beta\alpha}}$ indicates that the spin connection is symmetric in these indices.

- **Gauge sector:**
  The Hermitian generators of the Yang-Mills gauge group are written as $\mathbf{T}_{(r)}$, and the (real) structure constants are defined by

$$[\mathbf{T}_{(p)}, \mathbf{T}_{(q)}] = ic_{(p)(q)}{}^{(r)}\mathbf{T}_{(r)}\,. \tag{2.82}$$

  Furthermore, the field strength tensor is given by

$$F_{\mu\nu}{}^{(r)} = \partial_\mu A_\nu{}^{(r)} - \partial_\nu A_\mu{}^{(r)} + c_{(p)(q)}{}^{(r)} A_\mu{}^{(p)} A_\nu{}^{(q)}\,. \tag{2.83}$$

- **Covariant derivatives:**
  The covariant derivatives of the scalar matter fields have the form (cf. Section 2.2.1)

$$\mathcal{D}_\mu \varphi^k = \partial_\mu \varphi^k - iA_\mu{}^{(r)}(\mathbf{T}_{(r)}\varphi)^k\,, \tag{2.84}$$

$$\mathcal{D}_\mu \bar{\varphi}^{\bar{k}} = \partial_\mu \bar{\varphi}^{\bar{k}} + iA_\mu{}^{(r)}(\bar{\varphi}\mathbf{T}_{(r)})^{\bar{k}}\,. \tag{2.85}$$

  The following derivatives correspond to the covariant derivatives of the respective fields, extended by two terms which contain matter fields:[7]

$$\begin{aligned}\nabla_\mu \chi^k{}_\alpha &= \partial_\mu \chi^k{}_\alpha - \omega_{\mu\alpha}{}^\beta \chi^k{}_\beta - iA_\mu{}^{(r)}(\mathbf{T}_{(r)}\chi_\alpha)^k + \Gamma^k{}_{ij}\chi^i{}_\alpha \mathcal{D}_\mu \varphi^j \\ &\quad - \frac{1}{4}(K_j \mathcal{D}_\mu \varphi^j - K_{\bar{j}} \mathcal{D}_\mu \bar{\varphi}^{\bar{j}})\chi^k{}_\alpha - \frac{i}{4} g_{j\bar{j}}(\chi^j \sigma_\mu \bar{\chi}^{\bar{j}})\chi^k{}_\alpha\,,\end{aligned} \tag{2.86}$$

$$\begin{aligned}\nabla_\mu \bar{\chi}^{\bar{k}\dot{\alpha}} &= \partial_\mu \bar{\chi}^{\bar{k}\dot{\alpha}} - \omega_\mu{}^{\dot{\alpha}}{}_{\dot{\beta}} \bar{\chi}^{\bar{k}\dot{\beta}} + iA_\mu{}^{(r)}(\bar{\chi}^{\dot{\alpha}}\mathbf{T}_{(r)})^{\bar{k}} + \Gamma^{\bar{k}}{}_{\bar{i}\bar{j}} \bar{\chi}^{\bar{i}\dot{\alpha}} \mathcal{D}_\mu \bar{\varphi}^{\bar{j}} \\ &\quad + \frac{1}{4}(K_j \mathcal{D}_\mu \varphi^j - K_{\bar{j}} \mathcal{D}_\mu \bar{\varphi}^{\bar{j}})\bar{\chi}^{\bar{k}\dot{\alpha}} + \frac{i}{4} g_{j\bar{j}}(\chi^j \sigma_\mu \bar{\chi}^{\bar{j}})\bar{\chi}^{\bar{k}\dot{\alpha}}\,,\end{aligned} \tag{2.87}$$

$$\begin{aligned}\nabla_\mu \lambda_\alpha{}^{(r)} &= \partial_\mu \lambda_\alpha{}^{(r)} - \omega_{\mu\alpha}{}^\beta \lambda_\beta{}^{(r)} + A_\mu{}^{(p)} c_{(p)(q)}{}^{(r)} \lambda_\alpha{}^{(q)} \\ &\quad + \frac{1}{4}(K_k \mathcal{D}_\mu \varphi^k - K_{\bar{k}} \mathcal{D}_\mu \bar{\varphi}^{\bar{k}})\lambda_\alpha{}^{(r)} + \frac{i}{4} g_{k\bar{k}}(\chi^k \sigma_\mu \bar{\chi}^{\bar{k}})\lambda_\alpha{}^{(r)}\,,\end{aligned} \tag{2.88}$$

$$\begin{aligned}\nabla_\mu \bar{\lambda}^{\dot{\alpha}(r)} &= \partial_\mu \bar{\lambda}^{\dot{\alpha}(r)} - \omega_\mu{}^{\dot{\alpha}}{}_{\dot{\beta}} \bar{\lambda}^{\dot{\beta}(r)} + A_\mu{}^{(p)} c_{(p)(q)}{}^{(r)} \bar{\lambda}^{\dot{\alpha}(q)} \\ &\quad - \frac{1}{4}(K_k \mathcal{D}_\mu \varphi^k - K_{\bar{k}} \mathcal{D}_\mu \bar{\varphi}^{\bar{k}})\bar{\lambda}^{\dot{\alpha}(r)} - \frac{i}{4} g_{k\bar{k}}(\chi^k \sigma_\mu \bar{\chi}^{\bar{k}})\bar{\lambda}^{\dot{\alpha}(r)}\,,\end{aligned} \tag{2.89}$$

$$\begin{aligned}\nabla_\nu \psi_\mu{}^\alpha &= \partial_\nu \psi_\mu{}^\alpha + \psi_\mu{}^\beta \omega_{\nu\beta}{}^\alpha \\ &\quad + \frac{1}{4}(K_k \mathcal{D}_\nu \varphi^k - K_{\bar{k}} \mathcal{D}_\nu \bar{\varphi}^{\bar{k}})\psi_\mu{}^\alpha + \frac{i}{4} g_{k\bar{k}}(\chi^k \sigma_\nu \bar{\chi}^{\bar{k}})\psi_\mu{}^\alpha\,,\end{aligned} \tag{2.90}$$

$$\begin{aligned}\nabla_\nu \bar{\psi}_{\mu\dot{\alpha}} &= \partial_\nu \bar{\psi}_{\mu\dot{\alpha}} + \bar{\psi}_{\mu\dot{\beta}} \omega_\nu{}^{\dot{\beta}}{}_{\dot{\alpha}} \\ &\quad - \frac{1}{4}(K_k \mathcal{D}_\nu \varphi^k - K_{\bar{k}} \mathcal{D}_\nu \bar{\varphi}^{\bar{k}})\bar{\psi}_{\mu\dot{\alpha}} - \frac{i}{4} g_{k\bar{k}}(\chi^k \sigma_\nu \bar{\chi}^{\bar{k}})\bar{\psi}_{\mu\dot{\alpha}}\,.\end{aligned} \tag{2.91}$$

[7] In these definitions, the covariant derivatives of the gravitino and its conjugate are not covariant with respect to the Levi-Civita connection of spacetime, since the terms which contain the corresponding Christoffel symbols drop out in the antisymmetric combination of the derivatives.

2.2.3 Supergravity transformations

Because the Wess-Zumino gauge of a vector supermultiplet is not preserved under supersymmetry transformations, supergravity transformations are introduced, which are local SUSY transformations followed by a chiral gauge transformation, such that the Wess-Zumino gauge is restored. Thus, they are also called Wess-Zumino transformations. Like local SUSY transformations, supergravity transformations are parametrized by a fermionic spacetime-dependent Weyl spinor ξ^α and its conjugate $\bar{\xi}_{\dot{\alpha}}$, with the mass dimension $[\xi^\alpha] = [\bar{\xi}_{\dot{\alpha}}] = -\frac{1}{2}$. Infinitesimal transformations are then written as δ_ξ^{SG}, and finite transformations are given by $\Delta_\xi^{\text{SG}} = \exp(\delta_\xi^{\text{SG}})$. In the following the (off-shell) supergravity transformations of the component fields in the supergravity, chiral and gauge multiplet are presented, under which the Lagrangian in Eq. (2.64) is invariant, up to total spacetime derivatives. Again, it is most convenient to derive these transformations by using superspace techniques.

- **Supergravity multiplet:**
  The supergravity transformation of the graviton and the gravitino is given by

$$\delta_\xi^{\text{SG}} e_\mu{}^a = +i(\xi\sigma^a\bar{\psi}_\mu) + i(\bar{\xi}\bar{\sigma}^a\psi_\mu)\,, \tag{2.92}$$

$$\begin{aligned}\delta_\xi^{\text{SG}}\psi_\mu{}^\alpha = {}& +2\nabla_\mu\xi^\alpha - ie_\mu{}^a b_a\xi^\alpha - \frac{i}{3}(\xi\sigma^a\bar{\sigma}_\mu)^\alpha b_a \\ & + \frac{i}{3}(\bar{\xi}\bar{\sigma}_\mu)^\alpha M - \frac{1}{2\sqrt{2}}\psi_\mu{}^\alpha(K_k\xi\chi^k - K_{\bar{k}}\bar{\xi}\bar{\chi}^{\bar{k}})\,,\end{aligned} \tag{2.93}$$

$$\begin{aligned}\delta_\xi^{\text{SG}}\bar{\psi}_{\mu\dot{\alpha}} = {}& +2\nabla_\mu\bar{\xi}_{\dot{\alpha}} + ie_\mu{}^a b_a\bar{\xi}_{\dot{\alpha}} + \frac{i}{3}(\bar{\xi}\bar{\sigma}^a\sigma_\mu)_{\dot{\alpha}} b_a \\ & + \frac{i}{3}(\xi\sigma_\mu)_{\dot{\alpha}}\overline{M} + \frac{1}{2\sqrt{2}}\bar{\psi}_{\mu\dot{\alpha}}(K_k\xi\chi^k - K_{\bar{k}}\bar{\xi}\bar{\chi}^{\bar{k}})\,,\end{aligned} \tag{2.94}$$

  with the derivatives

$$\begin{aligned}\nabla_\mu\xi^\alpha = {}& \partial_\mu\xi^\alpha + \xi^\beta\omega_{\mu\beta}{}^\alpha \\ & + \frac{1}{4}(K_k\mathcal{D}_\mu\varphi^k - K_{\bar{k}}\mathcal{D}_\mu\bar{\varphi}^{\bar{k}})\xi^\alpha + \frac{i}{4}g_{k\bar{k}}(\chi^k\sigma_\mu\bar{\chi}^{\bar{k}})\xi^\alpha\,,\end{aligned} \tag{2.95}$$

$$\begin{aligned}\nabla_\mu\bar{\xi}_{\dot{\alpha}} = {}& \partial_\mu\bar{\xi}_{\dot{\alpha}} + \bar{\xi}_{\dot{\beta}}\omega_\mu{}^{\dot{\beta}}{}_{\dot{\alpha}} \\ & - \frac{1}{4}(K_k\mathcal{D}_\mu\varphi^k - K_{\bar{k}}\mathcal{D}_\mu\bar{\varphi}^{\bar{k}})\bar{\xi}_{\dot{\alpha}} - \frac{i}{4}g_{k\bar{k}}(\chi^k\sigma_\mu\bar{\chi}^{\bar{k}})\bar{\xi}_{\dot{\alpha}}\,.\end{aligned} \tag{2.96}$$

  The inhomogeneous transformation terms $2\nabla_\mu\xi^\alpha$ and $2\nabla_\mu\bar{\xi}_{\dot{\alpha}}$ indicate, that the gravitino is the gauge field of local supersymmetry. In addition, the supergravity transformations of the auxiliary fields read

$$\begin{aligned}\delta_\xi^{\text{SG}} M = {}& -i\sqrt{2}g_{k\bar{k}}(\xi\sigma^\mu\bar{\chi}^{\bar{k}})\Big(\mathcal{D}_\mu\varphi^k - \frac{1}{\sqrt{2}}\psi_\mu\chi^k\Big) + \sqrt{2}g_{k\bar{k}}(\xi\chi^k)\overline{F}^{\bar{k}} \\ & + i(\xi\lambda^{(r)})\big(K_k(\mathbf{T}_{(r)}\varphi)^k + K_{\bar{k}}(\bar{\varphi}\mathbf{T}_{(r)})^{\bar{k}}\big) - \frac{1}{\sqrt{2}}M(K_k\xi\chi^k - K_{\bar{k}}\bar{\xi}\bar{\chi}^{\bar{k}}) \\ & + 4(\xi\sigma^{\nu\mu}\mathcal{D}_\nu\psi_\mu) - i(\xi\sigma^\mu\bar{\sigma}^a\psi_\mu)b_a - i(\xi\sigma^\mu\bar{\psi}_\mu)M\,,\end{aligned} \tag{2.97}$$

$$\begin{aligned}\delta_\xi^{\rm SG}\overline{M} = &-i\sqrt{2}g_{k\bar{k}}(\bar{\xi}\bar{\sigma}^\mu\chi^k)\Big(\mathcal{D}_\mu\bar{\varphi}^{\bar{k}} - \frac{1}{\sqrt{2}}\bar{\psi}_\mu\bar{\chi}^{\bar{k}}\Big) + \sqrt{2}g_{k\bar{k}}(\bar{\xi}\bar{\chi}^{\bar{k}})F^k \\ &- i(\bar{\xi}\bar{\lambda}^{(r)})\big(K_k(\mathbf{T}_{(r)}\varphi)^k + K_{\bar{k}}(\bar{\varphi}\mathbf{T}_{(r)})^{\bar{k}}\big) + \frac{1}{\sqrt{2}}\overline{M}(K_k\xi\chi^k - K_{\bar{k}}\bar{\xi}\bar{\chi}^{\bar{k}}) \\ &+ 4(\bar{\xi}\bar{\sigma}^{\nu\mu}\mathcal{D}_\nu\bar{\psi}_\mu) + i(\bar{\xi}\bar{\sigma}^\mu\sigma^a\bar{\psi}_\mu)b_a - i(\bar{\xi}\bar{\sigma}^\mu\psi_\mu)\overline{M}\,,\end{aligned} \tag{2.98}$$

$$\begin{aligned}\delta_\xi^{\rm SG}b_a = &+\frac{1}{2}(\xi\sigma_a\bar{\sigma}^{\nu\mu} - 3\xi\sigma^{\nu\mu}\sigma_a)\mathcal{D}_\nu\bar{\psi}_\mu - \frac{1}{2}(\bar{\xi}\bar{\sigma}_a\sigma^{\nu\mu} - 3\bar{\xi}\bar{\sigma}^{\nu\mu}\bar{\sigma}_a)\mathcal{D}_\nu\psi_\mu \\ &- \frac{i}{2}e_a{}^\mu(\xi\sigma^d\bar{\psi}_\mu + \bar{\xi}\bar{\sigma}^d\psi_\mu)b_d - \frac{i}{2}e_a{}^\mu(\bar{\xi}\bar{\psi}_\mu)M + \frac{i}{2}e_a{}^\mu(\xi\psi_\mu)\overline{M} \\ &- \frac{i}{\sqrt{2}}g_{k\bar{k}}(\xi\sigma_a\bar{\sigma}^\mu\chi^k)\Big(\mathcal{D}_\mu\bar{\varphi}^{\bar{k}} - \frac{1}{\sqrt{2}}\bar{\psi}_\mu\bar{\chi}^{\bar{k}}\Big) + \frac{1}{\sqrt{2}}g_{k\bar{k}}(\xi\sigma_a\bar{\chi}^{\bar{k}})F^k \\ &+ \frac{i}{\sqrt{2}}g_{k\bar{k}}(\bar{\xi}\bar{\sigma}_a\sigma^\mu\bar{\chi}^{\bar{k}})\Big(\mathcal{D}_\mu\varphi^k - \frac{1}{\sqrt{2}}\psi_\mu\chi^k\Big) - \frac{1}{\sqrt{2}}g_{k\bar{k}}(\bar{\xi}\bar{\sigma}_a\chi^k)\overline{F}^{\bar{k}} \\ &- \frac{i}{2}(\xi\sigma_a\bar{\lambda}^{(r)} + \bar{\xi}\bar{\sigma}_a\lambda^{(r)})\big(K_k(\mathbf{T}_{(r)}\varphi)^k + K_{\bar{k}}(\bar{\varphi}\mathbf{T}_{(r)})^{\bar{k}}\big)\,,\end{aligned} \tag{2.99}$$

where the covariant derivatives $\mathcal{D}_\nu\psi_\mu$ and $\mathcal{D}_\nu\bar{\psi}_\mu$ correspond to the first line in Eq. (2.90) and (2.91), respectively.

- **Chiral multiplet:**
  The scalar fields of the chiral multiplets and the corresponding fermionic superpartners have the following supergravity transformations:

$$\delta_\xi^{\rm SG}\varphi^k = +\sqrt{2}\xi\chi^k\,, \tag{2.100}$$

$$\delta_\xi^{\rm SG}\bar{\varphi}^{\bar{k}} = +\sqrt{2}\bar{\xi}\bar{\chi}^{\bar{k}}\,, \tag{2.101}$$

$$\begin{aligned}\delta_\xi^{\rm SG}\chi^k{}_\alpha = &+i\sqrt{2}(\bar{\xi}\bar{\sigma}^\mu\epsilon)_\alpha\Big(\mathcal{D}_\mu\varphi^k - \frac{1}{\sqrt{2}}\psi_\mu\chi^k\Big) + \sqrt{2}\xi_\alpha F^k \\ &+ \frac{1}{\sqrt{2}}\xi_\alpha\Gamma^k{}_{ij}(\chi^i\chi^j) + \frac{1}{2\sqrt{2}}\chi^k{}_\alpha(K_k\xi\chi^k - K_{\bar{k}}\bar{\xi}\bar{\chi}^{\bar{k}})\,,\end{aligned} \tag{2.102}$$

$$\begin{aligned}\delta_\xi^{\rm SG}\bar{\chi}^{\bar{k}\dot{\alpha}} = &+i\sqrt{2}(\xi\sigma^\mu\epsilon)^{\dot{\alpha}}\Big(\mathcal{D}_\mu\bar{\varphi}^{\bar{k}} - \frac{1}{\sqrt{2}}\bar{\psi}_\mu\bar{\chi}^{\bar{k}}\Big) + \sqrt{2}\bar{\xi}^{\dot{\alpha}}\overline{F}^{\bar{k}} \\ &+ \frac{1}{\sqrt{2}}\xi^{\dot{\alpha}}\Gamma^{\bar{k}}{}_{\bar{i}\bar{j}}(\bar{\chi}^{\bar{i}}\bar{\chi}^{\bar{j}}) - \frac{1}{2\sqrt{2}}\bar{\chi}^{k\dot{\alpha}}(K_k\xi\chi^k - K_{\bar{k}}\bar{\xi}\bar{\chi}^{\bar{k}})\,.\end{aligned} \tag{2.103}$$

Moreover, the supergravity transformations of the auxiliary fields have the form

$$\begin{aligned}\delta_\xi^{\rm SG} F^k = &+i\sqrt{2}(\bar\xi\bar\sigma^\mu\nabla_\mu\chi^k) - i(\bar\xi\bar\sigma^\mu\psi_\mu)F^k + (\bar\xi\bar\sigma^\mu\sigma^\nu\bar\psi_\mu)\Big(\mathcal{D}_\nu\varphi^k - \frac{1}{\sqrt{2}}\psi_\nu\chi^k\Big)\\ &+\frac{\sqrt{2}}{3}\overline{M}(\xi\chi^k) - \frac{\sqrt{2}}{6}(\bar\xi\bar\sigma^a\chi^k)b_a - 2i(\bar\xi\bar\lambda^{(r)})(\mathbf{T}_{(r)}\varphi)^k - \sqrt{2}\Gamma^k{}_{ij}(\xi\chi^i)F^j\\ &-\frac{1}{\sqrt{2}}g^{\bar k k}R_{i\bar k j\bar l}(\chi^i\chi^j)(\bar\xi\bar\chi^{\bar l}) + \frac{1}{\sqrt{2}}F^k(K_j\xi\chi^j - K_{\bar j}\bar\xi\bar\chi^{\bar j})\,,\end{aligned} \tag{2.104}$$

$$\begin{aligned}\delta_\xi^{\rm SG} \overline{F}^{\bar k} = &+i\sqrt{2}(\xi\sigma^\mu\nabla_\mu\bar\chi^{\bar k}) - i(\xi\sigma^\mu\bar\psi_\mu)\overline{F}^{\bar k} + (\xi\sigma^\mu\bar\sigma^\nu\psi_\mu)\Big(\mathcal{D}_\nu\bar\varphi^{\bar k} - \frac{1}{\sqrt{2}}\bar\psi_\nu\bar\chi^{\bar k}\Big)\\ &+\frac{\sqrt{2}}{3}M(\bar\xi\bar\chi^{\bar k}) + \frac{\sqrt{2}}{6}(\xi\sigma^a\bar\chi^{\bar k})b_a + 2i(\xi\lambda^{(r)})(\bar\varphi\mathbf{T}_{(r)})^{\bar k} - \sqrt{2}\Gamma^{\bar k}{}_{\bar i\bar j}(\bar\xi\bar\chi^{\bar i})\overline{F}^{\bar j}\\ &-\frac{1}{\sqrt{2}}g^{\bar k k}R_{k\bar i l\bar j}(\bar\chi^{\bar i}\bar\chi^{\bar j})(\xi\chi^l) - \frac{1}{\sqrt{2}}\overline{F}^{\bar k}(K_j\xi\chi^j - K_{\bar j}\bar\xi\bar\chi^{\bar j})\,.\end{aligned} \tag{2.105}$$

- **Gauge multiplet:**
  Under supergravity transformations, a gauge boson and the associated gaugino transform as

$$\delta_\xi^{\rm SG} A_\mu{}^{(r)} = +i(\xi\sigma_\mu\bar\lambda^{(r)}) + i(\bar\xi\bar\sigma_\mu\lambda^{(r)})\,, \tag{2.106}$$

$$\begin{aligned}\delta_\xi^{\rm SG}\lambda_\alpha{}^{(r)} = &+(\xi\sigma^{\mu\nu}\epsilon)_\alpha(F_{\mu\nu}{}^{(r)} - i\psi_\mu\sigma_\nu\bar\lambda^{(r)} - i\bar\psi_\mu\bar\sigma_\nu\lambda^{(r)})\\ &+i\xi_\alpha D^{(r)} - \frac{1}{2\sqrt{2}}\lambda^{\alpha(r)}(K_k\xi\chi^k - K_{\bar k}\bar\xi\bar\chi^{\bar k})\,,\end{aligned} \tag{2.107}$$

$$\begin{aligned}\delta_\xi^{\rm SG}\bar\lambda^{\dot\alpha(r)} = &+(\bar\xi\bar\sigma^{\mu\nu}\epsilon)^{\dot\alpha}(F_{\mu\nu}{}^{(r)} - i\psi_\mu\sigma_\nu\bar\lambda^{(r)} - i\bar\psi_\mu\bar\sigma_\nu\lambda^{(r)})\\ &-i\bar\xi^{\dot\alpha}D^{(r)} + \frac{1}{2\sqrt{2}}\bar\lambda^{\dot\alpha(r)}(K_k\xi\chi^k - K_{\bar k}\bar\xi\bar\chi^{\bar k})\,.\end{aligned} \tag{2.108}$$

Furthermore, the supergravity transformation of the auxiliary field is given by

$$\begin{aligned}\delta_\xi^{\rm SG} D^{(r)} = &-(\xi\sigma^\mu\mathcal{D}_\mu\bar\lambda^{(r)}) + (\bar\xi\bar\sigma^\mu\mathcal{D}_\mu\lambda^{(r)}) + \frac{i}{2}(\bar\psi_\mu\bar\sigma^\mu\xi + \psi_\mu\sigma^\mu\bar\xi)D^{(r)}\\ &+\frac{1}{2}(\bar\psi_\mu\bar\sigma^{\rho\tau}\bar\sigma^\mu\xi - \psi_\mu\sigma^{\rho\tau}\sigma^\mu\bar\xi)(F_{\rho\tau}{}^{(r)} - i\psi_\rho\sigma_\tau\bar\lambda^{(r)} - i\bar\psi_\rho\bar\sigma_\tau\lambda^{(r)})\,,\end{aligned} \tag{2.109}$$

where the covariant derivatives $\mathcal{D}_\mu\lambda^{(r)}$ and $\mathcal{D}_\mu\bar\lambda^{(r)}$ correspond to the first line in Eq. (2.88) and (2.89), respectively.

2.2.4 R-symmetry

In supergravity, an R-symmetry $\mathrm{U}(1)_{\rm R}$ is a special type of U(1) symmetry, whose transformations consist of a Yang-Mills gauge transformation and a simultaneous Kähler

transformation. Analogous to ordinary U(1) Yang-Mills gauge symmetries, the matter scalar fields φ^k and $\bar{\varphi}^{\bar{k}}$ transform under $\mathrm{U}(1)_\mathrm{R}$ as

$$\varphi^k \mapsto e^{+iw_\mathrm{R}(\varphi^k)\alpha_\mathrm{R}}\varphi^k\,, \qquad \bar{\varphi}^{\bar{k}} \mapsto e^{-iw_\mathrm{R}(\varphi^k)\alpha_\mathrm{R}}\bar{\varphi}^{\bar{k}}\,, \tag{2.110}$$

where $w_\mathrm{R}(\varphi^k)$ is the corresponding weight of φ^k, also called R-charge, and α_R is a real function. If it is assumed that the superpotential $W(\varphi^k)$, as a function of the fields φ^k, has a definite weight $w_\mathrm{R}(W)$, W and $\overline{W}$ have well defined transformation properties under $\mathrm{U}(1)_\mathrm{R}$, namely [8]

$$W \mapsto e^{+iw_\mathrm{R}(W)\alpha_\mathrm{R}}W\,, \qquad \overline{W} \mapsto e^{-iw_\mathrm{R}(W)\alpha_\mathrm{R}}\overline{W}\,. \tag{2.111}$$

In contrast to ordinary Yang-Mills gauge symmetries, the superpotential is not invariant with respect to an R-symmetry. However, it is still assumed that the Kähler potential $K(\varphi^k, \bar{\varphi}^{\bar{k}})$ and the gauge kinetic function $f_{(r)(s)}(\varphi^k)$ are a singlets under $\mathrm{U}(1)_\mathrm{R}$ transformations, i.e.

$$w_\mathrm{R}(K) = 0\,, \tag{2.112}$$

$$w_\mathrm{R}(f_{(r)(s)}) = 0\,, \qquad w_\mathrm{R}(\bar{f}_{(r)(s)}) = 0\,. \tag{2.113}$$

The superpotential appears in the Lagrangian given in Eq. (2.64) only in combination with the term $e^{K/2}$, such that a Kähler transformation $F(\varphi^k)$ induces a U(1) transformation (see Eq. (2.32)):

$$e^{K/2}W \mapsto e^{-i\,\mathrm{Im}\,F}e^{K/2}W\,, \qquad e^{K/2}\overline{W} \mapsto e^{+i\,\mathrm{Im}\,F}e^{K/2}\overline{W}\,. \tag{2.114}$$

If the $\mathrm{U}(1)_\mathrm{R}$ transformation takes the value $\alpha_\mathrm{R} = -\frac{1}{2}\,\mathrm{Im}\,F$, i.e. it is parametrized by a Kähler transformation, and the superpotential has the weight

$$w_\mathrm{R}(W) = +2\,, \qquad w_\mathrm{R}(\overline{W}) = -2\,, \tag{2.115}$$

the Yang-Mills transformation in Eq. (2.110) corresponds to the Kähler transformation in Eq. (2.114). Since Kähler and Yang-Mills transformations leave the action invariant, this holds true for $\mathrm{U}(1)_\mathrm{R}$ transformations, if and only if Eq. (2.112), (2.113) and (2.115) apply.

The R-charge of a component field is given by an overall R-charge of the supermultiplet plus the particular weight w_F of that field with respect to Kähler transformations, cf. Eqs (2.60)–(2.63). In the following, the R-charges of the component fields in the supergravity, chiral and gauge multiplet are listed.

- **Supergravity multiplet:**
  The overall R-charge of the supergravity multiplet is zero. Thus, the weights w_R of the component fields take the values

$$w_\mathrm{R}(e_\mu{}^a) = 0\,, \tag{2.116}$$

$$w_\mathrm{R}(\psi_\mu{}^\alpha) = +1\,, \qquad w_\mathrm{R}(\bar{\psi}_{\mu\dot{\alpha}}) = -1\,, \tag{2.117}$$

$$w_\mathrm{R}(M) = +2\,, \qquad w_\mathrm{R}(\overline{M}) = -2\,, \tag{2.118}$$

$$w_\mathrm{R}(G_a) = 0\,. \tag{2.119}$$

[8] The assignment of an R-charge to the superpotential is compatible with covariant derivatives with respect to the matter scalar fields, e.g. $w_\mathrm{R}(D_kW) = w_\mathrm{R}(W_k) = w_\mathrm{R}(W) - w_\mathrm{R}(\varphi^k)$ where the first identity holds under the assumption of Eq. (2.112).

- **Chiral multiplet:**
  For a chiral multiplet the overall R-charge is not fixed and is written as $w_{\mathrm{R}}(\phi^k)$. The weights w_{R} of the component fields are then given by

$$w_{\mathrm{R}}(\varphi^k) = w_{\mathrm{R}}(\phi^k)\,, \quad w_{\mathrm{R}}(\chi^k{}_\alpha) = w_{\mathrm{R}}(\phi^k) - 1\,, \quad w_{\mathrm{R}}(F^k) = w_{\mathrm{R}}(\phi^k) - 2\,, \tag{2.120}$$

$$w_{\mathrm{R}}(\bar{\varphi}^{\bar{k}}) = w_{\mathrm{R}}(\bar{\phi}^{\bar{k}})\,, \quad w_{\mathrm{R}}(\bar{\chi}^{\bar{k}\dot{\alpha}}) = w_{\mathrm{R}}(\bar{\phi}^{\bar{k}}) + 1\,, \quad w_{\mathrm{R}}(\overline{F}^{\bar{k}}) = w_{\mathrm{R}}(\bar{\phi}^{\bar{k}}) + 2\,, \tag{2.121}$$

  where $w_{\mathrm{R}}(\bar{\phi}^{\bar{k}}) = -w_{\mathrm{R}}(\phi^k)$.

- **Gauge multiplet:**
  The overall R-charge of a gauge multiplet is always equal to zero and the corresponding component fields have the following weights w_{R}:

$$w_{\mathrm{R}}(A_\mu) = 0\,, \qquad w_{\mathrm{R}}(\lambda_\alpha) = +1\,, \qquad w_{\mathrm{R}}(\bar{\lambda}^{\dot{\alpha}}) = -1\,, \qquad w_{\mathrm{R}}(D) = 0\,. \tag{2.122}$$

  The gauge boson which belongs to the $\mathrm{U}(1)_{\mathrm{R}}$ symmetry transforms as $A^{\mathrm{R}}_\mu \mapsto A^{\mathrm{R}}_\mu + \frac{i}{2}\partial_\mu \operatorname{Im} F$.

As discussed in Section 2.1.2, there may be multiple $\mathrm{U}(1)_{\mathrm{R}}$ symmetries in a supergravity model. Furthermore, an R-symmetry can be present as a discrete symmetry, namely as a discrete subgroup of $\mathrm{U}(1)_{\mathrm{R}}$. In that case, as for any discrete symmetry, the R-symmetry transformations are global transformations.

2.3 Supersymmetry breaking

As discussed in Section 2.1.3, the basic building blocks of supersymmetric theories are supermultiplets. Although in Section 2.2.2 the general off-shell supersymmetric Lagrangian of the supergravity/matter/Yang-Mills system is presented, only the case where the auxiliary fields are integrated out is physically relevant, i.e. the on-shell supersymmetric Lagrangian. In this case a supermultiplet just contains the physical component fields, where all of them have the same mass. Furthermore, the component fields within a chiral multiplet have the same transformation properties under Yang-Mills gauge symmetries. Thus, if supersymmetry were an exact symmetry, a supersymmetric extension of the SM would contain scalar sfermions and a fermionic Higgsino with the same gauge interactions and masses as the chiral fermions and the Higgs boson, respectively. In addition, massless gauginos would be present in such a theory with couplings to the SM fields. However, these additional particles have not been detected, which implies that if supersymmetry indeed exists, it can not be exact at low energies. There are two possible scenarios to account for this, either there are interactions which manifestly break supersymmetry, or supersymmetry is an exact symmetry but spontaneously broken in the present ground state. In the remainder of this section the latter case is considered.

In the context of supergravity, in Section 2.3.1 the conditions for spontaneous SUSY breaking are worked out and in Section 2.3.2 the super-Higgs mechanism is discussed. In addition, in Section 2.3.3 it is shown that under certain conditions the phenomenology of a model is described by a globally supersymmetric theory augmented by soft supersymmetry breaking interactions, if supersymmetry breaking is mediated via Planck scale suppressed interactions from a hidden sector.

2.3.1 Spontaneous supersymmetry breaking

In a supergravity theory, supersymmetry is spontaneously broken, if the ground state is not invariant under SUSY transformations, except for the inhomogeneous transformation of the gravitino, which is always non-zero in case of a local supersymmetry transformations. The inhomogeneous transformation indicates that the gravitino is the gauge field of local supersymmetry. The measured value of the vacuum energy ρ_{vac} is roughly given by $\rho_{\text{vac}}^{\text{exp}} \approx (10^{-12}\,\text{GeV})^4$ [13], which is many orders of magnitude smaller than the mass scales involved in supersymmetry breaking. Thus, in the following the value of ρ_{vac}, or equivalently the value of the cosmological constant, is set equal to zero in order to describe a realistic ground state. Furthermore, it is assumed that only scalar fields, which are singlets under Lorentz transformations, can acquire a non-zero vacuum expectation value, and that these vevs are constant in spacetime.[9] Hence, the only fields which potentially have a non-zero SUSY transformation in the ground state are the gravitino, the chiral fermions and the gauginos (cf. Section 2.2.3):

$$\langle \delta_\xi^{\text{SG}} \psi_\mu{}^\alpha \rangle = 2\langle \mathcal{D}_\mu \xi^\alpha \rangle - \frac{i}{3}(\bar{\xi}\bar{\sigma}_\mu)^\alpha \langle M \rangle\,, \qquad \langle \delta_\xi^{\text{SG}} \bar{\psi}_{\mu\dot{\alpha}} \rangle = 2\langle \mathcal{D}_\mu \bar{\xi}_{\dot{\alpha}} \rangle + \frac{i}{3}(\xi\sigma_\mu)_{\dot{\alpha}} \langle \overline{M} \rangle\,, \tag{2.123}$$

$$\langle \delta_\xi^{\text{SG}} \chi^k{}_\alpha \rangle = +\sqrt{2}\xi_\alpha \langle F^k \rangle\,, \qquad \langle \delta_\xi^{\text{SG}} \bar{\chi}^{\bar{k}\dot{\alpha}} \rangle = +\sqrt{2}\bar{\xi}^{\dot{\alpha}} \langle \overline{F}^{\bar{k}} \rangle\,, \tag{2.124}$$

$$\langle \delta_\xi^{\text{SG}} \lambda_\alpha{}^{(r)} \rangle = +i\xi_\alpha \langle D^{(r)} \rangle\,, \qquad \langle \delta_\xi^{\text{SG}} \lambda^{\dot{\alpha}(r)} \rangle = -i\bar{\xi}^{\dot{\alpha}} \langle D^{(r)} \rangle\,, \tag{2.125}$$

where the infinitesimal Weyl spinor $\xi^\alpha(\bar{\xi}_{\dot{\alpha}})$ parametrizes the supergravity transformation, and the covariant derivatives $\mathcal{D}_\mu \xi^\alpha$ and $\mathcal{D}_\mu \bar{\xi}_{\dot{\alpha}}$ correspond to the first line in Eq. (2.95) and (2.96), respectively. Furthermore, the vevs of the auxiliary fields are given by

$$\langle M \rangle = -3\big\langle e^{K/2} W \big\rangle\,, \qquad \langle \overline{M} \rangle = -3\big\langle e^{K/2} \overline{W} \big\rangle\,, \tag{2.126}$$

$$\langle F^k \rangle = -\big\langle g^{\bar{k}k} e^{K/2} D_{\bar{k}} \overline{W} \big\rangle\,, \qquad \langle \overline{F}^{\bar{k}} \rangle = -\big\langle g^{\bar{k}k} e^{K/2} D_k W \big\rangle\,, \tag{2.127}$$

$$\langle D^{(r)} \rangle = +\big\langle (\text{Re}\, f_{(r)(s)})^{-1} K_k (\mathbf{T}_{(r)}\varphi)^k \big\rangle\,, \tag{2.128}$$

using the corresponding equations of motion from Eq. (2.65). Ignoring the inhomogeneous term $2\mathcal{D}_\mu \xi^\alpha$ in the transformation of the gravitino, the identities in Eqs. (2.123)–(2.125) imply that supersymmetry is broken, if and only if at least one of the auxiliary fields M, F^k or $D^{(r)}$ has a non-vanishing vev.

After the auxiliary fields are integrated out, the scalar potential V in supergravity has the form (cf. Eq. (2.66))

$$V = V_F + V_D\,, \tag{2.129}$$

with the F-term contribution

$$e^{-1} V_F = e^K \Big(g^{\bar{k}k} D_k W D_{\bar{k}} \overline{W} - 3 W \overline{W} \Big)\,, \tag{2.130}$$

and the D-term contribution

$$e^{-1} V_D = \frac{1}{2} \big(\text{Re}\, f_{(r)(s)} \big)^{-1} \Big(K_k (\mathbf{T}_{(r)}\varphi)^k K_{\bar{k}} (\bar{\varphi}\mathbf{T}_{(s)})^{\bar{k}} \Big)\,. \tag{2.131}$$

[9] Another mechanism to break supersymmetry spontaneously in supergravity, which is not considered in the subsequent discussion, is via gaugino condensate, where a pair of gauginos gets a non-zero vev [71].

In contrast to globally supersymmetric theories, the scalar potential is not positive definite, because of the term $-3e^K W\overline{W}$ in V_F.

The vev of the scalar potential corresponds to the vacuum energy ρ_{vac}. In supergravity it is possible that the vacuum energy is equal to zero in a ground state with spontaneously broken supersymmetry. To discuss this point, it is convenient to use Eqs. (2.126)–(2.128) in order to write the vev of the scalar potential in the compact form:

$$\langle e^{-1}V\rangle = \langle g_{k\bar{k}}\rangle\langle F^k\rangle\langle\overline{F}^{\bar{k}}\rangle - \frac{1}{3}\langle M\rangle\langle\overline{M}\rangle + \frac{1}{2}\langle \operatorname{Re} f_{(r)(s)}\rangle\langle D^{(r)}\rangle\langle D^{(s)}\rangle\,. \tag{2.132}$$

The first and the third term on the right-hand side in Eq. (2.132) are positive semi-definite, whereas the second term is negative semi-definite. The breaking of supersymmetry implies that one or more vevs of the auxiliary fields are not equal to zero. This means, if SUSY is spontaneously broken in a ground state with $\langle V\rangle = 0$, the vev $\langle M\rangle$ and at least one of the vevs $\langle F^k\rangle$ and $\langle D^{(r)}\rangle$ are non-zero. SUSY breaking due to a non-zero $\langle F^k\rangle$ is referred to as F-term supersymmetry breaking, and it is called D-term supersymmetry breaking in case of a non-vanishing $\langle D^{(r)}\rangle$. Furthermore, since $\langle M\rangle \neq 0$ implies that $\langle W\rangle \neq 0$, in such a ground state an R-symmetry is broken spontaneously, because the superpotential has R-charge 2.

A necessary condition for a (local) minimum of the scalar potential is, that the derivative of V with respect to the scalar fields φ^k vanishes in the ground state. The derivative is given by

$$\begin{aligned}\partial_k(e^{-1}V) = {}& +e^K g^{\bar{l}l}\tilde{D}_k D_l W D_{\bar{l}}\overline{W} - 2e^K D_k W\overline{W} \\ & + (\operatorname{Re} f_{(t)(r)})^{-1} K_l(\mathbf{T}_{(t)}\varphi)^l\Big(g_{k\bar{i}}(\bar{\varphi}\mathbf{T}_{(r)})^{\bar{i}} - \frac{1}{4}(\operatorname{Re} f_{(s)(p)})^{-1}K_i(\mathbf{T}_{(s)}\varphi)^i\partial_k f_{(p)(r)}\Big)\,,\end{aligned} \tag{2.133}$$

and the corresponding vev is written in the convenient form

$$\begin{aligned}\langle\partial_k(e^{-1}V)\rangle = {}& -\langle e^{K/2}\tilde{D}_k D_l W\rangle\langle F^l\rangle + \frac{2}{3}\langle e^{K/2}D_k W\rangle\langle\overline{M}\rangle \\ & + \langle D^{(r)}\rangle\Big\langle g_{k\bar{i}}(\bar{\varphi}\mathbf{T}_{(r)})^{\bar{i}} - \frac{1}{4}(\operatorname{Re} f_{(s)(p)})^{-1}K_i(\mathbf{T}_{(s)}\varphi)^i\partial_k f_{(p)(r)}\Big\rangle\,,\end{aligned} \tag{2.134}$$

where $\partial_k \operatorname{Re} f_{(r)(s)} = \frac{1}{2}\partial_k f_{(r)(s)}$ and the identity from Eq. (2.52) are used.

2.3.2 Super-Higgs mechanism

From the theory of gauge symmetries it is known, that the spontaneous breaking of a continuous symmetry implies the existence of a massless Goldstone boson. If the symmetry is a local symmetry, the Goldstone boson can be absorbed by an appropriate gauge transformation into the gauge boson of the broken symmetry, which acquired a mass. The same systematics is valid for supersymmetry. Since supersymmetry is parametrized by a Weyl spinor, the Goldstone particle is a fermion and is called Goldstino. Locally supersymmetric theories are described by supergravity, where the gauge field of SUSY is the gravitino. In the following, the Goldstone theorem in case of supersymmetry is derived and the super-Higgs mechanism [72–74] is discussed for the realistic scenario with vanishing vacuum energy.

For the subsequent calculations it is convenient to use the notation $\mathcal{F}_I$, where the index I runs over all different bosonic and fermionic fields and their conjugates in the supergravity theory. A ground state has the property that

$$\left\langle \frac{\delta \mathcal{L}}{\delta \mathcal{F}_I} \right\rangle = 0 \,. \tag{2.135}$$

The variation of the Lagrangian with respect to the field $\mathcal{F}_I$ has the standard form

$$\frac{\delta \mathcal{L}}{\delta \mathcal{F}_I} = \frac{\partial \mathcal{L}}{\partial \mathcal{F}_I} - \partial_\mu \frac{\partial \mathcal{L}}{\partial(\partial_\mu \mathcal{F}_I)} \tag{2.136}$$

for all fields except the graviton, since $\mathcal{L}$ contains second order derivatives of ${e_\mu}^a$. In the vacuum, Eq. (2.135) is trivially satisfied for all fields except scalar fields and the graviton, because of Lorentz invariance. For scalar fields φ^k, Eq. (2.135) corresponds to the stationarity condition of the scalar potential in a (local) minimum

$$\left\langle \frac{\partial V}{\partial \varphi^k} \right\rangle = 0 \,. \tag{2.137}$$

In case of the graviton ${e_\mu}^a$, Eq. (2.135) represents the Einstein field equations in empty space with a cosmological constant $\langle V \rangle$, namely

$$\left\langle \frac{\delta \mathcal{L}_{\text{EH}}}{\delta {e_\mu}^a} - {e_a}^\mu V \right\rangle = 0 \,, \tag{2.138}$$

where $\mathcal{L}_{\text{EH}} = -\frac{1}{2} e \mathcal{R}$ is the Einstein-Hilbert action. If the vacuum energy vanishes, i.e. $\langle V \rangle = 0$, Eq. (2.138) is solved by the Minkowski metric, which describes flat spacetime. In that case, the vev of the graviton $\langle {e_\mu}^a \rangle = \delta_\mu^a$ is set equal to the identity matrix with no loss of generality. In such a vacuum the spin connection $\langle {\omega_{\mu a}}^b \rangle$ vanishes; thus the covariant derivative is equal to the normal derivative with respect to spacetime indices: $\langle \mathcal{D}_\mu \rangle = \langle \partial_\mu \rangle$.

In the following, global supersymmetry transformations and constant fields are considered. From the invariance of the action under supergravity transformations follows that

$$(\delta^{\text{SG}}_{\text{glob}} \mathcal{F}_I) \frac{\partial \mathcal{L}}{\partial \mathcal{F}_I} = (\delta^{\text{SG}}_{\text{glob}} \mathcal{F}_I) \frac{\delta \mathcal{L}}{\delta \mathcal{F}_I} = 0 + \dots \,, \tag{2.139}$$

where the ellipses indicate total derivative terms. The first identity follows from the assumption of constant fields. Taking another derivative with respect to $\mathcal{F}_J$, Eq. (2.139) reads

$$\frac{\partial(\delta^{\text{SG}}_{\text{glob}} \mathcal{F}_I)}{\partial \mathcal{F}_J} \frac{\partial \mathcal{L}}{\partial \mathcal{F}_I} + \delta^{\text{SG}}_{\text{glob}} \mathcal{F}_I \frac{\partial^2 \mathcal{L}}{\partial \mathcal{F}_I \partial \mathcal{F}_J} = 0 + \dots \,. \tag{2.140}$$

The vacuum condition in Eq. (2.135) implies that the first term vanishes in the ground state, thus

$$\langle \delta^{\text{SG}}_{\text{glob}} \mathcal{F}_I \rangle \left\langle \frac{\partial^2 \mathcal{L}}{\partial \mathcal{F}_I \partial \mathcal{F}_J} \right\rangle = 0 \,, \tag{2.141}$$

where the vevs $\langle \delta^{\mathrm{SG}}_{\mathrm{glob}} \mathcal{F}_I \rangle$ parametrize a massless state, namely the Goldstino. According to Eqs. (2.123)–(2.125), $\langle \delta^{\mathrm{SG}}_{\mathrm{glob}} \mathcal{F}_I \rangle$ can only be non-zero, if $\mathcal{F}_I$ represents either ψ_μ, χ^k, $\lambda^{(r)}$ or one of the conjugated fields. The inhomogeneous transformation $\langle \mathcal{D}_\mu \xi^\alpha \rangle$ of the gravitino vanishes in case of global supersymmetry transformations and vanishing vacuum energy, as discussed above. Thus, the term $\langle \frac{\partial^2 \mathcal{L}}{\partial \mathcal{F}_I \partial \mathcal{F}_J} \rangle$ is just the fermionic mass matrix, and the Goldstino is only non-zero if supersymmetry is spontaneously broken.

The above statements are illustrated by an explicit calculation in the following. Considering infinitesimal spinors, the transformation of the ground state in Eqs. (2.123)–(2.125) shows that the Goldstino ζ_α is contained in the gravitino, the chiral fermions and the gauginos, and that the contributions in these fields are given by

$$\begin{pmatrix} \bar{\psi}_\nu{}^{\dot{\alpha}} \\ \chi^l{}_\alpha \\ \lambda_\alpha{}^{(s)} \end{pmatrix} \supset \frac{1}{\sqrt{c}} \begin{pmatrix} -\frac{i}{3}\langle \overline{M} \rangle \bar{\sigma}_\nu^{\dot{\alpha}\gamma} \\ +\sqrt{2}\langle F^l \rangle \delta_\alpha^\gamma \\ +i\langle D^{(s)} \rangle \delta_\alpha^\gamma \end{pmatrix} \zeta_\gamma \,. \tag{2.142}$$

The constant c has the value

$$c = \frac{10}{9}\langle M\overline{M} \rangle \,, \tag{2.143}$$

such that ζ_α is canonically normalized. The Goldstino is non-zero, exactly if at least one of the auxiliary fields has a non-vanishing vev, which is equivalent to spontaneously broken supersymmetry. Inverting Eq. (2.142), ζ_α takes the form

$$\zeta_\alpha = \frac{1}{\sqrt{c}} \Big(-\frac{i}{3}\langle M \rangle (\sigma^\mu \bar{\psi}_\mu)_\alpha + \sqrt{2}\langle g_{k\bar{k}} \overline{F}^{\bar{k}} \rangle \chi^k{}_\alpha - i\langle \mathrm{Re}\, f_{(r)(s)} D^{(s)} \rangle \lambda_\alpha{}^{(r)} \Big) \,. \tag{2.144}$$

In order to check that the Goldstino is indeed massless, the mass term of the fermions in the Lagrangian is considered:[10]

$$\begin{aligned} e^{-1}\mathcal{L}^m_{\mathrm{F}} = & -\big\langle e^{K/2} W \big\rangle (\bar{\psi}_\mu \bar{\sigma}^{\mu\nu} \bar{\psi}_\nu) - \frac{1}{2}\big\langle e^{K/2} \tilde{D}_j D_k W \big\rangle (\chi^j \chi^k) + \frac{1}{4}\big\langle g^{\bar{k}k} e^{K/2} \partial_k f_{(r)(s)} D_{\bar{k}} \overline{W} \big\rangle (\lambda^{(r)} \lambda^{(s)}) \\ & + \frac{i}{\sqrt{2}}\big\langle e^{K/2} D_k W \big\rangle (\bar{\psi}_\mu \bar{\sigma}^\mu \chi^k) - \frac{1}{2}\big\langle K_k (\mathbf{T}_{(r)} \varphi)^k \big\rangle (\bar{\psi}_\mu \bar{\sigma}^\mu \lambda^{(r)}) \\ & - i\sqrt{2}\big\langle g_{k\bar{k}} (\bar{\varphi} \mathbf{T}_{(r)})^{\bar{k}} \big\rangle (\chi^k \lambda^{(r)}) + \frac{i}{2\sqrt{2}}\big\langle (\mathrm{Re}\, f_{(s)(p)})^{-1} K_j (\mathbf{T}_{(s)} \varphi)^j \partial_k f_{(p)(r)} \big\rangle (\chi^k \lambda^{(r)}) \\ & + c.c. \,, \end{aligned} \tag{2.145}$$

where *c.c.* signifies the complex conjugated terms. It is worth to mention, that in the mass term the coupling of the gravitino to the chiral fermions and the gauginos is present only via the Goldstino, as can be seen by comparing Eq. (2.144) with the second line in Eq. (2.145) and using the expressions from Eqs. (2.126)–(2.128). The fact that the vev of the scalar potential and its derivative with respect to the scalar fields vanishes, namely

[10] Although the spin connection contains quadratic terms of the gravitino (cf. Eq. (2.69)), the contribution of the Einstein-Hilbert action $\mathcal{L}_{\mathrm{EH}} = -\frac{1}{2} e \mathcal{R}$ to the mass term of the fermions is not present, because the spacetime metric is the Minkowski metric in a ground state with vanishing energy.

$\langle V\rangle = 0$ and $\langle \partial_k V\rangle = 0$ (cf. Eq. (2.132) and (2.134)), implies that the vector on the right-hand side in Eq. (2.142) representing the Goldstino is an eigenvector with eigenvalue zero of the fermionic mass matrix

$$\mathbf{M}_{\mathrm{F}} = \begin{pmatrix} (\mathbf{M}^{\mu\nu})^{\dot\beta}{}_{\dot\alpha} & (\mathbf{M}^{\mu}{}_{l})^{\dot\beta\alpha} & (\mathbf{M}^{\mu}{}_{(s)})^{\dot\beta\alpha} \\ (\mathbf{M}_{k}{}^{\nu})_{\beta\dot\alpha} & (\mathbf{M}_{kl})_{\beta}{}^{\alpha} & (\mathbf{M}_{k(s)})_{\beta}{}^{\alpha} \\ (\mathbf{M}_{(r)}{}^{\nu})_{\beta\dot\alpha} & (\mathbf{M}_{(r)l})_{\beta}{}^{\alpha} & (\mathbf{M}_{(r)(s)})_{\beta}{}^{\alpha} \end{pmatrix}, \tag{2.146}$$

written in the basis $(\bar\psi_\nu{}^{\dot\alpha}, \chi^l{}_\alpha, \lambda_\alpha{}^{(s)})$. This is in agreement with the identity in Eq. (2.141). The form of the submatrices of $\mathbf{M}_{\mathrm{F}}$ can be read off from Eq. (2.145); they are given by

$$\begin{aligned}
(\mathbf{M}^{\mu\nu})^{\dot\beta}{}_{\dot\alpha} &= +2\big\langle e^{K/2}W\big\rangle(\bar\sigma^{\mu\nu})^{\dot\beta}{}_{\dot\alpha}\,,\\
(\mathbf{M}_{kl})_{\beta}{}^{\alpha} &= +\big\langle e^{K/2}\tilde D_k D_l W\big\rangle\delta^{\alpha}_{\beta}\,,\\
(\mathbf{M}_{(r)(s)})_{\beta}{}^{\alpha} &= -\frac{1}{2}\big\langle g^{\bar i i}e^{K/2}\partial_i f_{(r)(s)}D_{\bar i}\overline{W}\big\rangle\delta^{\alpha}_{\beta}\,,\\
(\mathbf{M}^{\mu}{}_{l})^{\dot\beta\alpha} &= -\frac{i}{\sqrt{2}}\big\langle e^{K/2}D_l W\big\rangle\bar\sigma^{\mu\dot\beta\alpha}\,,\\
(\mathbf{M}_{k}{}^{\nu})_{\beta\dot\alpha} &= +\frac{i}{\sqrt{2}}\big\langle e^{K/2}D_k W\big\rangle\sigma^{\nu}_{\beta\dot\alpha}\,,\\
(\mathbf{M}^{\mu}{}_{(s)})^{\dot\beta\alpha} &= +\frac{1}{2}\big\langle K_i(\mathbf{T}_{(s)}\varphi)^i\big\rangle\bar\sigma^{\mu\dot\beta\alpha}\,,\\
(\mathbf{M}_{(r)}{}^{\nu})_{\beta\dot\alpha} &= -\frac{1}{2}\big\langle K_i(\mathbf{T}_{(r)}\varphi)^i\big\rangle\sigma^{\nu}_{\beta\dot\alpha}\,,\\
(\mathbf{M}_{k(s)})_{\beta}{}^{\alpha} &= +i\sqrt{2}\Big\langle g_{k\bar i}(\bar\varphi\mathbf{T}_{(r)})^{\bar i} - \frac{1}{4}(\mathrm{Re}\, f_{(s)(p)})^{-1}K_i(\mathbf{T}_{(s)}\varphi)^i\partial_k f_{(p)(r)}\Big\rangle\delta^{\alpha}_{\beta}\,,\\
(\mathbf{M}_{(r)l})_{\beta}{}^{\alpha} &= +i\sqrt{2}\Big\langle g_{l\bar i}(\bar\varphi\mathbf{T}_{(r)})^{\bar i} - \frac{1}{4}(\mathrm{Re}\, f_{(s)(p)})^{-1}K_i(\mathbf{T}_{(s)}\varphi)^i\partial_l f_{(p)(r)}\Big\rangle\delta^{\alpha}_{\beta}\,.
\end{aligned} \tag{2.147}$$

From Eq. (2.142) follows, that by performing a supergravity transformation with $\xi = -\zeta$, the contribution of the Goldstino in the chiral fermions and gauginos is removed. The Goldstino is absorbed by the gravitino, where it appears in the term $-2\partial_\nu\bar\zeta^{\dot\alpha} \subset \bar\psi_\nu{}^{\dot\alpha}$. In this particular gauge, the mixing terms between the gravitino and the chiral fermions or the gauginos are not present anymore in the fermionic mass term.

In the realistic scenario, where the scalar potential vanishes in the supersymmetry breaking ground state, the vev $\langle M\rangle$ has a finite value. Thus, the first term in Eq. (2.145), which is the mass term of the gravitino, is non-zero and the corresponding mass $m_{3/2}$ is given by

$$m_{3/2} = e^{\langle K\rangle/2M_{\mathrm{P}}^2}\frac{|\langle W\rangle|}{M_{\mathrm{P}}^2}\,, \tag{2.148}$$

where the correct mass dimension was restored by using powers of the (reduced) Planck mass M_{P}. In addition, the supersymmetry breaking scale $\Lambda_{\not{\mathrm{SUSY}}}$ is defined by

$$\Lambda_{\not{\mathrm{SUSY}}} := \sqrt{m_{3/2}M_{\mathrm{P}}}\,, \tag{2.149}$$

representing the size of the vevs of the auxiliary fields which cause spontaneous supersymmetry breaking.

2.3.3 Planck scale mediated supersymmetry breaking

The idea of Planck scale mediated supersymmetry breaking, also called gravity mediated supersymmetry breaking, is that a supergravity theory consists of a hidden sector, where spontaneous SUSY breaking happens, and an observable sector, which contains all fields relevant for the phenomenology. Moreover, the interactions between the two sectors are suppressed by the (reduced) Planck mass M_{P}. To account for that, it is convenient to write the Kähler potential, the superpotential and the gauge kinetic function in the form

$$K(\varphi_h, \bar{\varphi}_h, \varphi_o, \bar{\varphi}_o) = K_h(\varphi_h, \bar{\varphi}_h) + K_o(\frac{\varphi_h}{M_{\mathrm{P}}}, \frac{\bar{\varphi}_h}{M_{\mathrm{P}}}, \varphi_o, \bar{\varphi}_o)\,, \tag{2.150}$$

$$W(\varphi_h, \varphi_o) = W_h(\varphi_h) + W_o(\frac{\varphi_h}{M_{\mathrm{P}}}, \varphi_o)\,, \tag{2.151}$$

$$f_{(r)(s)}(\varphi_h, \varphi_o) = (f_h)_{(r)(s)}(\varphi_h) + (f_o)_{(r)(s)}(\frac{\varphi_h}{M_{\mathrm{P}}}, \varphi_o)\,, \tag{2.152}$$

where fields in the hidden and observable sector are labelled by a subscript h and o, respectively. It is further assumed that the Yang-Mills gauge group $\mathrm{G} = \mathrm{G}_h \times \mathrm{G}_o$ of the whole theory is a direct product, and that the adjoint indices of $(f_h)_{(r)(s)}$ and $(f_o)_{(r)(s)}$ belong to the gauge group G_h of the hidden sector and to the gauge group G_o of the observable sector, respectively.

In the hidden sector, the typical mass scale, including possible vevs of the scalar fields, is the (reduced) Planck mass M_{P}, except in W_h where the highest power of the Planck mass is assumed to be M_{P}^2. This restriction is necessary, in order that there appear no positive powers of the Planck mass in the observable sector after supersymmetry is spontaneously broken [75, 76]. The vevs $\langle\varphi_h\rangle$ cause spontaneous supersymmetry breaking, such that the gravitino gets a mass $m_{3/2}$ much smaller than M_{P}, as described by the super-Higgs mechanism. The effects of supersymmetry breaking are mediated to the observable sector via the Planck scale suppressed interactions.

If the mass scales in the observable sector are of the order of the gravitino mass or smaller, all interactions between fields from the hidden and the observable sector are suppressed by the ratio $m_{3/2}/M_{\mathrm{P}} \ll 1$ once supersymmetry is spontaneously broken, which means that the two sectors are basically decoupled. In that case, the observable sector is described by a globally supersymmetric theory augmented by supersymmetry breaking interactions. These interactions are soft supersymmetry breaking, if there are only renormalizable terms in K_o, W_o and $(f_o)_{(r)(s)}$ with respect to the fields φ_o and $\bar{\varphi}_o$. All other interactions which involve fields of the observable sector are suppressed by the ratio $m_{3/2}/M_{\mathrm{P}}$, and can be neglected in a good approximation for the phenomenology of the model. This regime is called flat limit, which formally is the limit $M_{\mathrm{P}} \mapsto \infty$ of a supergravity theory, where $m_{3/2}$ is kept fixed. Taking into account the above stated assumptions, the flat limit is calculated for a general hidden and observable sector in the remainder of this section.

In Section 2.3.3.1, preliminary calculations are performed, which are used to determine the globally supersymmetric Lagrangian plus the supersymmetry breaking terms of the observable sector in the flat limit. The result is then presented in Section 2.3.3.2, where the Kähler potential, the superpotential and the gauge kinetic function may contain non-renormalizable terms with respect to the observable sector fields. In addition, the result for the renormalizable case is given in Section 2.3.3.3.

2.3.3.1 Preliminary calculations

In order to perform the subsequent calculations, the correct mass dimension, which is equal to four, of the terms in the general supergravity Lagrangian (see Eq. (2.64)) has to be restored by multiplying with an appropriate power of the (reduced) Planck mass M_{P}. The component fields of the supergravity, chiral and gauge multiplets have mass dimensions according to Eq. (2.19), (2.21) and (2.23), respectively. Furthermore, the mass dimensions of the Kähler potential, the superpotential and the gauge kinetic function are given in Eqs. (2.56)–(2.58). Finally, derivatives with respect to matter scalar fields and with respect to spacetime coordinates have the mass dimensions $[\partial_k] = [\partial_{\bar{k}}] = -1$ and $[\partial_\mu] = +1$, respectively.

It is convenient to distinguish the matter field indices k in the hidden and observable sector by an additional label, namely k_h and k_o, whereas for the adjoint indices (r) of the gauge group this label is omitted for the sake of readability. In order to take account of the mass scales in the hidden and in the observable sector, the dimensionless scalar fields

$$\hat{\varphi}_h^{k_h} := \frac{\varphi_h^{k_h}}{M_{\mathrm{P}}}\,, \qquad\qquad \hat{\varphi}_o^{k_o} := \frac{\varphi_o^{k_o}}{m_o}\,, \tag{2.153}$$

are introduced, where m_o is the biggest mass scale in the observable sector, including possible vevs $\langle\varphi_o\rangle$, which is present with a positive power. It is assumed that this mass scale is of the same order or smaller as the gravitino mass, i.e. $\mathcal{O}(m_o) \leq \mathcal{O}(m_{3/2})$.[11] According to the definition of the dimensionless fields in Eq. (2.153), the derivative with respect to the scalar fields takes the from

$$\frac{\partial}{\partial\varphi_h^{k_h}} = \frac{1}{M_{\mathrm{P}}}\frac{\partial}{\partial\hat{\varphi}_h^{k_h}}\,, \qquad\qquad \frac{\partial}{\partial\varphi_o^{k_o}} = \frac{1}{m_o}\frac{\partial}{\partial\hat{\varphi}_o^{k_o}}\,. \tag{2.154}$$

In terms of the dimensionless fields, the Kähler potential, the superpotential and the gauge kinetic function from Eqs. (2.150)–(2.152) are written as

$$\begin{aligned} K(\varphi_h,\bar{\varphi}_h,\varphi_o,\bar{\varphi}_o) &= K_h(\varphi_h,\bar{\varphi}_h) + K_o(\frac{\varphi_h}{M_{\mathrm{P}}},\frac{\bar{\varphi}_h}{M_{\mathrm{P}}},\varphi_o,\bar{\varphi}_o) \\ &= M_{\mathrm{P}}^2\,\hat{K}_h(\hat{\varphi}_h,\hat{\bar{\varphi}}_h) + m_o^2\,\hat{K}_o(\hat{\varphi}_h,\hat{\bar{\varphi}}_h,\hat{\varphi}_o,\hat{\bar{\varphi}}_o)\,, \end{aligned} \tag{2.155}$$

$$\begin{aligned} W(\varphi_h,\varphi_o) &= W_h(\varphi_h) + W_o(\frac{\varphi_h}{M_{\mathrm{P}}},\varphi_o) \\ &= m_h\,M_{\mathrm{P}}^2\,\hat{W}_h(\hat{\varphi}_h) + m_o^3\,\hat{W}_o(\hat{\varphi}_h,\hat{\varphi}_o)\,, \end{aligned} \tag{2.156}$$

$$\begin{aligned} f_{(r)(s)}(\varphi_h,\varphi_o) &= (f_h)_{(r)(s)}(\varphi_h) + (f_o)_{(r)(s)}(\frac{\varphi_h}{M_{\mathrm{P}}},\varphi_o) \\ &= (\hat{f}_h)_{(r)(s)}(\hat{\varphi}_h) + (\hat{f}_o)_{(r)(s)}(\hat{\varphi}_h,\hat{\varphi}_o)\,, \end{aligned} \tag{2.157}$$

such that the parameters in $\hat{K}_{h/o}$, $\hat{W}_{h/o}$ and $(\hat{f}_{h/o})_{(r)(s)}$, and possible vevs $\langle\hat{\varphi}_h^{k_h}\rangle$ and $\langle\hat{\varphi}_o^{k_o}\rangle$ are of $\mathcal{O}(1)$ or smaller. The mass scale m_h in Eq. (2.156) is introduced to make sure that

[11] There may be much bigger mass scales like the GUT or the Planck scale in the observable sector which are present with a negative power in non-renormalizable operators.

there are no M_{P}^3 terms in W_h, and it is fixed by the value of the gravitino mass as shown below. For later use it is convenient to define the dimensionless quantities

$$\begin{aligned}
\lambda &:= \langle e^{\hat{K}_h/2} \rangle \,, & & \\
\lambda' &:= \langle \hat{W}_h \rangle \,, & \bar{\lambda}' &:= \langle \hat{\overline{W}}_h \rangle \,, \\
\lambda_{k_h} &:= \langle D_{k_h} \hat{W}_h \rangle \,, & \lambda_{\bar{k}_h} &:= \langle D_{\bar{k}_h} \hat{\overline{W}}_h \rangle \,, \\
\lambda'_{k_h} &:= \langle (\hat{K}_h)_{k_h} \rangle \,, & \lambda'_{\bar{k}_h} &:= \langle (\hat{K}_h)_{\bar{k}_h} \rangle \,, \\
\lambda''_{k_h} &:= \langle (\hat{W}_h)_{k_h} \rangle \,, & \lambda''_{\bar{k}_h} &:= \langle (\hat{W}_h)_{\bar{k}_h} \rangle \,, \\
\lambda^{\bar{k}_h k_h} &:= \langle (g_h)^{\bar{k}_h k_h} \rangle \,,
\end{aligned} \tag{2.158}$$

which are naturally of $\mathcal{O}(1)$, and the small parameter

$$\varepsilon := \frac{\tilde{m}_{3/2}}{M_{\mathrm{P}}} \ll 1 \,, \quad \text{with} \quad \tilde{m}_{3/2} := \max(m_{3/2}, m_h, m_o), \tag{2.159}$$

which will be used as an expansion parameter in the following. To determine m_h, the vev of the superpotential is written as

$$|\langle W \rangle| = m_{3/2}\, M_{\mathrm{P}}^2\, e^{-\langle K \rangle / 2 M_{\mathrm{P}}^2} \,, \tag{2.160}$$

using the expression for the gravitino mass from Eq. (2.148). On the other hand, according to Eq. (2.155) and (2.156), $\langle K \rangle$ and $|\langle W \rangle|$ have the form

$$\begin{aligned}
\langle K \rangle &= M_{\mathrm{P}}^2 \langle \hat{K}_h \rangle + m_o^2 \langle \hat{K}_o \rangle \\
&= M_{\mathrm{P}}^2 \left(\langle \hat{K}_h \rangle + \mathcal{O}(\varepsilon^2) \right) ,
\end{aligned} \tag{2.161}$$

$$\begin{aligned}
|\langle W \rangle| &= \left| m_h\, M_{\mathrm{P}}^2 \langle \hat{W}_h \rangle + m_o^3 \langle \hat{W}_o \rangle \right| \\
&= m_h\, M_{\mathrm{P}}^2 \left(|\langle \hat{W}_h \rangle| + \mathcal{O}(\varepsilon^2) \right) .
\end{aligned} \tag{2.162}$$

Plugging Eq. (2.161) and (2.162) in Eq. (2.160) leads to

$$m_h = m_{3/2} \left(\frac{1}{\lambda |\lambda'|} + \mathcal{O}(\varepsilon^2) \right) , \tag{2.163}$$

which shows that $\mathcal{O}(m_h) = \mathcal{O}(m_{3/2})$, if $\mathcal{O}(|\lambda'|) = \mathcal{O}(1)$. In case that $\mathcal{O}(|\lambda'|) < \mathcal{O}(1)$ such that $\mathcal{O}(m_h) > \mathcal{O}(m_{3/2})$, the definition of ε in Eq. (2.159) is still valid because of the big hierarchy between $m_{3/2}$ and M_{P}.

In the following, the general supergravity Lagrangian from Eq. (2.64), where the auxiliary fields are integrated out, is expanded in ε after supersymmetry is spontaneously broken in the hidden sector. In particular, the terms which contain observable sector fields and are not suppressed by ϵ are determined, by using the form of the Kähler potential, superpotential and gauge kinetic function stated in Eqs. (2.155)–(2.157) and the dimensionless quantities from Eq. (2.158).

For most of the terms in the supergravity Lagrangian which include fields of the observable sector it is apparent, whether they are suppressed by ε or not. The ones which are not suppressed by ε are part of a globally supersymmetric Lagrangian. However, there are two exceptions, namely the scalar potential V and the quadratic fermion interaction term $\mathcal{L}_{\mathrm{F}}$, which have to be discussed in more detail. This is done in the following:

- **Scalar potential:**
  The F-term contribution to the scalar potential from (2.130) with the correct mass dimension is given by

$$e^{-1}V_F = e^{K/M_{\rm P}^2}\Big(g^{\bar{k}k}D_k W\, D_{\bar{k}}\overline{W} - 3\frac{W\overline{W}}{M_{\rm P}^2}\Big)\,, \tag{2.164}$$

  where

$$D_k W = \frac{K_k W}{M_{\rm P}^2} + W_k\,, \qquad\qquad D_{\bar{k}}\overline{W} = \frac{K_{\bar{k}}\overline{W}}{M_{\rm P}^2} + \overline{W}_{\bar{k}}\,. \tag{2.165}$$

  In order to figure out which parts of V_F are not suppressed by ε, the expansion of the different constituents with respect to ε is considered. These expansions are given by

$$e^{K/M_{\rm P}^2} = e^{\hat{K}_h + m_o^2/M_{\rm P}^2\,\hat{K}_o} = e^{\hat{K}_h}\Big(1 + \frac{m_o^2}{M_{\rm P}^2}\hat{K}_o + \mathcal{O}(\varepsilon^4)\Big)\,, \tag{2.166}$$

$$\frac{W\overline{W}}{M_{\rm P}^2} = m_h^2\, M_{\rm P}^2\, \hat{W}_h\hat{\overline{W}}_h + m_h\, m_o^3\,\big(\hat{W}_h\hat{\overline{W}}_o + \hat{\overline{W}}_h\hat{W}_o\big) + \tilde{m}_{3/2}^4\,\mathcal{O}(\varepsilon^2)\,, \tag{2.167}$$

  and

$$\begin{aligned}
D_{k_h}W &= m_h\, M_{\rm P}\, D_{k_h}\hat{W}_h + \frac{m_h\, m_o^2}{M_{\rm P}}(\hat{K}_o)_{k_h}\hat{W}_h + \frac{m_o^3}{M_{\rm P}}\big((\hat{K}_h)_{k_h}\hat{W}_o + (\hat{W}_o)_{k_h}\big) \\
&\quad + \tilde{m}_{3/2}^2\,\mathcal{O}(\varepsilon^3)\,, \\
D_{\bar{k}_h}\overline{W} &= m_h\, M_{\rm P}\, D_{\bar{k}_h}\hat{\overline{W}}_h + \frac{m_h\, m_o^2}{M_{\rm P}}(\hat{K}_o)_{\bar{k}_h}\hat{\overline{W}}_h + \frac{m_o^3}{M_{\rm P}}\big((\hat{K}_h)_{\bar{k}_h}\hat{\overline{W}}_o + (\hat{\overline{W}}_o)_{\bar{k}_h}\big) \\
&\quad + \tilde{m}_{3/2}^2\,\mathcal{O}(\varepsilon^3)\,, \\
D_{k_o}W &= m_h\, m_o\,(\hat{K}_o)_{k_o}\hat{W}_h + m_o^2\,(\hat{W}_o)_{k_o} + \tilde{m}_{3/2}^2\,\mathcal{O}(\varepsilon^2)\,, \\
D_{\bar{k}_o}\overline{W} &= m_h\, m_o\,(\hat{K}_o)_{\bar{k}_o}\hat{\overline{W}}_h + m_o^2\,(\hat{\overline{W}}_o)_{\bar{k}_o} + \tilde{m}_{3/2}^2\,\mathcal{O}(\varepsilon^2)\,,
\end{aligned} \tag{2.168}$$

  where $D_{k_h}\hat{W}_h = (\hat{K}_h)_{k_h}\hat{W}_h + (\hat{W}_h)_{k_h}$ and $D_{\bar{k}_h}\hat{\overline{W}}_h = (\hat{K}_h)_{\bar{k}_h}\hat{\overline{W}}_h + (\hat{\overline{W}}_h)_{\bar{k}_h}$. In addition, the Kähler metric has the matrix form

$$g_{k\bar{k}} = \begin{pmatrix} g_{k_h\bar{k}_h} & g_{k_h\bar{k}_o} \\ g_{k_o\bar{k}_h} & g_{k_o\bar{k}_o} \end{pmatrix}, \tag{2.169}$$

  where the submatrices are given by

$$\begin{aligned}
g_{k_h\bar{k}_h} &= (g_h)_{k_h\bar{k}_h} + \frac{m_o^2}{M_{\rm P}^2}(\hat{K}_o)_{k_h\bar{k}_h}\,, \\
g_{k_h\bar{k}_o} &= \frac{m_o}{M_{\rm P}}(\hat{K}_o)_{k_h\bar{k}_o}\,, \\
g_{k_o\bar{k}_h} &= \frac{m_o}{M_{\rm P}}(\hat{K}_o)_{k_o\bar{k}_h}\,, \\
g_{k_o\bar{k}_o} &= (g_o)_{k_o\bar{k}_o}\,,
\end{aligned} \tag{2.170}$$

with $(g_h)_{k_h\bar{k}_h} = (\hat{K}_h)_{k_h\bar{k}_h}$ and $(g_o)_{k_o\bar{k}_o} = (\hat{K}_o)_{k_o\bar{k}_o}$. The expansion with respect to ε of the submatrices of the inverse Kähler metric

$$g^{\bar{k}k} = \begin{pmatrix} g^{\bar{k}_h k_h} & g^{\bar{k}_h k_o} \\ g^{\bar{k}_o k_h} & g^{\bar{k}_o k_o} \end{pmatrix}, \tag{2.171}$$

is then given by

$$\begin{aligned}
g^{\bar{k}_h k_h} &= (g_h)^{\bar{k}_h k_h} + \frac{m_o^2}{M_\mathrm{P}^2}(g_h)^{\bar{k}_h i_h}\Big(- (\hat{K}_o)_{i_h\bar{i}_h} + (\hat{K}_o)_{i_h\bar{j}_o}(g_o)^{\bar{j}_o j_o}(\hat{K}_o)_{j_o\bar{i}_h}\Big)(g_h)^{\bar{i}_h k_h} \\
&\quad + \mathcal{O}(\varepsilon^3)\,, \\
g^{\bar{k}_h k_o} &= -\frac{m_o}{M_\mathrm{P}}(g_h)^{\bar{k}_h i_h}(\hat{K}_o)_{i_h\bar{i}_o}(g_o)^{\bar{i}_o k_o} + \mathcal{O}(\varepsilon^2)\,, \\
g^{\bar{k}_o k_h} &= -\frac{m_o}{M_\mathrm{P}}(g_o)^{\bar{k}_o i_o}(\hat{K}_o)_{i_o\bar{i}_h}(g_h)^{\bar{i}_h k_h} + \mathcal{O}(\varepsilon^2)\,, \\
g^{\bar{k}_o k_o} &= (g_o)^{\bar{k}_o k_o} + \mathcal{O}(\varepsilon^2)\,,
\end{aligned} \tag{2.172}$$

where $(g_h)^{\bar{k}_h k_h}$ and $(g_o)^{\bar{k}_o k_o}$ are the inverses of $(g_h)_{k_h\bar{k}_h}$ and $(g_o)_{k_o\bar{k}_o}$, respectively. Using the expressions from Eqs. (2.166)–(2.168) and (2.172), V_F takes the form

$$\begin{aligned}
e^{-1}V_F = +\;& m_h^2\,(\hat{V}_F)_h\,(M_\mathrm{P}^2 + m_o^2\,\hat{K}_o) \\
+\;& m_h^2\,m_o^2\,e^{\hat{K}_h}(g_h)^{\bar{k}_h k_h}\Big(\hat{W}_h(D_{\bar{k}_h}\overline{\hat{W}}_h)(\hat{K}_o)_{k_h} + \overline{\hat{W}}_h(D_{k_h}\hat{W}_h)(\hat{K}_o)_{\bar{k}_h}\Big) \\
+\;& m_h\,m_o^3\,e^{\hat{K}_h}(g_h)^{\bar{k}_h k_h}\Big((D_{\bar{k}_h}\overline{\hat{W}}_h)\big((\hat{K}_h)_{k_h}\hat{W}_o + (\hat{W}_o)_{k_h}\big) \\
&\qquad + (D_{k_h}\hat{W}_h)\big((\hat{K}_h)_{\bar{k}_h}\overline{\hat{W}}_o + (\overline{\hat{W}}_o)_{\bar{k}_h}\big)\Big) \\
+\;& m_h^2\,m_o^2\,e^{\hat{K}_h}(g_o)^{\bar{k}_o k_o}\,\hat{W}_h\overline{\hat{W}}_h\,(\hat{K}_o)_{k_o}(\hat{K}_o)_{\bar{k}_o} \\
+\;& m_h\,m_o^3\,e^{\hat{K}_h}(g_o)^{\bar{k}_o k_o}\Big(\overline{\hat{W}}_h\,(\hat{K}_o)_{\bar{k}_o}(\hat{W}_o)_{k_o} + \hat{W}_h\,(\hat{K}_o)_{k_o}(\overline{\hat{W}}_o)_{\bar{k}_o}\Big) \\
+\;& m_o^4\,e^{\hat{K}_h}(g_o)^{\bar{k}_o k_o}(\hat{W}_o)_{k_o}(\overline{\hat{W}}_o)_{\bar{k}_o} \\
+\;& m_h^2\,m_o^2\,e^{\hat{K}_h}\Big(\big(g^{\bar{k}_h k_o}\frac{M_\mathrm{P}}{m_o}\big)\,\hat{W}_h(D_{\bar{k}_h}\overline{\hat{W}}_h)(\hat{K}_o)_{k_o} \\
&\qquad + \big(g^{\bar{k}_o k_h}\frac{M_\mathrm{P}}{m_o}\big)\,\overline{\hat{W}}_h(D_{k_h}\hat{W}_h)(\hat{K}_o)_{\bar{k}_o}\Big) \\
+\;& m_h\,m_o^3\,e^{\hat{K}_h}\Big(\big(g^{\bar{k}_h k_o}\frac{M_\mathrm{P}}{m_o}\big)\,(D_{\bar{k}_h}\overline{\hat{W}}_h)(\hat{W}_o)_{k_o} + \big(g^{\bar{k}_o k_h}\frac{M_\mathrm{P}}{m_o}\big)\,(D_{k_h}\hat{W}_h)(\overline{\hat{W}}_o)_{\bar{k}_o}\Big) \\
+\;& m_h^2\,m_o^2\,e^{\hat{K}_h}\big(g_2^{\bar{k}_h k_h}\frac{M_\mathrm{P}^2}{m_o^2}\big)(D_{k_h}\hat{W}_h)(D_{\bar{k}_h}\overline{\hat{W}}_h) \\
-\;& 3\,m_h\,m_o^3\,e^{\hat{K}_h}\Big(\overline{\hat{W}}_h\hat{W}_o + \hat{W}_h\overline{\hat{W}}_o\Big) \\
+\;& \tilde{m}_{3/2}^4\,\mathcal{O}(\varepsilon)\,,
\end{aligned} \tag{2.173}$$

with $g_2^{\bar{k}_h k_h} = g^{\bar{k}_h k_h} - (g_h)^{\bar{k}_h k_h}$ (cf. first line in Eq. (2.172)) and

$$(\hat{V}_F)_h = e^{\hat{K}_h}\big((g_h)^{\bar{k}_h k_h}(D_{k_h}\hat{W}_h)(D_{\bar{k}_h}\overline{\hat{W}}_h) - 3\hat{W}_h\overline{\hat{W}}_h\big)\,. \tag{2.174}$$

According to Eq. (2.173), the F-term contribution to the scalar potential can be written as

$$V_F = (V_F)_h + (V_F)_o^{\text{global}} + (V_F)_{o,1}^{\cancel{\text{SUSY}}} + (V_F)_{o,2}^{\cancel{\text{SUSY}}} + \tilde{m}_{3/2}^4\,\mathcal{O}(\varepsilon)\,, \tag{2.175}$$

where the first term contains only hidden sector fields and the other three terms contain only observable sector fields. In particular, $(V_F)_h$ is the F-term contribution to the scalar potential in the hidden sector. Furthermore, $(V_F)_o^{\text{global}}$ is the F-term contribution to the scalar potential in global supersymmetry in the observable sector

$$e^{-1}(V_F)_o^{\text{global}} = \lambda^2\,(g_o)^{\bar{k}_o k_o}\,(W_o)_{k_o}(\overline{W}_o)_{\bar{k}_o}\,, \tag{2.176}$$

and $(V_F)_{o,1}^{\cancel{\text{SUSY}}}$ and $(V_F)_{o,2}^{\cancel{\text{SUSY}}}$ are additional supersymmetry breaking terms

$$\begin{aligned}
e^{-1}(V_F)_{o,1}^{\cancel{\text{SUSY}}} = {}& +\frac{1}{M_{\text{P}}^2}\,\langle V_F\rangle K_o \\
& + m_{3/2}^2\,\lambda^{\bar{k}_h k_h}\Big(\frac{\lambda_{\bar{k}_n}}{\lambda'}\,M_{\text{P}}\,(K_o)_{k_h} + c.c.\Big) \\
& + m_{3/2}^2\,(g_o)^{\bar{k}_o k_o}\,(K_o)_{k_o}(K_o)_{\bar{k}_o} \\
& - m_{3/2}^2\,\frac{\lambda_{k_h}\,\lambda_{\bar{k}_h}}{|\lambda'|^2}\,\lambda^{\bar{k}_h i_h}\,\lambda^{\bar{i}_h k_h}\Big(M_{\text{P}}^2\,(K_o)_{i_h\bar{i}_h} - M_{\text{P}}^2\,(g_o)^{\bar{j}_o j_o}\,(K_o)_{i_h\bar{j}_o}(K_o)_{j_o\bar{i}_h}\Big) \\
& - m_{3/2}^2\,\lambda^{\bar{i}_h k_h}\Big(\frac{\lambda_{k_h}}{\lambda'}\,M_{\text{P}}\,(g_o)^{\bar{k}_o i_o}\,(K_o)_{i_o\bar{i}_h}(K_o)_{\bar{k}_o} + c.c.\Big)\,,
\end{aligned} \tag{2.177}$$

$$\begin{aligned}
e^{-1}(V_F)_{o,2}^{\cancel{\text{SUSY}}} = {}& +\;\; m_{3/2}\,\lambda\,\lambda^{\bar{k}_h k_h}\frac{\lambda_{\bar{k}_h}}{|\lambda'|}\,\big(\lambda'_{k_h}\,W_o + M_{\text{P}}\,(W_o)_{\bar{k}_h}\big) \\
& +\;\; m_{3/2}\,\lambda\,\frac{\bar{\lambda}'}{|\lambda'|}\,(g_o)^{\bar{k}_o k_o}\,(K_o)_{\bar{k}_o}(W_o)_{k_o} \\
& +\;\; m_{3/2}\,\lambda\,\frac{\lambda_{\bar{k}_h}}{|\lambda'|}\,\lambda^{\bar{k}_h i_h}\,M_{\text{P}}\,(g_o)^{\bar{i}_o k_o}\,(K_o)_{i_h\bar{i}_o}(W_o)_{k_o} \\
& - 3\,m_{3/2}\,\lambda\,\frac{\bar{\lambda}'}{|\lambda'|}\,W_o \\
& + c.c.\,,
\end{aligned} \tag{2.178}$$

using the definitions from Eq. (2.158). All terms in Eqs. (2.176)–(2.178) are evaluated at $\langle\varphi_h\rangle$. Since $0 \geq \langle V_F\rangle \geq -3m_{3/2}^2 M_{\text{P}}^2$ in the realistic scenario where $\langle V\rangle = 0$, the coefficient of the first term of Eq. (2.177) is of $\mathcal{O}(m_{3/2}^2)$ or smaller.

The D-term contribution to the scalar potential from Eq. (2.131) with the correct mass dimension reads

$$e^{-1}V_D = \frac{1}{2}\big(\,\text{Re}\,f_{(r)(s)}\big)^{-1}\Big(K_k(\mathbf{T}_{(r)}\varphi)^k K_{\bar{k}}(\bar{\varphi}\mathbf{T}_{(s)})^{\bar{k}}\Big)\,. \tag{2.179}$$

Since the fields in the hidden and in the observable sector have no common gauge interaction, V_D can be written as

$$V_D = (V_D)_h + (V_D)_o^{\text{global}} + \tilde{m}_{3/2}^4\mathcal{O}(\varepsilon)\,, \tag{2.180}$$

where $(V_D)_h$ and $(V_D)_o^{\text{global}}$ contain only hidden and observable sector fields, respectively. In particular, $(V_D)_h$ is the D-term contribution to the scalar potential in the hidden sector and $(V_D)_o^{\text{global}}$ is the D-term contribution to the scalar potential in global supersymmetry in the observable sector, namely

$$e^{-1}(V_D)_o^{\text{global}} = \frac{1}{2}\big(\operatorname{Re}(f_o)_{(r)(s)}\big)^{-1}\Big((K_o)_{k_o}(\mathbf{T}_{(r)}\varphi_o)^{k_o}(K_o)_{\bar{k}_o}(\bar{\varphi}_o\mathbf{T}_{(s)})^{\bar{k}_o}\Big)\,, \tag{2.181}$$

where all terms are evaluated at $\langle\varphi_h\rangle$. In fact, the D-term contribution to the scalar potential is the same in global and local SUSY.

- **Quadratic fermion interaction term:**
  The quadratic fermion interaction term, which among others contains the fermionic mass term (cf. Eq. (2.145)), is written as

$$\mathcal{L}_{\text{F}} = \mathcal{L}_{\bar{\psi}\bar{\psi}} + \mathcal{L}_{\chi\chi} + \mathcal{L}_{\lambda\lambda} + \mathcal{L}_{\bar{\psi}\chi} + \mathcal{L}_{\bar{\psi}\lambda} + \mathcal{L}_{\chi\lambda} + c.c.\,, \tag{2.182}$$

where the different parts are given by

$$e^{-1}\mathcal{L}_{\bar{\psi}\bar{\psi}} = -e^{K/2M_{\text{P}}^2}\frac{W}{M_{\text{P}}^2}(\bar{\psi}_\mu\bar{\sigma}^{\mu\nu}\bar{\psi}_\nu)\,, \tag{2.183a}$$

$$e^{-1}\mathcal{L}_{\chi\chi} = -\frac{1}{2}e^{K/2M_{\text{P}}^2}\tilde{D}_j D_k W(\chi^j\chi^k)\,, \tag{2.183b}$$

$$e^{-1}\mathcal{L}_{\lambda\lambda} = +\frac{1}{4}g^{\bar{k}k}e^{K/2M_{\text{P}}^2}\partial_k f_{(r)(s)}D_{\bar{k}}\overline{W}(\lambda^{(r)}\lambda^{(s)})\,, \tag{2.183c}$$

$$e^{-1}\mathcal{L}_{\bar{\psi}\chi} = +\frac{i}{\sqrt{2}M_{\text{P}}}e^{K/2M_{\text{P}}^2}D_k W(\bar{\psi}_\mu\bar{\sigma}^\mu\chi^k)\,, \tag{2.183d}$$

$$e^{-1}\mathcal{L}_{\bar{\psi}\lambda} = -\frac{1}{2M_{\text{P}}}K_k(\mathbf{T}_{(r)}\varphi)^k(\bar{\psi}_\mu\bar{\sigma}^\mu\lambda^{(r)})\,, \tag{2.183e}$$

$$e^{-1}\mathcal{L}_{\chi\lambda} = -i\sqrt{2}g_{k\bar{k}}(\bar{\varphi}\mathbf{T}_{(r)})^{\bar{k}}(\chi^k\lambda^{(r)}) + \frac{i}{2\sqrt{2}}(\operatorname{Re}f_{(s)(p)})^{-1}K_j(\mathbf{T}_{(s)}\varphi)^j\partial_k f_{(p)(r)}(\chi^k\lambda^{(r)})\,. \tag{2.183f}$$

First, Eq. (2.183a), (2.183d) and (2.183e) are considered, which take the form

$$\begin{aligned} e^{-1}\mathcal{L}_{\bar{\psi}\bar{\psi}} &= -m_h\, e^{\hat{K}_h/2}\hat{W}_h(\bar{\psi}_\mu\bar{\sigma}^{\mu\nu}\bar{\psi}_\nu) + \tilde{m}_{3/2}\,\mathcal{O}(\varepsilon)\,(\bar{\psi}\bar{\psi}) \\ &= -m_{3/2}\,\frac{\lambda'}{|\lambda'|}\,(\bar{\psi}_\mu\bar{\sigma}^{\mu\nu}\bar{\psi}_\nu) + \tilde{m}_{3/2}\,\mathcal{O}(\varepsilon)\,(\bar{\psi}\bar{\psi})\,, \end{aligned} \tag{2.184}$$

$$\begin{aligned} e^{-1}\mathcal{L}_{\bar{\psi}\chi} &= +m_h\,\frac{i}{\sqrt{2}}e^{\hat{K}_h/2}D_{k_h}\hat{W}_h(\bar{\psi}_\mu\bar{\sigma}^\mu\chi_h^{k_h}) + \tilde{m}_{3/2}\,\mathcal{O}(\varepsilon)\,(\bar{\psi}\chi) \\ &= e^{-1}(\mathcal{L}_{\bar{\psi}\chi})_h + \tilde{m}_{3/2}\,\mathcal{O}(\varepsilon)\,(\bar{\psi}\chi)\,, \end{aligned} \tag{2.185}$$

$$\begin{aligned} e^{-1}\mathcal{L}_{\bar{\psi}\lambda} &= -\frac{1}{2M_{\text{P}}}(K_h)_{k_h}(\mathbf{T}_{(r)}\varphi_h)^{k_h}(\bar{\psi}_\mu\bar{\sigma}^\mu\lambda_h^{(r)}) + \tilde{m}_{3/2}\,\mathcal{O}(\varepsilon)\,(\bar{\psi}\lambda) \\ &= e^{-1}(\mathcal{L}_{\bar{\psi}\lambda})_h + \tilde{m}_{3/2}\,\mathcal{O}(\varepsilon)\,(\bar{\psi}\lambda)\,, \end{aligned} \tag{2.186}$$

where the expressions $(\bar{\psi}\bar{\psi})$, $(\bar{\psi}\chi)$ and $(\bar{\psi}\lambda)$ are written symbolically. Thus, $\mathcal{L}_{\bar{\psi}\bar{\psi}}$, $\mathcal{L}_{\bar{\psi}\chi}$ and $\mathcal{L}_{\bar{\psi}\lambda}$ contain no terms with observable sector fields which are not suppressed by ε. As discussed in Section 2.3.2, the mixing of the gravitino with the chiral fermions and the gauginos in the fermionic mass matrix takes place only via the Goldstino. In case of hidden sector supersymmetry breaking, the Goldstino is contained in $\bar{\psi}_\mu$ and in the hidden sector fields χ_h and λ_h up to terms of $\mathcal{O}(\varepsilon)$, and it can be absorbed by the gravitino using an appropriate supersymmetry transformation. Hence, the mass terms in $\mathcal{L}_{\bar{\psi}\chi}$ and $\mathcal{L}_{\bar{\psi}\lambda}$ vanish.

Next, the quadratic chiral fermion interaction in Eq. (2.183b) is considered. In order to determine which parts are not suppressed by ε, the following expansion is performed:

$$\begin{aligned}\tilde{D}_j D_k W = W_{jk} - \Gamma^i{}_{jk} W_i + \frac{1}{M_{\mathrm{P}}^2}\Big(K_{jk}W + K_j W_k + K_k W_j - \Gamma^i{}_{jk} K_i W\Big) \\ + \frac{1}{M_{\mathrm{P}}^4} K_i K_j W\,.\end{aligned} \tag{2.187}$$

Using the identities from Eq. (2.172), the Christoffel symbols $\Gamma^i{}_{jk} = g^{\bar{i}i} g_{j\bar{i},k}$ are determined:

$$\begin{aligned}\Gamma^{i_h}{}_{j_h k_h} &= \frac{1}{M_{\mathrm{P}}}\left(\hat{\Gamma}^{i_h}{}_{j_h k_h} + \mathcal{O}(\varepsilon^2)\right), \\ \Gamma^{i_h}{}_{j_h k_o} = \Gamma^{i_h}{}_{k_o j_h} &= \frac{1}{M_{\mathrm{P}}}\,\mathcal{O}(\varepsilon)\,, \\ \Gamma^{i_o}{}_{j_h k_h} &= \frac{1}{M_{\mathrm{P}}}\,\mathcal{O}(\varepsilon)\,, \\ \Gamma^{i_h}{}_{j_o k_o} &= \frac{1}{M_{\mathrm{P}}}\left((g_h)^{\bar{i}_h i_h}\,(\hat{K}_o)_{j_o \bar{i}_h k_o} + \big(\frac{M_{\mathrm{P}}}{m_o}\, g^{\bar{i}_o i_h}\big)(\hat{K}_o)_{j_o \bar{i}_o k_o} + \mathcal{O}(\varepsilon)\right), \\ \Gamma^{i_o}{}_{j_h k_o} = \Gamma^{i_o}{}_{k_o j_h} &= \frac{1}{M_{\mathrm{P}}}\left((g_o)^{\bar{i}_o i_o}\,(\hat{K}_o)_{j_h \bar{i}_o k_o} + \mathcal{O}(\varepsilon^2)\right), \\ \Gamma^{i_o}{}_{j_o k_o} &= \frac{1}{m_o}\left(\hat{\Gamma}^{i_o}{}_{j_o k_o} + \mathcal{O}(\varepsilon^2)\right),\end{aligned} \tag{2.188}$$

with

$$\begin{aligned}\hat{\Gamma}^{i_h}{}_{j_h k_h} &= (g_h)^{\bar{i}_h i_h}\,(\hat{K}_h)_{j_h \bar{i}_h k_h}\,, \\ \hat{\Gamma}^{i_o}{}_{j_o k_o} &= (g_o)^{\bar{i}_o i_o}\,(\hat{K}_o)_{j_o \bar{i}_o k_o}\,.\end{aligned} \tag{2.189}$$

Thus, Eq. (2.187) takes the form

$$\begin{aligned}\tilde{D}_{j_h} D_{k_h} W &= m_h\,\tilde{D}_{j_h} D_{k_h} \hat{W}_h + \tilde{m}_{3/2}\,\mathcal{O}(\varepsilon)\,, \\ \tilde{D}_{j_h} D_{k_o} W = \tilde{D}_{k_o} D_{j_h} W &= \tilde{m}_{3/2}\,\mathcal{O}(\varepsilon)\,, \\ \tilde{D}_{j_o} D_{k_o} W &= m_o\left((\hat{W}_o)_{j_o k_o} - \hat{\Gamma}^{i_o}{}_{j_o k_o}(\hat{W}_o)_{i_o}\right) - m_h\, M_{\mathrm{P}}\,\Gamma^{i_h}{}_{j_o k_o}(\hat{W}_h)_{i_h} \\ &\quad + m_h\Big((\hat{K}_o)_{j_o k_o} - \hat{\Gamma}^{i_o}{}_{j_o k_o}(\hat{K}_o)_{i_o}\Big)\hat{W}_h + \tilde{m}_{3/2}\,\mathcal{O}(\varepsilon)\,,\end{aligned} \tag{2.190}$$

where

$$\begin{aligned}\tilde{D}_{j_h} D_{k_h} \hat{W}_h = {} & (\hat{W}_h)_{j_h k_h} - \hat{\Gamma}^{i_h}{}_{j_h k_h} \hat{W}_{i_h} + (\hat{K}_h)_{j_h k_h} \hat{W}_h + (\hat{K}_h)_{j_h} (\hat{W}_h)_{k_h} + (\hat{K}_h)_{k_h} (\hat{W}_h)_{j_h} \\ & - \hat{\Gamma}^{i_h}{}_{j_h k_h} (\hat{K}_h)_{i_h} \hat{W}_h + (\hat{K}_h)_{i_h} (\hat{K}_h)_{j_h} \hat{W}_h \,,\end{aligned} \tag{2.191}$$

and $\mathcal{L}_{\chi\chi}$ is then given by

$$\begin{aligned} e^{-1} \mathcal{L}_{\chi\chi} = {} & -\frac{1}{2}\, m_h\, e^{(\hat{K}_h)/2}\, (\tilde{D}_{j_h} D_{k_h} \hat{W}_h)(\chi_h^{j_h} \chi_h^{k_h}) \\ & - \frac{1}{2}\, m_o\, e^{(\hat{K}_h)/2} \Big((\hat{W}_o)_{j_o k_o} - \hat{\Gamma}^{i_o}{}_{j_o k_o} (\hat{W}_o)_{i_o} \Big) (\chi_o^{j_o} \chi_o^{k_o}) \\ & - \frac{1}{2}\, m_h\, e^{(\hat{K}_h)/2}\, \hat{W}_h \Big((\hat{K}_o)_{j_o k_o} - \hat{\Gamma}^{i_o}{}_{j_o k_o} (\hat{K}_o)_{i_o} \Big) (\chi_o^{j_o} \chi_o^{k_o}) \\ & + \frac{1}{2}\, m_h\, e^{(\hat{K}_h)/2}\, M_{\rm P}\, \Gamma^{i_h}{}_{j_o k_o} (\hat{W}_h)_{i_h}\, (\chi_o^{j_o} \chi_o^{k_o}) \\ & + \tilde{m}_{3/2}\, \mathcal{O}(\varepsilon)\, (\chi\chi)\,. \end{aligned} \tag{2.192}$$

According to Eq. (2.192), the quadratic chiral fermion interaction can be written as

$$\mathcal{L}_{\chi\chi} = (\mathcal{L}_{\chi\chi})_h + (\mathcal{L}_{\chi\chi})_o^{\rm global} + (\mathcal{L}_{\chi\chi})_o^{\not{\rm SUSY}} + \tilde{m}_{3/2}\, \mathcal{O}(\varepsilon)\, (\chi\chi)\,, \tag{2.193}$$

where the first term contains only hidden sector fields and the other two terms contain only observable sector fields. In particular, $(\mathcal{L}_{\chi\chi})_h$ is the quadratic chiral fermion interaction in the hidden sector. Furthermore, $(\mathcal{L}_{\chi\chi})_o^{\rm global}$ is the quadratic chiral fermion interaction in global supersymmetry in the observable sector

$$e^{-1} (\mathcal{L}_{\chi\chi})_o^{\rm global} = -\frac{1}{2}\, \lambda \Big((W_o)_{j_o k_o} - \Gamma^{i_o}{}_{j_o k_o} (W_o)_{i_o} \Big) (\chi_o^{j_o} \chi_o^{k_o})\,, \tag{2.194}$$

and $(\mathcal{L}_{\chi\chi})_o^{\not{\rm SUSY}}$ contains additional supersymmetry breaking terms

$$\begin{aligned} e^{-1} (\mathcal{L}_{\chi\chi})_o^{\not{\rm SUSY}} = {} & -\frac{1}{2}\, m_{3/2}\, \frac{\lambda'}{|\lambda'|} \Big((K_o)_{j_o k_o} - \Gamma^{i_o}{}_{j_o k_o} (K_o)_{i_o} \Big) (\chi_o^{j_o} \chi_o^{k_o}) \\ & + \frac{1}{2}\, m_{3/2}\, \frac{\lambda''_{i_h}}{|\lambda'|}\, M_{\rm P}\, \Gamma^{i_h}{}_{j_o k_o} (\chi_o^{j_o} \chi_o^{k_o})\,. \end{aligned} \tag{2.195}$$

All terms in Eq. (2.194) and (2.195) are evaluated at $\langle \varphi_h \rangle$.

The quadratic gaugino interaction in Eq. (2.183c) contains the derivative of the gauge kinetic function with respect to the scalar fields, which is given by

$$\begin{aligned} \partial_{k_h} f_{(r)(s)} &= \frac{1}{M_{\rm P}}\, \partial_{k_h} (\hat{f}_h)_{(r)(s)} + \frac{1}{M_{\rm P}}\, \partial_{k_h} (\hat{f}_o)_{(r)(s)}\,, \\ \partial_{k_o} f_{(r)(s)} &= \frac{1}{m_o}\, \partial_{k_o} (\hat{f}_o)_{(r)(s)}\,. \end{aligned} \tag{2.196}$$

In addition, using the identities from Eq. (2.168) and (2.172), $\mathcal{L}_{\lambda\lambda}$ takes the form

$$\begin{aligned} e^{-1}\mathcal{L}_{\lambda\lambda} = &+\frac{1}{4}\, m_h\, e^{(\hat{K}_h)/2}\, (g_h)^{\bar{k}_h k_h}\, \partial_{k_h}(\hat{f}_h)_{(r)(s)}\, (D_{\bar{k}_h}\hat{\overline{W}}_h)(\lambda_h^{(r)}\lambda_h^{(s)}) \\ &+\frac{1}{4}\, m_h\, e^{(\hat{K}_h)/2}\, (g_h)^{\bar{k}_h k_h}\, \partial_{k_h}(\hat{f}_o)_{(r)(s)}\, (D_{\bar{k}_h}\hat{\overline{W}}_h)(\lambda_o^{(r)}\lambda_o^{(s)}) \\ &+\frac{1}{4}\, m_h\, e^{(\hat{K}_h)/2}\, (g_o)^{\bar{k}_o k_o}\, \partial_{k_o}(\hat{f}_o)_{(r)(s)}\, \hat{\overline{W}}_h(\hat{K}_o)_{\bar{k}_o}\, (\lambda_o^{(r)}\lambda_o^{(s)}) \\ &+\frac{1}{4}\, m_o\, e^{(\hat{K}_h)/2}\, (g_o)^{\bar{k}_o k_o}\, \partial_{k_o}(\hat{f}_o)_{(r)(s)}\, (\hat{\overline{W}}_o)_{\bar{k}_o}\, (\lambda_o^{(r)}\lambda_o^{(s)}) \\ &+\frac{1}{4}\, m_h\, e^{(\hat{K}_h)/2}\, \Big(g^{\bar{k}_h k_o}\, \frac{M_{\mathrm{P}}}{m_o}\Big)\, \partial_{k_o}(\hat{f}_o)_{(r)(s)}\, (D_{\bar{k}_h}\hat{\overline{W}}_h)(\lambda_o^{(r)}\lambda_o^{(s)}) \\ &+ m_h\, \mathcal{O}(\varepsilon)\, (\lambda\lambda)\,, \end{aligned} \tag{2.197}$$

which can also be written as

$$\mathcal{L}_{\lambda\lambda} = (\mathcal{L}_{\lambda\lambda})_h + (\mathcal{L}_{\lambda\lambda})_o^{\mathrm{global}} + (\mathcal{L}_{\lambda\lambda})_o^{\cancel{\mathrm{SUSY}}} + \tilde{m}_{3/2}\, \mathcal{O}(\varepsilon)\, (\lambda\lambda)\,. \tag{2.198}$$

The first term $(\mathcal{L}_{\lambda\lambda})_h$ is the quadratic gaugino interaction in the hidden sector. Moreover, $(\mathcal{L}_{\lambda\lambda})_o^{\mathrm{global}}$ is the quadratic gaugino interaction in global supersymmetry in the observable sector

$$e^{-1}(\mathcal{L}_{\lambda\lambda})_o^{\mathrm{global}} = +\frac{1}{4}\lambda\, (g_o)^{\bar{k}_o k_o}\, (\overline{W}_o)_{\bar{k}_o}\, \partial_{k_o}(f_o)_{(r)(s)}(\lambda_o^{(r)}\lambda_o^{(s)})\,, \tag{2.199}$$

and $(\mathcal{L}_{\lambda\lambda})_o^{\cancel{\mathrm{SUSY}}}$ contains additional supersymmetry breaking terms

$$\begin{aligned} e^{-1}(\mathcal{L}_{\lambda\lambda})_o^{\cancel{\mathrm{SUSY}}} = &+\frac{1}{4}\, m_{3/2}\, \frac{\lambda_{\bar{k}_h}}{|\lambda'|}\, \lambda^{\bar{k}_h k_h}\, M_{\mathrm{P}}\, \partial_{k_h}(f_o)_{(r)(s)}(\lambda_o^{(r)}\lambda_o^{(s)}) \\ &+\frac{1}{4}\, m_{3/2}\, \frac{\bar{\lambda}'}{|\lambda'|}\, (g_o)^{\bar{k}_o k_o}\, (K_o)_{\bar{k}_o}\, \partial_{k_o}(f_o)_{(r)(s)}(\lambda_o^{(r)}\lambda_o^{(s)}) \\ &-\frac{1}{4}\, m_{3/2}\, \frac{\lambda_{\bar{k}_h}}{|\lambda'|}\, \lambda^{\bar{k}_h i_h}\, M_{\mathrm{P}}\, (g_o)^{\bar{i}_o k_o}\, (K_o)_{i_h \bar{i}_o}\, \partial_{k_o}(f_o)_{(r)(s)}(\lambda_o^{(r)}\lambda_o^{(s)})\,. \end{aligned} \tag{2.200}$$

All terms in Eq. (2.199) and (2.200) are evaluated at $\langle\varphi_h\rangle$.

Finally, Eq. (2.183f) can be written as

$$\mathcal{L}_{\chi\lambda} = (\mathcal{L}_{\chi\lambda})_h + (\mathcal{L}_{\chi\lambda})_o^{\mathrm{global}} + \tilde{m}_{3/2}\, \mathcal{O}(\varepsilon)\, (\chi\lambda)\,, \tag{2.201}$$

where $(\mathcal{L}_{\chi\lambda})_h$ represents the quadratic chiral fermion-gaugino interaction term in the hidden sector, and $(\mathcal{L}_{\chi\lambda})_o^{\mathrm{global}}$ is the corresponding term in global supersymmetry in the observable sector, namely

$$\begin{aligned} e^{-1}(\mathcal{L}_{\chi\lambda})_o^{\mathrm{global}} = &-i\sqrt{2}(g_o)_{k_o\bar{k}_o}(\bar{\varphi}_o \mathbf{T}_{(r)})^{\bar{k}_o}(\chi_o^{k_o}\lambda_o^{(r)}) \\ &+\frac{i}{2\sqrt{2}}(\mathrm{Re}(f_o)_{(s)(p)})^{-1}(K_o)_{j_o}(\mathbf{T}_{(s)}\varphi_o)^{j_o}\partial_{k_o}(f_o)_{(p)(r)}(\chi_o^{k_o}\lambda_o^{(r)})\,, \end{aligned} \tag{2.202}$$

which has the same form as in local supersymmetry. The terms in Eq. (2.202) are evaluated at $\langle\varphi_h\rangle$.

2.3.3.2 Flat limit for a general observable sector

In Section 2.3.3.1, preliminary calculations have been performed in order to determine the terms in the supergravity Lagrangian which contain fields of the observable sector and survive in the flat limit, i.e. they are not suppressed by a factor of $\mathcal{O}(m_{3/2}/M_{\mathrm{P}})$. It turned out, that these terms are described by a globally supersymmetric Lagrangian plus additional supersymmetry breaking terms

$$\mathcal{L}_o = \mathcal{L}_o^{\text{global}} + (\mathcal{L}_\varphi)_{o,1}^{\not{\text{SUSY}}} + (\mathcal{L}_\varphi)_{o,2}^{\not{\text{SUSY}}} + (\mathcal{L}_{\chi\chi})_o^{\not{\text{SUSY}}} + (\mathcal{L}_{\lambda\lambda})_o^{\not{\text{SUSY}}} + \tilde{m}_{3/2}^4\,\mathcal{O}(\varepsilon)\,, \tag{2.203}$$

where $\tilde{m}_{3/2}$ and ε are defined in Eq. (2.159). For the sake of readability, in the following the label o is omitted, namely $K \equiv K_o$, $W \equiv W_o$, $f_{(r)(s)} \equiv (f_o)_{(r)(s)}$, $\varphi \equiv \varphi_o$, $\chi \equiv \chi_o$, $A \equiv A_o$, $\lambda \equiv \lambda_o$ and $k \equiv k_o$, whereas the label h is restored. Furthermore, the dimensionless quantities from Eq. (2.158) are used. In particular, λ is absorbed into the superpotential W, and all subsequent terms are evaluated at $\langle\varphi_h\rangle$. The (on-shell) globally supersymmetric Lagrangian has the standard form

$$\begin{aligned}
e^{-1}\mathcal{L}_o^{\text{global}} = {} & -g_{k\bar{k}}\,g^{\mu\nu}\mathcal{D}_\mu\varphi^k\mathcal{D}_\nu\bar{\varphi}^{\bar{k}} - \frac{i}{2}g_{k\bar{k}}(\chi^k\sigma^\mu\mathcal{D}_\mu\bar{\chi}^{\bar{k}} + \bar{\chi}^{\bar{k}}\bar{\sigma}^\mu\mathcal{D}_\mu\chi^k) \\
& - \frac{1}{4}\,\mathrm{Re}\,f_{(r)(s)}F^{\mu\nu(r)}F_{\mu\nu}{}^{(s)} + \frac{1}{8}\,\mathrm{Im}\,f_{(r)(s)}\epsilon_{\mu\nu\rho\tau}F^{\mu\nu(r)}F^{\rho\tau(s)} \\
& - \frac{i}{2}\Big(f_{(r)(s)}\lambda^{(r)}\sigma^\mu\mathcal{D}_\mu\bar{\lambda}^{(s)} + \bar{f}_{(r)(s)}\bar{\lambda}^{(r)}\bar{\sigma}^\mu\mathcal{D}_\mu\lambda^{(s)}\Big) \\
& + g^{\bar{k}k}\,W_k\overline{W}_{\bar{k}} - \frac{1}{2}\tilde{\partial}_j\partial_k W(\chi^j\chi^k) - \frac{1}{2}\tilde{\partial}_{\bar{j}}\partial_{\bar{k}}\overline{W}(\bar{\chi}^{\bar{j}}\bar{\chi}^{\bar{k}}) \\
& + \frac{1}{4}R_{k\bar{k}j\bar{j}}(\chi^k\chi^j)(\bar{\chi}^{\bar{k}}\bar{\chi}^{\bar{j}}) \\
& - i\sqrt{2}g_{k\bar{k}}(\chi^k\lambda^{(r)})(\bar{\varphi}\mathbf{T}_{(r)})^{\bar{k}} + i\sqrt{2}g_{k\bar{k}}(\bar{\chi}^{\bar{k}}\bar{\lambda}^{(r)})(\mathbf{T}_{(r)}\varphi)^k \\
& - \frac{1}{2\sqrt{2}}\Big(\partial_k f_{(r)(s)}(\chi^k\sigma^{\mu\nu}\lambda^{(r)}) + \partial_{\bar{k}}\bar{f}_{(r)(s)}(\bar{\chi}^{\bar{k}}\bar{\sigma}^{\mu\nu}\bar{\lambda}^{(r)})\Big)F_{\mu\nu}{}^{(s)} \\
& + \frac{1}{8}\tilde{\partial}_j\partial_k f_{(r)(s)}(\chi^j\chi^k)(\lambda^{(r)}\lambda^{(s)}) + \frac{1}{8}\tilde{\partial}_{\bar{j}}\partial_{\bar{k}}\bar{f}_{(r)(s)}(\bar{\chi}^{\bar{j}}\bar{\chi}^{\bar{k}})(\bar{\lambda}^{(r)}\bar{\lambda}^{(s)}) \\
& + \frac{1}{4}g^{\bar{k}k}\partial_k f_{(r)(s)}\overline{W}_{\bar{k}}(\lambda^{(r)}\lambda^{(s)}) + \frac{1}{4}g^{\bar{k}k}\partial_{\bar{k}}\bar{f}_{(r)(s)}W_k(\bar{\lambda}^{(r)}\bar{\lambda}^{(s)}) \\
& - \frac{1}{16}g^{k\bar{k}}\partial_k f_{(r)(s)}\partial_{\bar{k}}\bar{f}_{(p)(q)}(\lambda^{(r)}\lambda^{(s)})(\bar{\lambda}^{(p)}\bar{\lambda}^{(q)}) \\
& - \frac{1}{2}\big(\,\mathrm{Re}\,f_{(r)(s)}\big)^{-1}\Big(K_k(\mathbf{T}_{(r)}\varphi)^k - \frac{i}{2\sqrt{2}}\partial_k f_{(r)(p)}(\chi^k\lambda^{(p)}) + \frac{i}{2\sqrt{2}}\partial_{\bar{k}}\bar{f}_{(r)(p)}(\bar{\chi}^{\bar{k}}\bar{\lambda}^{(p)})\Big) \\
& \qquad \times \Big(K_{\bar{j}}(\bar{\varphi}\mathbf{T}_{(s)})^{\bar{j}} - \frac{i}{2\sqrt{2}}\partial_j f_{(s)(q)}(\chi^j\lambda^{(q)}) + \frac{i}{2\sqrt{2}}\partial_{\bar{j}}\bar{f}_{(s)(q)}(\bar{\chi}^{\bar{j}}\bar{\lambda}^{(q)})\Big)\,,
\end{aligned} \tag{2.204}$$

for a general, potentially non-renormalizable, Kähler potential, superpotential and gauge kinetic function in the observable sector. The covariant derivatives are given by

$$\begin{aligned}
\mathcal{D}_\mu\varphi^k &= \partial_\mu\varphi^k - iA_\mu{}^{(r)}(\mathbf{T}_{(r)}\varphi)^k\,, \\
\mathcal{D}_\mu\bar{\varphi}^{\bar{k}} &= \partial_\mu\bar{\varphi}^{\bar{k}} + iA_\mu{}^{(r)}(\bar{\varphi}\mathbf{T}_{(r)})^{\bar{k}}\,,
\end{aligned} \tag{2.205}$$

$$\begin{aligned}\mathcal{D}_\mu \chi^k{}_\alpha &= \partial_\mu \chi^k{}_\alpha - \omega_{\mu\alpha}{}^\beta \chi^k{}_\beta - iA_\mu{}^{(r)}(\mathbf{T}_{(r)}\chi_\alpha)^k + \Gamma^k{}_{ij}\chi^i{}_\alpha \mathcal{D}_\mu \varphi^j \,, \\ \mathcal{D}_\mu \bar{\chi}^{\bar{k}\dot{\alpha}} &= \partial_\mu \bar{\chi}^{\bar{k}\dot{\alpha}} - \omega_\mu{}^{\dot{\alpha}}{}_{\dot{\beta}} \bar{\chi}^{\bar{k}\dot{\beta}} + iA_\mu{}^{(r)}(\bar{\chi}^{\dot{\alpha}}\mathbf{T}_{(r)})^{\bar{k}} + \Gamma^{\bar{k}}{}_{\bar{i}\bar{j}}\bar{\chi}^{\bar{i}\dot{\alpha}} \mathcal{D}_\mu \bar{\varphi}^{\bar{j}} \,,\end{aligned} \tag{2.206}$$

$$\begin{aligned}\mathcal{D}_\mu \lambda_\alpha{}^{(r)} &= \partial_\mu \lambda_\alpha{}^{(r)} - \omega_{\mu\alpha}{}^\beta \lambda_\beta{}^{(r)} + A_\mu{}^{(p)} c_{(p)(q)}{}^{(r)} \lambda_\alpha{}^{(q)} \,, \\ \mathcal{D}_\mu \bar{\lambda}^{\dot{\alpha}(r)} &= \partial_\mu \bar{\lambda}^{\dot{\alpha}(r)} - \omega_\mu{}^{\dot{\alpha}}{}_{\dot{\beta}} \bar{\lambda}^{\dot{\beta}(r)} + A_\mu{}^{(p)} c_{(p)(q)}{}^{(r)} \bar{\lambda}^{\dot{\alpha}(q)} \,,\end{aligned} \tag{2.207}$$

where the spin connection only contains the graviton

$$\begin{aligned}e_\nu{}^b e_{\rho a} \omega_{\mu b}{}^a = \omega_{\mu\nu\rho} = &+\frac{1}{2}(e_\mu{}^a \partial_\nu e_{\rho a} - e_\rho{}^a \partial_\mu e_{\nu a} - e_\nu{}^a \partial_\rho e_{\mu a}) \\ &- \frac{1}{2}(e_\mu{}^a \partial_\rho e_{\nu a} - e_\nu{}^a \partial_\mu e_{\rho a} - e_\rho{}^a \partial_\nu e_{\mu a}) \,,\end{aligned} \tag{2.208}$$

and it is written in terms of spinor indices by using Eq. (2.70). Furthermore, the supersymmetry breaking terms are given by (cf. Eq. (2.177), (2.178), (2.195) and (2.200))

$$\begin{aligned}e^{-1}(\mathcal{L}_\varphi)_{o,1}^{\cancel{\text{SUSY}}} = &-\frac{1}{M_\text{P}^2}\langle V_F \rangle K \\ &- m_{3/2}^2 \lambda^{\bar{k}_h k_h}\Big(\frac{\lambda_{\bar{k}_n}}{\lambda'} M_\text{P} K_{k_h} + c.c.\Big) \\ &- m_{3/2}^2 g^{\bar{k}k} K_k K_{\bar{k}} \\ &+ m_{3/2}^2 \frac{\lambda_{k_h}\lambda_{\bar{k}_h}}{|\lambda'|^2} \lambda^{\bar{k}_h i_h} \lambda^{\bar{i}_h k_h} \Big(M_\text{P}^2 K_{i_h \bar{i}_h} - M_\text{P}^2 g^{\bar{j}j} K_{i_h \bar{j}} K_{j \bar{i}_h}\Big) \\ &+ m_{3/2}^2 \lambda^{\bar{i}_h k_h}\Big(\frac{\lambda_{k_h}}{\lambda'} M_\text{P} g^{\bar{k}i} K_{i\bar{i}_h} K_{\bar{k}} + c.c.\Big) \,,\end{aligned} \tag{2.209}$$

$$\begin{aligned}e^{-1}(\mathcal{L}_\varphi)_{o,2}^{\cancel{\text{SUSY}}} = &-m_{3/2} \lambda^{\bar{k}_h k_h} \frac{\lambda_{\bar{k}_h}}{|\lambda'|}\left(\lambda'_{k_h} W + M_\text{P} W_{\bar{k}_h}\right) \\ &- m_{3/2} \frac{\bar{\lambda}'}{|\lambda'|} g^{\bar{k}k} K_{\bar{k}} W_k \\ &- m_{3/2} \frac{\lambda_{\bar{k}_h}}{|\lambda'|} \lambda^{\bar{k}_h i_h} M_\text{P} g^{\bar{i}k} K_{i_h \bar{i}} W_k \\ &+ 3\, m_{3/2} \frac{\bar{\lambda}'}{|\lambda'|} W \\ &+ c.c. \,,\end{aligned} \tag{2.210}$$

$$\begin{aligned}e^{-1}(\mathcal{L}_{\chi\chi})_o^{\cancel{\text{SUSY}}} = &-\frac{1}{2} m_{3/2} \frac{\lambda'}{|\lambda'|}\Big(K_{jk} - \Gamma^i{}_{jk} K_i\Big)(\chi^j \chi^k) \\ &+ \frac{1}{2} m_{3/2} \frac{\lambda''_{i_h}}{|\lambda'|} M_\text{P} \Gamma^{i_h}{}_{jk} (\chi^j \chi^k) \\ &+ c.c. \,,\end{aligned} \tag{2.211}$$

$$
\begin{aligned}
e^{-1}(\mathcal{L}_{\lambda\lambda})_o^{\cancel{\text{SUSY}}} = &+\frac{1}{4}\, m_{3/2}\, \frac{\lambda_{\bar{k}_h}}{|\lambda'|}\, \lambda^{\bar{k}_h k_h}\, M_{\mathrm{P}}\, \partial_{k_h} f_{(r)(s)} (\lambda^{(r)}\lambda^{(s)}) \\
&+\frac{1}{4}\, m_{3/2}\, \frac{\bar{\lambda}'}{|\lambda'|}\, g^{\bar{k}k}\, K_{\bar{k}}\, \partial_k f_{(r)(s)} (\lambda^{(r)}\lambda^{(s)}) \\
&-\frac{1}{4}\, m_{3/2}\, \frac{\lambda_{\bar{k}_h}}{|\lambda'|}\, \lambda^{\bar{k}_h i_h}\, M_{\mathrm{P}}\, g^{\bar{i}k}\, K_{i_h \bar{i}}\, \partial_k f_{(r)(s)} (\lambda^{(r)}\lambda^{(s)}) \\
&+ c.c.\,.
\end{aligned}
\tag{2.212}
$$

The vev $\langle V_F \rangle$ is the vacuum expectation value of the F-term contribution to the scalar potential of the whole theory, including the hidden sector. In a realistic scenario, where V vanishes in the ground state, $M_{\mathrm{P}}^{-2}\langle V_F \rangle$ is of $\mathcal{O}(m_{3/2}^2)$ or smaller. Hence, the gravitino mass $m_{3/2}$ determines the mass scale of all supersymmetry breaking terms. Furthermore, in the flat limit the only term in the supergravity Lagrangian which is proportional to M_{P}^2 is the Einstein-Hilbert action $\mathcal{L}_{\mathrm{EH}} = -\frac{1}{2} M_{\mathrm{P}}^2\, e\mathcal{R}$. Thus, the equation of motion of the graviton is decoupled from the matter fields and is solved by the Minkowski metric, which describes flat spacetime. The determinant $e = \det e_\mu{}^a$ is then equal to one and the spin connection $\omega_{\mu b}{}^a$, given in Eq. (2.208), vanishes.

2.3.3.3 Flat limit for a renormalizable observable sector

If the Kähler potential, the superpotential and the gauge kinetic function are renormalizable with respect to the observable sector fields, the terms in Eq. (2.209)–(2.212) correspond to soft supersymmetry breaking terms. In a good approximation this is also valid, if non-renormalizable terms in K, W or $f_{(r)(s)}$ are suppressed by a mass scale which is much bigger than the gravitino mass, e.g. the GUT scale or the Planck scale. Using the same conventions as in Section 2.3.3.2, the Lagrangian of the observable sector is then written as

$$
\mathcal{L}_o = \mathcal{L}_o^{\text{global}} + (\mathcal{L}_\varphi)_{m^2}^{\text{soft}} + (\mathcal{L}_\varphi)_A^{\text{soft}} + (\mathcal{L}_\chi)_m^{\text{soft}} + (\mathcal{L}_\lambda)_m^{\text{soft}} + \tilde{m}_{3/2}^4\, \mathcal{O}(\varepsilon)\,,
\tag{2.213}
$$

where the (on-shell) globally supersymmetric part has the standard form

$$
\begin{aligned}
e^{-1}\mathcal{L}_o^{\text{global}} = &-g_{k\bar{k}}\, g^{\mu\nu} \mathcal{D}_\mu \varphi^k \mathcal{D}_\nu \bar{\varphi}^{\bar{k}} - \frac{i}{2} g_{k\bar{k}} (\chi^k \sigma^\mu \mathcal{D}_\mu \bar{\chi}^{\bar{k}} + \bar{\chi}^{\bar{k}} \bar{\sigma}^\mu \mathcal{D}_\mu \chi^k) \\
&-\frac{1}{4}\, \mathrm{Re}\, f_{(r)(s)} F^{\mu\nu(r)} F_{\mu\nu}{}^{(s)} + \frac{1}{8}\, \mathrm{Im}\, f_{(r)(s)} \epsilon_{\mu\nu\rho\tau} F^{\mu\nu(r)} F^{\rho\tau(s)} \\
&-\frac{i}{2}\Big(f_{(r)(s)} \lambda^{(r)} \sigma^\mu \mathcal{D}_\mu \bar{\lambda}^{(s)} + \bar{f}_{(r)(s)} \bar{\lambda}^{(r)} \bar{\sigma}^\mu \mathcal{D}_\mu \lambda^{(s)} \Big) \\
&+ g^{\bar{k}k}\, W_k \overline{W}_{\bar{k}} - \frac{1}{2} W_{jk} (\chi^j \chi^k) - \frac{1}{2} \overline{W}_{\bar{j}\bar{k}} (\bar{\chi}^{\bar{j}} \bar{\chi}^{\bar{k}}) \\
&- i\sqrt{2} g_{k\bar{k}} (\chi^k \lambda^{(r)}) (\bar{\varphi} \mathbf{T}_{(r)})^{\bar{k}} + i\sqrt{2} g_{k\bar{k}} (\bar{\chi}^{\bar{k}} \bar{\lambda}^{(r)}) (\mathbf{T}_{(r)} \varphi)^k \\
&-\frac{1}{2} \big(\mathrm{Re}\, f_{(r)(s)} \big)^{-1} \Big(K_k (\mathbf{T}_{(r)} \varphi)^k \Big) \Big(K_{\bar{j}} (\bar{\varphi} \mathbf{T}_{(s)})^{\bar{j}} \Big)\,,
\end{aligned}
\tag{2.214}
$$

and the soft supersymmetry breaking part is given by

$$\begin{aligned} e^{-1}(\mathcal{L}_\varphi)^{\text{soft}}_{m^2} = &-\frac{1}{M_{\text{P}}^2}\,\langle V_F\rangle K \\ &- m_{3/2}^2\,\lambda^{\bar{k}_h k_h}\Big(\frac{\lambda_{\bar{k}_n}}{\lambda'}\,M_{\text{P}}\,K_{k_h} + c.c.\Big) \\ &- m_{3/2}^2\,g^{\bar{k}k}\,K_k K_{\bar{k}} \\ &+ m_{3/2}^2\,\frac{\lambda_{k_h}\,\lambda_{\bar{k}_h}}{|\lambda'|^2}\,\lambda^{\bar{k}_h i_h}\,\lambda^{\bar{i}_h k_h}\,\Big(M_{\text{P}}^2\,K_{i_h\bar{i}_h} - M_{\text{P}}^2\,g^{\bar{j}j}\,K_{i_h\bar{j}}K_{j\bar{i}_h}\Big) \\ &+ m_{3/2}^2\,\lambda^{\bar{i}_h k_h}\,\Big(\frac{\lambda_{k_h}}{\lambda'}\,M_{\text{P}}\,g^{\bar{k}i}\,K_{i\bar{i}_h}K_{\bar{k}} + c.c.\Big)\,, \end{aligned} \tag{2.215}$$

$$\begin{aligned} e^{-1}(\mathcal{L}_\varphi)^{\text{soft}}_{A} = &-m_{3/2}\,\lambda^{\bar{k}_h k_h}\frac{\lambda_{\bar{k}_h}}{|\lambda'|}\,\big(\lambda'_{k_h}\,W + M_{\text{P}}\,W_{\bar{k}_h}\big) \\ &- m_{3/2}\,\frac{\bar{\lambda}'}{|\lambda'|}\,g^{\bar{k}k}\,K_{\bar{k}}W_k \\ &- m_{3/2}\,\frac{\lambda_{\bar{k}_h}}{|\lambda'|}\,\lambda^{\bar{k}_h i_h}\,M_{\text{P}}\,g^{\bar{i}k}\,K_{i_h\bar{i}}W_k \\ &+ 3\,m_{3/2}\,\frac{\bar{\lambda}'}{|\lambda'|}\,W \\ &+ c.c.\,, \end{aligned} \tag{2.216}$$

$$\begin{aligned} e^{-1}(\mathcal{L}_\chi)^{\text{soft}}_{m} = &-\frac{1}{2}\,m_{3/2}\,\frac{\lambda'}{|\lambda'|}\,K_{jk}(\chi^j\chi^k) \\ &+ \frac{1}{2}\,m_{3/2}\,\frac{\lambda''_{i_h}}{|\lambda'|}\,\lambda^{\bar{i}_h i_h}\,M_{\text{P}}\,K_{j\bar{i}_h k}(\chi^j\chi^k) \\ &+ c.c.\,, \end{aligned} \tag{2.217}$$

$$\begin{aligned} e^{-1}(\mathcal{L}_\lambda)^{\text{soft}}_{m} = &+\frac{1}{4}\,m_{3/2}\,\frac{\lambda_{\bar{k}_h}}{|\lambda'|}\,\lambda^{\bar{k}_h k_h}\,M_{\text{P}}\,\partial_{k_h} f_{(r)(s)}(\lambda^{(r)}\lambda^{(s)}) \\ &+ c.c.\,. \end{aligned} \tag{2.218}$$

If the Kähler potential contains no terms which are holomorphic or antiholomorphic in the observable sector fields, i.e. $K = f(\varphi_h/M_{\text{P}}, \bar{\varphi}_h/M_{\text{P}})\varphi\bar{\varphi}$ with some real function f, the term $(\mathcal{L}_\chi)^{\text{soft}}_m$ vanishes. In that case, $(\mathcal{L}_\varphi)^{\text{soft}}_{m^2}$ and $(\mathcal{L}_\varphi)^{\text{soft}}_A$ correspond to soft mass terms and soft linear terms, respectively, of the scalar fields. The soft gaugino mass term is contained in $(\mathcal{L}_\lambda)^{\text{soft}}_m$. Finally, Eqs. (2.215)–(2.218) show that the mass scale of the soft supersymmetry breaking terms in the observable sector is determined by the gravitino mass $m_{3/2}$ in scenarios where supersymmetry breaking is mediated via Planck scale suppressed interactions from a hidden sector.

2.4 The minimal supersymmetric Standard Model

The minimal supersymmetric Standard Model [77–79] is the minimal extension of the SM, such that supersymmetry is realized. In particular, the MSSM has the same gauge group (internal symmetry) as the SM, and for each SM fermion and gauge boson there is a corresponding chiral and gauge multiplet, respectively. Furthermore, the MSSM contains two chiral multiplets associated with EW Higgs fields, which are both doublets under $\mathrm{SU}(2)_\mathrm{L}$, but with opposite charges under $\mathrm{U}(1)_\mathrm{Y}$. This is necessary in order that gauge anomalies are cancelled, which includes the condition $\mathrm{tr}(I_3^2\, q_\mathrm{Y}) = 0$ for the (left-handed) Weyl fermions, where I_3 is the third component of the weak isospin and q_Y the weak hypercharge. The condition is fulfilled in the SM, thus the additional Weyl fermions which are present in the supermultiplets associated with the EW Higgs fields have to respect this condition as well, which would not be possible with only one supermultiplet. An overview of the chiral and the gauge multiplets in the MSSM extended by right-handed neutrinos is given in Table 2.1 and 2.2, respectively. The superpartners of the SM particles are also referred to as sparticles. Furthermore, the supermultiplets Q, u^c, d^c, L, ν^c, e^c are often called "fermionic multiplets", because they contain SM fermions, and H_u and H_d are denoted as "Higgs multiplets".

Table 2.1: List of the chiral multiplets which are present in the MSSM extended by right-handed neutrinos (cf. [45]). For a specific supermultiplet, in the first column the names of the scalar and left-handed Weyl spinor component fields are stated and the label of the multiplet is specified. Furthermore, the labels of the component fields are written in the second and third column. In the last column the representation with respect to the SM gauge group is given.

Names/Multiplet		Spin 0	Spin $\frac{1}{2}$	$\mathrm{SU}(3)_\mathrm{C} \times \mathrm{SU}(2)_\mathrm{L} \times \mathrm{U}(1)_\mathrm{Y}$
squarks, quarks (×3 families)	Q	$(\widetilde{u}_L \;\; \widetilde{d}_L)$	$(u_L \;\; d_L)$	$(\mathbf{3},\mathbf{2})(+\frac{1}{6})$
	u^c	$\widetilde{u}_R^*$	$u_R^\dagger$	$(\overline{\mathbf{3}},\mathbf{1})(-\frac{2}{3})$
	d^c	$\widetilde{d}_R^*$	$d_R^\dagger$	$(\overline{\mathbf{3}},\mathbf{1})(+\frac{1}{3})$
sleptons, leptons (×3 families)	L	$(\widetilde{\nu}_L \;\; \widetilde{e}_L)$	$(\nu_L \;\; e_L)$	$(\mathbf{1},\mathbf{2})(-\frac{1}{2})$
	ν^c	$\widetilde{\nu}_R^*$	$\nu_R^\dagger$	$(\mathbf{1},\mathbf{1})(\;\;0)$
	e^c	$\widetilde{e}_R^*$	$e_R^\dagger$	$(\mathbf{1},\mathbf{1})(+1)$
Higgs, higgsinos	H_u	$(H_u^+ \;\; H_u^0)$	$(\widetilde{H}_u^+ \;\; \widetilde{H}_u^0)$	$(\mathbf{1},\mathbf{2})(+\frac{1}{2})$
	H_d	$(H_d^0 \;\; H_d^-)$	$(\widetilde{H}_d^0 \;\; \widetilde{H}_d^-)$	$(\mathbf{1},\mathbf{2})(-\frac{1}{2})$

The superpotential contains only renormalizable terms, namely the Yukawa coupling terms $\mathbf{Y}$, the Majorana mass term of the right-handed neutrinos $\mathbf{M}_R$, and the μ term, which is the supersymmetric version of the mass term of the EW Higgs field in the SM.

Table 2.2: List of the gauge multiplets which are present in the MSSM. For a specific supermultiplet, in the first column the names of the gaugino and gauge boson are stated, and the corresponding labels are written in the second and third column. Moreover, the representation concerning the SM gauge group is given in the last column.

Names	spin $\frac{1}{2}$	spin 1	$\mathrm{SU(3)_C \times SU(2)_L \times U(1)_Y}$
gluinos, gluons	$\widetilde{G}$	G	$(\mathbf{8},\mathbf{1})(0)$
winos, W bosons	$\widetilde{W}$	W	$(\mathbf{1},\mathbf{3})(0)$
bino, B boson	$\widetilde{B}$	B	$(\mathbf{1},\mathbf{1})(0)$

In left-right notation the superpotential reads

$$\begin{aligned} W_{\mathrm{MSSM}} = &-(\mathbf{Y}_u)_{IJ}\; H_u \cdot Q_I^\alpha\, u^c_{J\alpha} + (\mathbf{Y}_d)_{IJ}\, H_d \cdot Q_I^\alpha\, d^c_{J\alpha} \\ &+ (\mathbf{Y}_e)_{IJ}\, H_d \cdot L_I\, e^c_J - (\mathbf{Y}_\nu)_{IJ}\, H_u \cdot L_I\, \nu^c_J + \frac{1}{2}(\mathbf{M}_R)_{IJ}\, \nu^c_I\, \nu^c_J \\ &+ \mu\, H_u \cdot H_d\,, \end{aligned} \tag{2.219}$$

where a (lower) upper index α represents the (anti)fundamental representation of $\mathrm{SU(3)_C}$, and $\Psi \cdot \Phi \equiv \epsilon_{ab}\, \Psi^a\, \Phi^b$ ($\epsilon_{12} = 1$) with the $\mathrm{SU(2)_L}$ indices a, b of the fundamental representation. Moreover, the family indices I, J rum from 1 to 3.

In order to avoid gauge invariant and renormalizable operators in the superpotential which lead to experimentally non-observed baryon number (B) and lepton number (L) violating processes like proton decay, matter parity

$$P_{\mathrm{M}} = (-1)^{3(\mathrm{B}-\mathrm{L})} \tag{2.220}$$

is introduced. The chiral multiplets carry the following baryon and lepton numbers: $\mathrm{B}(Q) = +\frac{1}{3}$, $\mathrm{B}(u^c) = \mathrm{B}(d^c) = -\frac{1}{3}$, $\mathrm{L}(L) = +1$ and $\mathrm{L}(e^c) = \mathrm{L}(\nu^c) = -1$, all other assignments are zero.[12] Thus, in order that operators have a vanishing matter parity, they have to contain an even number of supermultiplets with SM fermions. An equivalent formulation of matter parity at the component field level, which has the properties of an R-symmetry, is R-parity

$$P_{\mathrm{R}} = (-1)^{3(\mathrm{B}-\mathrm{L})+2s}\,, \tag{2.221}$$

where s is the spin of the component field. In a Lorentz invariant operator, fermions always appear in pairs. Hence, the term $(-1)^{2s}$ does not contribute to the overall R-parity of the operator. The definition of R-parity shows that the SM fermions and the scalar Higgs bosons have charge 0 under this symmetry, whereas their superpartners carry charge 1. Thus, if R-parity is indeed realized, the decay product of such a superpartner has to contain an odd number supersymmetric particles, which implies that the lightest

[12] Although the Majorana mass operator of the right-handed neutrinos has $L = -2$, which violates lepton number conservation, this is not in conflict with experimental observations if $\mathbf{M}_R$ is much above the EW scale.

supersymmetric particle is completely stable, and consequently a possible candidate for dark matter if it is uncharged under $\mathrm{U}(1)_{\mathrm{EM}}$.

The Kähler potential is given by $K = \sum_k \varphi^k \bar{\varphi}^{\bar{k}}$, where φ^k runs over all scalar fields of the MSSM, which provides minimal kinetic terms. Furthermore, the gauge kinetic function $f_{(r)(s)} = \delta_{(r)(s)}$ is equal to the Kronecker delta, where $(r), (s)$ are adjoint indices of the SM gauge group.

If the MSSM describes the observable sector of a theory with hidden sector supersymmetry breaking, then, in the flat limit, the corresponding Lagrangian is globally supersymmetric with additional soft supersymmetry breaking terms (cf. Section 2.3.3). The soft supersymmetry breaking terms in the context of the MSSM are given by

$$\begin{aligned}
-\mathcal{L}^{\mathrm{soft}}_{\mathrm{MSSM}} = &-\frac{1}{2}\big[M_3\,\widetilde{G}\,\widetilde{G} + M_2\,\widetilde{W}\,\widetilde{W} + M_1\,\widetilde{B}\,\widetilde{B} + c.c.\big] \\
&+ \Big[-(\mathbf{A}_u)_{IJ}\,H_u\cdot\widetilde{Q}_I\,\widetilde{u}^*_{R_J} + (\mathbf{A}_d)_{IJ}\,H_d\cdot\widetilde{Q}_I\,\widetilde{d}^*_{R_J} \\
&+ (\mathbf{A}_e)_{IJ}\,H_d\cdot\widetilde{L}_I\,\widetilde{e}^*_{R_J} + (\mathbf{A}_\nu)_{IJ}\,H_u\cdot\widetilde{L}_I\,\widetilde{\nu}^*_{R_J} + c.c.\Big] \\
&+ (\mathbf{m}^2_{\widetilde{Q}})_{IJ}\,\widetilde{Q}_I\,\overline{\widetilde{Q}}_J + (\mathbf{m}^2_{\widetilde{u}})_{IJ}\,\widetilde{u}^*_{R_I}\,\overline{\widetilde{u}}^*_{R_J} + (\mathbf{m}^2_{\widetilde{d}})_{IJ}\,\widetilde{d}^*_{R_I}\,\overline{\widetilde{d}}^*_{R_J} \\
&+ (\mathbf{m}^2_{\widetilde{L}})_{IJ}\,\widetilde{L}_I\,\overline{\widetilde{L}}_J + (\mathbf{m}^2_{\widetilde{e}})_{IJ}\,\widetilde{e}^*_{R_I}\,\overline{\widetilde{e}}^*_{R_J} + (\mathbf{m}^2_{\widetilde{\nu}})_{IJ}\,\widetilde{\nu}^*_{R_I}\,\overline{\widetilde{\nu}}^*_{R_J} \\
&+ m^2_{H_u}\,H_u\,\overline{H}_u + m^2_{H_d}\,H_d\,\overline{H}_d + \big[b\,H_u\cdot H_d + c.c.\big]\,,
\end{aligned} \tag{2.222}$$

with the gaugino mass terms M, the scalar squared-mass terms $\mathbf{m}^2$ and m^2, the scalar trilinear terms $\mathbf{A}$, and the scalar bilinear term b. The $\mathrm{SU}(3)_{\mathrm{C}}$ indices are suppressed, and the same convention for the contraction of $\mathrm{SU}(2)_{\mathrm{L}}$ indices is used as in Eq. (2.219). In case of hidden sector supersymmetry breaking, the mass scale of the supersymmetry breaking terms is determined by the mass $m_{3/2}$ of the gravitino. Consequently, at this mass scale the superpartners of the SM particles are integrated out and the MSSM is matched to the SM.

Universal boundary conditions of the soft terms in Eq. (2.222), neglecting the b-term, at an energy scale Λ are referred to as mSUGRA or constrained MSSM (CMSSM) boundary conditions. These boundary conditions are parametrized by a universal gaugino mass $M_{1/2}$, a universal proportionality factor a_0 for the trilinear couplings and a universal scalar mass m_0, namely

$$\begin{aligned}
M_i\big|_\Lambda &= M_{1/2}\,, & i &\in \{1,2,3\}\,, \\
\mathbf{A}_x\big|_\Lambda &= a_0\,\mathbf{Y}_x\,, & x &\in \{u,d,e,\nu\}\,, \\
\mathbf{m}^2_x\big|_\Lambda &= m_0^2\,\mathbb{1}_{3\times3}\,, & x &\in \{\widetilde{Q},\widetilde{u},\widetilde{d},\widetilde{L},\widetilde{e},\widetilde{\nu}\}\,, \\
m^2_{H_x}\big|_\Lambda &= m_0^2\,, & x &\in \{u,d\}\,.
\end{aligned} \tag{2.223}$$

In the MSSM, electroweak symmetry breaking $\mathrm{SU}(2)_{\mathrm{L}}\times\mathrm{U}(1)_{\mathrm{Y}} \to \mathrm{U}(1)_{\mathrm{EM}}$ takes place if the neutral components concerning $\mathrm{U}(1)_{\mathrm{EM}}$ of the scalar fields H_u and H_d acquire non-vanishing vevs, namely

$$\langle H^0_u\rangle = v_u := v\,\sin\beta\,, \qquad\qquad \langle H^0_d\rangle = v_d := v\,\cos\beta\,, \tag{2.224}$$

with $v = 174\,\mathrm{GeV}$ and $\tan\beta = v_u/v_d$, where $0 \le \beta \le \frac{\pi}{2}$. The stationarity condition for

the corresponding local minimum of the scalar potential (at tree-level) then reads

$$\sin(2\beta) = \frac{2b}{m_{H_u}^2 + m_{H_d}^2 + 2|\mu|^2}\,, \tag{2.225}$$

$$M_Z^2 = \frac{m_{H_d}^2 - m_{H_u}^2}{\sqrt{1-\sin^2(2\beta)}} - m_{H_u}^2 - m_{H_d}^2 - 2|\mu|^2\,. \tag{2.226}$$

After the EW symmetry is broken, three real degrees of freedom of H_u and H_d are absorbed into the massive gauge bosons $W^\pm$ and Z^0 by the Higgs mechanism. The remaining five physical degrees of freedom are labelled by h^0, H^0, A^0, H^+ and H^-, where the superscripts indicate the corresponding EM charges. The light Higgs field at 125 GeV is denoted by h^0, while H^0 and A^0 denote heavier neutral scalar fields with even and odd parity P, respectively. The masses of these fields (at tree-level) are given by

$$m_{A^0}^2 = 2|\mu|^2 + m_{H_u}^2 + m_{H_d}^2\,, \tag{2.227}$$

$$m_{h^0}^2 = \frac{1}{2}m_{A^0}^2 + \frac{1}{2}M_Z^2 - \frac{1}{2}\sqrt{(m_{A^0}^2 - M_Z^2)^2 + 4M_Z^2\, m_{A^0}^2\, \sin^2(2\beta)}\,, \tag{2.228}$$

$$m_{H^0}^2 = \frac{1}{2}m_{A^0}^2 + \frac{1}{2}M_Z^2 + \frac{1}{2}\sqrt{(m_{A^0}^2 - M_Z^2)^2 + 4M_Z^2\, m_{A^0}^2\, \sin^2(2\beta)}\,, \tag{2.229}$$

$$m_{H^\pm}^2 = m_{A^0}^2 + M_W^2\,. \tag{2.230}$$

where the expressions for M_W and M_Z are stated in Eq. (1.11).

In the electroweak broken phase of the MSSM, the mass matrices of the squarks and charged sleptons are 6×6-dimensional, whereas the one of the sneutrinos is 3×3-dimensional, assuming no right-handed (s)neutrinos. A suitable basis to write the mass matrices of the squarks and the charged sleptons is given by the so-called super-CKM (SCKM) basis. To get this basis, a rotation at the level of supermultiplet is performed, i.e. the fermions and the sfermions are rotated in the same way, such that the mass matrices of the quarks and the charged leptons are diagonal.

After the EW symmetry is broken, the bino, and the neutral wino and Higgsino states form the so-called neutralinos $\widetilde{\chi}_i^0$. In the basis $(\widetilde{B}, \widetilde{W}^0, \widetilde{H}_d^0, \widetilde{H}_u^0)$ the corresponding mass matrix (at tree-level) is given by (cf. [45])

$$\mathbf{M}_{\widetilde{\chi}^0} = \begin{pmatrix} M_1 & 0 & -\frac{1}{\sqrt{2}}g_1 v_d & \frac{1}{\sqrt{2}}g_1 v_u \\ 0 & M_2 & \frac{1}{\sqrt{2}}g_2 v_d & -\frac{1}{\sqrt{2}}g_2 v_u \\ -\frac{1}{\sqrt{2}}g_1 v_d & \frac{1}{\sqrt{2}}g_2 v_d & 0 & -\mu \\ \frac{1}{\sqrt{2}}g_1 v_u & -\frac{1}{\sqrt{2}}g_2 v_u & -\mu & 0 \end{pmatrix}. \tag{2.231}$$

Furthermore, the charged wino and Higgsino states form the so-called charginos $\widetilde{\chi}_i^\pm$, where the mass matrix (at tree-level) in the basis $(\widetilde{W}^+, \widetilde{H}_u^+, \widetilde{W}^-, \widetilde{H}_d^-)$ has the form

$$\mathbf{M}_{\widetilde{\chi}^\pm} = \begin{pmatrix} 0 & \mathbf{X}^\mathsf{T} \\ \mathbf{X} & 0 \end{pmatrix}, \quad \text{with} \quad \mathbf{X} = \begin{pmatrix} M_2 & g_2 v_u \\ g_2 v_d & \mu \end{pmatrix}. \tag{2.232}$$

CHAPTER 3

Grand Unified Theories

The idea of unification in physics is that two or more apparently distinct phenomena can be traced back to a common, more fundamental principle. For example, in this sense the weak and the electromagnetic force are two different phenomena which are unified in the electroweak theory. The separation occurs because of the spontaneous breaking of the EW symmetry $\mathrm{SU(2)_L} \times \mathrm{U(1)_Y}$ into $\mathrm{U(1)_{EM}}$ by the vev of the EW Higgs field H in the context of the SM. The full gauge group of the SM is given by the reductive Lie group $\mathrm{SU(3)_C} \times \mathrm{SU(2)_L} \times \mathrm{U(1)_Y}$, where for each of the three components there is a different gauge coupling. A Grand Unified Theory [80–82] is a theory where the SM gauge group $\mathrm{G_{321}}$ is embedded into a simple Lie group. The unification of the gauge couplings takes place at the so-called GUT scale M_{GUT}, where the GUT gauge group is spontaneously broken into the SM one by the vev of one or multiple scalar (Higgs) fields. Furthermore, in a Grand Unified Theory the SM fields are embedded into bigger representations of the GUT gauge group. Depending on the GUT gauge group and on the choice of the Higgs representations involved in the GUT operators for the Yukawa couplings, the unification of the fermions leads to a variety of relations between the entries of the Yukawa matrices at the SM level, once the GUT symmetry is spontaneously broken. Typically the entries are related via Clebsch-Gordan (CG) coefficients, or linear combinations of them, which are purely group theoretic quantities.

A hint that the SM is indeed a low energy manifestation of a GUT is given by the running of the three gauge couplings. By solving the renormalization group equations (RGEs), it turns out that g_1, g_2 and g_3 run towards each other above the EW scale. However, they do not meet exactly, which would be necessary in order to unify them in the gauge coupling of the GUT. This shortcoming can be overcome by adding intermediate states, i.e. particles with a mass between the EW and the GUT scale, to the theory, so that the running of the gauge couplings gets modified. A suitable set of such extra particles is provided by the superpartners of the SM fields in the MSSM. If the masses of these fields are located at about $10^3\,\mathrm{GeV}$, the gauge couplings meet at around 10^{16} - $10^{17}\,\mathrm{GeV}$.[1] Thus, supersymmetric GUTs are promising candidates for the unification of the three interactions of the SM.

There are several Lie groups which are suitable for GUT gauge groups. The most common ones are the SU(5) and the SO(10) group. A short review about these two groups is given in Section 3.1 and 3.2.

[1] The matching of the gauge couplings may not be exact because of threshold corrections near the GUT scale.

3.1 The group SU(5)

The group SU(5) is a 24-dimensional simple Lie group of rank 4, with the maximal subgroups

$$\begin{aligned} \mathrm{G}_{321} &\equiv \mathrm{SU}(3)_\mathrm{C} \times \mathrm{SU}(2)_\mathrm{L} \times \mathrm{U}(1)_\mathrm{Y} \subseteq \mathrm{SU}(5)\,, \\ \mathrm{G}_{41} &\equiv \mathrm{SU}(4) \times \mathrm{U}(1) \subseteq \mathrm{SU}(5)\,. \end{aligned} \tag{3.1}$$

In the following, only the maximal subgroup G_{321} is considered. In the fundamental representation the generators of SU(5) are given by Hermitian and traceless matrices, with the convention that the Dynkin index is $\frac{1}{2}$, which corresponds to the usual normalization for SU(N) groups. The four diagonal generators have the form

$$\begin{aligned} \mathbf{T}_1^{\mathrm{diag}} &= \frac{1}{2}\,\mathrm{diag}(1,-1,0,0,0)\,, & \mathbf{T}_2^{\mathrm{diag}} &= \frac{1}{2\sqrt{3}}\,\mathrm{diag}(1,1,-2,0,0)\,, \\ \mathbf{T}_3^{\mathrm{diag}} &= \frac{1}{2}\,\mathrm{diag}(0,0,0,1,-1)\,, & \mathbf{T}_4^{\mathrm{diag}} &= \frac{1}{2\sqrt{15}}\,\mathrm{diag}(-2,-2,-2,3,3)\,. \end{aligned} \tag{3.2}$$

Furthermore, there are ten pairs of raising and lowering operators, which are defined as

$$\mathbf{T}^+_{ij} := \begin{pmatrix} & j & \\ & \vdots & \\ \dots & 1 & \dots \\ & \vdots & \end{pmatrix} i\,, \qquad \mathbf{T}^-_{ij} := (\mathbf{T}^+_{ij})^\mathsf{T} = \begin{pmatrix} & i & \\ & \vdots & \\ \dots & 1 & \dots \\ & \vdots & \end{pmatrix} j\,, \tag{3.3}$$

where $i,j \in \{1,...,5\}$ and $i<j$. The remaining twenty generators are then given by the linear combinations $+\frac{1}{2}\big(\mathbf{T}^+_{ij}+\mathbf{T}^-_{ij}\big)$ and $-\frac{i}{2}\big(\mathbf{T}^+_{ij}-\mathbf{T}^-_{ij}\big)$. The definition of the diagonal generators $\mathbf{T}_1^{\mathrm{diag}}$, $\mathbf{T}_2^{\mathrm{diag}}$ and $\mathbf{T}_3^{\mathrm{diag}}$ indicates, that the 3×3 block with $i,j \in \{1,2,3\}$ represents the $\mathrm{SU}(3)_\mathrm{C}$ subgroup, and the 2×2 block with $i,j \in \{4,5\}$ describes the $\mathrm{SU}(2)_\mathrm{L}$ subgroup. Moreover, the $\mathrm{U}(1)_\mathrm{Y}$ subgroup is generated by $\mathbf{T}_4^{\mathrm{diag}}$.

The components of the 5-dimensional fundamental and the corresponding conjugate representation are written as $\mathbf{5}^i$ and $\overline{\mathbf{5}}_i$, with an upper and a lower index, respectively. The irreducible representations of SU(5) are located in tensor products of the $\mathbf{5}^i$ and $\overline{\mathbf{5}}_i$. The lowest dimensional representations thus have the following index structure:

$$\begin{aligned} &\mathbf{5}^i,\ \overline{\mathbf{5}}_i,\ \mathbf{10}^{[ij]},\ \overline{\mathbf{10}}_{[ij]},\ \mathbf{15}^{(ij)},\ \overline{\mathbf{15}}_{(ij)},\ \mathbf{24}^i{}_j,\ \mathbf{35}^{(ijk)},\ \overline{\mathbf{35}}_{(ijk)},\ \mathbf{40}^{[ij]k},\ \overline{\mathbf{40}}_{[ij]k},\ \mathbf{45}^{[ij]}{}_k,\ \overline{\mathbf{45}}_{[ij]}{}^k, \\ &\mathbf{50}^{[ij][kl]},\ \overline{\mathbf{50}}_{[ij][kl]},\ \mathbf{70}^{(ij)}{}_k,\ \overline{\mathbf{70}}_{(ij)}{}^k,\ \mathbf{70}'^{(ijkl)},\ \overline{\mathbf{70}}'_{(ijkl)},\ \mathbf{75}^{[ij]}{}_{[kl]}, \end{aligned} \tag{3.4}$$

where parentheses indicate symmetrization and square brackets indicate antisymmetrization of the indices. The components of the **24**, **40**, **45**, **50**, **70** and **75**, are projected out

of the tensor products

$$\begin{aligned}
(\mathbf{5}\otimes\overline{\mathbf{5}})^{i}{}_{j} &= (\mathbf{24}\oplus\mathbf{1})^{i}{}_{j}\,,\\
(\mathbf{10}\otimes\mathbf{5})^{[ij]k} &= (\mathbf{40}\oplus\overline{\mathbf{10}})^{[ij]k}\,,\\
(\mathbf{10}\otimes\overline{\mathbf{5}})^{[ij]}{}_{k} &= (\mathbf{45}\oplus\mathbf{5})^{[ij]}{}_{k}\,,\\
(\mathbf{10}\otimes\mathbf{10})^{[ij][kl]} &= (\mathbf{50}\oplus\overline{\mathbf{45}}\oplus\overline{\mathbf{5}})^{[ij][kl]}\,,\\
(\mathbf{15}\otimes\overline{\mathbf{5}})^{(ij)}{}_{k} &= (\mathbf{70}\oplus\mathbf{5})^{(ij)}{}_{k}\,,\\
(\mathbf{10}\otimes\overline{\mathbf{10}})^{[ij]}{}_{[kl]} &= (\mathbf{75}\oplus\mathbf{24}\oplus\mathbf{1})^{[ij]}{}_{[kl]}\,,
\end{aligned} \tag{3.5}$$

by imposing the relations

$$\mathbf{24}^{i}{}_{i}=0\,,\quad \epsilon_{ijklm}\mathbf{40}^{ijk}=0\,,\quad \mathbf{45}^{ij}{}_{j}=0\,,\quad \epsilon_{ijklm}\mathbf{50}^{ijkn}=0\,,\quad \mathbf{70}^{ij}{}_{j}=0\,,\quad \mathbf{75}^{ij}{}_{kj}=0\,, \tag{3.6}$$

where ϵ_{ijklm} is the rank 5 completely antisymmetric Levi-Civita symbol, which is an invariant SU(5) tensor. Similar relations hold true for the corresponding conjugate representations. Invariants concerning SU(5) transformations are formed by contracting lower with upper indices, where the height of an index is changed by complex conjugation.

The decomposition of the $\mathbf{1}$, $\overline{\mathbf{5}}$ and $\mathbf{10}$ into irreducible representations of the maximal subgroup G_{321} is given by [2]

$$\begin{aligned}
\mathbf{1} &= (\mathbf{1},\mathbf{1})(0)\,,\\
\overline{\mathbf{5}} &= (\mathbf{1},\mathbf{2})(-\tfrac{1}{2})\oplus(\overline{\mathbf{3}},\mathbf{1})(+\tfrac{1}{3})\,,\\
\mathbf{10} &= (\mathbf{1},\mathbf{1})(+1)\oplus(\overline{\mathbf{3}},\mathbf{1})(-\tfrac{2}{3})\oplus(\mathbf{3},\mathbf{2})(+\tfrac{1}{6})\,,
\end{aligned} \tag{3.7}$$

which leads to the following embedding of the MSSM supermultiplets: $\nu^c\in\mathbf{1}$, $L,d^c\in\overline{\mathbf{5}}$ and $e^c,u^c,Q\in\mathbf{10}$ (cf. Table 2.1). This implies the general relation $\mathbf{Y}_d\sim\mathbf{Y}_e^{\mathsf{T}}$ between the Yukawa matrices of the down-quark and charged lepton sector at the GUT scale, where the exact form depends on how the Yukawa terms at the SU(5) level are realized, and how GUT symmetry breaking is implemented. In addition, the weak doublets H_u and H_d can be embedded into multiple representations of SU(5), namely $H_u\in\mathbf{5}$, $\mathbf{45}$, $\mathbf{70}$ and $H_d\in\overline{\mathbf{5}}$, $\overline{\mathbf{45}}$, $\overline{\mathbf{70}}$. Finally, the representations $\mathbf{24}$ and $\mathbf{75}$ contain both a singlet $(\mathbf{1},\mathbf{1})(0)$ of G_{321}, thus these two representations are appropriate to implement spontaneous symmetry breaking of SU(5) to the SM gauge group.

3.2 The group SO(10)

The group SO(10) is a 45-dimensional simple Lie group of rank 5, with the maximal subgroups

$$\begin{aligned}
\mathrm{G}_{51} &\equiv \mathrm{SU}(5)\times\mathrm{U}(1)_{\mathrm{X}}\subseteq\mathrm{SO}(10)\,,\\
\mathrm{G}_{422} &\equiv \mathrm{SU}(4)_{\mathrm{C}}\times\mathrm{SU}(2)_{\mathrm{L}}\times\mathrm{SU}(2)_{\mathrm{R}}\subseteq\mathrm{SO}(10)\,,
\end{aligned} \tag{3.8}$$

[2] For a proper SU(5) normalization corresponding to a Dynkin index $\frac{1}{2}$, the $\mathrm{U}(1)_{\mathrm{Y}}$ charges need to be multiplied with the factor $\sqrt{3/5}$.

where G_{422} is the Pati-Salam group. The 45 generators $\mathbf{T}_{pq}$ of SO(10), with antisymmetric indices p and q ($p, q \in \{1, ..., 10\}$), fulfil the commutation relations

$$[\mathbf{T}_{pq}, \mathbf{T}_{rs}] = -\tfrac{i}{\sqrt{2}}(\delta_{pr}\mathbf{T}_{qs} + \delta_{qs}\mathbf{T}_{pr} - \delta_{ps}\mathbf{T}_{qr} - \delta_{qr}\mathbf{T}_{ps})\,, \tag{3.9}$$

which can be realized by the following set of 10×10-dimensional matrices

$$(\mathbf{T}_{pq})_{rs} = \tfrac{i}{\sqrt{2}}(\delta_{pr}\delta_{qs} - \delta_{ps}\delta_{qr})\,. \tag{3.10}$$

The normalization of the generator $\mathbf{T}_{pq}$ complies with a Dynkin index 1, which is the typical normalization for SO(N) groups. This set of generators corresponds to the 10-dimensional fundamental representation of SO(10) in the so-called "real" basis, which has lower indices only. The indices $p, q, r, ...$ are referred to as real fundamental indices, and the components of the representation are written as $\mathbf{10}_p$ in that basis. Since the decomposition of the fundamental representation with respect to the SU(5) subgroup is given by $\mathbf{10} = \mathbf{5} \oplus \overline{\mathbf{5}}$, it is convenient to introduce a "complex" basis, which is adapted to that embedding. The components of the $\mathbf{10}$ in the complex basis are either written with an upper or a lower index i:

$$\mathbf{10}^i : \begin{pmatrix} \mathbf{5} \\ \overline{\mathbf{5}} \end{pmatrix}, \qquad\qquad \mathbf{10}_i : \begin{pmatrix} \overline{\mathbf{5}} \\ \mathbf{5} \end{pmatrix}. \tag{3.11}$$

In the following, the $\mathbf{10}^i$ and $\mathbf{10}_i$ are referred to as complex and anticomplex basis, respectively. Furthermore, the indices $i, j, k, ...$ are called complex or anticomplex fundamental indices, depending on whether they are raised or lowered. The relation between the real and the complex basis of the fundamental representation is the following: the components of the $\mathbf{5}$ in Eq. (3.11) are of the form $\frac{1}{\sqrt{2}}(\mathbf{10}_p + i\,\mathbf{10}_{p+1})$, where p is odd. Moreover, the $\overline{\mathbf{5}}$ contains the same entries, but with i replaced by $-i$. The transition from the real to the complex basis (which has an upper index) is performed by the unitary matrix $P^i{}_p \equiv \mathbf{P}$, where the first five rows, corresponding to the $\mathbf{5}$, have the form $\frac{1}{\sqrt{2}}(0 \;\; ... \;\; 0 \;\; 1 \;\; +i \;\; 0 \;\; ... \;\; 0)$, and the last five rows, corresponding to the $\overline{\mathbf{5}}$, have the same form but with $-i$. The matrix $\mathbf{P}$ then defines all other possible transition matrices between the real and the (anti)complex basis, namely

$$\begin{aligned} &\text{real to complex:} && P^i{}_p \equiv \mathbf{P}\,, \\ &\text{real to anticomplex:} && P_{ip} \equiv \mathbf{P}^*\,, \\ &\text{complex to real:} && P_{pi} \equiv \mathbf{P}^{-1} = \mathbf{P}^\dagger\,, \\ &\text{anticomplex to real:} && P_p{}^i \equiv (\mathbf{P}^*)^{-1} = \mathbf{P}^\mathsf{T}\,. \end{aligned} \tag{3.12}$$

The index notation of the transition matrices is adapted to the heights of the indices in the different bases. For example, the transition from the real to the complex basis is given by $\mathbf{10}^i = P^i{}_p \mathbf{10}_p$, whereas the inverse transformation, from the complex to the real basis, has the form $\mathbf{10}_p = P_{pi}\mathbf{10}^i$. Since the real indices are always lowered, repeated indices of this type are just summed over.

The definitions of the transition matrices in Eq. (3.12) implies the following relations:

$$\begin{aligned} P^i{}_p\, P_{pj} &= \delta^i{}_j\,, & P_{pi}\, P^i{}_q &= \delta_{pq}\,, \\ P_{ip}\, P_p{}^j &= \delta_i{}^j\,, & P_p{}^i\, P_{iq} &= \delta_{pq}\,. \end{aligned} \tag{3.13}$$

In addition, the complex and the anticomplex bases are related by raising or lowering the index i with the following two matrices:

$$\begin{aligned} P^{ij} &= P^i{}_p P_p{}^j \equiv \begin{pmatrix} 0 & \mathbb{1}_{5\times5} \\ \mathbb{1}_{5\times5} & 0 \end{pmatrix}, \\ P_{ij} &= P_{ip} P_{pj} = (P^{ij})^* \equiv \begin{pmatrix} 0 & \mathbb{1}_{5\times5} \\ \mathbb{1}_{5\times5} & 0 \end{pmatrix}. \end{aligned} \tag{3.14}$$

The fundamental representation **10** is self-conjugate, since it is equivalent to its conjugate representation. Furthermore, in the real basis the components $\mathbf{10}_p$ can be chosen real, hence **10** is a real representation, and the components of the **5** and $\overline{\mathbf{5}}$ in the complex basis are related by complex conjugation. However, in supersymmetric theories the complexified version of **10** is used, because the fields are complex. The **10** thus contains ten complex degrees of freedom, and the $\overline{\mathbf{5}}$ is no longer the conjugate of **5**.

The spinor representation in SO(10) is the 16-dimensional irreducible representation **16**. Since the spinor representation is complex, it is not equivalent to the conjugate representation $\overline{\mathbf{16}}$. It is convenient to write the direct sum $\mathbf{16} \oplus \overline{\mathbf{16}}$ as an reducible 32-dimensional representation **32**, which either carries an upper or a lower spinor index $A \in \{1, ..., 32\}$, depending on the particular embedding of the components of the **16** and $\overline{\mathbf{16}}$:

$$\mathbf{32}^A : \begin{pmatrix} \mathbf{16} \\ \overline{\mathbf{16}} \end{pmatrix}, \qquad\qquad \mathbf{32}_A : \begin{pmatrix} -\overline{\mathbf{16}} \\ \mathbf{16} \end{pmatrix}. \tag{3.15}$$

The minus sign in $\mathbf{32}_A$ is introduced, such that the definitions in Eq. (3.15) are consistent with raising and lowering the spinor index by the charge conjugation matrix C, which is defined below.

The basic objects in the construction of the SO(10) generators in the spinor representation are the gamma matrices Γ_p, where p is a real fundamental index. With respect to the basis $\mathbf{32}^A$, the gamma matrices have the spinor index structure $(\Gamma_p)^A{}_B$. Furthermore, the ten matrices Γ_p form an orthogonal basis of a Clifford algebra, which is defined by the following anticommutation relations:

$$\{\Gamma_p, \Gamma_q\} = 2\delta_{pq}\mathbb{1}\,. \tag{3.16}$$

A particular set of gamma matrices, such that the Clifford algebra relations in Eq. (3.16) are fulfilled, can be constructed by means of the Kronecker product of five Pauli matrices σ^a ($a \in \{0, 1, 2, 3\}$) in the following way:

$$\begin{aligned} \Gamma_{2k-1} &:= \sigma^0 \otimes ... \otimes \sigma^0 \otimes \sigma^1 \otimes \sigma^3 \otimes ... \otimes \sigma^3\,, \\ \Gamma_{2k} &:= \underbrace{\sigma^0 \otimes ... \otimes \sigma^0}_{k-1} \otimes \sigma^2 \otimes \underbrace{\sigma^3 \otimes ... \otimes \sigma^3}_{5-k}, \end{aligned} \tag{3.17}$$

where $k = 1, ..., 5$. The explicit construction in Eq. (3.17) implies, that the gamma matrices are Hermitian, i.e. $\Gamma_p = (\Gamma_p)^\dagger$. Furthermore, the matrices $(\Gamma_p)^A{}_B$ have the block structure

$$\Gamma_p = \begin{pmatrix} \square & \blacksquare \\ \blacksquare & \square \end{pmatrix}, \tag{3.18}$$

where each square represents a 16×16-dimensional block. The blocks which are indicated by a white square have all entries equal to zero, which implies an off-diagonal structure of the matrices. Thus, a product of an odd number of gamma matrices has an off-diagonal structure as well, whereas a product of an even number of gamma matrices has a diagonal structure:

$$\text{odd number of } \Gamma_p\text{:} \begin{pmatrix} \square & \blacksquare \\ \blacksquare & \square \end{pmatrix}, \qquad \text{even number of } \Gamma_p\text{:} \begin{pmatrix} \blacksquare & \square \\ \square & \blacksquare \end{pmatrix}. \tag{3.19}$$

The 45 generators in the spinor representation are formed by the commutator of two gamma matrices in each case, namely

$$\mathbf{T}^{\text{spinor}}_{pq} := \tfrac{i}{4\sqrt{2}}[\Gamma_p, \Gamma_q]\,. \tag{3.20}$$

With respect to the basis $\mathbf{32}^A$, the generators a have the index structure $(\mathbf{T}^{\text{spinor}}_{pq})^A{}_B$, and from the construction in Eq. (3.20) follows, that they are Hermitian and have a block diagonal form. The two non-zero blocks on the diagonal correspond to the generators in the irreducible representations **16** and $\overline{\mathbf{16}}$, respectively, which is consistent with the embedding in Eq. (3.15). Moreover, the Clifford algebra relations in Eq. (3.16) imply, that the generators $\mathbf{T}^{\text{spinor}}_{pq}$ fulfil the commutation relations in Eq. (3.9).

The so-called "charge conjugation matrix" C of SO(10) is a 32×32-dimensional matrix, which satisfies the identity

$$C\,\Gamma_p\,C^{-1} = -\Gamma_p^{\mathsf{T}} \tag{3.21}$$

for each of the gamma matrices. Using the fact that the generators in the spinor representation are Hermitian, Eq. (3.21) implies the relation

$$C\,\mathbf{T}^{\text{spinor}}_{pq}\,C^{-1} = -(\mathbf{T}^{\text{spinor}}_{pq})^*\,, \tag{3.22}$$

which means that C is the transition matrix between the 32-dimensional spinor representation and its conjugate representation. Concerning the basis $\mathbf{32}^A$, the charge conjugation matrix has the index structure $C \equiv C_{AB}$, whereas its inverse is written as $C^{-1} \equiv (C_{AB})^{-1} = C^{AB}$. The two matrices have the explicit form

$$C_{AB} \equiv \begin{pmatrix} 0 & -\mathbb{1}_{16\times 16} \\ +\mathbb{1}_{16\times 16} & 0 \end{pmatrix}, \qquad C^{AB} \equiv \begin{pmatrix} 0 & +\mathbb{1}_{16\times 16} \\ -\mathbb{1}_{16\times 16} & 0 \end{pmatrix}, \tag{3.23}$$

and they are used to lower and raise spinor indices, namely

$$\mathbf{32}_A = C_{AB}\,\mathbf{32}^B\,, \quad \mathbf{32}^A = C^{AB}\,\mathbf{32}_B\,. \tag{3.24}$$

This is consistent with the embedding of the **16** and $\overline{\mathbf{16}}$ into $\mathbf{32}^A$ and $\mathbf{32}_A$ in Eq. (3.15).

For the construction of SO(10) invariants, it is often convenient to use a set of gamma matrices Γ_i with an anticomplex index i, instead of the real index p. The conversion of the fundamental index is realised by means of the transition matrix P_{ip} from Eq. (3.12):

$$(\Gamma_i)^A{}_B = P_{ip}\,(\Gamma_p)^A{}_B\,. \tag{3.25}$$

This transformation does not affect the block structure of the gamma matrices in Eq. (3.18). Furthermore, the irreducible representation **16** is typically embedded into the reducible representation $\mathbf{32}^A$ along the lines of Eq. (3.15), by setting the components corresponding to the $\overline{\mathbf{16}}$ equal to zero. Analogously, the $\overline{\mathbf{16}}$ is embedded into the $\mathbf{32}^A$ as well. Hence, in this notation both 16-dimensional representations carry an upper spinor index:

$$\mathbf{16}^A : \begin{pmatrix} \mathbf{16} \\ 0 \end{pmatrix}, \quad \overline{\mathbf{16}}^A : \begin{pmatrix} 0 \\ \overline{\mathbf{16}} \end{pmatrix}. \tag{3.26}$$

All irreducible representations of SO(10) are contained in tensor products of the **10**, **16** and $\overline{\mathbf{16}}$, where the lowest dimensional ones have the following index structure

$$\begin{aligned} &\mathbf{10}^i,\ \mathbf{16}^A,\ \overline{\mathbf{16}}^A,\ \mathbf{45}^{[ij]},\ \mathbf{54}^{(ij)},\ \mathbf{120}^{[ijk]},\ \mathbf{126}^{[ijklm]},\ \overline{\mathbf{126}}^{[ijklm]}, \\ &\mathbf{144}^{Ai},\ \overline{\mathbf{144}}^{Ai},\ \mathbf{210}^{[ijkl]},\ \mathbf{210'}^{(ijk)}. \end{aligned} \tag{3.27}$$

To specify the representations in Eq. (3.27) only upper indices are used, and the parentheses and square brackets indicate symmetrization and antisymmetrization of complex fundamental indices, respectively. These symmetry properties are restored, if real indices are used instead. All the representations which carry a spinor index are complex representations, whereas the ones with fundamental indices only are real, except the **126** and $\overline{\mathbf{126}}$, which are complex as well.

Since the number of components indicated by the index structures and the actual sizes of the **54**, **210′**, **144** and $\overline{\mathbf{144}}$ in Eq. (3.27) do not match, irreducible representations of smaller dimensions have to be projected out of the tensor product in each case:

$$\begin{aligned} (\mathbf{10}\otimes\mathbf{10})^{(ij)} &= (\mathbf{54}\oplus\mathbf{1})^{(ij)}\,, \\ (\mathbf{10}\otimes\mathbf{10}\otimes\mathbf{10})^{(ijk)} &= (\mathbf{210'}\oplus\mathbf{10})^{(ijk)}\,, \\ (\mathbf{16}\otimes\mathbf{10})^{Ai} &= (\mathbf{144}\oplus\overline{\mathbf{16}})^{Ai}\,, \\ (\overline{\mathbf{16}}\otimes\mathbf{10})^{Ai} &= (\overline{\mathbf{144}}\oplus\mathbf{16})^{Ai}\,. \end{aligned} \tag{3.28}$$

This is achieved by imposing the following conditions

$$\mathbf{54}^{ij}\,P_{ij} = 0\,, \qquad \mathbf{210'}^{ijk}\,P_{jk} = 0\,, \qquad \Gamma_i{}^A{}_B\,\mathbf{144}^{Bi} = 0\,, \qquad \Gamma_i{}^A{}_B\,\overline{\mathbf{144}}^{Bi} = 0\,. \tag{3.29}$$

Furthermore, the components of the **126** and $\overline{\mathbf{126}}$ are distinguished by the (anti)self-duality identities using the real basis

$$\mathbf{126}_{[pqrst]} = -\frac{i}{5!}\epsilon_{pqrstvwxyz}\mathbf{126}_{[vwxyz]}\,, \qquad \overline{\mathbf{126}}_{[pqrst]} = +\frac{i}{5!}\epsilon_{pqrstvwxyz}\overline{\mathbf{126}}_{[vwxyz]}\,, \tag{3.30}$$

where $\epsilon_{pqrstvwxyz}$ is the rank 10 completely antisymmetric Levi-Civita symbol, which is an invariant SO(10) tensor.

Invariants concerning SO(10) transformations are formed by summing over indices of the same type. While in the case of spinor or (anti)complex indices, only indices of different heights can be contracted, there is no restriction for real indices, because they are all lowered. A (anti)complex index is raised or lowered by using the matrices P^{ij} and

P_{ij}, given in Eq. (3.14), whereas the height of a spinor index is changed by means of the charge conjugation matrix C_{AB} and its inverse C^{AB}, defined in Eq. (3.23). In addition, a fundamental index is converted into a pair of spinor indices via the gamma matrices.

Irreducible representations with antisymmetric fundamental indices can be written as 32×32-dimensional matrices in spinor space as follows

$$\begin{aligned}
\mathbf{10}^A{}_B &:= \mathbf{10}^i \, (\Gamma_i)^A{}_B \,, \\
\mathbf{45}^A{}_B &:= \mathbf{45}^{[ij]} \, (\Gamma_i \Gamma_j)^A{}_B \,, \\
\mathbf{120}^A{}_B &:= \mathbf{120}^{[ijk]} \, (\Gamma_i \Gamma_j \Gamma_k)^A{}_B \,, \\
\mathbf{210}^A{}_B &:= \mathbf{210}^{[ijkl]} \, (\Gamma_i \Gamma_j \Gamma_k \Gamma_l)^A{}_B \,, \\
\mathbf{126}^A{}_B &:= \mathbf{126}^{[ijklm]} \, (\Gamma_i \Gamma_j \Gamma_k \Gamma_l \Gamma_m)^A{}_B \,, \\
\overline{\mathbf{126}}^A{}_B &:= \overline{\mathbf{126}}^{[ijklm]} \, (\Gamma_i \Gamma_j \Gamma_k \Gamma_l \Gamma_m)^A{}_B \,,
\end{aligned} \tag{3.31}$$

which is not possible for representations with symmetric indices, because of the Clifford algebra relations of the gamma matrices. The defined representations in Eq. (3.31) have block structures according to Eq. (3.19).

The decompositions of the irreducible representations listed in Eq. (3.27) under the maximal subgroup G_{51} are stated in Table 3.1, where in addition the locations of the SM singlets and $\mathrm{SU}(2)_\mathrm{L}$ (anti)doublets are indicated (cf. [83]). The decomposition of the **16** under G_{321}, namely

$$\mathbf{16} = \underbrace{(\mathbf{1},\mathbf{1})(0)}_{\mathbf{1}\text{ of SU(5)}} \oplus \underbrace{(\mathbf{1},\mathbf{2})(-\tfrac{1}{2}) \oplus (\overline{\mathbf{3}},\mathbf{1})(+\tfrac{1}{3})}_{\overline{\mathbf{5}}\text{ of SU(5)}} \oplus \underbrace{(\mathbf{1},\mathbf{1})(+1) \oplus (\overline{\mathbf{3}},\mathbf{1})(-\tfrac{2}{3}) \oplus (\mathbf{3},\mathbf{2})(+\tfrac{1}{6})}_{\mathbf{10}\text{ of SU(5)}} , \tag{3.32}$$

shows, that the SM fermions of one generation, including a right-handed neutrino, can be embedded into the **16** (cf. Table 2.1). This implies the general relation $\mathbf{Y}_u \sim \mathbf{Y}_d \sim \mathbf{Y}_e \sim \mathbf{Y}_\nu$ between the Yukawa matrices of the different fermion sectors at the GUT scale, where the exact form depends on the realization of the Yukawa terms at the SO(10) level and on the implementation of GUT symmetry breaking. Moreover, the embedding of the SM fermions into the **16** provides a natural explanation for the existence of right-handed neutrinos.

Table 3.1: Decomposition of the lowest dimensional irreducible representations of SO(10), neglecting corresponding conjuagte representations, into irreducible representations of the maximal subgroup G_{51}. The $U(1)_X$ charges have to be multiplied by the factor $(2\sqrt{10})^{-1}$, corresponding to a Dynkin index 1. A straight underline denotes that the representation contains one SM singlet, while a wavy underline indicates one $SU(2)_L$ (anti)doublet $(\mathbf{1},\mathbf{2})(\pm\frac{1}{2})$, according to the label $\pm$.

SO(10)	$\supset$	$SU(5)\times U(1)_X$
10	=	$\underset{\sim}{\mathbf{5}}(+2)_+ \oplus \underset{\sim}{\overline{\mathbf{5}}}(-2)_-$
16	=	$\underline{\mathbf{1}}(-5) \oplus \underset{\sim}{\overline{\mathbf{5}}}(+3)_- \oplus \mathbf{10}(-1)$
45	=	$\underline{\mathbf{1}}(0) \oplus \mathbf{10}(+4) \oplus \overline{\mathbf{10}}(-4) \oplus \underline{\mathbf{24}}(0)$
54	=	$\mathbf{15}(+4) \oplus \overline{\mathbf{15}}(-4) \oplus \underline{\mathbf{24}}(0)$
120	=	$\underset{\sim}{\mathbf{5}}(+2)_+ \oplus \underset{\sim}{\overline{\mathbf{5}}}(-2)_- \oplus \mathbf{10}(-6) \oplus \overline{\mathbf{10}}(+6) \oplus \underset{\sim}{\mathbf{45}}(+2)_+ \oplus \underset{\sim}{\overline{\mathbf{45}}}(-2)_-$
126	=	$\underline{\mathbf{1}}(-10) \oplus \underset{\sim}{\overline{\mathbf{5}}}(-2)_- \oplus \mathbf{10}(-6) \oplus \overline{\mathbf{15}}(+6) \oplus \underset{\sim}{\mathbf{45}}(+2)_+ \oplus \overline{\mathbf{50}}(-2)$
144	=	$\underset{\sim}{\mathbf{5}}(-3)_+ \oplus \underset{\sim}{\overline{\mathbf{5}}}(-7)_- \oplus \overline{\mathbf{10}}(+1) \oplus \overline{\mathbf{15}}(+1) \oplus \underline{\mathbf{24}}(+5) \oplus \overline{\mathbf{40}}(+1) \oplus \underset{\sim}{\mathbf{45}}(-3)_+$
210	=	$\underline{\mathbf{1}}(0) \oplus \underset{\sim}{\mathbf{5}}(-8)_+ \oplus \underset{\sim}{\overline{\mathbf{5}}}(+8)_- \oplus \mathbf{10}(+4) \oplus \overline{\mathbf{10}}(-4) \oplus \underline{\mathbf{24}}(0) \oplus \mathbf{40}(-4) \oplus \overline{\mathbf{40}}(+4) \oplus \underline{\mathbf{75}}(0)$
210′	=	$\mathbf{35}(-6) \oplus \overline{\mathbf{35}}(+6) \oplus \underset{\sim}{\mathbf{70}}(+2)_+ \oplus \underset{\sim}{\overline{\mathbf{70}}}(-2)_-$

3.3 Doublet-triplet splitting and the MSSM Higgs location

In Grand Unified Theories, $SU(2)_L$ doublets $(\mathbf{1},\mathbf{2})(+\frac{1}{2})$ and antidoublets $(\mathbf{1},\mathbf{2})(-\frac{1}{2})$ are typically embedded into GUT representations, which at the same time also contain color triplets $(\mathbf{3},\mathbf{1})(-\frac{1}{3})$ and antitriplets $(\overline{\mathbf{3}},\mathbf{1})(+\frac{1}{3})$, as for example the $\mathbf{5}$ and $\overline{\mathbf{5}}$ of SU(5) or the $\mathbf{10}$ of SO(10). In general, there may be multiple doublet-antidoublet pairs in a GUT model. The corresponding masses are typically of the order M_{GUT}, however there is one light pair of mass eigenstates which corresponds to the EW doublets, namely to the H_u and H_d of the MSSM. On the other hand, in supersymmetric theories the (anti)triplets mediate dimension 5 proton decay, thus all of these states must be heavy in order that the predictions for proton decay of a GUT model are compatible with the experimental bounds (see Section 3.4). Due to the GUT embedding, the doublet and the triplet mass matrices $\mathbf{M}_D$ and $\mathbf{M}_T$, respectively, are related. Thus, naturally it is expected, that all doublets are heavy as well. The feature, that one doublet-antidoublet pair has a mass at the EW scale, while all other doublet and triplet masses are located at around the GUT scale is referred to as doublet-triplet (DT) splitting.

Possible solutions to the DT splitting problem are given by the (double) missing partner mechanism in SU(5) [84–86] or SO(10) [87, 88], or by the Dimopoulos-Wilczek mechanism in SO(10) [89, 90]. The missing partner mechanism exploits the fact that

certain representations in SU(5) and SO(10) contain more (anti)triplet than (anti)doublet states. In particular, the **50** of SU(5) contains one triplet, but no doublet, while the **126** of SO(10) contains one doublet and one triplet pair, but also an additional antitriplet state. Thus, $\mathbf{M}_D$ and $\mathbf{M}_T$ have different dimensions, which allows to make one doublet light, while keeping all triplets heavy. In the Dimopoulos-Wilczek mechanism, the **45** of SO(10) acquires a specially aligned vev, which breaks GUT symmetry but leaves one of the doublet states massless.

Another possibility to implement DT splitting is given by fine-tuning. Since the rank of a mass matrix indicates whether there is massless state or not, the condition $\det \mathbf{M}_D = 0$ (the MSSM pair of doublets is almost massless compared to the GUT scale), such that at the same time $\det \mathbf{M}_T \neq 0$, satisfies DT splitting. A vanishing determinant of $\mathbf{M}_D$ is achieved by imposing a specific relation on the parameters in the Higgs sector, i.e. by fine-tuning one of the parameters. Doublet-triplet splitting by fine-tuning can typically be imposed in any model.

In a concrete model with the superpotential W of the Higgs sector, the doublet and triplet mass matrices are calculates as

$$(\mathbf{M}_D)_{ij} = \frac{\partial^2 W}{\partial D_i \partial \overline{D}_j}\Big|_{\text{vacuum}}\,, \tag{3.33}$$

$$(\mathbf{M}_T)_{ij} = \frac{\partial^2 W}{\partial T_i \partial \overline{T}_j}\Big|_{\text{vacuum}}\,, \tag{3.34}$$

where D_i and $\overline{D}_j$ are doublet and antidoublet states, and T_i and $\overline{T}_j$ are triplet and antitriplet states embedded into GUT representations. The dimensions of $\mathbf{M}_D$ and $\mathbf{M}_T$ are given by the number of doublet-antidoublet and triplet-antitriplet pairs in the Higgs sector. Since H_u and H_d are almost massless compared to the GUT scale, they correspond to the left and right zero eigenmodes of $\mathbf{M}_D$, respectively, and can be expressed as a linear combination of the doublets D_i and antidoublets $\overline{D}_j$:

$$H_u = \sum_i a_i\, D_i\,, \qquad\qquad H_d = \sum_j b_j\, \overline{D}_j\,, \tag{3.35}$$

where the complex coefficients a_i and b_j have the normalization $\sum_k |a_k|^2 = \sum_l |b_l|^2 = 1$. On the other hand, D_i and $\overline{D}_j$ can be written in terms of states in the mass eigenbasis

$$D_i = a_i^*\, H_u + \dots\,, \qquad\qquad \overline{D}_j = b_j^*\, H_d + \dots\,. \tag{3.36}$$

The dots indicate mass eigenstates whose vevs are equal to zero. Because non-vanishing vevs of doublets or antidoublets break EW symmetry, it is assumed that only the light mass eigenstates H_u and H_d can acquire a vev. The vevs of D_i and $\overline{D}_j$ are thus given by

$$\langle D_i \rangle = a_i^*\, v_u\,, \qquad\qquad \langle \overline{D}_j \rangle = b_j^*\, v_d\,, \tag{3.37}$$

where $v_u = \langle H_u^0 \rangle$ and $v_d = \langle H_d^0 \rangle$ as defined in Eq. (2.224).

If there are multiple doublet-antidoublet pairs in a concrete model, the contribution of the light MSSM Higgses in the states D_i and $\overline{D_j}$, which are embedded into GUT representations, depends on the coefficients a_i and b_j via Eq. (3.36). These coefficients in

turn depend on the superpotential parameters of the Higgs sector, and are therefore also linked to the particular implementation of DT splitting.

In SU(5) theories, where only $\mathbf{Y}_d$ and $\mathbf{Y}_e$ are connected via GUT relations, the parameters a_i and b_j can be absorbed into the Yukawa couplings, since the down-type quarks and the charged leptons couple both to H_d. Thus, these extra parameters do not affect predictions in the Yukawa sector.

In contrast, in SO(10) theories the parameters a_i and b_j can generally not be absorbed into Yukawa couplings, because the Yukawa matrices of all fermion sectors arise from the same GUT operator. This implies, that there is in principle extra freedom to the SO(10) "Clebsch-Gordan" relations between the Yukawa matrices, due to the parameters a_i and b_j, which depend on the form of the superpotential in the Higgs sector.

3.4 Proton decay

A general feature of Grand Unified Theories is that they predict proton decay, induced by baryon and lepton number violating (but B-L preserving) operators of dimension 6 at the Lagrangian level. These effective four-fermion operators form invariants under the SM gauge group and are schematically written as

$$\mathcal{L} \supset \frac{1}{M^2}\left(Q\,L\,Q\,Q + u_R^\dagger\, d_R^\dagger\, e_R^\dagger\, u_R^\dagger + Q\,Q\,\overline{e}_R^\dagger\,\overline{u}_R^\dagger + Q\,L\,\overline{u}_R^\dagger\,\overline{d}_R^\dagger\right) + c.c.\,. \tag{3.38}$$

They are generated by integrating out heavy scalar or vector (gauge boson) leptoquarks with mass M, which are present in GUTs due to the embedding of the SM fields into bigger GUT representations and the embedding of the SM gauge group into the bigger GUT gauge group. For example, the first two operators in Eq. (3.38) are generated via the scalar leptoquarks $(\mathbf{3},\mathbf{1})(-\frac{1}{3})$ and $(\overline{\mathbf{3}},\mathbf{1})(+\frac{1}{3})$ (i.e. triplets and antitriplets), which are present in the $\mathbf{5}$ and $\overline{\mathbf{5}}$, respectively, of SU(5). Moreover, the last two operators in Eq. (3.38) are generated via the vector leptoquarks $(\mathbf{3},\mathbf{2})(-\frac{5}{6})$ and $(\overline{\mathbf{3}},\mathbf{2})(+\frac{5}{6})$, which are part of the adjoint representation of SU(5). A naive estimate based on dimensional analysis for the decay width of the proton in these two cases is given by [91]

$$\Gamma_p \approx |y_u y_d|^2 \frac{m_p^5}{M_T^4}\,, \qquad\qquad \Gamma_p \approx \alpha_{\mathrm{GUT}}^2 \frac{m_p^5}{M_V^4}\,, \tag{3.39}$$

where m_p is the proton mass, $\alpha_{\mathrm{GUT}} = g_{\mathrm{GUT}}^2/(4\pi)$ the unified structure constant, and M_T and M_V are the masses of the scalar and the vector leptoquarks, respectively. So far, proton decay has not been measured, but the most stringent bounds on the lifetime of the proton currently come from the Super-Kamiokande experiment [92]. Using the experimental constraint $\tau(p \to K^+\bar{\nu}) \gtrsim 6.5\cdot 10^{33}\,\mathrm{yr}$ [93], which is one of the decay channels with the strictest bound, and the realistic values $g_{\mathrm{GUT}} \approx 0.7$, $y_u \approx 2.7\cdot 10^{-6}/\sin\beta$ and $y_d \approx 5.0\cdot 10^{-6}/\cos\beta$ (with $\tan\beta = 20$) for the unified gauge coupling and the Yukawa couplings at the GUT scale [94], rough lower bounds for M_T and M_V are obtained:

$$M_T \gtrsim 3.6\cdot 10^{11}\,\mathrm{GeV}\,, \qquad\qquad M_V \gtrsim 4.3\cdot 10^{15}\,\mathrm{GeV}\,. \tag{3.40}$$

The estimate shows that proton decay from dimension 6 operators as in Eq. (3.38) is compatible with a typical GUT scale $\gtrsim 10^{16}\,\mathrm{GeV}$, and triplet masses which are even several orders of magnitude below M_{GUT}.

Proton decay from dimension 6 operators, which are generated by heavy scalar and vector leptoquarks, is present in any GUT and is typically not in conflict with the experimental bounds. However, in SUSY theories, the dimension 6 operators can also be generated via dimension 4 and 5 operators (at the Lagrangian level), which contain two fermions and one or two scalar superpartners. The dimension 6 operators are then generated by integrating out the sparticles. Since the sparticle masses are typically much smaller than the GUT scale, in order to account for the hierarchy problem of the EW Higgs mass, the induced proton decay is in general much stronger than in the above scenario. In fact, proton decay from dimension 4 operators is far above the experimental bounds, thus such operators must not be present in the Lagrangian, which, for example, is achieved by introducing R-parity (matter parity) as discussed in Section 2.4.

The dimension 5 operators are formed by integrating out heavy triplet states, which typically have masses $\gtrsim 10^{17}\,\text{GeV}$ in order that the induced proton decay is consistent with the experimental bounds (see e.g. [95]). At the SUSY scale M_{SUSY}, the dimension 6 operators are then built at 1-loop level by "dressing" the dimension 5 operators with gluino, chargino and neutralino exchange diagrams. Again, a naive estimate based on dimensional analysis can be made for dimension 5 proton decay

$$\Gamma_p \propto \frac{m_p^5}{M_T^2\, M_{\text{SUSY}}^2}\,, \tag{3.41}$$

however, the determination of the constant represented by $\propto$ is more involved in this case, because of the loop structure of the dimension 6 operator. An example diagram for the proton decay channel $p \to K^+\bar{\nu}$ via the dressing of a dimension 5 operator is shown in Figure 3.1. In this example the dressing takes place by means of a mass insertion of the winos $\widetilde{W}^{\pm}$, and the big black circle indicates the effective dimension 5 operator. The two different diagrams with renormalizable interactions, which lead to the effective dimension 5 operator by integrating out a heavy triplet are drawn in Figure 3.2 (cf. [96]). The right diagram contains a scalar triplet T, whereas in the left digram a mass insertion of the fermionic superpartner $\widetilde{T}$ is present.

Figure 3.1: An example diagram for the proton decay channel $p \to K^+\bar{\nu}$. The big black circle represents the effective dimension 5 operator, and the dressing of this operator takes place by using a mass insertion of the winos $\widetilde{W}^{\pm}$.

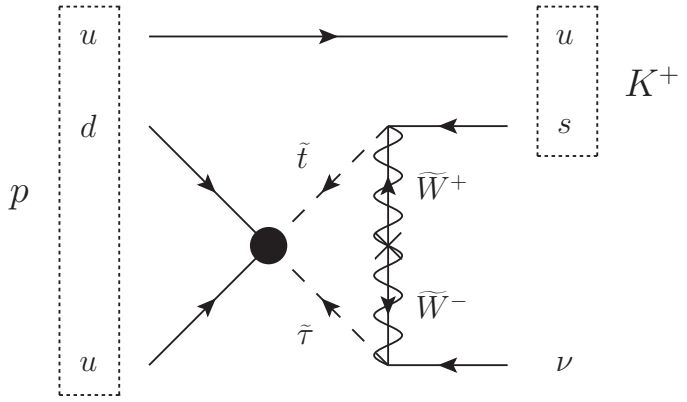

Figure 3.2: The two different diagrams with renormalizable interactions, which lead to the effective dimension 5 operator in Figure 3.1. The scalar triplets and antitriplets are labelled by T and $\overline{T}$, respectively, while their fermionic superpartners are written as $\widetilde{T}$ and $\widetilde{\overline{T}}$.

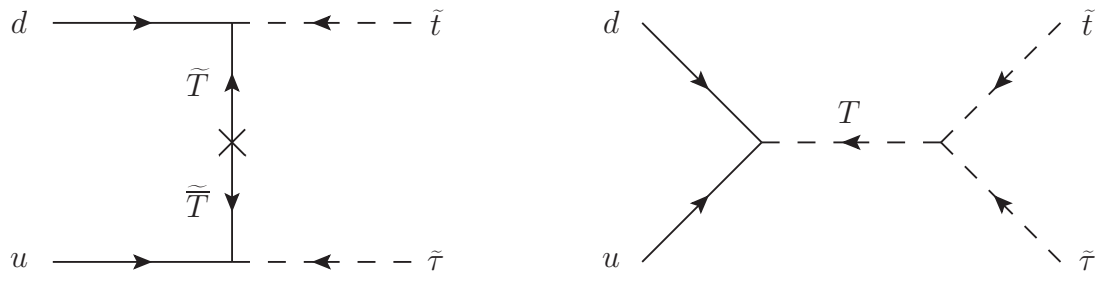

In general, multiple triplet and antitriplet superfields T_i and $\overline{T}_j$, respectively, with a mass matrix $(\mathbf{M}_T)_{ij}$ are present in a GUT model (cf. Section 3.3). At the superpotential level the interactions between the (anti)triplet and the MSSM superfields form so called "quasi-Yukawa" terms with quasi-Yukawa matrices $\tilde{\mathbf{Y}}_{iIJ}$. Apart from the two family indices I, J, the quasi-Yukawa matrices carry also a triplet index i. The quasi-Yukawa operators and the mass term for the (anti)triplets are given by

$$\begin{aligned} W_{\mathrm{T}} = &+\tfrac{1}{2}(\tilde{\mathbf{Y}}_{qq})_{iIJ}\,\epsilon_{\alpha\beta\gamma}\,Q_I^\alpha\cdot Q_J^\beta\,T_i^\gamma + (\tilde{\mathbf{Y}}_{eu})_{iIJ}\,e_I^c\,u_{J\alpha}^c\,T_i^\alpha \\ &+ (\tilde{\mathbf{Y}}_{ql})_{jIJ}\,Q_I^\alpha\cdot L_j\,\overline{T}_{j\alpha} + (\tilde{\mathbf{Y}}_{ud})_{jIJ}\,\epsilon^{\alpha\beta\gamma}\,u_{I\alpha}^c\,d_{J\beta}^c\,\overline{T}_{j\gamma} \\ &+ (\mathbf{M}_T)_{ij}\,T_i^\alpha\,\overline{T}_{j\alpha}\,, \end{aligned} \tag{3.42}$$

where the indices α, β, γ belong to the (anti)fundamental representation of $\mathrm{SU}(3)_C$, with $\epsilon_{123} = \epsilon^{123} = 1$. Moreover, the contraction of fundamental $\mathrm{SU}(2)_L$ indices is written as $\Psi\cdot\Phi = \epsilon_{ab}\,\Psi^a\,\Phi^b$ with $\epsilon_{12} = 1$. After integrating out the (anti)triplets, the effective baryon and lepton number violating operators are obtained

$$\begin{aligned} W_5 = &-\tfrac{1}{2}(\mathbf{M}_T^{-1})_{ij}\,(\tilde{\mathbf{Y}}_{ql})_{iIJ}\,(\tilde{\mathbf{Y}}_{qq})_{jKN}\,\epsilon_{\alpha\beta\gamma}\,(Q_I^\alpha\cdot L_J)(Q_K^\beta\cdot Q_N^\gamma) \\ &- (\mathbf{M}_T^{-1})_{ij}\,(\tilde{\mathbf{Y}}_{ud})_{iIJ}\,(\tilde{\mathbf{Y}}_{eu})_{jKN}\,\epsilon^{\alpha\beta\gamma}\,u_{I\alpha}^c\,d_{J\beta}^c\,e_K^c\,u_{N\gamma}^c \\ &+ \dots\,. \end{aligned} \tag{3.43}$$

where the dots indicate terms which are not relevant for proton decay, and $I, J, K, N \in \{1, 2, 3\}$ represent family indices. Since the superpotential is holomorphic in the superfields, only the $Q\,L\,Q\,Q$ and the $u_R^\dagger\,d_R^\dagger\,e_R^\dagger\,u_R^\dagger$ operators from Eq. (3.38) are present in Eq. (3.43). Using the following definitions of the dimension 5 operators $\mathbf{C}_{5L}^{IJKN}$ and $\mathbf{C}_{5R}^{IJKN}$:

$$\mathbf{C}_{5L}^{IJKN} := +(\mathbf{M}_T^{-1})_{ij}\,(\tilde{\mathbf{Y}}_{ql})_{iIJ}\,(\tilde{\mathbf{Y}}_{qq})_{jKN}\,, \tag{3.44}$$

$$\mathbf{C}_{5R}^{IJKN} := +(\mathbf{M}_T^{-1})_{ij}\,(\tilde{\mathbf{Y}}_{ud})_{iIJ}\,(\tilde{\mathbf{Y}}_{eu})_{jKN}\,, \tag{3.45}$$

the effective superpotential in Eq. (3.43) is written as

$$\begin{aligned} W_5 = &-\tfrac{1}{2}\mathbf{C}_{5L}^{IJKN}\,\epsilon_{\alpha\beta\gamma}\,(Q_I^\alpha\cdot L_J)(Q_K^\beta\cdot Q_N^\gamma) \\ &- \mathbf{C}_{5R}^{IJKN}\,\epsilon^{\alpha\beta\gamma}\,u_{I\alpha}^c\,d_{J\beta}^c\,e_K^c\,u_{N\gamma}^c \\ &+ \dots\,, \end{aligned} \tag{3.46}$$

which matches the conventions in [97]. The definitions in Eq. (3.44) and (3.45) show, that the dimension 5 operators, and therefore also the predictions for proton decay, depend on the form of the quasi-Yukawa matrices, as well as on the form of the triplet mass matrix.

Since the triplet states are present in the same GUT representations as the doublet states, which contain the H_u and H_d of the MSSM, the quasi-Yukawa matrices are related to the Yukawa matrices at the GUT scale. For example, in SU(5) the following general relations in family space hold: $\tilde{\mathbf{Y}}_{qq} \sim \tilde{\mathbf{Y}}_{eu} \sim \mathbf{Y}_u$ and $\tilde{\mathbf{Y}}_{ql} \sim \tilde{\mathbf{Y}}_{ud} \sim \mathbf{Y}_d$, using the conventions from Eq. (2.219) for $\mathbf{Y}_u$ and $\mathbf{Y}_d$, where the exact form depends on the choice of the SU(5) operators. In SO(10), on the other hand, the Yukawa and quasi-Yukawa operators originate from the same GUT operators, thus all Yukawa and quasi-Yukawa matrices are related.

As discussed in Section 3.3, due to the GUT embeddings the doublet and the triplet mass matrices $\mathbf{M}_D$ and $\mathbf{M}_T$ are related, so doublet-triplet splitting is necessary in order that all triplet states are heavy, namely at the GUT sale or higher, while one doublet pair is light, namely at the EW scale. Hence, the form of the triplet mass matrix $\mathbf{M}_T$ depends on the implementation of DT splitting, what finally impacts the predictions for proton decay.

A detailed discussion about the dressing of the dimension 5 operators and how the decay width of the proton for different decay channels is calculated is given in Chapter 7.

PART III

Flavour model building in SUSY GUTs

CHAPTER 4

Predictions from a flavour GUT model combined with a SUSY breaking sector

4.1 Motivation

The framework of supersymmetric flavour GUT models has the attractive feature that it is capable to resolve several shortcomings of the SM. Because of the embedding of multiple SM representations into one bigger GUT representation, such models predict relations between the Yukawa couplings of the different fermion sectors at the GUT scale, after the GUT symmetry is spontaneously broken. Moreover, if the GUT representations used for the embedding of the SM fermions also contain an SM singlet state, as for example the **16** of SO(10), there is a straight forward explanation for the existence of right-handed neutrinos, so that the SM neutrinos get small masses via the seesaw mechanism. A discrete flavour symmetry can be introduced in order to explain the structure of the Yukawa matrices in family space. Particular Yukawa structures at the GUT scale are conveniently implemented in models, where the flavour symmetry is spontaneously broken by vevs of flavour-Higgs fields, so-called flavon fields. Supersymmetry, on the other hand, provides a solution to the hierarchy problem of the EW Higgs mass, and the lightest superpartner of the SM particles is a suitable candidate for cold dark matter, assuming matter parity.

If supersymmetry indeed exists, it must be spontaneously broken, since no superpartners of the SM particles have been detected so far. The appropriate framework to consider spontaneous SUSY breaking is supergravity, where SUSY is implemented as a local symmetry. In contrast to global SUSY, in supergravity it is possible to form SUSY breaking ground states which have a vanishing vacuum energy at the same time. In particular, SUSY breaking in a hidden sector has the appealing property that under certain conditions only soft SUSY breaking terms are generated in the matter (observable) sector, as discussed in Section 2.3.3, such that there is still a systematic cancellation of loop corrections to the EW Higgs mass.

Roughly speaking, a complete supersymmetric flavour GUT model consists of four distinct sectors, so that the superpotential has the schematic form

$$W = W_{\text{mat}} + W_{\text{fl}} + W_{\cancel{\text{GUT}}} + W_{\cancel{\text{SUSY}}}\,. \tag{4.1}$$

The part W_{mat} gives rise to the Yukawa and mass terms of the matter sector once the GUT and the family symmetry are spontaneously broken. Family symmetry breaking is caused by flavon vevs, which are generated in the flavon sector W_{fl}, and $W_{\cancel{\text{GUT}}}$ represents the sector, where GUT symmetry breaking takes place. Finally, the part $W_{\cancel{\text{SUSY}}}$ describes the SUSY breaking sector of the model. Flavour GUT models typically focus on the matter

and flavon part of the superpotential, without explaining the origin of GUT symmetry and SUSY breaking. The incorporation of a SUSY breaking sector in the model has the feature, that in case of gravity mediated SUSY breaking the form of the soft SUSY breaking terms in the matter sector is predicted at the GUT scale.

The purpose of this chapter is to investigate in a first step how a generic flavon sector W_{fl} can be combined with a simple SUSY breaking sector $W_{\not{\text{SUSY}}}$, such that family symmetry and SUSY breaking takes place in the desired manner. In a second step, we consider the flavour GUT model from [98] with slight modifications, and calculate the predictions of this model in the presence of a SUSY breaking sector.

This chapter is based on the publication [1] and is organized as follows: after discussing the combination of a flavon sector with a SUSY breaking sector in Section 4.2, the conclusions are applied on an example model in Section 4.3. Finally, a complete fit of this model to experimental data is performed in Section 4.4.

4.2 Combining a flavon with a SUSY breaking sector

4.2.1 Generic flavon superpotential

In the following, we consider SUSY flavour GUT models with a (discrete) family symmetry $\mathrm{G_F}$. In order that the family symmetry is spontaneously broken by vevs of flavon fields, such that the flavour structure of the model is generated at the GUT scale, at least some of the flavons must be in non-singlet representations of $\mathrm{G_F}$. The part of the superpotential which realizes a non-trivial vev alignment of the flavon fields is labelled by W_{fl}. A typical term in W_{fl} which generates such a vev alignment for a flavon field θ has the schematic form

$$W_{\text{fl}}^{\theta} = P(\kappa\,\theta^n - M^2)\,, \tag{4.2}$$

where P is a so-called driving field, M a mass scale of the order M_{GUT}, and $n \geq 2$ an integer. Furthermore, the complex parameter κ has mass dimension $-(n-2)$ and is of the order $1/\Lambda^{n-2}$, with a mass scale $\Lambda > M$. Although θ transforms in a non-trivial way under the family symmetry, the n-th power θ^n must have the form of a singlet. For the sake of readability, we set the (reduced) Planck mass $M_{\text{P}} = 1$ in the subsequent calculations. With the covariant derivatives

$$D_P W_{\text{fl}}^{\theta} = \kappa\,\theta^n - M^2 + W_{\text{fl}}^{\theta}\,\partial_P K\,, \tag{4.3}$$

$$D_\theta W_{\text{fl}}^{\theta} = n\,\kappa\,P\,\theta^{n-1} + W_{\text{fl}}^{\theta}\,\partial_\theta K\,, \tag{4.4}$$

the scalar potential reads

$$V = e^K \left(g^{\bar{k}k} D_k W_{\text{fl}}^{\theta}\, D_{\bar{k}} \overline{W}_{\text{fl}}^{\theta} - 3|W_{\text{fl}}^{\theta}|^2\right), \tag{4.5}$$

where $k \in \{P, \theta\}$. For any Kähler potential K the scalar potential has a local minimum at

$$\langle P \rangle = 0\,, \qquad\qquad \langle \theta \rangle = \left(\frac{M^2}{\kappa}\right)^{1/n}, \tag{4.6}$$

with

$$\langle V \rangle = 0\,, \tag{4.7}$$

since $\langle W_{\text{fl}}^{\theta} \rangle = 0$ and $\langle D_P W_{\text{fl}}^{\theta} \rangle = \langle D_\theta W_{\text{fl}}^{\theta} \rangle = 0$.[1] Thus, SUSY is not broken in that minimum. Moreover, the positive definiteness of the Kähler metric $g_{k\bar{k}}$ guarantees, that for the field values in Eq. (4.6) the scalar potential indeed has a (local) minimum, i.e. the masses of the fields are positive.

The form of W_{fl}^{θ} can be protected by introducing a $\mathrm{U}(1)_{\mathrm{R}}$ symmetry, as well as a global $\mathbb{Z}_n$ symmetry. In order that the weight w_{R} of W_{fl}^{θ} is equal to 2, the R-charges of the driving and the flavon field must be $w_{\mathrm{R}}(P) = 2$ and $w_{\mathrm{R}}(\theta) = 0$. Furthermore, with respect to the $\mathbb{Z}_n$ symmetry P and θ have the charges 0 and 1, respectively.[2] For the construction of a simple SUSY breaking sector as in Section 4.2.2, it turns out though, that it is more appropriate to consider a discrete $\mathbb{Z}_m^{\mathrm{R}}$ symmetry instead of the $\mathrm{U}(1)_{\mathrm{R}}$ symmetry. In that case, higher powers of the driving field $P^{m+1} + \ldots$ (or $P^{m/2+1} + \ldots$ if m is even) are compatible with the symmetries, and thus, they are generally also present in W_{fl}^{θ}. If these terms are added to the superpotential, additional minima of the scalar potential with $\langle P \rangle \neq 0$ appear. However, the minimum from Eq. (4.6) still exists and can be used for model building.

As a basic principle in model building one may assume "spontaneous CP violation", which means that the fundamental theory is CP symmetric, and CP violation is only induced after spontaneous symmetry breaking. In the context of the flavon superpotential form Eq. (4.2) this means, that the parameters κ and M are real, and therefore, the argument of $\langle \theta \rangle$ can only take the discrete values $2\pi p/n$ ($p \in \{0, ..., n-1\}$), which may correspond to a CP violation phase. Spontaneous CP violation is implemented in the example model which we consider in Section 4.3.

In principle, a flavour model contains multiple flavon and driving fields, which form superpotential terms as in Eq. 4.2. The general case will be discussed in Section 4.2.3.

4.2.2 Simple SUSY breaking setup

In order to spontaneously break SUSY in the context of supergravity, we consider a simple setup with one chiral superfield φ. The form of the corresponding superpotential $W_{\not{\text{SUSY}}}^{\varphi}$ is given by

$$W_{\not{\text{SUSY}}}^{\varphi} = \mu^2(\varphi + \lambda\varphi^p)\,, \tag{4.8}$$

where the parameters μ and λ have mass dimensions 1 and $1-p$, respectively. Since the overall phase of the superpotential is not physical, we can choose μ and λ to be real, by applying the redefinition $\varphi \to \exp(i\alpha/(1-p))\varphi$ where α is the phase of λ. If the model contains a $\mathbb{Z}_m^{\mathrm{R}}$ symmetry, the R-charge of φ must be equal to 2, and the power p is restricted to values like $1+m$, or $1+m/2$ if m is even. Using the covariant derivative

$$D_\varphi W_{\not{\text{SUSY}}}^{\varphi} = \mu^2(1 + p\,\lambda\varphi^{p-1}) + W_{\not{\text{SUSY}}}^{\varphi}\partial_\varphi K\,, \tag{4.9}$$

[1] Note, the conditions $\langle W_{\text{fl}}^{\theta} \rangle = 0$ and $\langle D_P W_{\text{fl}}^{\theta} \rangle = \langle D_\theta W_{\text{fl}}^{\theta} \rangle = 0$ imply that $\langle \partial_P W_{\text{fl}}^{\theta} \rangle = \langle \partial_\theta W_{\text{fl}}^{\theta} \rangle = 0$, which corresponds to vanishing F-terms in global SUSY.

[2] In principle, superpotential terms like θ^{2n} are also compatible with the $\mathbb{Z}_n$ symmetry. However, such terms are highly suppressed by a large power of the mass scale Λ and are therefore neglected.

the corresponding scalar potential is written as

$$V = e^K \left(g^{\bar{\varphi}\varphi} D_\varphi W^\varphi_{\not{\text{SUSY}}} D_{\bar{\varphi}} \overline{W}^\varphi_{\not{\text{SUSY}}} - 3 |W^\varphi_{\not{\text{SUSY}}}|^2 \right) , \tag{4.10}$$

where K is the Kähler potential of φ. If a (local) minimum exists, it typically satisfies $\langle F_\varphi \rangle \neq 0$, thus SUSY is spontaneously broken (cf. Section 2.3.1). The fermionic superpartner of the scalar field φ is then absorbed by the gravitino, which gets the mass $m_{3/2}$. Furthermore, the parameters μ and λ can be adjusted (without affecting SUSY breaking), such that the two conditions

$$\langle V \rangle = 0 , \tag{4.11}$$

$$\left\langle e^{K/2} |W^\varphi_{\not{\text{SUSY}}}| \right\rangle = m_{3/2} , \tag{4.12}$$

are satisfied, for a given value of $m_{3/2}$. The first constraint is fulfilled by an appropriate choice of λ. Once λ is fixed, the factor μ^2 is used to rescale $W^\varphi_{\not{\text{SUSY}}}$, such that the second identity holds.

In general, the vev of φ is located above the Planck scale, if the Kähler potential is minimal, i.e. $K = \varphi\bar{\varphi}$. However, by adding additional terms of the form $\gamma_{\varphi\varphi}(\varphi\bar{\varphi})^2 + \ldots$ to the Kähler potential, where the dots indicate terms with higher powers in $\varphi\bar{\varphi}$, the vev can be shifted to values below M_{P}.

4.2.3 General scenario with multiple driving and flavon fields

In the following we will argue, that the general scenario with N_{D} driving fields P'_j ($j \in \{1, ..., N_{\text{D}}\}$) and N_{F} flavon fields θ_i ($i \in \{1, ..., N_{\text{F}}\}$), where the number of driving fields is bigger than the one of flavon fields (i.e. $N_{\text{D}} > N_{\text{F}}$), is suitable to combine a flavon and a SUSY breaking sector as described in Section 4.2.1 and 4.2.2, respectively. In particular, after a change of basis in the fields P'_j, N_{F} of these fields serve as driving fields for the flavons, whereas the remaining $N_{\text{D}} - N_{\text{F}}$ fields can be used to implement SUSY breaking. The prime in the label of the driving fields is used to distinguish the two different bases. We assume again, that the theory contains a $\mathbb{Z}^{\text{R}}_m$ symmetry, where the driving and the flavon fields have R-charges $w_{\text{R}}(P'_j) = 2$ and $w_{\text{R}}(\theta_i) = 0$. Moreover, each flavon transforms under a separate global $\mathbb{Z}_{n_i}$ symmetry with charge 1. The driving fields are singlets concerning these symmetries. The general ansatz for the superpotential is then given by

$$\begin{aligned}
W_{\text{fl}+\not{\text{SUSY}}} = \quad & P'_1 \left(\kappa'_{11}\theta_1^{n_1} + \kappa'_{12}\theta_2^{n_2} + \kappa'_{13}\theta_3^{n_3} + \ldots + \kappa'_{1N_{\text{F}}}\theta_{N_{\text{F}}}^{n_{N_{\text{F}}}} - M'^2_1 \right) \\
+ \quad & P'_2 \left(\kappa'_{21}\theta_1^{n_1} + \kappa'_{22}\theta_2^{n_2} + \kappa'_{23}\theta_3^{n_3} + \ldots + \kappa'_{2N_{\text{F}}}\theta_{N_{\text{F}}}^{n_{N_{\text{F}}}} - M'^2_2 \right) \\
+ \quad & P'_3 \left(\kappa'_{31}\theta_1^{n_1} + \kappa'_{32}\theta_2^{n_2} + \kappa'_{33}\theta_3^{n_3} + \ldots + \kappa'_{3N_{\text{F}}}\theta_{N_{\text{F}}}^{n_{N_{\text{F}}}} - M'^2_3 \right) \\
& \vdots \\
& + P'_{N_{\text{D}}} \left(\kappa'_{N_{\text{D}}1}\theta_1^{n_1} + \kappa'_{N_{\text{D}}2}\theta_2^{n_2} + \kappa'_{N_{\text{D}}3}\theta_3^{n_3} + \ldots + \kappa'_{N_{\text{D}}N_{\text{F}}}\theta_{N_{\text{F}}}^{n_{N_{\text{F}}}} - M'^2_{N_{\text{D}}} \right) \\
+ \quad & \ldots ,
\end{aligned} \tag{4.13}$$

where the dots in the last line indicate terms which contain higher powers of the fields P'_j. The couplings between the driving and the flavon fields are implemented by the matrix κ',

where each entry κ'_{ji} has the required mass dimension, and the additional mass scales are written as M'_j.

Like every complex rectangular matrix, the coupling matrix κ' can be decomposed by a QR decomposition into a unitary matrix and an upper triangular matrix. The unitary matrix induces a new basis in the driving fields, which is denoted by P_j, and the resulting upper triangular coupling matrix is labelled by κ. Consequently, the $N_\mathrm{D}-N_\mathrm{F}$ driving fields $P_{N_\mathrm{F}+1}, ..., P_{N_\mathrm{D}}$ do not couple to the flavon fields. Furthermore, the mass scales are rotated as well, and are now written as M_j. With respect to this new basis, the superpotential $W_{\text{fl+}\cancel{\text{SUSY}}}$ reads

$$\begin{aligned}
W_{\text{fl+}\cancel{\text{SUSY}}} = \quad & P_1\big(\kappa_{11}\theta_1^{n_1} + \kappa_{12}\theta_2^{n_2} + \kappa_{13}\theta_3^{n_3} + \ldots + \kappa_{1N_\mathrm{F}}\theta_{N_\mathrm{F}}^{n_{N_\mathrm{F}}} - M_1^2\big) \\
+ \quad & P_2\big(\phantom{\kappa_{11}\theta_1^{n_1} +}\ 0\ \phantom{\theta_1^{n_1}} + \kappa_{22}\theta_2^{n_2} + \kappa_{23}\theta_3^{n_3} + \ldots + \kappa_{2N_\mathrm{F}}\theta_{N_\mathrm{F}}^{n_{N_\mathrm{F}}} - M_2^2\big) \\
+ \quad & P_3\big(\phantom{\kappa_{11}\theta_1^{n_1} +}\ 0\ \phantom{\theta_1^{n_1}} + \phantom{\kappa_{22}\theta_2^{n_2} +}\ 0\ \phantom{\theta_2^{n_2}} + \kappa_{33}\theta_3^{n_3} + \ldots + \kappa_{3N_\mathrm{F}}\theta_{N_\mathrm{F}}^{n_{N_\mathrm{F}}} - M_3^2\big) \\
& \vdots \\
+ \quad & P_{N_\mathrm{F}}\big(\phantom{\kappa_{11}\theta_1^{n_1} +}\ 0\ \phantom{\theta_1^{n_1}} + \phantom{\kappa_{22}\theta_2^{n_2} +}\ 0\ \phantom{\theta_2^{n_2}} + \phantom{\kappa_{33}\theta_3^{n_3} +}\ 0\ \phantom{\theta_3^{n_3}} + \ldots + \kappa_{N_\mathrm{F}N_\mathrm{F}}\theta_{N_\mathrm{F}}^{n_{N_\mathrm{F}}} - M_{N_\mathrm{F}}^2\big) \\
+ \quad & P_{N_\mathrm{F}+1}\big(\phantom{\kappa_{11}\theta_1^{n_1} +}\ 0\ \phantom{\theta_1^{n_1}} + \phantom{\kappa_{22}\theta_2^{n_2} +}\ 0\ \phantom{\theta_2^{n_2}} + \phantom{\kappa_{33}\theta_3^{n_3} +}\ 0\ \phantom{\theta_3^{n_3}} + \ldots + \phantom{\kappa_{N_\mathrm{F}N_\mathrm{F}}\theta_{N_\mathrm{F}}^{n_{N_\mathrm{F}}}}\ 0\ \phantom{\theta_{N_\mathrm{F}}^{n_{N_\mathrm{F}}}} - M_{N_\mathrm{F}+1}^2\big) \\
& \vdots \\
+ \quad & P_{N_\mathrm{D}}\big(\phantom{\kappa_{11}\theta_1^{n_1} +}\ 0\ \phantom{\theta_1^{n_1}} + \phantom{\kappa_{22}\theta_2^{n_2} +}\ 0\ \phantom{\theta_2^{n_2}} + \phantom{\kappa_{33}\theta_3^{n_3} +}\ 0\ \phantom{\theta_3^{n_3}} + \ldots + \phantom{\kappa_{N_\mathrm{F}N_\mathrm{F}}\theta_{N_\mathrm{F}}^{n_{N_\mathrm{F}}}}\ 0\ \phantom{\theta_{N_\mathrm{F}}^{n_{N_\mathrm{F}}}} - M_{N_\mathrm{D}}^2\big) \\
+ \quad & \ldots\,,
\end{aligned} \tag{4.14}$$

where the last line again indicates terms which contain higher powers, such as $m+1$ (or $m/2+1$ if m even), of the driving fields, which are compatible with the $\mathbb{Z}_m^\mathrm{R}$ symmetry. Such a term may contain different fields P_j.

In order to establish the connection with the SUSY breaking scenario from Section 4.2.2, we make the following relabelling: the driving fields $P_{N_\mathrm{F}+l}$ with $l \in \{1, ..., N_\mathrm{D} - N_\mathrm{F}\}$ are written as φ_l, and the corresponding mass scales $M_{N_\mathrm{F}+l}$ as μ_l. In addition, the higher order terms $\lambda_l\,\varphi_l^{m+1}$ are explicitly considered. The superpotential is then given by

$$\begin{aligned}
W_{\text{fl+}\cancel{\text{SUSY}}} = \quad & P_1\big(\kappa_{11}\theta_1^{n_1} + \kappa_{12}\theta_2^{n_2} + \kappa_{13}\theta_3^{n_3} + \cdots + \kappa_{1N_\mathrm{F}}\theta_{N_\mathrm{F}}^{n_{N_\mathrm{F}}} - M_1^2\big) \\
& + P_2\big(\kappa_{22}\theta_2^{n_2} + \kappa_{23}\theta_3^{n_3} + \cdots + \kappa_{2N_\mathrm{F}}\theta_{N_\mathrm{F}}^{n_{N_\mathrm{F}}} - M_2^2\big) \\
& + P_3\big(\kappa_{33}\theta_3^{n_3} + \cdots + \kappa_{3N_\mathrm{F}}\theta_{N_\mathrm{F}}^{n_{N_\mathrm{F}}} - M_3^2\big) \\
& \vdots \\
& + P_{N_\mathrm{F}}\big(\kappa_{N_\mathrm{F}N_\mathrm{F}}\theta_{N_\mathrm{F}}^{n_{N_\mathrm{F}}} - M_{N_\mathrm{F}}^2\big) \\
& + \big(\mu_1^2\varphi_1 + \lambda_1\varphi_1^{m+1}\big) + \cdots + \big(\mu_{N_\mathrm{D}-N_\mathrm{F}}^2\varphi_{N_\mathrm{D}-N_\mathrm{F}} + \lambda_{N_\mathrm{D}-N_\mathrm{F}}\varphi_{N_\mathrm{D}-N_\mathrm{F}}^{m+1}\big) \\
& + \ldots\,.
\end{aligned} \tag{4.15}$$

The above discussion shows, that starting with a general setup of N_D driving fields and $N_\mathrm{F} < N_\mathrm{D}$ flavon fields, one can perform a unitary rotation in the space of driving fields, so that one ends up with N_F driving fields P_i associated to the flavon fields θ_i, and $N_\mathrm{D} - N_\mathrm{F}$ fields φ_l, which do not directly couple to the flavon fields and which can be used to implement spontaneous SUSY breaking.

Using $\langle P_i \rangle = 0$ and neglecting possible coupling terms between P_i and φ_l, the conditions for the vevs of the flavon fields are recovered iteratively: in a first step, the term $\langle D_P W \rangle$ as in Eq. (4.3) for the field P_{N_F} is set equal to zero which fixes the vev $\langle \theta_{N_\mathrm{F}} \rangle$ (cf. Section 4.2.1). In a second step, by using the value of $\langle \theta_{N_\mathrm{F}} \rangle$, the vanishing term $\langle D_P W \rangle$ for the field $P_{N_\mathrm{F}-1}$ fixes the vev $\langle \theta_{N_\mathrm{F}-1} \rangle$. In the same manner the value of $\langle \theta_{N_\mathrm{F}-2} \rangle$ is determined. This procedure continuous until the vev $\langle \theta_1 \rangle$ is fixed in a last step.

In general, there are couplings between the flavon fields P_i and the SUSY breaking fields φ_l. We will argue in Section 4.2.4, that these additional coupling terms do not qualitatively change the SUSY and family symmetry breaking minimum of the scalar potential corresponding to the combined superpotential $W_{\mathrm{fl}+\cancel{\mathrm{SUSY}}}$, i.e. to a good approximation the flavon and the SUSY breaking sector can be considered separately.

4.2.4 Example: one driving and one SUSY breaking field

To investigate the influence of coupling terms between the driving and the SUSY breaking fields in the superpotential $W_{\mathrm{fl}+\cancel{\mathrm{SUSY}}}$ from Eq. (4.15) on the spontaneous breaking of SUSY and $\mathrm{G_F}$, we consider the simplified scenario, where $N_\mathrm{D} = 2$ and $N_\mathrm{F} = 1$, and where the R-symmetry is given by $\mathbb{Z}_4^\mathrm{R}$. Hence, there is only one driving field P and one SUSY breaking field φ after the rotation of the fields, and the superpotential reads

$$W_{\mathrm{fl}+\cancel{\mathrm{SUSY}}} = \mu^2(\varphi + \lambda\varphi^3) + P(\kappa\theta^n - M^2) + a_1 P^3 + a_2 \varphi P^2 + a_3 \varphi^2 P \,. \tag{4.16}$$

In addition, the Kähler potential has the following form:

$$K = \widetilde{K}(\varphi, \bar{\varphi}) + P\overline{P} + \theta\bar{\theta} \,, \tag{4.17}$$

where $\widetilde{K}$ corresponds to the Kähler potential of the SUSY breaking field φ from Section 4.2.2. Since K is canonically normalized, there is no renormalizable term which mixes φ and P. All other mixing terms between the fields, which are suppressed by the Planck scale, are neglected. In the following analysis we assume that $M \gg m_{3/2}$, what is well justified because the gravitino mass is typically much smaller than the GUT scale, where family symmetry breaking takes place.

In a first step, we discuss the case where the couplings a_i ($i \in \{1,2,3\}$) between the driving and the SUSY breaking field are equal to zero. Using the covariant derivatives

$$D_\varphi W_{\mathrm{fl}+\cancel{\mathrm{SUSY}}} = \mu^2(1 + 3\lambda\varphi^2) + W_{\mathrm{fl}+\cancel{\mathrm{SUSY}}}\, \partial_\varphi K \,, \tag{4.18}$$

$$D_P W_{\mathrm{fl}+\cancel{\mathrm{SUSY}}} = \kappa\theta^n - M^2 + W_{\mathrm{fl}+\cancel{\mathrm{SUSY}}}\, \partial_P K \,, \tag{4.19}$$

$$D_\theta W_{\mathrm{fl}+\cancel{\mathrm{SUSY}}} = n\kappa P\, \theta^{n-1} + W_{\mathrm{fl}+\cancel{\mathrm{SUSY}}}\, \partial_\theta K \,, \tag{4.20}$$

the scalar potential is given by

$$V = e^K \left(g^{\bar{k}k} D_k W_{\mathrm{fl}+\cancel{\mathrm{SUSY}}}\, D_{\bar{k}} \overline{W}_{\mathrm{fl}+\cancel{\mathrm{SUSY}}} - 3|W_{\mathrm{fl}+\cancel{\mathrm{SUSY}}}|^2 \right) , \tag{4.21}$$

with the index $k \in \{\varphi, P, \theta\}$. Because in $W_{\mathrm{fl}+\cancel{\mathrm{SUSY}}}$ the superpotential W_fl from Eq. (4.2) is combined with $W_{\cancel{\mathrm{SUSY}}}$ from Eq. (4.8), the values of $\langle P \rangle$ and $\langle \theta \rangle$ in Eq. (4.6) describe no longer a minimum of the scalar potential. Also the vev of φ changes and the values of the parameters μ and λ have to be adjusted, such that the two conditions in Eq. (4.11)

and (4.12) are still fulfilled. A numerical analysis of the scalar potential in Eq. (4.21) showed, that all these shifts are small when the flavon and the SUSY breaking sector are combined, and that the qualitative picture of the discussions in the previous sections does not change.

At the analytical level this result can be understood in the following way: in a local minimum of V the two necessary conditions $\langle \partial V/\partial P \rangle = 0$ and $\langle \partial V/\partial \theta \rangle = 0$ have to be satisfied. In a first approximation this is achieved by a shift of $\langle P \rangle$ away from zero of the order $\mathcal{O}(m_{3/2} \cdot \Lambda^2/M^2)$, which corresponds to $\langle D_\theta W \rangle = 0$, and a relative shift of θ^n away from M^2/κ of the order $\mathcal{O}(m_{3/2}^2/M^2 \cdot \Lambda^2/M^2)$, which corresponds to $\langle D_P W \rangle = 0$. Because the contribution from the flavon sector to $\langle W \rangle$ is only of the order $\mathcal{O}(m_{3/2}^3)$, the vev of φ experiences only a negligible relative correction of the order $\mathcal{O}(m_{3/2}^2/M_{\mathrm{P}}^2)$. Furthermore, the relative adjustment of the parameter λ is of the order $\mathcal{O}(m_{3/2}^2/M_{\mathrm{P}}^2)$ as well, so that $\langle V \rangle = 0$.

The impact of the additional coupling terms $a_1 P^3$, $a_2 \varphi P^2$ and $a_3 \varphi^2 P$ is discussed in the following: if the first term is present, additional minima with $\langle P \rangle \neq 0$ appear, however the minimum with $\langle P \rangle \approx 0$ still exists as discussed in Section 4.2.1. The other two terms leave $\langle D_\theta W \rangle$ unchanged but modify $\langle D_P W \rangle$ and $\langle D_\varphi W \rangle$. The numerical analysis showed, that although the vev of φ can be of the order of the Planck scale, the two terms do not qualitatively change the picture, because they can be absorbed by a redefinition of M when plugging in the vev of φ. The only condition which the parameters a_i have to satisfy is $a_3 \langle \varphi \rangle^2 \leq M^2$, such that the relative correction of M is at most of order one. Furthermore, the relative shifts of $\langle \varphi \rangle$ and λ are up to $\mathcal{O}(m_{3/2}/M_{\mathrm{P}})$.

The above discussion can also be applied to the case of a more general flavon superpotential.

4.3 An example flavour GUT model

Having discussed the combination of a general flavon sector with a SUSY breaking sector in Section 4.2, we consider in this section the implementation of a specific flavour GUT model in the presence of a SUSY breaking sector. For the flavour GUT model we take the one from [98], with slight modifications, which is based on an SU(5) GUT symmetry and an A_4 family symmetry $\mathrm{G_F}$, in combination with additional discrete "shaping symmetries".

The main features related to the flavon sector of this model are, that CP symmetry is spontaneously broken by discrete vacuum alignments of the flavons, as discussed in [99]. The CP violation phase in the CKM matrix is then realized by a unitarity triangle angle $\alpha_{\mathrm{UT}} \approx 90^\circ$ via the phase sum rule [100] in the quark sector. Furthermore, the "Constrained Sequential Dominance 2" scheme [101] for the neutrino sector is implemented, which, in combination with contributions from the charged lepton sector, predicts the PMNS mixing angles and phases.

The most important modifications of the flavour model we consider compared to the one from [98] are the following: instead of a $\mathrm{U}(1)_{\mathrm{R}}$ symmetry, we use a $\mathbb{Z}_4^{\mathrm{R}}$ symmetry,[3] such

[3] We have checked that the only new terms which appear in the renormalizable superpotential, due to the choice of a $\mathbb{Z}_4^{\mathrm{R}}$ instead of a $\mathrm{U}(1)_{\mathrm{R}}$ symmetry, are trilinear couplings between messenger fields, which however only induce suppressed higher order operators in the matter sector, such that the model predictions are not changed.

that we can add a simple SUSY breaking sector. Moreover, we choose different relations between the entries of the down-quark and the charged lepton Yukawa matrices at the GUT scale, e.g. we predict the approximate ratios $y_\mu = -3y_s$ and $y_\tau = y_b$ for the second and third family.

An overview of all fields of the flavour model, including driving and messenger fields, with the corresponding representations and charges under all symmetries of the model, as well as the full superpotential of the renormalizable theory is given in Appendix A.1.

4.3.1 The flavon potential and the flavon vevs

We take the same flavon superpotential W_{fl} as given in [98]. Since in our model we include a SUSY breaking sector in the context of supergravity, the flavon vev alignments get slightly modified. However, as discussed in Section 4.2.4, these shifts are suppressed by the small ratio between the gravitino mass and the GUT scale. In addition, although we consider a $\mathbb{Z}_4^{\text{R}}$ instead of a $\text{U}(1)_{\text{R}}$ symmetry, which allows for additional coupling terms between the driving fields, the original vev alignment of the driving fields at approximately zero still exists. Hence, the predictions of the flavon sector get not spoiled.

The most important flavons to generate the flavour structure in the up-quark/charged lepton sector and in the CSD2 scheme of the neutrino sector are the fields $\theta_{23}, \theta_{102}, \theta_2$ and θ_3, which are all triplets under the A_4 family symmetry. They acquire the following vev alignments in flavour space:

$$\langle\theta_{23}\rangle \propto \begin{pmatrix} 0 \\ 1 \\ -1 \end{pmatrix}, \qquad \langle\theta_{102}\rangle \propto \begin{pmatrix} 1 \\ 0 \\ 2 \end{pmatrix}, \qquad \langle\theta_2\rangle \propto \begin{pmatrix} 0 \\ 1 \\ 0 \end{pmatrix}, \qquad \langle\theta_3\rangle \propto \begin{pmatrix} 0 \\ 0 \\ 1 \end{pmatrix}, \tag{4.22}$$

where the symbol $\propto$ indicates proportionality (with a real factor). The additional flavon fields which appear in the matter sector are θ_2', θ_{102}', ξ_1, ξ_2 and ξ_u, which form singlets under A_4. Moreover, the vevs of ξ_1 and ξ_u are real, whereas the ones of θ_2', θ_{102}' and ξ_2 have the complex phases $\pi/2$, $4\pi/3$ and $-\pi/3$, respectively.

4.3.2 SUSY breaking sector and the matter superpotential

For the SUSY breaking sector we choose the simple setup from Section 4.2.2, which contains one chiral superfield φ with an R-charge $w_{\text{R}}(\varphi) = 2$. Apart from that, the field φ is a complete singlet under all symmetries of the model, namely the SU(5) GUT symmetry, the A_4 family symmetry and the additional discrete shaping symmetries. Since in our flavour model the R-symmetry is given by $\mathbb{Z}_4^{\text{R}}$, the superpotential of the SUSY breaking sector from Eq. (4.8) reads

$$W_{\not{\text{SUSY}}} = \mu^2(\varphi + \lambda\varphi^3)\,. \tag{4.23}$$

The set of matter superfields in the model is given by F, T_1, T_2, T_3, N_1 and N_2, where F and T_I are in the $\overline{\mathbf{5}}$ and $\mathbf{10}$ representation of SU(5), respectively. Furthermore, the F is a triplet under A_4, whereas the T_I are singlets. The N_1 and N_2 are singlets under SU(5) as well as under A_4, and represent the right-handed neutrinos (cf. Table A.1). The MSSM

Higgs doublet H_u is embedded into H_5, and the antidoublet H_d is contained in $\overline{H}_5$ and $\overline{H}'_5$.[4] Moreover, the H_{24} acquires an SM singlet GUT scale vev v_{24}, which breaks the SU(5) symmetry. After the heavy messenger fields, whose masses are above the GUT scale, are integrated out, the superpotential W_{mat} of the matter sector consists of four terms, namely

$$W_{\text{mat}} = W_u + W_d + W_\nu + W_R \,, \tag{4.24}$$

where these terms are given by

$$\begin{aligned}
W_u &= \frac{1}{\Lambda^2} T_1^2 H_5 \xi_u \xi_1 + \frac{1}{\Lambda^2} T_1 T_2 H_5 \xi_u^2 + \frac{1}{\Lambda^2} T_2^2 H_5 \xi_1^2 + \frac{1}{\Lambda} T_2 T_3 H_5 \xi_1 + T_3^2 H_5 \,, \\
W_d &= \frac{1}{\Lambda^3} \theta'_2 \overline{H}_5 F(T_1 \theta_2) H_{24} + \frac{1}{\Lambda^3} \theta'_{102} \overline{H}_5 F(T_2 \theta_{102}) H_{24} + \frac{1}{\Lambda^2} F(T_2 \theta_{23}) \overline{H}'_5 H_{24} + \frac{1}{\Lambda} \overline{H}_5 F(T_3 \theta_3), \\
W_\nu &= \frac{1}{\Lambda} (H_5 F)(\theta_{23} N_1) + \frac{1}{\Lambda} (H_5 F)(\theta_{102} N_2) \,, \\
W_R &= \xi_1 N_1^2 + \xi_2 N_2^2 \,,
\end{aligned} \tag{4.25}$$

with the messenger mass scale Λ. Note that the coefficients in front of each operator are omitted. The labels indicate that the Yukawa terms of the up-quark, the down-quark/charged lepton and the neutrino sector emerge from W_u, W_d and W_ν, respectively. Moreover, the Majorana mass term of the right-handed neutrinos results from W_R. After the flavons acquired their vevs, the Yukawa matrices at the GUT scale are given by

$$\mathbf{Y}_u = \begin{pmatrix} a_u & b_u & 0 \\ b_u & c_u & d_u \\ 0 & d_u & e_u \end{pmatrix}, \qquad \mathbf{Y}_d = \begin{pmatrix} 0 & i\epsilon_2 & 0 \\ \bar{\omega}\epsilon_{102} & \epsilon_{23} & 2\bar{\omega}\epsilon_{102} - \epsilon_{23} \\ 0 & 0 & \epsilon_3 \end{pmatrix},$$

$$\mathbf{Y}_e = \begin{pmatrix} 0 & \bar{\omega}\epsilon_{102} & 0 \\ i\epsilon_2 & -3\epsilon_{23} & 0 \\ 0 & 2\bar{\omega}\epsilon_{102} + 3\epsilon_{23} & \epsilon_3 \end{pmatrix}, \qquad \mathbf{Y}_\nu = \begin{pmatrix} 0 & b \\ a & 0 \\ -a & 2b \end{pmatrix}, \tag{4.26}$$

using the left-right convention from Section 2.4, and the right-handed neutrino mass matrix takes the form

$$\mathbf{M}_R = \begin{pmatrix} M_A & 0 \\ 0 & M_B \end{pmatrix}. \tag{4.27}$$

The real parameters in $\mathbf{Y}_u$ are defined as

$$a_u \propto \frac{|\langle \xi_u \rangle \langle \xi_1 \rangle|}{\Lambda^2} \,, \qquad b_u \propto \frac{|\langle \xi_u \rangle|^2}{\Lambda^2} \,, \qquad c_u \propto \frac{|\langle \xi_1 \rangle|^2}{\Lambda^2} \,, \qquad d_u \propto \frac{|\langle \xi_u \rangle|}{\Lambda} \,, \tag{4.28}$$

[4] A complete Higgs sector may contain additional doublet and antidoublet states. Since in SU(5) GUTs the form of the doublet mass matrix does not affect the predictions in the Yukawa sector, we do not consider a particular scenario for doublet-triplet splitting.

whereas e_u is not suppressed by the mass scale Λ, since it belongs to a renormalizable operator. Furthermore, the real parameters in $\mathbf{Y}_d$ and $\mathbf{Y}_e$ are given by

$$\epsilon_{23} \propto \frac{v_{24}}{\Lambda^2}|\langle\theta_{23}\rangle|\,, \quad \epsilon_{102} \propto \frac{v_{24}}{\Lambda^3}|\langle\theta'_{102}\rangle\langle\theta_{102}\rangle|\,, \quad \epsilon_2 \propto \frac{v_{24}}{\Lambda^3}|\langle\theta'_2\rangle\langle\theta_2\rangle|\,, \quad \epsilon_3 \propto \frac{1}{\Lambda}|\langle\theta_3\rangle|\,, \tag{4.29}$$

where the phase factor $\bar{\omega}$ is equal to $\mathrm{e}^{4\pi i/3}$, corresponding to the phase of $\langle\theta'_{102}\rangle$, and the factor i next to the parameter ϵ_2 in $\mathbf{Y}_d$ and $\mathbf{Y}_e$ is induced by $\langle\theta_2\rangle$. Finally, the real parameters in $\mathbf{Y}_\nu$ read

$$a \propto \frac{|\langle\theta_{23}\rangle|}{\Lambda}\,, \qquad\qquad b \propto \frac{|\langle\theta_{102}\rangle|}{\Lambda}\,, \tag{4.30}$$

and the mass parameters M_A and M_B in $\mathbf{M}_R$ get the complex phases 0 and $-\pi/3$ from the vevs $\langle\xi_1\rangle$ and $\langle\xi_2\rangle$, respectively. If the right-handed neutrinos are integrated out at their corresponding mass scale, the mass matrix of the left-handed neutrinos is calculated by the seesaw formula

$$\mathbf{M}_\nu = \frac{v_u^2}{2}\mathbf{Y}_\nu\mathbf{M}_R^{-1}\mathbf{Y}_\nu^\mathsf{T}\,, \tag{4.31}$$

where $v_u = v\sin\beta$, and $v = 174\,\mathrm{GeV}$ is the EW Higgs vev. Using the neutrino Yukawa matrix and the Majorana mass matrix from Eq. (4.26) and (4.27), we get

$$\mathbf{M}_\nu = \begin{pmatrix} m_b & 0 & 2m_b \\ 0 & m_a & -m_a \\ 2m_b & -m_a & m_a + 4m_b \end{pmatrix}, \quad \text{with} \quad m_a := \frac{v_u^2 a^2}{2M_A},\; m_b := \frac{v_u^2 b^2}{2M_B}\,. \tag{4.32}$$

Note that $\mathbf{M}_\nu$ only depends on the ratios a^2/M_A and b^2/M_B.

4.3.3 Soft SUSY breaking terms

The coefficients in front of each superpotential operator in Eq. (4.25) are in general functions of the SUSY breaking field φ, i.e. beside a constant factor a coefficient contains a term proportional to φ^2/M_P^2, or even higher order terms of φ. Furthermore, after the flavon fields acquired their vevs, the matter sector contains only MSSM fields and the mass scale is given by the EW scale, which is smaller than the gravitino mass.[5] Thus, SUSY breaking takes place in a hidden sector and we can consider the matter sector in the flat limit, where the theory is globally supersymmetric with additional soft SUSY breaking terms (see Section 2.3.3). The mass scale of these terms is determined by the gravitino mass.

The soft trilinear couplings of the squarks and the sleptons have the same structure as the Yukawa matrices in Eq. (4.26), due to the transformation properties of the fields

[5]The only exceptions are the Majorana masses of the right-handed neutrinos, which are typically much bigger than the gravitino mass. However, these heavy masses do not affect the mass scale of the soft trilinear couplings and the soft masses, which is given by $m_{3/2}$. The only soft terms which get a bigger mass scale are bilinear terms of right-handed sneutrinos. Since such terms have no effect on the running of the other soft terms, and the right-handed (s)neutrinos are integrated out at high mass scales, they can safely be ignored.

under the symmetries of the model. However, the different terms of the from $\langle\varphi^2\rangle/M_{\mathrm{P}}^2$ in each operator coefficient give, in general, non-universal contributions to the soft trilinear couplings. These contributions are indicated by an additional parameter k_i, with mass dimension one, in each non-zero entry of the matrices. At the GUT scale the trilinear couplings are then written as

$$\mathbf{A}_u = \begin{pmatrix} k_5 a_u & k_6 b_u & 0 \\ k_6 b_u & k_7 c_u & k_8 d_u \\ 0 & k_8 d_u & k_9 e_u \end{pmatrix}, \qquad \mathbf{A}_d = \begin{pmatrix} 0 & i k_1 \epsilon_2 & 0 \\ k_2 \bar{\omega} \epsilon_{102} & k_3 \epsilon_{23} & 2 k_2 \bar{\omega} \epsilon_{102} - k_3 \epsilon_{23} \\ 0 & 0 & k_4 \epsilon_3 \end{pmatrix},$$

$$\mathbf{A}_e = \begin{pmatrix} 0 & k_2 \bar{\omega} \epsilon_{102} & 0 \\ i k_1 \epsilon_2 & -3 k_3 \epsilon_{23} & 0 \\ 0 & 2 k_2 \bar{\omega} \epsilon_{102} + 3 k_4 \epsilon_{23} & \epsilon_3 \end{pmatrix}, \quad \mathbf{A}_\nu = \begin{pmatrix} 0 & k_{11} b \\ k_{10} a & 0 \\ -k_{10} a & 2 k_{11} b \end{pmatrix}, \tag{4.33}$$

where again left-right notation is used.

Since the three matter 5-plets are embedded into the representation F, which forms a triplet under the family symmetry A_4, the corresponding soft mass matrix has to be proportional to the identity matrix at the GUT scale. Although the matter 10-plets are singlets under A_4, the different transformations under the shaping symmetries require that their soft mass matrix is diagonal as well, but in general it is not proportional to the identity matrix. According to the embedding of the MSSM fields into the GUT representations, the squared soft masses of the squarks and the sleptons have the form

$$\mathbf{m}_{\widetilde{L}}^2 = \mathbf{m}_{\widetilde{d}}^2 = \begin{pmatrix} m_F^2 & 0 & 0 \\ 0 & m_F^2 & 0 \\ 0 & 0 & m_F^2 \end{pmatrix}, \qquad \mathbf{m}_{\widetilde{Q}}^2 = \mathbf{m}_{\widetilde{u}}^2 = m_{\widetilde{e}}^2 = \begin{pmatrix} m_{T_1}^2 & 0 & 0 \\ 0 & m_{T_2}^2 & 0 \\ 0 & 0 & m_{T_3}^2 \end{pmatrix}, \tag{4.34}$$

where the parameters m_F^2 and $m_{T_I}^2$ have mass dimension 2. Moreover, the squared soft masses of the right-handed sneutrinos are given by

$$\mathbf{m}_{\widetilde{\nu}}^2 = \begin{pmatrix} m_{\nu_1}^2 & 0 \\ 0 & m_{\nu_2}^2 \end{pmatrix}, \tag{4.35}$$

and for the squared soft masses of the MSSM Higgs doublets, we use the usual labellings $m_{H_u}^2$ and $m_{H_d}^2$, respectively.

Under the assumption that the gauge kinetic function has the simple form $f_{(r)(s)} = f(\varphi) \cdot \delta_{(r)(s)}$, all three soft masses of the gauginos in the MSSM have the same value $M_{1/2}$ at the GUT scale, because SU(5) is a simple Lie group.

4.4 Numerical analysis of the example model

4.4.1 Model implementation

The Yukawa matrices of the quarks and the leptons, as well as the mass matrix of the right-handed neutrinos at the GUT scale are stated in Eq. (4.26) and (4.27), after spontaneous

breaking of the SU(5) gauge symmetry and the A_4 family symmetry. Moreover, the form of the soft terms at the GUT scale is given in Eqs. (4.33)–(4.35), by assuming spontaneous SUSY breaking in a hidden sector.

In order to reduce the number of free parameters in our model, we fix the values of the three gauge couplings at the GUT scale: $g_3 = 0.698$, $g_2 = 0.697$ and $g_1 = 0.704$, which is consistent with the experimental values at low energies. Furthermore, we choose for the right-handed neutrino masses $|M_A| = 2 \cdot 10^{10}\,\text{GeV}$ and $|M_B| = 2 \cdot 10^{11}\,\text{GeV}$, assuming that we are in the regime of small neutrino Yukawa couplings, where the values of these masses (to a good approximation) only affect the left-handed neutrino mass matrix, which now only depends on the parameters a and b. Finally, we choose $\text{sign}\,\mu = -1$ and assume normal ordering for the left-handed neutrino masses, which is basically predicted by the CSD2 scheme.

- **Parameters**:
  The model contains 30 free parameters: the Yukawa matrices from Eq. (4.26) are specified by the eleven parameters ϵ_2, ϵ_{102}, ϵ_{23}, ϵ_3, a_u, b_u, c_u, d_u, e_u, a, b. Furthermore, there are the eleven parameters k_i in the soft trilinear couplings stated in Eq. (4.33), the six parameters m_F, m_{T_1}, m_{T_2}, m_{T_3}, m_{H_u}, m_{H_d} in the soft masses from Eq. (4.34),[6] and the gaugino mass $M_{1/2}$. Finally, the ratio of the MSSM Higgs vevs $\tan\beta$ is a free parameter of the model as well. All these values (except $\tan\beta$) are input at the GUT scale.

- **Observables**:
  The 30 parameters are fitted to 30 observables at low energies. In the Yukawa sector there are the nine Yukawa couplings y_u, y_c, y_t, y_d, y_s, y_b, y_e, y_μ, y_τ of the quarks and the charged leptons, and the four CKM parameters θ_{12}^{CKM}, θ_{23}^{CKM}, θ_{13}^{CKM}, δ^{CKM}, where the corresponding experimental values at M_Z are given in [94]. Although the values of the charged lepton Yukawa couplings are measured very precisely, we take a standard deviation of 1% of the central value, which roughly corresponds to the precision of the running. In the neutrino sector we fit the three PMNS angles $\sin^2(\theta_{12}^{\text{PMNS}})$, $\sin^2(\theta_{23}^{\text{PMNS}})$, $\sin^2(\theta_{13}^{\text{PMNS}})$, and the two mass-squared differences of the light neutrinos Δm_{21}^2, Δm_{31}^2, where the experimental values are taken from NuFIT 3.0 (2016) [54]. Moreover, we fit the dark matter relic density Ω and the EW Higgs mass m_h, whose experimental values are given in PDG (2016) [102]. For the Higgs mass we take a standard deviation of 3 GeV, which roughly corresponds to the error in the theoretical calculation. Finally, we calculate the branching ratios of the nine flavour violation processes $\mu \to e\gamma$, $\tau \to e\gamma$, $\tau \to \mu\gamma$, $K_L^0 \to \pi^0\bar{\nu}\nu$, $K^+ \to \pi^+\bar{\nu}\nu$, $B_S^0 \to e^+e^-$, $B_S^0 \to \mu^+\mu^-$, $B_S^0 \to e^\pm\mu^\mp$, $B \to \tau\nu$, and the quantity ϵ_K, which gives a measure for CP violation in the Kaon decay $K \to \pi\pi$. The experimental values/bounds of these observables are taken from PDG (2016) [102]. In order to account for the uncertainty in the theoretical calculation of ϵ_K, we normalize the predicted and the experimental value with ϵ_K^{SM}, which is the value calculated by SUSY FLAVOR v2.54 [103–105] for the SM, i.e. we consider the ratio $\epsilon_K/\epsilon_K^{\text{SM}}$ as the observable.

[6] Note that the parameters m_{ν_1} and m_{ν_2} are not included in the fit, because the right-handed (s)neutrinos are integrated out at a high energy scale and $\mathbf{m}_{\tilde{\nu}}^2$ gives a negligible contribution to the running of the other soft masses in the regime where the neutrino Yukawa couplings are $\ll 1$.

- **Predictions**:
  Apart from the observables from above, the model has the capability to predict, among others, the mass spectrum of superpartners of the SM particles, as well as the WIMP-nucleon cross section of dark matter.

4.4.2 Numerical procedure

The numerical procedure for the analysis of the model is the following: we apply 1-loop RGEs of the MSSM to run the Yukawa matrices and the soft terms from the GUT scale $M_{\text{GUT}} = 2 \cdot 10^{16}\,\text{GeV}$ to the SUSY scale M_{SUSY} by using the Mathematica package SusyTC [106], which is an extension of the Mathematica package REAP [107]. The right-handed neutrinos are integrated out at the corresponding mass scales, generating the left-handed neutrino masses, and the SUSY scale is determined dynamically by the geometric mean of the two up-type squark masses which have the largest mixing with the stop flavour eigenstates $\widetilde{t}_1$ and $\widetilde{t}_2$, namely $M_{\text{SUSY}} = \sqrt{m_{\widetilde{t}_1} m_{\widetilde{t}_1}}$. All superpartners of the SM particles are integrated out at that scale, and the MSSM is matched to the SM by taking into account the SUSY threshold corrections. Moreover, the model quantities at the SUSY scale are used to calculate the sparticle spectrum with SusyTC, the masses of the extra MSSM Higgs states with FeynHiggs 2.12.0 [108–115], the properties of dark matter with MicrOMEGAs 4.3.5 [116], and the observables related to flavour violating processes with SUSY FLAVOR v2.54 [103–105]. Finally, we use 1-loop RGEs of the SM in SusyTC to run the Yukawa matrices and the mass matrix of the left-handed neutrinos from the SUSY scale the Z boson mass scale $M_Z = 91.2\,\text{GeV}$. At this energy scale, the Yukawa couplings of the SM fermions, the neutrino masses, as well as the CKM and PMNS angles and phases are calculated.

As a measure for the goodness of the fit we apply the χ^2 function. Moreover, to calculate the posterior density of the parameters and the observables, we perform an MCMC analysis by using an adaptive Metropolis-Hastings algorithm [117]. In order to get a better resolution of the regions with a good fit for the DM relic density, we use ten times the experimental error for Ω in the MCMC analysis. This modification has no influence on the predictions for the other observables. In addition, to avoid a short lifetime of the metastable EW symmetry breaking vacuum, we confine the values of the parameters k_i to the interval $[-10^4\,\text{GeV}, +10^4\,\text{GeV}]$, where the numerical analysis showed, that only trilinear terms may escape this interval, which have no big impact on the low energy observables. We choose all prior distributions to be flat.

4.4.3 Results

Applying the numerical procedure as described in Section 4.4.3, we calculate for each parameter and for each observable the 1σ highest posterior density (HPD) interval and the mode value, i.e. the maximal value of the corresponding density function. The values are listed in Table 4.1 and 4.2, respectively. For the points with lowest χ^2 in the MCMC analysis we checked that the lifetime of the EW vacuum in the presence of unbounded from below (UFB) directions or charge and colour breaking (CCB) minima is much bigger than the age of the universe, by applying the procedures described in [118–121]. The χ^2 values of these best-fit points are at around 20.

In the following we comment on selected results of the MCMC analysis:

- Since all free parameters of our model, including the ones in the soft terms, are fitted by the observables, we can predict the mass spectrum of the SM superpartners and of the extra MSSM Higgs states. The corresponding 1σ HPD intervals of the masses are shown in Figure 4.1. Note that for the SM superpartners the running masses are used. As expected, in all the calculated parameter points in the MCMC analysis the lightest supersymmetric particle is a neutralino $\widetilde{\chi}^0$, because in our model DM matter consists of weakly interacting massive particles, which are given by the LSPs. In addition, in the calculated points the next-to-LSP (NLSP) is either a chargino, a stau or a sneutrino. The heaviest particles in the spectrum are typically the gluino and the up- and down-type squarks. The predicted mass spectrum is at the edge of the reach of 100 TeV pp colliders (see e.g. [122]).

- Using MicrOMEGAs, we calculate in each point of the MCMC analysis the (spin independent) WIMP-nucleon cross section. Since in our model the WIMP is always the lightest neutralino, we can correlate the predictions for the mass of the WIMP and for the cross section with nucleons, as shown in Figure 4.2, where on the x-axis the mass and on the y-axis the cross section is plotted. The darker and the lighter red areas correspond the 1σ and the 2σ HPD regions, respectively, predicted by the model. Moreover, in the same plot we indicate the sensitivity of the XENON1T experiment [123] by a solid blue line, as well as the predicted sensitivity of the future XENONnT experiment by a dashed blue line. We see that there is no overlap of our model prediction with the sensitivity of XENON1T, however, the prediction is in the reach of XENONnT.

- The branching ratio $\mathrm{Br}(\mu \to e\gamma)$ is sensitive to off-diagonal entries in the mass matrix of the charged sleptons, written in the SCKM basis, which mix the selectron and the smuon. Such off-diagonal terms are induced by a 1-2 mixing in the Yukawa matrix of the charged leptons, and non-universal diagonal soft masses in the 2×2 block of the first two families in $m^2_{\widetilde{e}}$. Since in our model a 1-2 mixing in $\mathbf{Y}_e$ is present, we expect a correlation between the parameters m_{T_1} and m_{T_2} from Eq. (4.34), in order that the experimental bound of $\mathrm{Br}(\mu \to e\gamma)$ is satisfied. In Figure 4.3 we show the combined predictions of these two parameters, where m_{T_1} is plotted on the x-axis and m_{T_2} on the y-axis. The 1σ and the 2σ HPD regions from the MCMC analysis are displayed by the darker and lighter red areas, respectively. We see that our model predicts a mild correlation between these two parameters.

- The predictions of the MCMC analysis for the branching ratios $\mathrm{Br}(K^+ \to \pi^+ \bar{\nu}\nu)$, $\mathrm{Br}(B_S^0 \to \mu^+\mu^-)$ and $\mathrm{Br}(B \to \tau\nu)$ lie at the edge of the 1σ intervals of the experimental data, as shown in Table (4.2). More precise measurements of these quantities in future experiments can test our model. Moreover, for the branching ratios $\mathrm{Br}(K_L^0 \to \pi^0 \bar{\nu}\nu)$ and $\mathrm{Br}(B_S^0 \to e^+e^-)$ our model makes precise predictions too, however the values are far below the experimental sensitivities.

- Typically, our model predicts values below 40° for the PMNS angle $\theta_{23}^{\mathrm{PMNS}}$, which is in tension with the experimental data where the central value is higher. The 1σ HPD interval from the MCMC analysis is given by $\theta_{23}^{\mathrm{PMNS}} = 39.9^\circ \pm 0.3^\circ$, which is still

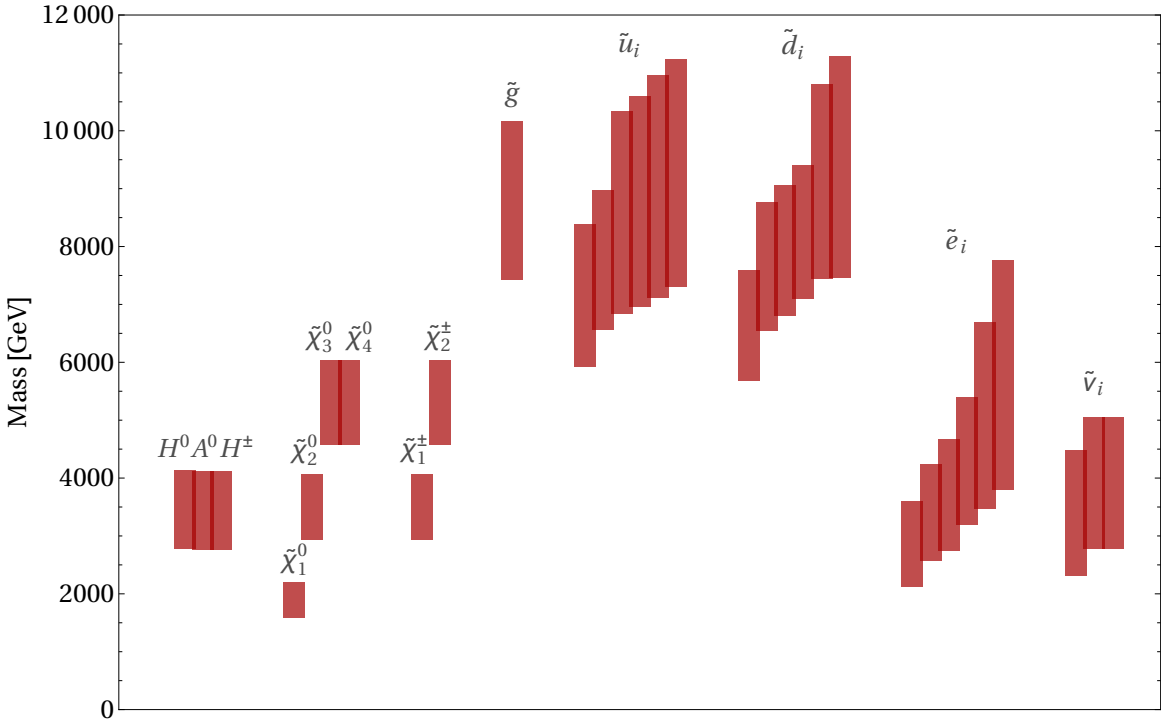

Figure 4.1: The 1σ HPD intervals of the SM superpartners and of the extra MSSM Higgs states from the MCMC analysis, indicated as red bars. The LSP is always the lightest neutralino $\tilde{\chi}_1^0$, which corresponds to the WIMP of DM.

within the 2σ range of the experimental data from NuFIT 3.0 (2016) [54], as used in the analysis. However, the newest data from NuFIT 4.1 (2019) [54] shows, that our prediction lies now even outside the experimental 3σ range given by $[40.8°, 51.3°]$. As can be seen from the plots provided by NuFIT, the χ^2 projection for this observable does not follow a Gaussian distribution, and the predicted value of $39.9°$ is even beyond a χ^2 of 15. This implies that in the context of the new data, our model is disfavoured. Though, in order to see whether the model is excluded or not, a fit with the data from NuFIT 4.1 (2019) [54] would be required.

In summary, with the above numerical analysis we showed that the integration of a SUSY breaking sector in a flavour GUT model, which specifies the form of the soft terms at the GUT scale, has the potential to be very predictive for the mass spectrum of the sparticles and the extra Higgs states, as well as for properties of the WIMP of cold DM, given by the lightest neutralino. Furthermore, precise predictions for branching ratios of flavour violating processes can be made. The predictions have the potential to be tested by a next generation of experiments. Although the example model we considered in this chapter is in tension with the experimental data in the neutrino sector, the general considerations from above can be applied to different flavour GUT models.

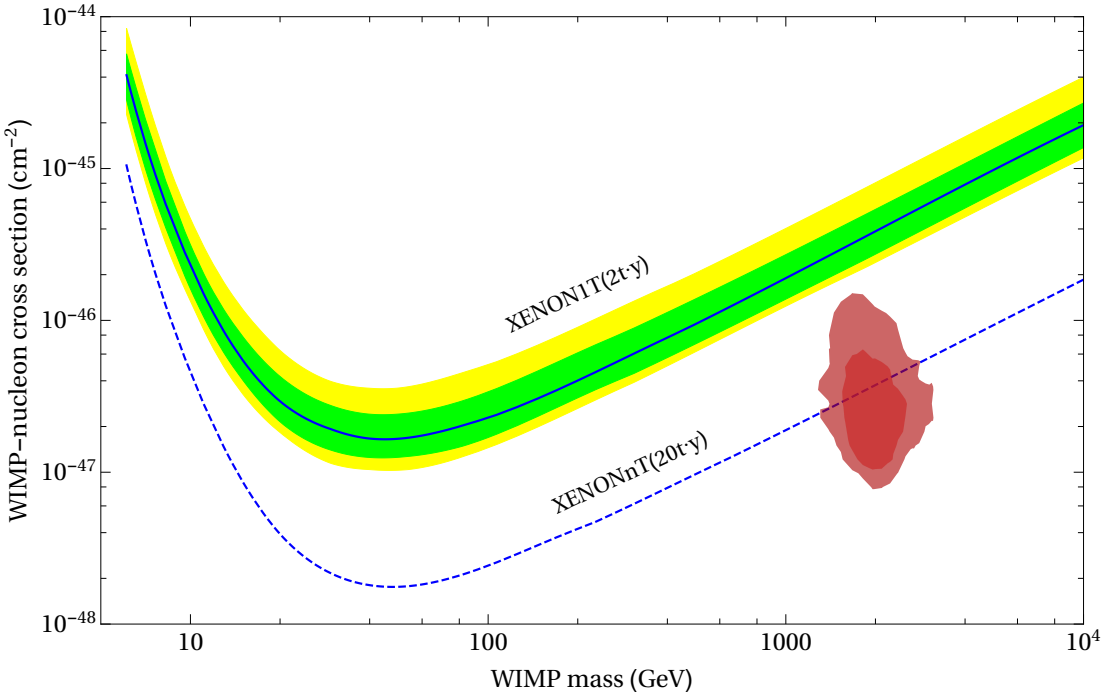

Figure 4.2: The spin-independent WIMP-nucleon cross section as a function of the WIMP mass. The darker and lighter read areas represent the 1σ and 2σ HPD regions from the MCMC analysis. The solid and dashed blue curves indicate the sensitivities of the XENON1T and the (planed) XENONnT experiment [123], respectively. In addition, the green and yellow bands correspond to the 1σ and 2σ sensitivities of XENON1T.

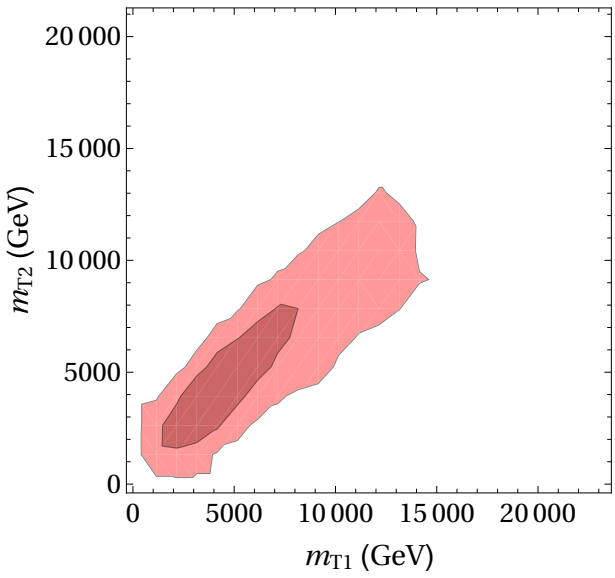

Figure 4.3: Correlation plot of the parameters m_{T_1} (on the x-axis) and m_{T_2} (on the y-axis) given in Eq. (4.34). The 1σ and 2σ HPD regions from the MCMC analysis correspond to the darker and lighter read areas, respectively.

Table 4.1: List of the mode values and the 1σ HPD intervals of the model parameters from the MCMC analysis. The values of the k_i are confined to the interval $[-10^4\,\mathrm{GeV}, +10^4\,\mathrm{GeV}]$, and the symbol $-$ indicates a (almost) uniform distribution of the respective parameter within that prior. The two values of a_u correspond to the two solutions of the (leading order) equation $y_u \approx |(\mathbf{Y}_u)_{11} - (\mathbf{Y}_u)_{12}^2/(\mathbf{Y}_u)_{22}|$, where $(\mathbf{Y}_u)_{11} = a_u$. The 1σ HPD interval of a_u is given by the union of the two stated intervals.

Parameter		MCMC	
ϵ_2	in 10^{-3}	1.639	$^{+0.971}_{-0.942}$
ϵ_{102}	in 10^{-3}	-1.428	$^{+0.071}_{-0.102}$
ϵ_{23}	in 10^{-3}	-7.369	$^{+0.423}_{-0.437}$
ϵ_3	in 10^{-1}	-4.226	$^{+0.159}_{-0.205}$
a_u	in 10^{-5}	-1.182	$^{+0.127}_{-0.118}$
		-0.741	$^{+0.117}_{-0.109}$
b_u	in 10^{-4}	1.102	$^{+0.054}_{-0.060}$
c_u	in 10^{-3}	-1.069	$^{+0.048}_{-0.046}$
d_u	in 10^{-3}	9.403	$^{+0.811}_{-0.877}$
e_u	in 10^{-1}	4.629	$^{+0.154}_{-0.143}$
a	in 10^{-3}	3.848	$^{+0.044}_{-0.046}$
b	in 10^{-3}	4.551	$^{+0.047}_{-0.060}$
$\tan\beta$		47.68	$^{+4.95}_{-3.11}$
k_1	in GeV	-8122	$^{+9686}_{-1.878}$
k_2	in GeV	$-$	
k_3	in GeV	8397	$^{+1603}_{-8233}$
k_4	in GeV	2	$^{+4201}_{-4745}$
k_5	in GeV	$-$	
k_6	in GeV	$-$	
k_7	in GeV	$-$	
k_8	in GeV	$-$	
k_9	in GeV	-3551	$^{+4062}_{-3679}$
k_{10}	in GeV	$-$	
k_{11}	in GeV	$-$	
m_F	in GeV	2595	$^{+1847}_{-1965}$
m_{T_1}	in GeV	3454	$^{+3299}_{-1908}$
m_{T_2}	in GeV	3314	$^{+2842}_{-1644}$
m_{T_3}	in GeV	4564	$^{+1930}_{-1556}$
m_{H_u}	in GeV	3294	$^{+2043}_{-2500}$
m_{H_d}	in GeV	2297	$^{+1581}_{-2171}$
$M_{1/2}$	in GeV	4193	$^{+638}_{-761}$

Table 4.2: List of the observables used to fit the model. For each observable the experimental central value and the 1σ range are stated, as well as the mode value and the 1σ HPD interval from the MCMC analysis. The experimental values of the Yukawa couplings and the CKM parameters are taken from [94], the ones related to the neutrino sector from NuFIT 3.0 (2016) [54] and the remaining ones from PDG (2016) [102]. For y_e, y_μ, y_τ we take a relative error of 1%, reflecting the precision of the running, and for m_h an error of $\pm 3\,\text{GeV}$, reflecting the uncertainty in the theoretical calculation. The symbol $\star$ indicates that ten times the listed experimental error of Ω is used in the MCMC analysis.

Observable		Experiment		MCMC	
y_u	in 10^{-6}	7.4	$^{+1.5}_{-3.0}$	7.0	$^{+1.8}_{-2.7}$
y_c	in 10^{-3}	3.60	± 0.11	3.61	$^{+0.10}_{-0.12}$
y_t		0.9861	$^{+0.0086}_{-0.0087}$	0.9883	$^{+0.0078}_{-0.0097}$
y_d	in 10^{-5}	1.58	$^{+0.23}_{-0.10}$	1.44	$^{+0.05}_{-0.05}$
y_s	in 10^{-4}	3.12	$^{+0.17}_{-0.16}$	3.55	$^{+0.12}_{-0.10}$
y_b	in 10^{-2}	1.639	± 0.015	1.636	$^{+0.016}_{-0.014}$
y_e	in 10^{-6}	2.795	$\pm 1\%$	2.808	$^{+0.027}_{-0.029}$
y_μ	in 10^{-4}	5.900	$\pm 1\%$	5.857	$^{+0.054}_{-0.064}$
y_τ	in 10^{-2}	1.003	$\pm 1\%$	1.003	$^{+0.009}_{-0.010}$
θ_{12}^{CKM}	in 10^{-1}	2.2735	± 0.0072	2.2729	$^{+0.0072}_{-0.0078}$
θ_{23}^{CKM}	in 10^{-2}	4.208	± 0.064	4.211	$^{+0.057}_{-0.073}$
θ_{13}^{CKM}	in 10^{-3}	3.64	± 0.13	3.676	$^{+0.116}_{-0.142}$
δ^{CKM}		1.208	± 0.054	1.207	$^{+0.015}_{-0.014}$
$\sin^2(\theta_{12}^{\text{PMNS}})$	in 10^{-1}	3.08	$^{+0.13}_{-0.12}$	3.08	$^{+0.02}_{-0.02}$
$\sin^2(\theta_{23}^{\text{PMNS}})$	in 10^{-1}	4.51	$^{+0.38}_{-0.25}$	4.11	$^{+0.06}_{-0.05}$
$\sin^2(\theta_{13}^{\text{PMNS}})$	in 10^{-2}	2.19	± 0.10	2.03	$^{+0.05}_{-0.04}$
Δm_{21}^2	in 10^{-5}	7.49	$^{+0.19}_{-0.17}$	7.671	$^{+0.174}_{-0.173}$
Δm_{31}^2	in 10^{-3}	2.477	± 0.042	2.505	$^{+0.036}_{-0.042}$
m_h	in GeV	125.6	± 3.0	125.7	$^{+0.9}_{-0.8}$
Ω	in 10^{-1}	1.186	$\pm 0.020\star$	1.219	$^{+0.219}_{-0.193}$
$\mu \to e\gamma$	in 10^{-13}	≤ 5.7		≤ 1.9	
$\tau \to e\gamma$	in 10^{-16}	$\leq 3.3 \cdot 10^8$		≤ 9.8	
$\tau \to \mu\gamma$	in 10^{-13}	$\leq 4.4 \cdot 10^5$		≤ 4.3	
$K_L^0 \to \pi^0 \bar{\nu}\nu$	in 10^{-11}	$\leq 2.6 \cdot 10^3$		2.839	$^{+0.007}_{-0.011}$
$K^+ \to \pi^+ \bar{\nu}\nu$	in 10^{-10}	1.73	$^{+1.15}_{-1.05}$	0.7798	$^{+0.0013}_{-0.0021}$
$B_S^0 \to e^+e^-$	in 10^{-14}	$\leq 2.8 \cdot 10^7$		4.97	$^{+0.55}_{-0.74}$
$B_S^0 \to \mu^+\mu^-$	in 10^{-9}	3.1	± 0.7	2.12	$^{+0.24}_{-0.32}$
$B_S^0 \to e^\pm\mu^\mp$	in 10^{-20}	$\leq 1.1 \cdot 10^{12}$		≤ 1.7	
$B \to \tau\nu$	in 10^{-4}	1.14	± 0.27	0.886	$^{+0.005}_{-0.006}$
$\epsilon_K^{\text{exp}}/\epsilon_K^{\text{SM}}$		1.09	± 0.16	1.01	$^{+0.10}_{-0.10}$

CHAPTER 5

Predicting δ^{PMNS}, $\theta_{23}^{\mathrm{PMNS}}$ and fermion mass ratios from flavour GUTs with CSD2

5.1 Motivation

Due to the embedding of the SM representations into bigger GUT representations, Grand Unified Theories are a natural framework to address the favour puzzle, namely to explain the observed masses, as well as the mixing angles and the CP violation phases in the fermion sector. In theories with an SU(5) gauge group, the Yukawa terms of the charged leptons originate from the same GUT operators as the ones of the down-type quarks, thus we typically expect that the charged lepton Yukawa matrix features some non-zero mixing of the order of the CKM angles. However, the observed mixing in the lepton sector is much bigger than the one in the quark sector, which implies that the main contribution to the mixing angles in the PMNS matrix must originate from the neutrino mass matrix. The mixing from the charged lepton sector then gives subleading corrections to the leading order mixing pattern of the neutrino sector. A suitable class of models to explain such a mixing pattern are flavour GUT models with a spontaneously broken family symmetry by flavon vevs.

A viable leading order mixing pattern in the neutrino sector is given by tri-bimaximal (TB) mixing [124, 125]. In flavour models with spontaneously broken family symmetry, the TB mixing pattern of the neutrino mass matrix can be realized via a type I seesaw mechanism with so-called Constrained Sequential Dominance (CSD, also referred to as CSD1) [126], which assumes the existence of two right-handed neutrinos. In this scenario, the columns of the neutrino Yukawa matrix are proportional to the two flavon vev alignments $(0, 1, -1)$ and $(1, 1, 1)$, respectively, in family space. The TB mixing pattern implies that in leading order the PMNS angle $\theta_{13}^{\mathrm{PMNS}}$ originates solely from the charged lepton sector and is given by the identity $\theta_{13}^{\mathrm{PMNS}} \approx \theta_{12}^{eL}/\sqrt{2}$. However, since in the context of SU(5) GUTs the 1-2 left angle θ_{12}^{eL} of the charged leptons is typically fixed by the values of the charged fermion masses and the CKM parameters, the above identity for $\theta_{13}^{\mathrm{PMNS}}$ is usually too stringent to reproduce the experimental value.

An improved version of Constrained Sequential Dominance is given by CSD2 [101]. In this setup, one of the flavon vevs, which generate the texture of the neutrino Yukawa matrix, is aligned in the direction $(0, 1, -1)$, and the other one in the direction $(1, 2, 0)$ or $(1, 0, 2)$, which corresponds to two different implementations of CSD2. The CSD2 scheme adopts the feature $\theta_{12}^{\nu} \approx 35^\circ$ for the 1-2 angle in the neutrino sector from TB mixing, which is close to the measured value. On the other hand, in contrast to the TB mixing pattern, CSD2 predicts a deviation of θ_{23}^{ν} from 45° as well as a non-vanishing θ_{13}^{ν}, such

that $\theta_{13}^{\text{PMNS}}$ is not solely generated from the charged lepton sector. In the context of SU(5) GUT models with the feature, that the mixing in the charged lepton sector is determined by the GUT relations, CSD2 offers an attractive setup in the neutrino sector to predict the PMNS angles and phases.

The purpose of this chapter is to systematically investigate a class of predictive SU(5) GUT models which feature the CSD2 setup in the neutrino sector. By performing a fit to the experimental data, we determine the most promising model candidates and investigate the predictive power of this class of models.

This chapter is based on the publication [2] and is organized as follows: in Section 5.2 the class of SU(5) models is specified, including a discussion on the chosen texture of the fermion sector. In Section 5.3 we state the predictive power of the models and describe the procedure for the numerical analysis. The results of the analysis are then discussed in Section 5.4.

5.2 CSD2 in a simple and predictive GUT setup

5.2.1 General model setup

The class of models we consider in this chapter are supersymmetric SU(5) models, where we choose the texture in the Yukawa sector at the GUT scale to be as predictive as possible. However, we do not consider any specific flavour model to generate this texture dynamically, as for example by spontaneous breaking of a family symmetry by flavon vevs, in order that the analysis is as model independent as possible. Moreover, we also do not consider any specific setup to achieve spontaneous GUT symmetry breaking.

We assume the standard embedding of the fermionic MSSM multiplets into the representations F_I, T_I, and, N_K, where F_I is a $\overline{\mathbf{5}}$, T_I a $\mathbf{10}$ and N_K a $\mathbf{1}$ of SU(5). The family index I runs from 1 to 3, while K can in principle be any positive integer, which means that the number of right-handed neutrinos can be different from three. The MSSM Yukawa terms emerge from SU(5) superpotential terms of the form

$$(\mathbf{Y}_u)_{IJ}: \qquad T_I\, T_J\, X\,, \tag{5.1}$$

$$(\mathbf{Y}_d)_{IJ}\ \&\ (\mathbf{Y}_e^{\mathsf{T}})_{IJ}: \qquad T_I\, F_J\, Y\,, \tag{5.2}$$

$$(\mathbf{Y}_\nu)_{IK}: \qquad F_I\, N_K\, Z\,, \tag{5.3}$$

where X, Y, Z represent Higgs fields, or products of Higgs fields, which are in general different for different tuples of family indices (I, J). In particular, X, Y, Z consist of SU(5) representations which contain the MSSM Higgs doublets, and possibly additional representations which acquire SM singlet GUT scale vevs. Since the down-quark and charged lepton Yukawa operators are embedded into the same GUT operator, the entries of the two Yukawa matrices are related by Clebsch-Gordan coefficients (or linear combinations of them) at the GUT scale. The CG coefficients depend on the specific choice of the Higgs field(s) Y and on the construction of the SU(5) invariant.

Since we do not consider any specific flavour model, the appropriate framework to specify the superpotential of the Yukawa sector at the GUT scale is the MSSM, by taking the SU(5) boundary conditions into account. For the definition of the superpotential the left-right convention from Eq. (2.219) is used.

Although we study the model setup in the context of supersymmetry, we are mainly interested in the predictions for the Yukawa couplings, the left-handed neutrino masses, and the CKM and PMNS parameters. The "SUSY part" of the model affects the predictions mainly via the RG running of the parameters from the GUT scale to low energy scales, and via the threshold corrections at the SUSY scale [127–131]. To implement the effect of the SUSY threshold corrections in a model independent way, we do not consider a particular texture for the soft SUSY breaking terms, but parametrize the threshold corrections directly by a set of free parameters [94], as discussed in Section 5.2.3.

5.2.2 Texture of the Yukawa sector

In the following we discuss the choice of the texture in the Yukawa sector at the GUT scale, which is based on the principles of simplicity and predictivity:

- **Phase sum rule for δ^{CKM}**:
  In order to predict a viable CP violating phase δ^{CKM} in the CKM matrix, we implement a unitary triangle angle $\alpha_{\mathrm{UT}} = \delta_{12}^{dL} - \delta_{12}^{uL} \approx 90^\circ$ [100], where δ_{12}^{dL} and δ_{12}^{uL} are the phases of the left 1-2 mixings in the down- and up-quark sector, respectively. A necessary condition for the phase sum rule in the quark sector to work are vanishing mixing angles $\theta_{13}^{uL} = \theta_{13}^{dL} = 0$ of the left-handed quarks. In addition, the generation of α_{UT} by a single imaginary entry in the up- or down-quark Yukawa matrix has the attractive feature, that it can easily be generated by discrete flavon vev alignments in flavour models with spontaneous CP violation (cf. [99]).

- **Simplicity in $\mathbf{Y}_d$**:
  We choose a $2 + 1$ block diagonal structure for $\mathbf{Y}_d$, meaning that there is no mixing between the first two families and the third family in the down-sector, i.e. $\theta_{23}^{dL} = \theta_{13}^{dL} = 0$, which is consistent with the conditions for the phase sum rule in the previous point. Thus, all CKM mixing between the first two and the third family comes from the up-sector, and only the largest CKM mixing angle $\theta_{12}^{\mathrm{CKM}}$ gets also a contribution from the down-sector. The structure can be further simplified by choosing $(\mathbf{Y}_d)_{11} = 0$. This still allows to fit the three down-type masses as well as the θ_{12}^{dL} contribution to the CKM angle. Moreover, it ensures that the right 1-2 mixing, which is used in the lepton sector, does not vanish. Complex phases in $\mathbf{Y}_d$ can be absorbed by redefinitions of the fields. In particular, with the freedom of the three phases in T_I we can make one entry in each row real. On the other hand, since in flavour models with flavon fields the F_I typically form a triplet under the family symmetry, there is only one overall phase which can be chosen. However, a redefinition of F_I would also modify the form of the neutrino mass matrix, so we do not absorb the one remaining phase in $\mathbf{Y}_d$ by F_I. Instead, we use this freedom to absorb a phase in the neutrino mass matrix, as discussed below. The texture of the down-quark Yukawa matrix at the GUT scale is thus given by

$$\mathbf{Y}_d = \begin{pmatrix} 0 & z & 0 \\ ye^{-i\gamma} & x & 0 \\ 0 & 0 & y_b \end{pmatrix}, \tag{5.4}$$

where x, y, z and y_b are real, positive parameters. Since x and z are positive, the phase of the left 1-2 mixing vanishes, i.e. $\delta_{12}^{dL} = 0$. The remaining complex phase γ will affect CP violation in the lepton sector.

- **CP violation in $\mathbf{Y}_u$**:
  Since the Yukawa terms in the up-quark sector originate from operators as in Eq. (5.1), the corresponding Yukawa matrix is symmetric at the GUT scale. In order that the conditions for the phase sum rule in the quark sector are satisfied, we require that the 1-3 mixing in $\mathbf{Y}_u$ vanishes. In a very good approximation this is fulfilled by setting $(\mathbf{Y}_u)_{13} = 0$ (and also $(\mathbf{Y}_u)_{31} = 0$ due to the symmetry of the matrix). Furthermore, because there is no contribution from the down-quark sector to the unitarity triangle α_{UT}, the phase of the left 1-2 mixing must have the value $\delta_{12}^{uL} = -\frac{\pi}{2}$. Due to the texture zero in the entries $(\mathbf{Y}_u)_{13}$ and $(\mathbf{Y}_d)_{13}$ the relation

$$\theta_{13}^{\mathrm{CKM}} \approx \theta_{12}^{uL}\, \theta_{23}^{uL} \tag{5.5}$$

  holds, where the 2-3 angle is given by $\theta_{23}^{uL} \approx \theta_{23}^{\mathrm{CKM}}$. Because $\mathbf{Y}_d$ has a block diagonal structure, the CKM angles $\theta_{13}^{\mathrm{CKM}}$ and $\theta_{23}^{\mathrm{CKM}}$ are entirely generated from the up-quark sector, whereas $\theta_{12}^{\mathrm{CKM}}$ gets contributions from the up- and the down-quark sector. We implement the phase $\delta_{12}^{uL} = -\frac{\pi}{2}$ by choosing all entries to be real, except the $(\mathbf{Y}_u)_{12}$ (and $(\mathbf{Y}_u)_{21}$) entry to be imaginary.[1] The texture of $\mathbf{Y}_u$ is thus given by

$$\mathbf{Y}_u = \begin{pmatrix} u_1 & -iu_2 & 0 \\ -iu_2 & u_3 & u_4 \\ 0 & u_4 & u_5 \end{pmatrix}, \tag{5.6}$$

  where the u_i are real, positive parameters. These parameters are used to fit the three up-type masses m_u, m_c and m_t, as well as the two CKM angles $\theta_{13}^{\mathrm{CKM}}$ and $\theta_{23}^{\mathrm{CKM}}$. Note that the phases of the T_I are set by the form of $\mathbf{Y}_d$, thus the basis for $\mathbf{Y}_u$ is fixed.

- **Single operator dominance**:
  In our model setup we assume single operator dominance, that is, for each tuple of family indices (I, J) the corresponding Yukawa terms are dominantly generated by a single (non-)renormalizable GUT operator as in Eqs. (5.1)–(5.3). Since at the SU(5) level $\mathbf{Y}_d$ and $\mathbf{Y}_e^{\mathsf{T}}$ are present in the same operator, cf. Eq (5.2), the entries of the two matrices are related by Clebsch-Gordan coefficients. For each entry, the value of the corresponding CG coefficient depends on the form of Y, which represents a Higgs field, or a product of Higgs fields. Thus, according to Eq. (5.4) $\mathbf{Y}_e$ has the form

$$\mathbf{Y}_e = \begin{pmatrix} 0 & c_y y e^{-i\gamma} & 0 \\ c_z z & c_x x & 0 \\ 0 & 0 & y_\tau \end{pmatrix}, \tag{5.7}$$

[1] Note that any implementation of the phase sum rule leads to the same predictions. Thus, with no loss of generality we can us the particular ansatz from Eq. (5.6) for the implementation of the up-quark Yukawa matrix.

where c_x, c_y and c_z label CG coefficients. In an explicit model there is also a CG coefficient relating y_b and y_τ, e.g. $y_\tau/y_b = 1$ (i.e. b-τ unification [132]) or $y_\tau/y_b = 3/2$ (see for example [133]), which gives an additional constraint on the sparticle spectrum via the SUSY threshold corrections. However, in order to be as model independent as possible, we will simply fit these two parameters to the experimental data. Furthermore, since $\mathbf{Y}_d$ and $\mathbf{Y}_e^\mathsf{T}$ are connected via the CG coefficients, the parameters x, y and z are used to fit the masses of the first two families in the down-quark and charged lepton sector, as well as to generate a suitable angle θ_{12}^{dL} such that, in combination with the contribution from the up-quark sector, the CKM angle θ_{12}^{CKM} is predicted correctly. Since θ_{12}^{CKM} and the electron and muon masses m_e and m_μ are very well measured, x, y and z are basically fixed by these three observables. The mass ratio m_d/m_s, which is approximately invariant under SUSY threshold corrections, is then predicted by the set of CG coefficients, whereas the overall scale of the two masses can be adjusted by the SUSY threshold parameter η_q of the first two families in the down-quark sector (see Section 5.2.3). Moreover, the left-mixing angle θ_{12}^{eL} in the charged lepton sector is determined as well and is typically small, namely of the order of the Cabibbo angle.

- **CSD2 in the neutrino sector**:
  We choose the CSD2 scheme [101] for the neutrino sector, which assumes two right-handed neutrinos with a Majorana mass matrix

$$\mathbf{M}_R = \begin{pmatrix} M_A & 0 \\ 0 & M_B \end{pmatrix} . \tag{5.8}$$

  Furthermore, the neutrino Yukawa matrix can be implemented in two different ways, namely

$$\mathbf{Y}_\nu^{(102)} = \begin{pmatrix} 0 & b \\ a & 0 \\ -a & 2b \end{pmatrix} , \qquad \mathbf{Y}_\nu^{(120)} = \begin{pmatrix} 0 & b \\ a & 2b \\ -a & 0 \end{pmatrix} , \tag{5.9}$$

  based on the two different flavon vev alignments $(1,0,2)$ or $(1,2,0)$ in family space, which determine the form of the second column of $\mathbf{Y}_\nu$. By using the seesaw formula

$$\mathbf{M}_\nu = \frac{v_u^2}{2} \mathbf{Y}_\nu \mathbf{M}_R^{-1} \mathbf{Y}_\nu^\mathsf{T} , \tag{5.10}$$

  and the textures from Eq. (5.8) and (5.9), the mass matrices for the left-handed

neutrinos are then given by:

$$\mathbf{M}_\nu^{(102)} = m_a \begin{pmatrix} 0 & 0 & 0 \\ 0 & 1 & -1 \\ 0 & -1 & 1 \end{pmatrix} + m_b \begin{pmatrix} 1 & 0 & 2 \\ 0 & 0 & 0 \\ 2 & 0 & 4 \end{pmatrix} = m_a \begin{pmatrix} \epsilon e^{i\alpha} & 0 & 2\epsilon e^{i\alpha} \\ 0 & 1 & -1 \\ 2\epsilon e^{i\alpha} & -1 & 1 + 4\epsilon e^{i\alpha} \end{pmatrix}, \tag{5.11}$$

$$\mathbf{M}_\nu^{(120)} = m_a \begin{pmatrix} 0 & 0 & 0 \\ 0 & 1 & -1 \\ 0 & -1 & 1 \end{pmatrix} + m_b \begin{pmatrix} 1 & 2 & 0 \\ 2 & 4 & 0 \\ 0 & 0 & 0 \end{pmatrix} = m_a \begin{pmatrix} \epsilon e^{i\alpha} & 2\epsilon e^{i\alpha} & 0 \\ 2\epsilon e^{i\alpha} & 1 + 4\epsilon e^{i\alpha} & -1 \\ 0 & -1 & 1 \end{pmatrix}, \tag{5.12}$$

where the complex mass parameters m_a and m_b are defined as

$$m_a := \frac{v_u^2 a^2}{2M_A}, \qquad m_b := \frac{v_u^2 b^2}{2M_B}, \tag{5.13}$$

while their ratio is parametrized by the modulus ϵ and the phase α:

$$\frac{m_b}{m_a} \equiv \epsilon e^{i\alpha}. \tag{5.14}$$

The overall phase of the F_I can be used to absorb the phase of m_a, thus the left-handed neutrino mass matrices in Eq. (5.11) and (5.12) are parametrized by the three real, positive parameters m_a, ϵ and α. While m_a determines the overall scale of the neutrino masses, the mixings and phases in the neutrino sector are parametrized by ϵ and α.

In our model setup, the PMNS matrix gets contributions from the neutrino sector, as well as from the 1-2 mixing in the charged lepton sector, which is typically small, i.e. $\theta_{12}^{eL} \ll 1$. Since in the CSD2 scheme the mass hierarchy $M_A \ll M_B$ of the right-handed neutrinos is assumed, we get from Eq. (5.13) and (5.14) that $\epsilon \ll 1$. Thus, we can use ϵ and θ_{12}^{eL} for a parameter expansion of the PMNS matrix. According to Eqs. (B.15)–(B.17) and Eqs. (B.20)–(B.22), the expansion of the PMNS angles reads

$$\theta_{12}^{\text{PMNS}} \approx 35.3^\circ - \frac{\theta_{12}^{eL}}{\sqrt{2}} \cos\gamma, \tag{5.15}$$

$$\theta_{13}^{\text{PMNS}} \approx \frac{1}{\sqrt{2}} \left(\epsilon^2 + {\theta_{12}^{eL}}^2 \pm 2\epsilon\theta_{12}^{eL} \cos(\alpha + \gamma)\right)^{1/2}, \tag{5.16}$$

$$\theta_{23}^{\text{PMNS}} \approx 45^\circ \mp \epsilon \cos\alpha, \tag{5.17}$$

for the two CSD2 scenarios $\mathbf{M}_\nu^{(102)}$ and $\mathbf{M}_\nu^{(120)}$, respectively (indicated by the $\pm$ and the $\mp$ sign), where γ is the complex phase from $\mathbf{Y}_e$ in Eq. (5.7).

Moreover, the mass hierarchy $M_A \ll M_B$ of the right-handed neutrinos in CSD2 implies normal ordering for the left-handed neutrino masses, where the lightest mass m_{ν_1} is predicted to be zero. The two parameters m_a and ϵ in $\mathbf{M}_\nu$ are then used to fit the non-zero neutrino masses m_{ν_2} and m_{ν_3}, which are represented by the two

mass-squared differences Δm^2_{21} and Δm^2_{31}, respectively. In addition, since θ_{12}^{eL} is fixed by the observables in the charged lepton and quark sector, the values of the two remaining parameters α and γ from $\mathbf{M}_\nu$ and $\mathbf{Y}_e$ determine the three angles, as well as the CP violating and Majorana phases of the PMNS matrix. Since the 2-3 angle is least accurately measured, the two parameters are basically fixed by $\theta_{12}^{\rm PMNS}$ and $\theta_{13}^{\rm PMNS}$, and we can view $\theta_{23}^{\rm PMNS}$, $\delta^{\rm PMNS}$ and $\varphi_2^{\rm PMNS}$ as predicted quantities. Note that only the Majorana phase $\varphi_2^{\rm PMNS}$ is physical, since the lightest neutrino mass vanishes.

The simple and predictive texture of the charged fermion Yukawa matrices in Eq. (5.4), (5.6) and (5.7), and the left-handed neutrino mass matrix in Eq. (5.11) or (5.12), depending on the implementation of CSD2, contains a significantly reduced set of parameters, such that, generally speaking, this class of models is able to make predictions for the following observables:

predicted quantity	root cause
$\delta^{\rm CKM}$	phase sum rule
m_d/m_s	GUT connection
$\theta_{23}^{\rm PMNS}$	$\mathbf{Y}_e$ texture and CSD2
$\delta^{\rm PMNS}$	$\mathbf{Y}_e$ texture and CSD2
$\varphi_2^{\rm PMNS}$	$\mathbf{Y}_e$ texture and CSD2

In addition to these observables, the charged lepton mixing angle θ_{12}^{eL} is predicted as well, which is an interesting quantity from the point of view of model building. The value of θ_{12}^{eL} can discriminate between different schemes in the neutrino sector, which are combined with the same setup in the charged fermion sector. A detailed analysis of the class of models, by taking the different energy scales and the RG running into account, is done Section 5.3.

5.2.3 Candidates for GUT operators in the Yukawa sector

The value of each of the Clebsch-Gordan coefficients c_x, c_y and c_z in $\mathbf{Y}_e$ depends on the particular choice of the Higgs field(s) Y in the SU(5) operator in Eq. (5.2). A classification of the available CG coefficients in such operators has been done in [133, 134] for superpotential operators up to dimension four, where H_d is either embedded into a $\overline{\mathbf{5}}$ or $\overline{\mathbf{45}}$ and the SM singlet GUT scale vev originates from a **24** or **75**. Since the exact relations between $\mathbf{Y}_d$ and $\mathbf{Y}_e^{\rm T}$ via CG coefficients only hold at the GUT scale, but get modified by the RG running and the SUSY threshold corrections, we consider the following double ratio d of Yukawa couplings

$$d := \frac{y_\mu y_d}{y_e y_s}\,, \tag{5.18}$$

in order to determine which combinations of c_x, c_y and c_z are not suitable to reproduce the experimental values of the Yukawa couplings at low energies. In a good approximation, at

the GUT scale the double ratio can entirely be expressed in terms of CG coefficients

$$d\big|_{M_{\rm GUT}} = \frac{y_\mu y_d}{y_e y_s}\Big|_{M_{\rm GUT}} \approx \left|\frac{c_x^2}{c_y c_z}\right|, \tag{5.19}$$

where for the second identity we used the approximate formulas for the Yukawa couplings of the first and second family

$$y_d \approx \left|\frac{yz}{x}\right|, \qquad y_s \approx |x|, \qquad y_e \approx \left|\frac{c_y c_z}{c_x}\right|\left|\frac{yz}{x}\right|, \qquad y_\mu \approx |c_x||x|, \tag{5.20}$$

assuming that $x \gg y, z$. On the other hand, at low energies (e.g. at the Z boson mass scale) the double ratio is given by the experimental data [94]:

$$d\big|_{M_Z} = \frac{m_\mu m_d}{m_e m_s} = 10.7\,^{+1.6}_{-0.9}, \tag{5.21}$$

where the uncertainty is mostly induced by the quark masses m_s and m_d. The expressions for d at $M_{\rm GUT}$ and M_Z in Eq. (5.19) and (5.21) are connected, because the double ratio is approximately stable under RG running and SUSY threshold corrections [127–131]. This follows directly from the fact that already the ratios y_d/y_s and y_μ/y_e of Yukawa couplings within the same sector have this property, which is discussed in the following:

- **RG running:**
  Since in the down-quark and charged lepton sector the Yukawa couplings of the third family are much bigger than the ones of the first and second family, the 1-loop RGEs in the MSSM (see e.g. [106,107,135]) of y_d, y_s, y_e and y_μ take the approximate forms

$$\tfrac{\rm d}{{\rm d}t} y_d \approx \tfrac{1}{16\pi^2}\, y_d \left(3|y_b|^2 + |y_\tau|^2 - \tfrac{16}{3} g_3^2 - 3 g_2^2 - \tfrac{7}{15} g_1^2\right), \tag{5.22}$$
$$\tfrac{\rm d}{{\rm d}t} y_s \approx \tfrac{1}{16\pi^2}\, y_s \left(3|y_b|^2 + |y_\tau|^2 - \tfrac{16}{3} g_3^2 - 3 g_2^2 - \tfrac{7}{15} g_1^2\right), \tag{5.23}$$
$$\tfrac{\rm d}{{\rm d}t} y_e \approx \tfrac{1}{16\pi^2}\, y_e \left(3|y_b|^2 + |y_\tau|^2 - 3 g_2^2 - \tfrac{9}{5} g_1^2\right), \tag{5.24}$$
$$\tfrac{\rm d}{{\rm d}t} y_\mu \approx \tfrac{1}{16\pi^2}\, y_\mu \left(3|y_b|^2 + |y_\tau|^2 - 3 g_2^2 - \tfrac{9}{5} g_1^2\right). \tag{5.25}$$

  Note that the contribution from the neutrino Yukawa couplings in the last two equations is neglected, as they are typically subdominant. Comparing the RGEs in Eq. (5.22) and (5.23), it follows directly that $\frac{\rm d}{{\rm d}t}(y_d/y_s) \approx 0$, and analogously from Eq. (5.24) and (5.25) we get $\frac{\rm d}{{\rm d}t}(y_\mu/y_e) \approx 0$. This implies that the two ratios are approximately invariant under RG running in the MSSM. The same holds true for the RG running in the SM below the SUSY scale.

- **SUSY threshold corrections:**
  We implement the threshold corrections at the SUSY scale, by using the (real) parameters η_b and η_q, in the following general way [94]:

$$\mathbf{Y}_u^{\rm MSSM} \approx \frac{\mathbf{Y}_u^{\rm SM}}{\sin\beta}, \tag{5.26}$$
$$\mathbf{Y}_d^{\rm MSSM} \approx {\rm diag}\left(\frac{1}{1+\eta_q}, \frac{1}{1+\eta_q}, \frac{1}{1+\eta_b}\right) \frac{\mathbf{Y}_d^{\rm SM}}{\cos\beta}, \tag{5.27}$$
$$\mathbf{Y}_e^{\rm MSSM} \approx \frac{\mathbf{Y}_e^{\rm SM}}{\cos\beta}, \tag{5.28}$$

where only $\tan\beta$-enhanced contributions are taken into account. The Yukawa matrices are written in a basis where $\mathbf{Y}_u$ is diagonal, and again the left-right convention is used. While η_q parametrizes the threshold corrections of the first two families in the down-quark sector, which are typically similar, the threshold correction of the third family is parametrized independently by η_b.[2] Since there is no mixing between the first two and the third family in the down-quark and charged lepton sector, from Eq. (5.27) and (5.28) follows immediately, that the ratios y_d/y_s and y_μ/y_e are not affected by the given implementation of the SUSY threshold corrections.

Since the value of the double ratio d is approximately independent of the energy scale, the comparison of Eq. (5.19) with Eq. (5.21) shows that the ratio of CG coefficients $|c_x^2/(c_y c_z)|$ must be roughly equal to the experimental value 10.7. The available CG coefficients can be read off from Table 2 in [134] and are given by

$$0,\ +\tfrac{1}{6},\ -\tfrac{1}{2},\ -\tfrac{2}{3},\ +1,\ \pm\tfrac{3}{2},\ +2,\ -3,\ +\tfrac{9}{2},\ +6,\ +9,\ -18. \tag{5.29}$$

In Section 5.3.1.3 we will argue, that the predictions of the model are only sensitive to the absolute values $|c_x|$, $|c_y|$ and $|c_z|$ of the CG coefficients. Furthermore, we consider only the cases where $|c_x| \in \{3, \frac{9}{2}, 6\}$, because when the experimental value of the ratio y_μ/y_s is run up to the GUT scale without SUSY threshold corrections we get roughly 4.5.[3] Threshold corrections can shift this value to 3 or 6, but no much further. In Table 5.1 we list all combinations of $|c_x|$, $|c_y|$ and $|c_z|$ for which the double ratio is between 9 and 14. This interval roughly corresponds to the experimental 2σ range of d from Eq. (5.21). Since the model predictions depend on the individual values of c_y and c_z, and not only on their product like the double ratio, we distinguish between exchanges of c_y and c_z in Table 5.1.

[2] In principle, there are also $\tan\beta$-enhanced threshold corrections for $\mathbf{Y}_e$, which can be parametrized in the same manner as the ones for $\mathbf{Y}_d$. However, the correction of the third family can be absorbed by a redefinition $\tan\beta \to \tan\bar{\beta}$, and the correction of the first two families corresponds to a shift of the parameters x, y, z and η_q. Since the threshold corrections of the charged leptons are typically small compared to the ones of the down-quarks, the shift of the parameter point is minor, and $\tan\beta \approx \tan\bar{\beta}$ in the moderate or large $\tan\beta$ regime.

[3] Generally speaking, we expect that in case of $c_x = \frac{9}{2}$ the SUSY threshold correction of the first two families has to vanish, i.e. $\eta_q \approx 0$, in order to reproduce the experimental data of y_μ and y_s. On the other hand, if $c_x \in \{3, 6\}$ we expect $\eta_q \approx \pm 0.33$, because the Yukawa ratio is raised/lowered by 33% at the GUT scale. This is indeed confirmed by the numerical analysis, see Table 5.3

Table 5.1: List of all combinations of SU(5) Clebsch-Gordan coefficients (only absolute values), which provide a Yukawa double ratio $d \approx |c_x^2/(c_y c_z)|$ between 9 and 14, and where $c_x \in \{3, \frac{9}{2}, 6\}$. The available values for the CG coefficients are listed in Eq. (5.29) and have been classified in [133, 134].

c_x, c_y, c_z	c_x, c_y, c_z	c_x, c_y, c_z
3, $\frac{1}{6}$, $\frac{9}{2}$	$\frac{9}{2}$, $\frac{1}{6}$, 9	6, $\frac{1}{2}$, 6
3, $\frac{1}{6}$, 6	$\frac{9}{2}$, $\frac{1}{2}$, 3	6, $\frac{2}{3}$, $\frac{9}{2}$
3, $\frac{1}{2}$, $\frac{3}{2}$	$\frac{9}{2}$, $\frac{1}{2}$, $\frac{9}{2}$	6, $\frac{2}{3}$, 6
3, $\frac{1}{2}$, 2	$\frac{9}{2}$, $\frac{2}{3}$, 3	6, 1, 3
3, $\frac{2}{3}$, 1	$\frac{9}{2}$, 1, $\frac{3}{2}$	6, $\frac{3}{2}$, 2
3, $\frac{2}{3}$, $\frac{3}{2}$	$\frac{9}{2}$, 1, 2	6, 2, $\frac{3}{2}$
3, 1, $\frac{2}{3}$	$\frac{9}{2}$, $\frac{3}{2}$, 1	6, 2, 2
3, 1, 1	$\frac{9}{2}$, $\frac{3}{2}$, $\frac{3}{2}$	6, 3, 1
3, $\frac{3}{2}$, $\frac{1}{2}$	$\frac{9}{2}$, 2, 1	6, $\frac{9}{2}$, $\frac{2}{3}$
3, $\frac{3}{2}$, $\frac{2}{3}$	$\frac{9}{2}$, 3, $\frac{1}{2}$	6, 6, $\frac{1}{2}$
3, 2, $\frac{1}{2}$	$\frac{9}{2}$, 3, $\frac{2}{3}$	6, 6, $\frac{2}{3}$
3, $\frac{9}{2}$, $\frac{1}{6}$	$\frac{9}{2}$, $\frac{9}{2}$, $\frac{1}{2}$	
3, 6, $\frac{1}{6}$	$\frac{9}{2}$, 9, $\frac{1}{6}$	

5.3 Model implementation and analysis

In this section we describe the analysis of the class of models from Section 5.2, that is performed to determine which tuples of Clebsch-Gordan coefficients c_x, c_y and c_z in combination with one of the two CSD2 scenarios ($\mathbf{M}_\nu^{(102)}$ or $\mathbf{M}_\nu^{(120)}$) are able to fit the experimental data at low energies, and what model predictions we get in those cases. Since the model is implemented at the GUT scale, we take the RG running and the SUSY threshold corrections into account for the fit to the experimental data. As a measure for the goodness of the fit the χ^2 function is used. In Section 5.3.1 we specify the implementation of the model at the GUT scale for the numerical analysis, as well as the parameters and observables which are used in the fit. Moreover, in Section 5.3.2 we discuss the fit of the PMNS angles and the CP violating phase at an analytical level.

5.3.1 Model setup

5.3.1.1 Texture

The Yukawa matrices in the down-quark and charged lepton sector are implemented according to the textures in Eq. (5.4) and (5.7), respectively, and are given by

$$\mathbf{Y}_d = \begin{pmatrix} 0 & z & 0 \\ ye^{-i\gamma} & x & 0 \\ 0 & 0 & y_b \end{pmatrix}, \qquad \mathbf{Y}_e = \begin{pmatrix} 0 & c_y y e^{-i\gamma} & 0 \\ c_z z & c_x x & 0 \\ 0 & 0 & y_\tau \end{pmatrix}. \tag{5.30}$$

The texture of the Yukawa matrix in the up-quark sector is specified in Eq. (5.6). However, in order to get direct control over the mixing angles and the singular values of the matrix, we choose a different parametrization, namely

$$\mathbf{Y}_u = \mathbf{U}_{23}(\theta_{23}^{\mathrm{CKM}})\, \mathbf{U}_{12}(\theta_{12}^{uL})\, \mathrm{diag}(y_u, y_c, y_t)\, \mathbf{U}_{12}^{\mathsf{T}}(\theta_{12}^{uL})\, \mathbf{U}_{23}^{\mathsf{T}}(\theta_{23}^{\mathrm{CKM}}), \tag{5.31}$$

where the two unitary matrices are given by

$$\mathbf{U}_{23}(\theta_{23}^{\mathrm{CKM}}) = \begin{pmatrix} 1 & 0 & 0 \\ 0 & \cos\theta_{23}^{\mathrm{CKM}} & \sin\theta_{23}^{\mathrm{CKM}} \\ 0 & -\sin\theta_{23}^{\mathrm{CKM}} & \cos\theta_{23}^{\mathrm{CKM}} \end{pmatrix}, \quad \mathbf{U}_{12}(\theta_{12}^{uL}) = \begin{pmatrix} \cos\theta_{12}^{uL} & -i\sin\theta_{12}^{uL} & 0 \\ -i\sin\theta_{12}^{uL} & \cos\theta_{12}^{uL} & 0 \\ 0 & 0 & 1 \end{pmatrix}. \tag{5.32}$$

Although the entry $(\mathbf{Y}_u)_{13}$ is only approximately equal to zero, the 1-3 mixing angle θ_{13}^{uL} vanishes exactly in this parametrization, thus the conditions for the phase sum rule in the quark sector are fulfilled. Furthermore, the complex rotation matrix $\mathbf{U}_{12}$ reproduces the factor $-i$ in $(\mathbf{Y}_u)_{12}$, such that $\delta_{12}^{uL} = -\frac{\pi}{2}$, and the parametrization ensures that $\mathbf{Y}_u$ is symmetric. Since each of the parameters y_b, y_τ, y_u, y_s, y_t and $\theta_{23}^{\mathrm{CKM}}$ in Eq. (5.30) and (5.31) corresponds to one observable, we set them to the experimental values at the GUT scale, which are provided in [94] (for given $\tan\beta$ and threshold parameters η_b and η_q).[4]

[4]Note, in fact $\theta_{23}^{\mathrm{CKM}}$ does not exactly correspond to the 2-3 angle in the CKM matrix, but only up to (negligible) corrections of quadratic order in the CKM angles.

Depending on the choice of the CSD2 setup, the left-handed neutrino mass matrix has one of the following two forms after the right-handed neutrinos are integrated out, as stated in Eq. (5.11) and (5.12):

$$\mathbf{M}_\nu^{(102)} = m_a \begin{pmatrix} \epsilon e^{i\alpha} & 0 & 2\epsilon e^{i\alpha} \\ 0 & 1 & -1 \\ 2\epsilon e^{i\alpha} & -1 & 1+4\epsilon e^{i\alpha} \end{pmatrix}, \quad \mathbf{M}_\nu^{(120)} = m_a \begin{pmatrix} \epsilon e^{i\alpha} & 2\epsilon e^{i\alpha} & 0 \\ 2\epsilon e^{i\alpha} & 1+4\epsilon e^{i\alpha} & -1 \\ 0 & -1 & 1 \end{pmatrix}. \quad (5.33)$$

Note, we make the simplification that we implement the left-handed neutrino mass matrices directly at the GUT scale, without considering the running of the neutrino Yukawa matrix and of the right-handed neutrino masses down to the corresponding energy scale. This is well justified, by assuming that we are in the regime were the neutrino Yukawa couplings are small and, thus, do not affect the running of the other quantities in the model.

Finally, the matching of the MSSM to the SM at the SUSY scale is parametrized by $\tan\beta$, η_b and η_q according to Eqs. (5.26)–(5.28).

5.3.1.2 Observables

For the fit of the models we use 12 observables which are measured by the experiments. These are the four Yukawa couplings y_d, y_s, y_e, y_μ of the first two families in the down-quark and charged lepton sector, the two CKM angles and CP violating phase $\theta_{12}^{\rm CKM}, \theta_{13}^{\rm CKM}, \delta^{\rm CKM}$, the two mass-squared differences $\Delta m_{21}^2, \Delta m_{31}^2$ of the left-handed neutrinos, and the three PMNS angles $\theta_{12}^{\rm PMNS}, \theta_{13}^{\rm PMNS}, \theta_{23}^{\rm PMNS}$. As discussed above, the CSD2 scheme in the neutrino sector predicts normal ordering for the left-handed neutrino masses, where the lightest one vanishes. Thus the mass-squared differences just correspond to the two non-zero masses squared. There are further measured observables which are not counted above, since each of them is in one-to-one correspondence with a parameter of the model, namely the bottom and the tau Yukawa couplings, the three up-type Yukawa couplings, and the 2-3 CKM angle.

In addition, the model setup allows to make predictions for the following two observables which are not (or not accurately) measured: the PMNS CP violating phase $\delta^{\rm PMNS}$ and the effective mass $\langle m_{\beta\beta}\rangle$ in neutrinoless double-beta decay. Although the PMNS angle $\theta_{23}^{\rm PMNS}$ is used for the fit, the model prediction is much more restricted than the experimental uncertainty. The same applies to the mass ratio m_d/m_s of the down and the strange quark, where the two individual Yukawa couplings are part of the fit, however, the prediction for their ratio is more confined than the experimental error. Thus, each model candidate basically makes specific predictions for four observables.[5] The effective mass $\langle m_{\beta\beta}\rangle$ works as a proxy for the Majorana phase $\varphi_2^{\rm PMNS}$ via the formula

$$\begin{aligned} \langle m_{\beta\beta}\rangle &= \Big| \sum_i (\mathbf{U}_{1i}^{\rm PMNS})^2 m_{\nu_i} \Big| \\ &= c_{12}^2 c_{13}^2 e^{-i\varphi_1^{\rm PMNS}} m_{\nu_1} + s_{12}^2 c_{13}^2 e^{-i\varphi_2^{\rm PMNS}} m_{\nu_2} + s_{13}^2 e^{-2i\delta^{\rm PMNS}} m_{\nu_3}\,, \end{aligned} \quad (5.34)$$

where $c_{ij} \equiv \cos\theta_{ij}^{\rm PMNS}$ and $s_{ij} \equiv \sin\theta_{ij}^{\rm PMNS}$. Since the lightest neutrino mass is equal to zero, the Majorana phase $\varphi_1^{\rm PMNS}$ is not physical.

[5] We do not consider here the prediction for the CKM phase $\delta^{\rm CKM}$, which is determined by the phase sum rule in the quark sector, and therefore independent of the chosen model candidate.

The experimental values for the Yukawa couplings and the CKM parameters are taken directly at the GUT scale M_{GUT}, where the data is provided in [94] (for $M_{\text{SUSY}} = 3\,\text{TeV}$), including the corresponding 1σ ranges, as a function of the parameters $\tan\beta, \eta_b, \eta_q$. On the other hand, the mass-squared differences in the neutrino sector and the PMNS parameters are calculated at the Z boson mass scale M_Z, where the experimental data is taken from NuFIT 3.2 (2018) [54].[6] A schematic illustration of the model quantities at the different energy scales is given in Figure 5.1.

For all measured observables we use the 1σ range from the experimental data to calculate the contribution to the χ^2, except for the PMNS angle $\theta_{23}^{\text{PMNS}}$ we use the χ^2 projection provided by NuFIT 3.2 (2018) [54].

5.3.1.3 Parameters

Once the CG coefficients c_x, c_y, c_z are fixed and one of the two CSD2 scenarios ($\mathbf{M}_\nu^{(102)}$ or $\mathbf{M}_\nu^{(120)}$) is chosen, the model contains 11 parameters, which are used for the fit of the 12 observables from above. These are the four parameters x, y, z, γ in $\mathbf{Y}_d$ and $\mathbf{Y}_e$, the one parameter θ_{12}^{uL} in $\mathbf{Y}_u$, the three parameters m_a, ϵ, α in $\mathbf{M}_\nu$, and the three threshold parameters $\tan\beta, \eta_b, \eta_q$. The other parameter $y_b, y_\tau, y_u, y_c, y_t, \theta_{23}^{\text{CKM}}$, which are in one-to-one correspondence with an observable and thus can be fitted independently, are not counted. In fact, for given threshold parameters we assign these parameters the correct values at the GUT scale, which are provided in [94].

The parameters $x, y, z, \theta_{12}^{uL}, \eta_b$ are used to fit the Yukawa couplings y_d, y_s, y_e, y_μ and the CKM quantities $\theta_{12}^{\text{CKM}}, \theta_{13}^{\text{CKM}}, \delta^{\text{CKM}}$, while the parameters $m_a, \epsilon, \alpha, \gamma$ determine the mass-squared differences $\Delta m_{21}^2, \Delta m_{31}^2$ and the PMNS angles $\theta_{12}^{\text{PMNS}}, \theta_{13}^{\text{PMNS}}, \theta_{23}^{\text{PMNS}}$. The threshold parameters $\tan\beta, \eta_b$ only have a minor effect via the RG running on these observables, thus we basically fit 12 observables with 9 parameters.

With no loss of generality we can assume that the CG coefficients c_x, c_y, c_z are positive, because a change of sign $c_x \mapsto -c_x$ or $c_y \mapsto -c_y$ can be compensated by a shift $\gamma \mapsto \gamma + \pi$, whereas the change of sign $c_z \mapsto -c_z$ has no effect on the calculated observables at all. For the numerical analysis we choose the following ranges for the parameters:

$$\begin{aligned} &x,\, \theta_{12}^{uL} \in [0, 0.1]\,, \quad y,\, z \in [0, 0.01]\,, \quad \gamma,\, \alpha \in [0, 2\pi]\,, \quad \epsilon \in [0, 1]\,, \quad m_a \in [0, 0.1]\,\text{eV}\,, \\ &\tan\beta \in [20, 50]\,, \quad \eta_b,\, \eta_q \in [-0.6, 0.6]\,. \end{aligned} \tag{5.35}$$

Note, due to the freedom of phase redefinitions of the fields at the SU(5) level, as discussed in Section (5.2), the parameters x, y, z, m_a can be restricted to positive values. Furthermore, for the Z boson mass scale, the SUSY scale and the GUT scale we use the following values:

$$M_Z = 91.2\,\text{GeV}\,, \qquad M_{\text{SUSY}} = 3 \cdot 10^3\,\text{GeV}\,, \qquad M_{\text{GUT}} = 2 \cdot 10^{16}\,\text{GeV}\,. \tag{5.36}$$

[6] To efficiently calculate the running from M_{GUT} to M_Z, we prepared a data table which contains the effect of the running for the seven quantities $\theta_{12}^{\text{PMNS}}, \theta_{13}^{\text{PMNS}}, \theta_{23}^{\text{PMNS}}, \delta^{\text{PMNS}}, \varphi_2^{\text{PMNS}}, m_{\nu_2}, m_{\nu_3}$ as a function of the five parameters $\tan\beta, \eta_b, \theta_{23}^{\text{PMNS}}, \delta^{\text{PMNS}}, \varphi_2^{\text{PMNS}}$. The data table was calculated by using 2-loop RGEs in the SM and MSSM [107, 135, 136], and a SUSY scale of 3 TeV.

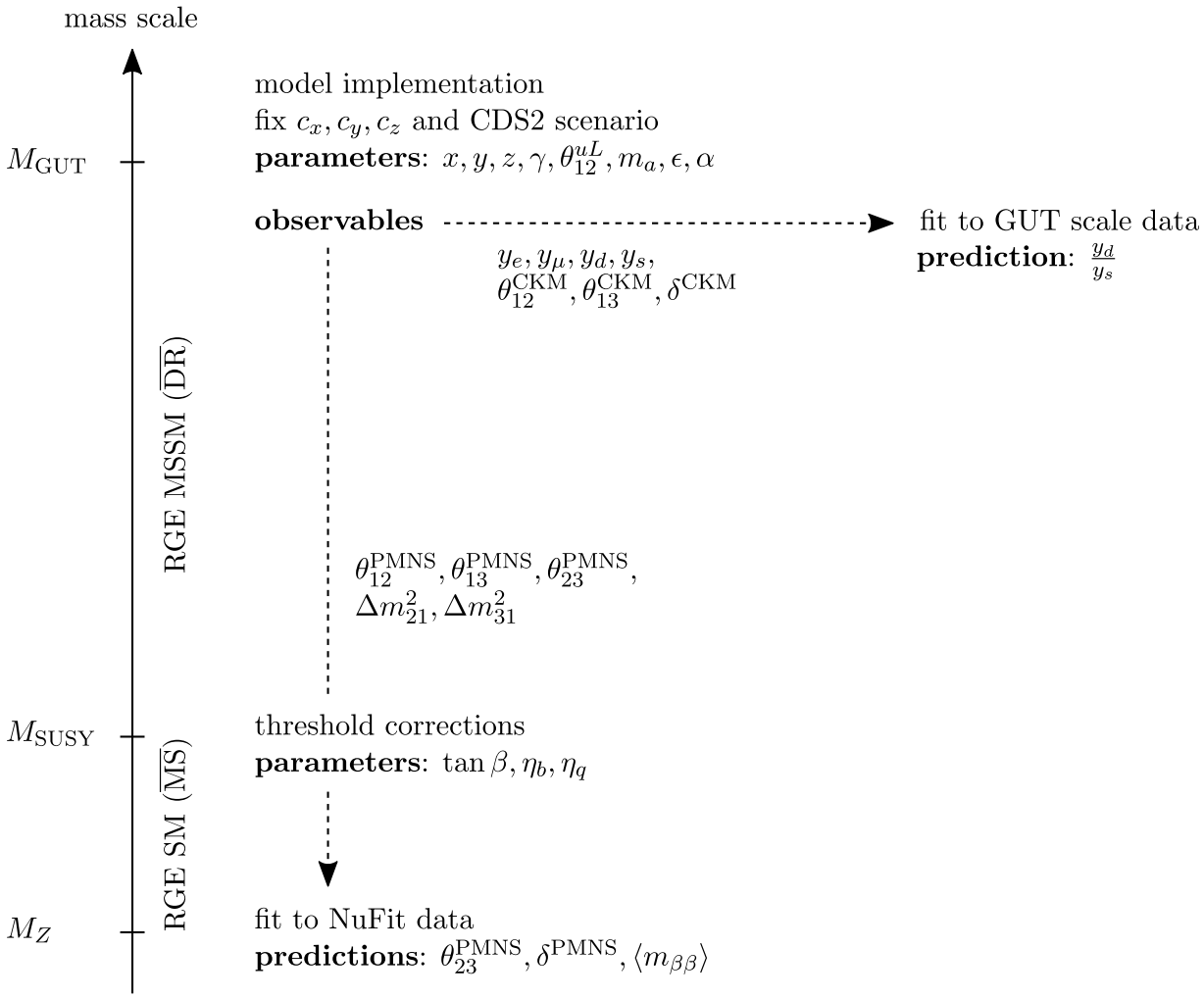

Figure 5.1: Schematic illustration of the model analysis. On the y-axis the involved mass scales as well as the type of RGEs used for the running are indicted. The model is implemented at the GUT scale by specifying the CG coefficients, the CSD2 scenario and the eight parameters in the Yukawa and the neutrino mass matrices. The Yukawa couplings and the CKM quantities are directly calculated at M_{GUT} and fitted to the experimental data given in [94]. The mass-squared differences of the left-handed neutrinos and the PMNS quantities are run down to the Z boson mass scale, where they are fitted to the experimental data from NuFIT 3.2 (2018) [54]. The matching of the MSSM to the SM at the SUSY scale is specified by the three threshold parameters. While the Yukawa ratio of the down and the strange quark is predicted at M_{GUT}, the predicted quantities in the lepton sector are run down to M_Z.

5.3.2 Analytical considerations in the lepton sector

For a given choice of the Clebsch-Gordan coefficients c_x, c_y, c_z the parameters $x, y, z, \theta_{12}^{uL}$ in the charged lepton and in the up- and down-quark Yukawa matrices, as well as the SUSY threshold parameter η_q, are completely fixed by the experimental values of the Yukawa couplings y_d, y_s, y_e, y_μ and the CKM quantities $\theta_{12}^{\mathrm{CKM}}, \theta_{13}^{\mathrm{CKM}}, \delta^{\mathrm{CKM}}$. In the lepton sector, the three parameters m_a, ϵ, α from the mass matrix of the left-handed neutrinos and the phase γ from the charged lepton Yukawa matrix are then used to fit the mass-squared differences $\Delta m_{21}^2, \Delta m_{31}^2$ and the PMNS angles $\theta_{12}^{\mathrm{PMNS}}, \theta_{13}^{\mathrm{PMNS}}, \theta_{23}^{\mathrm{PMNS}}$. It turns out, that for a given point in the space of these four parameters with a low χ^2, there are additional parameter points with the same or a similar χ^2 value. From an analytical point of view, this feature can be understood by means of the below-mentioned three steps. Since the considerations take place at a qualitative level, we neglect the effects of the RG running in the following.

1. The two non-zero neutrino masses correspond to the two non-vanishing singular values of $\mathbf{M}_\nu$. Thus, by fitting Δm_{21}^2 and Δm_{31}^2, the parameters m_a and ϵ can be expressed as functions of α, where the sign of α is irrelevant.

2. Since the angle $\theta_{12}^{eL} \approx |(c_y y)/(c_x x)|$ of the charged lepton sector is determined by the fit of the Yukawa couplings and the CKM angles, the parameter γ is fixed too, up to a minus sign, by the fit of $\theta_{12}^{\mathrm{PMNS}}$ via the approximate identity (cf. Eq. (B.15))

$$\theta_{12}^{\mathrm{PMNS}} \approx 35.3^\circ - \frac{\theta_{12}^{eL}}{\sqrt{2}} \cos\gamma \,. \tag{5.37}$$

   Thus, suitable values of γ appear always in pairs.

3. The last step in the analytic consideration depends on the choice of the CSD2 scenario. We discuss here the scenario $\mathbf{M}_\nu^{102}$, however the other case works analogously. The PMNS angle $\theta_{13}^{\mathrm{PMNS}}$ and the CP phase δ^{PMNS} can be calculated by means of the approximate identity (cf. Eq. (B.25))

$$\theta_{13}^{\mathrm{PMNS}} e^{i\delta^{\mathrm{PMNS}}} \approx \frac{\epsilon}{\sqrt{2}} e^{i(\pi+\alpha)} + \frac{\theta_{12}^{eL}}{\sqrt{2}} e^{i(\pi-\gamma)} \,. \tag{5.38}$$

   According to the first two steps, we can view the right-hand side of the equation as a function of α only. Thus, in order to get a low χ^2 in the fit of the model, we have to find an appropriate value for α.

   In Figure 5.2 the identity from Eq. (5.38) is graphically illustrated in the complex plane for the CG coefficients $(c_x, c_y, c_z) = (3, \frac{3}{2}, \frac{1}{2})$ and the CSD2 scenario $\mathbf{M}_\nu^{102}$. The left-hand side of Eq. (5.38) is represented by the solid red circle, whose radius is equal to the experimental central value of $\theta_{13}^{\mathrm{PMNS}}$. The darker red part of the circle corresponds to the experimental 3σ range of δ^{PMNS} (see NuFIT 3.2 (2018) [54]). The dashed blue line corresponds to the first term on right-hand side of Eq. (5.38). According to the dependence of ϵ on α, the line forms an approximate off-centred circle. The two solid blue circles, which represent the right-hand side of the identity, are then obtained by a shift of the dashed circle according to the second term, which

contains θ_{12}^{eL} and γ. There are two circles because of the unspecified sign of γ. The darker blue parts indicate the experimental 1σ range of $\theta_{23}^{\rm PMNS}$, whose value is determined by ϵ and α via Eq. (B.17).

The intersections of the solid red and blue circles correspond to values of α, where Eq. (5.38) is fulfilled, and thus χ^2 has a low value. Each blue circle has typically 0 or 2 intersection points with the red circle, thus, if there exist such points, we generically expect 4 of them, what is indeed the case in Figure 5.2. Concerning a point (γ, α) with low χ^2, the other intersection points are located at $(-\gamma, -\alpha)$, $(\gamma, 2\gamma - \alpha)$ and $(-\gamma, -2\gamma + \alpha)$. Since the first two points differ only by an overall minus sign, they give exactly the same value for χ^2; this also applies to the last two points. However, the relation between the two pairs is only approximate, because the center of the dashed blue circle is not located at the origin of the complex plane.

Since the observable $\theta_{23}^{\rm PMNS}$ is part of the χ^2 as well, we see that only 2 out of the 4 intersection points are compatible with the corresponding 1σ range (dark blue lines). Thus, in a fit of the model we expect either no point with a low χ^2, or two best-fit points with the same χ^2. Moreover, typically only one of the two best-fit points predicts a value for $\delta^{\rm PMNS}$ which lies within the experimental 3σ range (dark red line). In Figure (5.2), the two best fit points predict 90° and 270° for $\delta^{\rm PMNS}$, where the second value is compatible with the 3σ range.

The above conclusion, that in a model fit two best-fit points with the same χ^2 are expected, where typically only one of them is compatible with the 3σ range of the PMNS CP violating phase, applies to all combinations of CG coefficients from Table 5.1 and both CSD2 scenarios. These statements are also confirmed by the numerical analysis of the models.

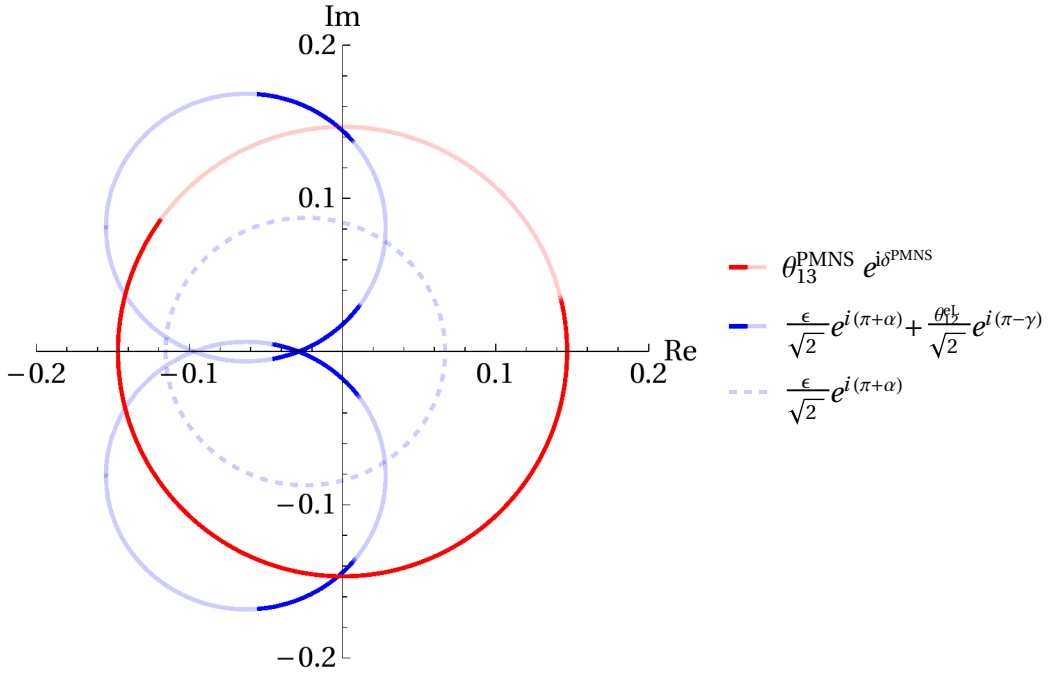

Figure 5.2: Graphical illustration of the individual terms in Eq. (5.38) for $(c_x, c_y, c_z) = (3, \frac{3}{2}, \frac{1}{2})$ and the CSD2 scenario $\mathbf{M}_\nu^{102}$. The fit of the two non-zero neutrino masses implies that ϵ is a function of α, and the two copies of the solid blue circle correspond to the two solutions of γ in the fit of $\theta_{12}^{\mathrm{PMNS}}$ (cf. Eq. (5.37)). Furthermore, $\theta_{12}^{eL} \approx |(c_y/c_x)(y/x)|$ is fixed by the fit of the Yukawa couplings and the CKM matrix, and the parameter α runs from 0 to 2π. The radius of the red circle is given by the experimental central value of $\theta_{13}^{\mathrm{PMNS}}$, and the darker red part corresponds to the experimental 3σ range of δ^{PMNS}. The dark blue line indicates the experimental 1σ range of $\theta_{23}^{\mathrm{PMNS}}$ for given ϵ and α using Eq. (B.17).

5.4 Results

In performing the numerical analysis as described in Section 5.3 for the simple and predictive class of models, we are mainly interested in two results: first, which combinations of Clebsch-Gordan coefficients (c_x, c_y, c_z) from Table 5.1, in combination with one of the two CSD2 scenarios $\mathbf{M}_\nu^{(102)}$ and $\mathbf{M}_\nu^{(120)}$, provide a good fit to the experimental data, and second, what are the predictions for the quantities $\theta_{23}^{\text{PMNS}}$, δ^{PMNS}, y_d/y_s and $\langle m_{\beta\beta}\rangle$ in those cases. The two issues are discussed in Section 5.4.1 and 5.4.2, respectively.

5.4.1 Suitable model candidates

In Table 5.2 a complete list of the model candidates from Table 5.1, which provide $\chi^2 < 15$, is shown. The models are ordered according to their best fit value and labelled by an integer. For each model the corresponding values of the CG coefficients (c_x, c_y, c_z) are specified, and the best-fit points for both CSD2 scenarios $\mathbf{M}_\nu^{(102)}$ and $\mathbf{M}_\nu^{(120)}$ are listed, where only points with $\chi^2 < 15$ are considered. The best-fit points always come in pairs and differ only in the signs (mod 2π) of the parameters α and γ, as discusses in Section 5.3.2. Each best-fit point is identified with an extra label a_i or b_i, according to the CSD2 scenario $\mathbf{M}_\nu^{(102)}$ or $\mathbf{M}_\nu^{(120)}$. For each best-fit point the following quantities are listed:

- The value χ^2_{Tot} represents the total χ^2 of the fit, whereas χ^2_{q} contains only the contributions from the Yukawa couplings and the CKM quantities, and χ^2_ν only the ones from the neutrino mass-squared differences and the PMNS angles. Because of the appropriate selection of CG-coefficients in Table 5.1, which was guided by the double ratio in Eq. (5.18), the contribution of χ^2_q to the total χ^2 is always small. Thus, in models with a big χ^2, the main contribution comes from χ^2_ν, and in general mainly from $\theta_{23}^{\text{PMNS}}$.

- The values for $\theta_{23}^{\text{PMNS}}$ and δ^{PMNS} are indicated by θ_{23} and δ, respectively, where a more detailed discussion of these predictions takes place in Section 5.4.2.

- The best-fit values of the parameters γ and α, as well as of the 1-2 left angle θ_{12}^{eL} in the charged lepton sector are instructive from a model building point of view.

  In a complete flavour model the values of the phases γ and α are preferably explained by a specific mechanism. A possible way to implement such phases is given by discrete flavon vev alignments in flavour models with spontaneous CP violation [99]. A common feature of almost all model candidates with a low χ^2 is, that γ is close to 70° or 290°.

  Since the angle θ_{12}^{eL} is fixed by the fit of the Yukawa couplings and the CKM matrix, the corresponding best-fit value can explore the viability of setups in the neutrino sector within the same class of models, which are different from CSD2. For example, the tri-bimaximal mixing pattern [124, 125] in the neutrino sector predicts $\theta_{13}^{\text{PMNS}} \approx \theta_{12}^{eL}/\sqrt{2}$. In order that the prediction is compatible with the experimental 3σ range of $\theta_{13}^{\text{PMNS}}$ from NuFIT 3.2 (2018) [54], the value of θ_{12}^{eL} must lie in the interval $[11.4^\circ, 12.7^\circ]$. However, we see in Table 5.2 that none of the models with a low χ^2 provides a suitable θ_{12}^{eL}.

The list in Table 5.2 shows that 20 out of the 37 model candidates from Table 5.1 have best-fit points with $\chi^2 < 15$, where for 10 models the total χ^2 is even smaller than 4. We see that overall there is no clear preference for one of the two CSD2 scenarios in the best-fit points. However, for a given tuple of CG coefficients usually one of the two scenarios provides a clearly better fit.

In Table 5.3 the model parameters for the 12 best-points with lowest χ^2 from Table 5.2 are listed, using the same labelling. Since there are always two best-fit points with the same χ^2, only the ones where the predicted value of δ^{PMNS} is compatible with the experimental 3σ range (see NuFIT 3.2 (2018) [54]) are considered. Furthermore, because the CG coefficients of model 1 and 2 differ only by an overall factor, the predictions of the two models are essentially equal. The same applies to model 4 and 5. Thus, the best-fit points of model 2 and 5 are not listed in the table.

5.4.2 Predictions

In the following we discuss the predictions for the PMNS angle $\theta_{23}^{\text{PMNS}}$, the CP violating phase δ^{PMNS}, the ratio y_d/y_s between the down and the strange quark Yukawa couplings (or equivalently the ratio between the two quark masses), and the effective mass $\langle m_{\beta\beta} \rangle$ in neutrinoless double-beta decay.

5.4.2.1 $\theta_{23}^{\text{PMNS}}$ and δ^{PMNS}

The predictions for $\theta_{23}^{\text{PMNS}}$ and δ^{PMNS} of the 12 best-fit points from Table 5.3 are illustrated in Figure 5.3. For each best-fit point a separate plot is shown with $\theta_{23}^{\text{PMNS}}$ on the x-axis and δ^{PMNS} on the y-axis, where the prediction of the best-fit point is indicated by a black $\times$. Around the best-fit point contours of minimal χ^2 are drawn, i.e. for given $\theta_{23}^{\text{PMNS}}$ and δ^{PMNS} the χ^2 is minimized with the condition, that $\theta_{23}^{\text{PMNS}}$ and δ^{PMNS} have the correct values. The χ^2 contours are drawn up to a certain threshold. Thus, for each model candidate the plots show which values of $\theta_{23}^{\text{PMNS}}$ and δ^{PMNS} are compatible with a low χ^2. Note that for all considered best-fit points the value of δ^{PMNS} lies within the experimental 3σ range.

From the plot we can see, that although $\theta_{23}^{\text{PMNS}}$ is included in the calculation of the χ^2, in most of the model candidates the predicted range for $\theta_{23}^{\text{PMNS}}$ is much smaller than the experimental 3σ range, which is given by $[40.3°, 51.5°]$ (see NuFIT 3.2 (2018) [54]). The same applies to the predicted ranges for δ^{PMNS}, where the experimental 3σ range is given by $[144°, 374°]$.

In Figure 5.4 the χ^2 contours from the 12 plots in Figure 5.3 are combined in one plot, where again $\theta_{23}^{\text{PMNS}}$ is on the x-axis and δ^{PMNS} on the y-axis. The grey areas represent the regions outside the 3σ ranges of $\theta_{23}^{\text{PMNS}}$ and δ^{PMNS}. We see, that the predicted ranges for $\theta_{23}^{\text{PMNS}}$ can be very different for different model candidates. Thus, a more precise measurement of this quantity in future experiments has the potential to discriminate, or even exclude some of the models. On the other hand, all the model candidates predict δ^{PMNS} within the (rough) interval $[230°, 290°]$, which is a feature of this particular class of models, independent of the choice of the CG coefficients or the CSD2 scenario. A more precise measurement of this quantity is therefore able to exclude the whole class of models.

5.4.2.2 Ratio of y_d and y_s

In contrast to the above analysis of the observables $\theta_{23}^{\text{PMNS}}$ and δ^{PMNS}, we calculate the posterior density for the different model candidates in order to determine the predictions of the Yukawa ratio y_d/y_s. The calculation is performed by means of an MCMC analysis, using an adaptive Metropolis-Hastings algorithm [117]. All prior distributions for the parameters are chosen to be flat within the corresponding intervals given in Eq. (5.35). Since the posterior density of the Yukawa ratio depends on the choice of the CG-coefficients, but not on the CSD2 scenario in the neutrino sector, we compute for each of the 20 models in Table 5.2 the 1σ HPD interval of y_d/y_s. In Figure 5.6 these intervals are shown as vertical red lines, where the labelling is the same as in Table 5.2. The dashed horizontal line indicates the experimental central value of y_d/y_s, and the grey areas represent the regions outside the 1σ range, which is given by $5.06\,^{+0.78}_{-0.42} \cdot 10^{-2}$ [94]. Note that the predictions for the Yukawa ratio are calculated at the GUT scale. However, since y_d/y_s is stable under RG running and SUSY threshold corrections, we can compare it directly with the experimental data at low energies.

The plot shows, that on the one hand the predicted ranges for y_d/y_s of the models are much smaller than the experimental 1σ range, and on the other hand the ranges may be quite different for different model candidates. Thus, more precise measurements of the quark masses m_d and m_s have the potential to distinguish between these models. The above observation is directly linked to the double ratio $d = (y_\mu/y_e)(y_d/y_s) \approx |c_x^2/(c_y c_z)|$ from Eq. (5.19), which is basically fixed for a given choice of CG coefficients. Since in addition the Yukawa couplings y_e and y_μ have much smaller experimental errors than y_d and y_s, the predicted range for y_d/y_s is small compared to the experimental uncertainty.

5.4.2.3 Effective mass in $0\nu\beta\beta$ decay

Since the CSD2 scenario predicts one left-handed neutrino mass to be zero, the two non-zero masses are predicted by a fit of the two neutrino mass-squared differences. Moreover, a model fit determines all quantities in the PMNS matrix, including the (physical) Majorana phase, so that the effective mass $\langle m_{\beta\beta}\rangle$ in neutrinoless double-beta decay can be calculated, by using Eq. (5.34). The effective mass works basically as a proxy for the Majorana phase, however the quantity $\langle m_{\beta\beta}\rangle$ is more interesting from an experimental point of view. Because the prediction for $\langle m_{\beta\beta}\rangle$ depends on the choice of the CG coefficients, as well as on the CSD2 scenario in the neutrino sector, we calculate for the 12 models with lowest χ^2 listed in Table 5.3 the corresponding 1σ HPD intervals, where δ^{PMNS} has to be compatible with the experimental 3σ range. In Figure 5.6 the 1σ HPD intervals are shown as vertical red lines with the corresponding labelling. The mass $\langle m_{\beta\beta}\rangle$ is given in eV. Although the different models predict different ranges for $\langle m_{\beta\beta}\rangle$, Figure 5.6 shows that all these predictions lie within the range $[2.5, 4.0] \cdot 10^{-3}\,\text{eV}$. However, these values are far beyond the reach of planned experiments, which have a sensitivity of around 0.1 eV (see e.g. Table II in [137]).

Table 5.2: List of all combinations of Clebsch-Gordan coefficients (c_x, c_y, c_z) which, in combination with one of the two CSD2 scenarios $\mathbf{M}_\nu^{102}$ and $\mathbf{M}_\nu^{120}$, provide a fit with $\chi^2 < 15$. The models are ordered according to their overall best-fit value. For each tuple of CG coefficients all the best-fit points with $\chi^2 < 15$ are stated. The first column assigns a unique label to the best-fit points, and the second column specifies the values of the CG coefficients and the CSD2 scenario. The total χ^2 of the fit is given by χ^2_{Tot}, whereas χ^2_{q} only contains the contributions from the Yukawa couplings and the CKM quantities, and χ^2_ν the ones from the neutrino mass-squared differences and the PMNS angles. Moreover, the predictions for the PMNS angle $\theta_{23}^{\text{PMNS}}$ and the CP violating phase δ^{PMNS} are labelled as θ_{23} and δ, respectively. The last three columns contain the best-fit values of the model parameters α and γ, and of the 1-2 left angle θ_{12}^{eL} in the charge lepton sector.

Label	(c_x, c_y, c_z)	χ^2_{Tot}	χ^2_{q}	χ^2_ν	$\theta_{23}[^\circ]$	$\delta[^\circ]$	$\gamma[^\circ]$	$\alpha[^\circ]$	$\theta_{12}^{eL}[^\circ]$
1	$\left(3, \frac{3}{2}, \frac{1}{2}\right)$								
a_1	(102)	0.17	0.06	0.11	47.9	92.7	68.7	233.1	7.23
a_2		0.17	0.06	0.11	47.9	267.3	291.3	126.9	7.23
b_1	(120)	4.05	0.06	3.99	41.6	120.1	71.6	148.2	7.22
b_2		4.05	0.06	3.99	41.6	239.9	288.4	211.8	7.22
2	$(6, 3, 1)$								
a_1	(102)	0.19	0.06	0.14	47.9	93.7	67.7	233.9	7.23
a_2		0.19	0.06	0.14	47.9	266.3	292.3	126.1	7.23
b_1	(120)	4.19	0.06	4.13	41.5	118.9	72.6	147.0	7.22
b_2		4.19	0.06	4.13	41.5	241.1	287.4	213.0	7.22
3	$\left(\frac{9}{2}, 2, 1\right)$								
a_1	(102)	1.62	1.06	0.56	43.9	103.0	72.9	263.2	5.49
a_2		1.62	1.06	0.56	43.9	257.0	287.1	96.8	5.49
b_1	(120)	1.06	1.06	0.00	47.2	90.2	71.0	90.5	5.49
b_2		1.06	1.06	0.00	47.2	269.8	289.0	269.5	5.49
4	$\left(\frac{9}{2}, \frac{3}{2}, 1\right)$								
a_1	(102)	1.81	1.12	0.69	43.7	110.9	66.2	272.3	5.33
a_2		1.81	1.12	0.69	43.7	249.1	293.8	87.7	5.33
b_1	(120)	1.24	1.12	0.12	47.4	93.0	68.8	94.0	5.33
b_2		1.24	1.12	0.12	47.4	267.0	291.2	266.0	5.33
5	$\left(3, 1, \frac{2}{3}\right)$								
a_1	(102)	1.82	1.12	0.70	43.7	110.7	66.5	272.1	5.32
a_2		1.82	1.12	0.70	43.7	249.3	293.5	87.9	5.32
b_1	(120)	1.24	1.12	0.12	47.4	93.1	68.7	94.1	5.32
b_2		1.24	1.12	0.12	47.4	266.9	291.3	265.9	5.32
6	$\left(\frac{9}{2}, 3, \frac{2}{3}\right)$								
a_1	(102)	1.64	0.92	0.72	48.8	83.9	72.5	215.3	8.29
a_2		1.64	0.92	0.72	48.8	276.1	287.5	144.7	8.29
b_1	(120)	9.68	0.93	8.75	40.4	117.1	78.4	155.0	8.28
b_2		9.68	0.93	8.75	40.4	242.9	281.6	205.0	8.28

Label	(c_x, c_y, c_z)	$\chi^2_{\rm Tot}$	$\chi^2_{\rm q}$	χ^2_{ν}	$\theta_{23}[^\circ]$	$\delta[^\circ]$	$\gamma[^\circ]$	$\alpha[^\circ]$	$\theta_{12}^{eL}[^\circ]$
7	$\left(6, 2, \frac{3}{2}\right)$								
a_1	(102)	2.97	0.06	2.91	42.3	117.7	64.3	283.7	4.80
a_2		2.97	0.06	2.91	42.3	242.3	295.7	76.3	4.80
b_1	(120)	1.77	0.05	1.72	48.3	84.7	77.8	87.7	4.80
b_2		1.77	0.05	1.72	48.3	275.3	282.2	272.3	4.80
8	$\left(6, 6, \frac{1}{2}\right)$								
a_1	(102)	2.37	0.38	1.99	49.6	84.4	71.5	147.4	14.90
a_2		2.37	0.38	1.99	49.6	275.6	288.5	212.6	14.90
a_3		8.62	0.43	8.19	40.9	133.9	64.5	63.6	14.93
a_4		8.62	0.43	8.19	40.9	226.1	295.5	296.4	14.93
b_1	(120)	3.11	0.38	2.74	42.1	121.6	68.9	218.5	14.90
b_2		3.11	0.38	2.74	42.1	238.4	291.1	141.5	14.90
9	$\left(3, 2, \frac{1}{2}\right)$								
a_1	(102)	3.24	3.12	0.12	47.9	87.4	72.7	226.9	7.42
a_2		3.24	3.12	0.12	47.9	272.6	287.3	133.1	7.42
b_1	(120)	8.59	3.15	5.45	41.2	114.2	77.5	144.0	7.41
b_2		8.59	3.15	5.45	41.2	245.8	282.5	216.0	7.41
b_3		11.64	3.19	8.45	49.2	97.0	49.2	75.2	7.40
b_4		11.64	3.19	8.45	49.2	263.0	310.8	284.8	7.40
10	$\left(3, \frac{3}{2}, \frac{2}{3}\right)$								
a_1	(102)	3.76	3.27	0.49	44.0	102.7	72.6	262.3	5.54
a_2		3.76	3.27	0.49	44.0	257.3	287.4	97.7	5.54
b_1	(120)	3.28	3.27	0.01	47.1	91.4	69.8	91.5	5.54
b_2		3.28	3.27	0.01	47.1	268.6	290.2	268.5	5.54
11	$\left(6, \frac{9}{2}, \frac{2}{3}\right)$								
a_1	(102)	4.87	0.14	4.73	50.6	82.0	70.5	187.2	10.97
a_2		4.87	0.14	4.73	50.6	278.0	289.5	172.8	10.97
b_1	(120)	8.16	0.14	8.01	40.5	128.9	69.9	188.8	10.98
b_2		8.16	0.14	8.01	40.5	231.1	290.1	171.2	10.98
12	$\left(6, 6, \frac{2}{3}\right)$								
a_1	(102)	5.98	2.65	3.32	50.2	78.0	73.6	182.1	11.28
a_2		5.98	2.65	3.32	50.2	282.0	286.4	177.9	11.28
b_1	(120)	14.58	2.66	11.92	39.8	125.1	72.7	187.3	11.28
b_2		14.58	2.66	11.92	39.8	234.9	287.3	172.7	11.28
13	$\left(\frac{9}{2}, \frac{9}{2}, \frac{1}{2}\right)$								
a_1	(102)	6.13	2.65	3.48	50.2	78.4	73.2	182.3	11.28
a_2		6.13	2.65	3.48	50.2	281.6	286.8	177.7	11.28
b_1	(120)	14.66	2.66	12.00	39.8	125.0	72.8	187.2	11.28
b_2		14.66	2.66	12.00	39.8	235.0	287.2	172.8	11.28
14	$\left(\frac{9}{2}, 3, \frac{1}{2}\right)$								
a_1	(102)	6.40	1.56	4.84	50.6	82.9	69.9	189.3	10.81
a_2		6.40	1.56	4.84	50.6	277.1	290.1	170.7	10.81
b_1	(120)	9.66	1.56	8.09	40.5	128.9	70.0	187.4	10.81
b_2		9.66	1.56	8.09	40.5	231.1	290.0	172.6	10.81

Label	(c_x, c_y, c_z)	χ^2_{Tot}	χ^2_{q}	χ^2_{ν}	$\theta_{23}[^\circ]$	$\delta[^\circ]$	$\gamma[^\circ]$	$\alpha[^\circ]$	$\theta_{12}^{eL}[^\circ]$
15	$\left(6, \frac{3}{2}, 2\right)$								
b_1	(120)	11.62	0.07	11.55	50.3	67.1	99.7	74.5	3.60
b_2		11.62	0.07	11.55	50.3	292.9	260.3	285.5	3.60
16	$\left(\frac{9}{2}, 1, \frac{3}{2}\right)$								
b_1	(120)	13.25	1.10	12.16	50.3	66.4	101.3	74.3	3.54
b_2		13.25	1.10	12.16	50.3	293.6	258.7	285.7	3.54
17	$\left(3, \frac{2}{3}, 1\right)$								
b_1	(120)	13.28	1.09	12.19	50.3	66.5	101.2	74.5	3.54
b_2		13.28	1.09	12.19	50.3	293.5	258.8	285.5	3.54
18	$\left(\frac{9}{2}, \frac{3}{2}, \frac{3}{2}\right)$								
b_1	(120)	13.30	3.35	9.95	50.2	62.0	103.7	68.4	3.69
b_2		13.30	3.35	9.95	50.2	298.0	256.3	291.6	3.69
19	$(6, 2, 2)$								
b_1	(120)	13.36	3.36	10.00	50.2	62.6	103.1	69.0	3.69
b_2		13.36	3.36	10.00	50.2	297.4	256.9	291.0	3.69
20	$(3, 1, 1)$								
b_1	(120)	13.41	3.35	10.06	50.2	63.1	102.7	69.6	3.69
b_2		13.41	3.35	10.06	50.2	296.9	257.3	290.4	3.69

Table 5.3: List of the 12 best-fit points from Table 5.2, with the corresponding labelling, which predict δ^{PMNS} within the experimental 3σ range (see NuFIT 3.2 (2018) [54]). For each best-fit point the values of the model parameters are stated. Note that model 2 and 5 are not considered, since they have essentially the same best-fit points as model 1 and 4, respectively (see main text).

Label	$\tan\beta$	η_b	η_q	x	y	z	$\gamma[^\circ]$	θ_{12}^{uL}	m_a[eV]	ϵ	$\alpha[^\circ]$
$1a_2$	46.9	0.45	−0.34	0.0072	0.00183	0.00164	291	0.087	0.028	0.103	127
$3b_2$	33.4	−0.17	0.02	0.0035	0.00075	0.00078	289	0.087	0.026	0.119	270
$4b_2$	48.5	0.60	−0.05	0.0050	0.00140	0.00115	291	0.087	0.027	0.117	266
$3a_2$	31.1	−0.15	0.02	0.0032	0.00069	0.00071	287	0.087	0.026	0.116	97
$6a_2$	31.0	−0.14	0.02	0.0031	0.00069	0.00070	288	0.087	0.029	0.099	145
$7b_2$	48.0	0.40	0.31	0.0037	0.00095	0.00085	282	0.087	0.026	0.121	272
$4a_2$	49.3	0.60	−0.05	0.0051	0.00142	0.00117	294	0.087	0.026	0.119	88
$8a_2$	48.7	0.57	0.33	0.0037	0.00097	0.00083	289	0.087	0.029	0.098	213
$7a_2$	49.1	0.49	0.31	0.0038	0.00096	0.00087	296	0.087	0.026	0.125	76
$8b_2$	49.6	0.59	0.33	0.0037	0.00099	0.00085	291	0.087	0.029	0.097	142
$9a_2$	32.5	−0.17	−0.31	0.0050	0.00098	0.00112	287	0.087	0.028	0.102	133
$10b_2$	35.0	−0.08	−0.31	0.0054	0.00105	0.00120	290	0.087	0.026	0.119	269

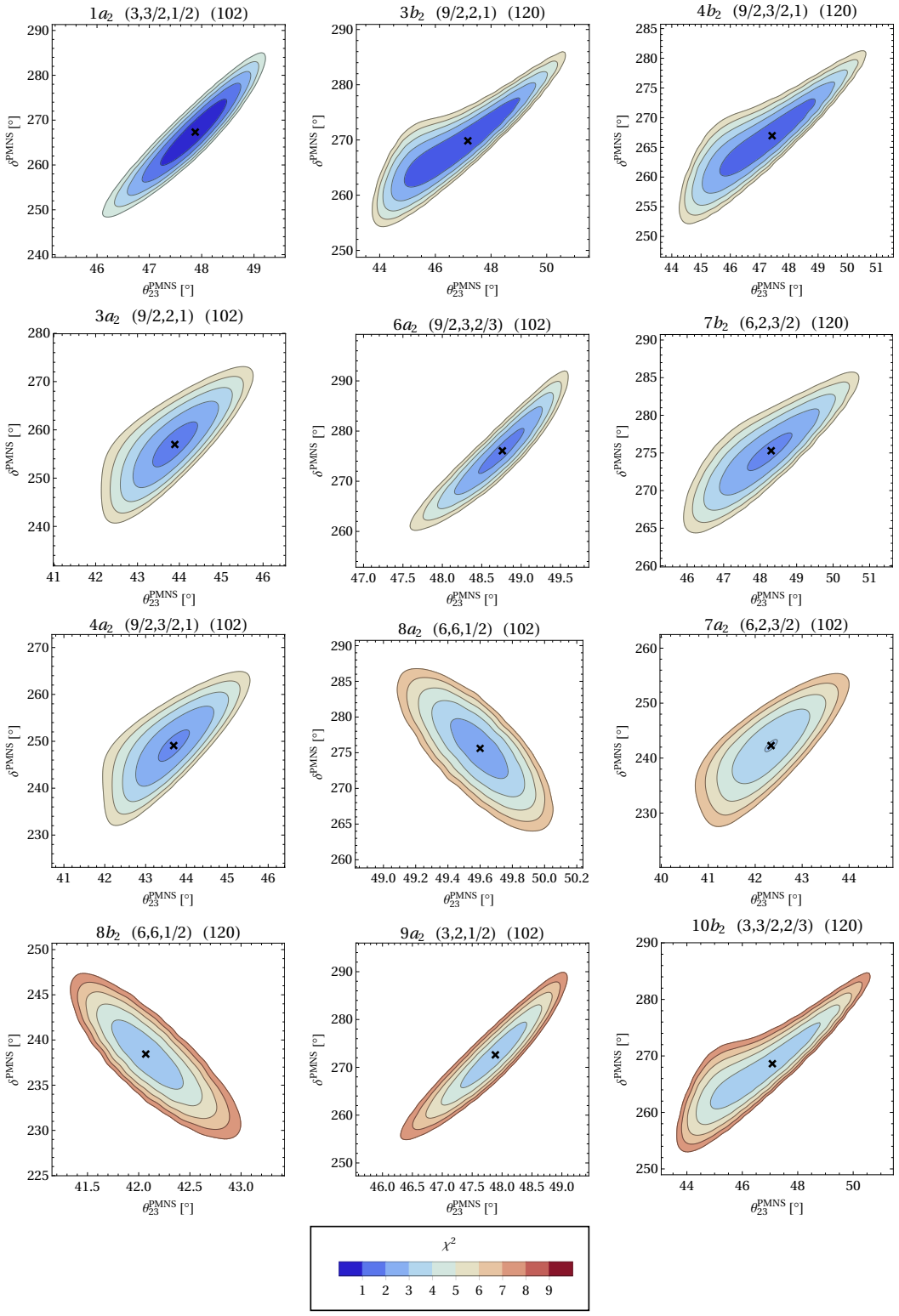

Figure 5.3: Graphical illustration of the predictions for $\theta_{23}^{\text{PMNS}}$ and δ^{PMNS}. From top left to bottom right, the plots correspond to the 12 best-fit points from Table 5.3. In each plot the minimal χ^2 contours for given values of $\theta_{23}^{\text{PMNS}}$ and δ^{PMNS} are shown, where the best fit-point is indcated by a black $\times$. Note, all the shown best-fit points predict δ^{PMNS} within the experimental 3σ range. The title of each plot contains the labelling of the best-fit point, as well as the corresponding values of (c_x, c_y, c_z) and the chosen CSD2 scenario.

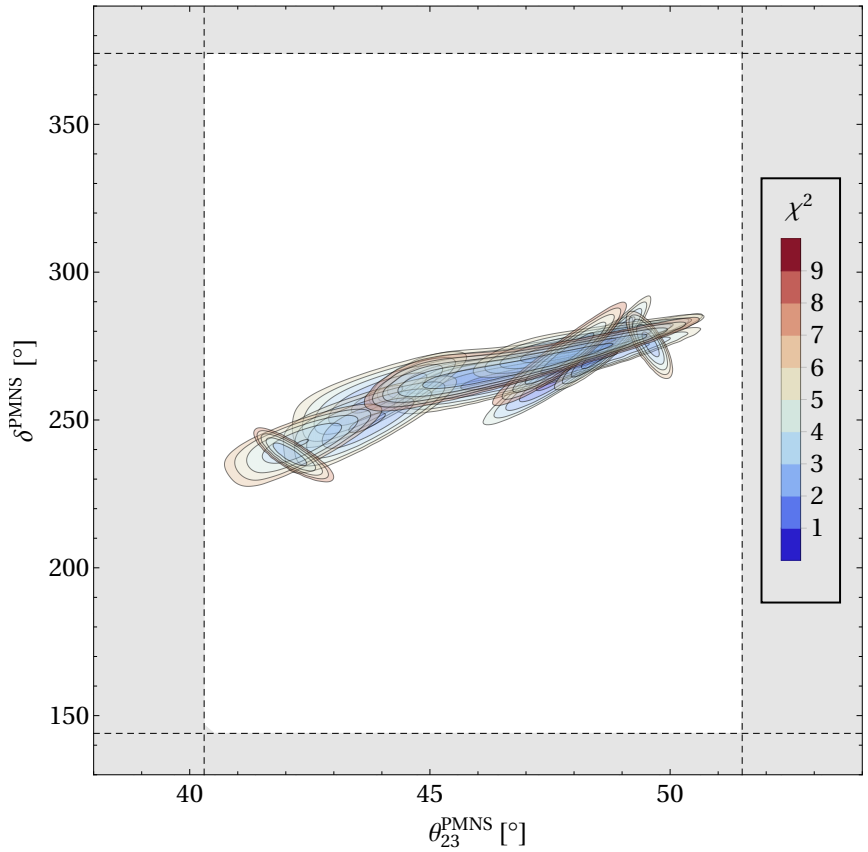

Figure 5.4: Combination of the χ^2 contours from the 12 plots in Figure 5.3 in the $\theta_{23}^{\text{PMNS}}$-$\delta^{\text{PMNS}}$ plane. The grey area represents the region outside the experimental 3σ ranges of $\theta_{23}^{\text{PMNS}}$ and δ^{PMNS}, which are given by $[40.3°, 51.5°]$ and $[144°, 374°]$, respectively (see NuFIT 3.2 (2018) [54]).

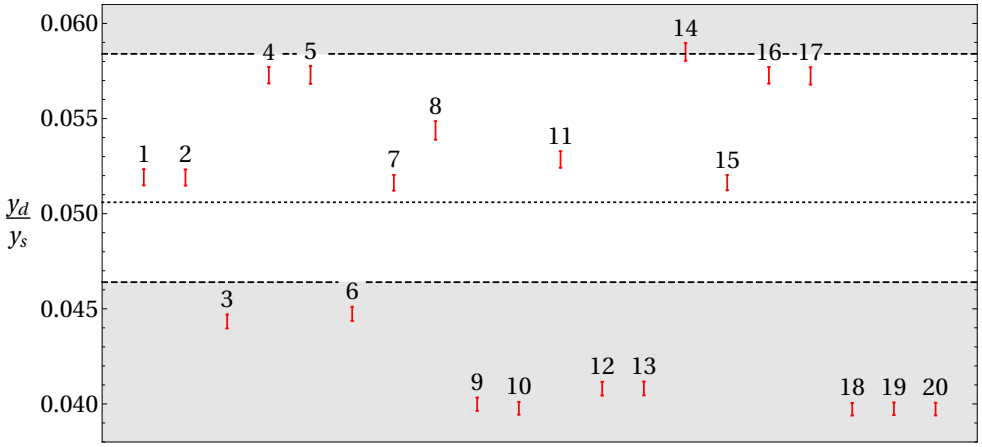

Figure 5.5: The 1σ HPD intervals of the Yukawa ratio y_d/y_s, shown as vertical red lines, for all the 20 combintions of CG coefficients listed in Table 5.3, where the intervals are independent of the choice of the CSD2 scenario. The horizontal dashed line indicates the experimental central value of the Yukawa ratio, and the grey areas represent the regions outside the experimental 1σ range. These values are is given by $y_d/y_s = 5.06\,^{+0.78}_{-0.42} \cdot 10^{-2}$ [94].

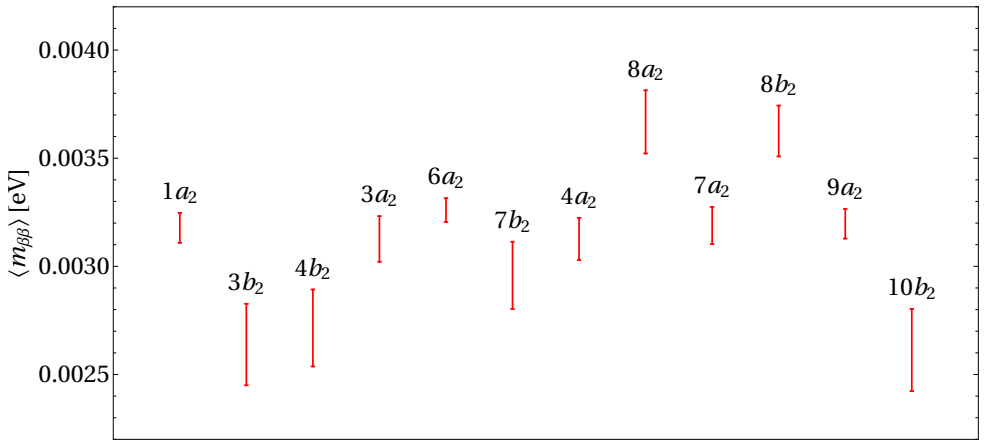

Figure 5.6: The 1σ HPD intervals of the effective mass $\langle m_{\beta\beta} \rangle$ in neutrinoless double-beta decay, shown as vertical red lines, for the 12 models with lowest χ^2 listed in Table 5.3. The mass is given in eV.

CHAPTER 6

Yukawa ratio predictions in non-renormalizable SO(10) GUT models

6.1 Motivation

In flavour GUT models, the concept of single operator dominance, where each entry of the MSSM Yukawa matrices is dominantly generated from one (non-)renormalizable GUT operator, has the attractive feature, that it can give rise to fixed ratios between the Yukawa couplings of different fermion sectors at the GUT scale. These ratios are typically given by group theoretical Clebsch-Gordan factors. Although models of this type have a larger particle content compared to minimal GUT models, which achieve GUT symmetry breaking and fitting of the experimental data by a minimal set of fields and parameters, they have the potential to be very predictive for mass ratios, mixing angles and CP violating phases in the fermion sector, especially in combination with a discrete flavour symmetry. The Yukawa terms at the MSSM level are formed, if the extra field representations, i.e. the ones which do not contain MSSM degrees of freedom, in the non-renormalizable operators of the Yukawa sector acquire vevs at the GUT scale, which break GUT symmetry but are singlets under the SM gauge group.

A possible way to generate the non-renormalizable operators from a renormalizable superpotential is to introduce so-called mediator fields, which have masses above the GUT scale. Once these mediators are integrated out at the GUT scale, the non-renormalizable operators are identified with the generated effective operators. The form of the effective operators, and thus also the predicted Clebsch-Gordan coefficients, depend on the representations of the mediators, and how exactly the renormalizable couplings are implemented. Along these lines, a classification of CG factors has been worked out in [133, 134] in the context of SU(5) for (non-) renormalizable superpotential operators up to dimension 4. This set of CG-coefficients we used in Chapter 5 to investigate a class of predictive SU(5) flavour GUT models.

A similar analysis of possible predictions for Yukawa ratios at the GUT scale can in principle be done in the context of SO(10). GUTs with an SO(10) gauge group have the attractive feature, that the MSSM Yukawa matrices of all fermion sectors are connected via GUT relations, because all SM fermions of one generation, including a right-handed neutrino, are embedded into a single irreducible representation. However, it turns out that such an analysis in SO(10) is more involved than in the SU(5) case, manly because of the following two points: first, irreducible SO(10) representations can contain more than one SM singlet state, which is not the case for (low-dimensional) SU(5) representations. Thus, the exact alignment of each of the SM singlet vevs at the GUT scale has an

influence on the predictions for the MSSM Yukawa couplings. Second, as discussed in Section 3.3, if the GUT representations in the Higgs sector of a model contain more than one doublet-antidoublet pair $(\mathbf{1},\mathbf{2})(\pm\frac{1}{2})$, the EW doublets H_u and H_d may not be well aligned with these states, depending on the form of the doublet mass matrix and thus also on the implementation of doublet-triplet splitting in the Higgs sector. Because of the stronger Yukawa relations in SO(10), this ambiguity can not be absorbed by redefinitions of parameters like in SU(5).

The purpose of this chapter is to investigate the predictions for the MSSM Yukawa couplings at the GUT scale for a class of non-renormalizable SO(10) Yukawa operators, by taking the above mentioned points into account. Our results are an extension of the analysis in [138]. We furthermore show, that single operator dominance can be achieved by constructing the non-renormalizable operators via mediators.

This chapter is based on the publication [3] and is organized as follows: in Section 6.2 the class of non-renormalizable Yukawa operators is defined and the predictions for the MSSM Yukawa couplings are worked out. Furthermore, in Section 6.3 we show how these operators can be generated from renormalizable interactions by using mediators, and in Section 6.4 we provide examples of predictive Higgs sectors.

6.2 A class of non-renormalizable Yukawa operators in SO(10)

The class of non-renormalizable SO(10) superpotential operators in the Yukawa sector, which we consider throughout this chapter, are of the schematic form

$$W \supset \mathbf{16}_I \cdot \mathbf{16}_J \cdot \mathbf{H} \cdot \mathbf{45}^n \cdot \mathbf{210}^m \,, \tag{6.1}$$

where $\mathbf{16}_{I,J}$ contains the fermionic supermultiplets of the MSSM (including a right-handed neutrino) with family indices $I, J \in \{1,2,3\}$. Furthermore, n and m are arbitrary powers, and it is assumed that the **45** and **210** acquire SM singlet vevs at the GUT scale. In principle, each **45** or **210** factor can correspond to a separate field. Because of the decomposition of the product

$$\mathbf{16} \otimes \mathbf{16} = \mathbf{10} \oplus \mathbf{126} \oplus \mathbf{120} \,, \tag{6.2}$$

we choose **H** to be a **10**, $\overline{\mathbf{126}}$ or **120**. Each of these representations contain $\mathrm{SU}(2)_\mathrm{L}$ doublets/antidoublets $(\mathbf{1},\mathbf{2})(\pm\frac{1}{2})$ (cf. Table 3.1), so they are suitable to form MSSM Yukawa terms.

As stated in Table 3.1, the **45** contains 2 SM singlet states, while **210** has 3 SM singlets. Thus, their vevs can lie in an arbitrary direction in the space of singlets, i.e. in $\mathbb{C}^2$ and $\mathbb{C}^3$, respectively. For specifying the singlet states, it is convenient to make use of a basis adapted to the maximal subgroup G_{51}, namely

$$\begin{aligned} X_1 &:= \langle \mathbf{1} \rangle_{\mathbf{45}} \,, & X_2 &:= \langle \mathbf{24} \rangle_{\mathbf{45}} \,, & & \\ Z_1 &:= \langle \mathbf{1} \rangle_{\mathbf{210}} \,, & Z_2 &:= \langle \mathbf{24} \rangle_{\mathbf{210}} \,, & Z_3 &:= \langle \mathbf{75} \rangle_{\mathbf{210}} \,. \end{aligned} \tag{6.3}$$

The angle brackets indicate the irreducible representation of G_{51} the singlets belong to, while their SO(10) origin is specified by the index. Alternatively, one can make use of a

basis adapted to the Pati-Salam group G_{422}:

$$\begin{aligned} \widetilde{X}_1 &:= \langle (\mathbf{1},\mathbf{1},\mathbf{3})\rangle_{\mathbf{45}}\,, & \widetilde{X}_2 &:= \langle (\mathbf{15},\mathbf{1},\mathbf{1})\rangle_{\mathbf{45}}\,, & \\ \widetilde{Z}_1 &:= \langle (\mathbf{1},\mathbf{1},\mathbf{1})\rangle_{\mathbf{210}}\,, & \widetilde{Z}_2 &:= \langle (\mathbf{15},\mathbf{1},\mathbf{1})\rangle_{\mathbf{210}}\,, & \widetilde{Z}_3 &:= \langle (\mathbf{15},\mathbf{1},\mathbf{3})\rangle_{\mathbf{210}}\,. \end{aligned} \tag{6.4}$$

The connection between the G_{51} and G_{422} adapted bases is given by

$$\begin{aligned} \widetilde{X}_1 &= \sqrt{\tfrac{2}{5}}\, X_1 - \sqrt{\tfrac{3}{5}}\, X_2\,, \\ \widetilde{X}_2 &= \sqrt{\tfrac{3}{5}}\, X_1 + \sqrt{\tfrac{2}{5}}\, X_2\,, \\ \widetilde{Z}_1 &= \tfrac{1}{\sqrt{10}}\, Z_1 - \sqrt{\tfrac{2}{5}}\, Z_2 + \tfrac{1}{\sqrt{2}}\, Z_3\,, \\ \widetilde{Z}_2 &= \sqrt{\tfrac{3}{10}}\, Z_1 + 2\sqrt{\tfrac{2}{15}}\, Z_2 + \tfrac{1}{\sqrt{6}}\, Z_3\,, \\ \widetilde{Z}_3 &= \sqrt{\tfrac{3}{5}}\, Z_1 - \tfrac{1}{\sqrt{15}}\, Z_2 - \tfrac{1}{\sqrt{3}}\, Z_3\,. \end{aligned} \tag{6.5}$$

Moreover, the SU(5) and Pati-Salam aligned states are normalized such that their vevs are orthonormal:

$$\begin{aligned} \langle \mathbf{45}^*_{ij} \cdot \mathbf{45}^{ij} \rangle &= |X_1|^2 + |X_2|^2 &&= |\widetilde{X}_1|^2 + |\widetilde{X}_2|^2\,, \\ \langle \mathbf{210}^*_{ijkl} \cdot \mathbf{210}^{ijkl} \rangle &= |Z_1|^2 + |Z_2|^2 + |Z_3|^2 &&= |\widetilde{Z}_1|^2 + |\widetilde{Z}_2|^2 + |\widetilde{Z}_3|^2\,, \end{aligned} \tag{6.6}$$

using the conventions from Section 3.2.

The **H**-representations **10**, $\overline{\mathbf{126}}$ and **120** contain doublets $(\mathbf{1},\mathbf{2})(+\frac{1}{2})$ and antidoublets $(\mathbf{1},\mathbf{2})(-\frac{1}{2})$ of the SM group G_{321}. While each of the two representations **10** and $\overline{\mathbf{126}}$ contains one doublet-antidoublet pair, the representation **120** contains two pairs. In addition, there is also an SM singlet in $\overline{\mathbf{126}}$. These states are labelled in the following under the embedding chain $G_{321} \subseteq G_{51} \subseteq \mathrm{SO}(10)$ (cf. Table 3.1): the doublets are

$$\begin{aligned} H^u_1 &\equiv (\mathbf{1},\mathbf{2})(+\tfrac{1}{2}) \subseteq \mathbf{5}(+2) \subseteq \mathbf{10}\,, \\ H^u_2 &\equiv (\mathbf{1},\mathbf{2})(+\tfrac{1}{2}) \subseteq \mathbf{5}(+2) \subseteq \overline{\mathbf{126}}\,, \\ H^u_3 &\equiv (\mathbf{1},\mathbf{2})(+\tfrac{1}{2}) \subseteq \mathbf{5}(+2) \subseteq \mathbf{120}\,, \\ H^u_4 &\equiv (\mathbf{1},\mathbf{2})(+\tfrac{1}{2}) \subseteq \mathbf{45}(+2) \subseteq \mathbf{120}\,, \end{aligned} \tag{6.7}$$

the antidoublets are

$$\begin{aligned} H^d_1 &\equiv (\mathbf{1},\mathbf{2})(-\tfrac{1}{2}) \subseteq \overline{\mathbf{5}}(-2) \subseteq \mathbf{10}\,, \\ H^d_2 &\equiv (\mathbf{1},\mathbf{2})(-\tfrac{1}{2}) \subseteq \overline{\mathbf{45}}(-2) \subseteq \overline{\mathbf{126}}\,, \\ H^d_3 &\equiv (\mathbf{1},\mathbf{2})(-\tfrac{1}{2}) \subseteq \overline{\mathbf{5}}(-2) \subseteq \mathbf{120}\,, \\ H^d_4 &\equiv (\mathbf{1},\mathbf{2})(-\tfrac{1}{2}) \subseteq \overline{\mathbf{45}}(-2) \subseteq \mathbf{120}\,, \end{aligned} \tag{6.8}$$

and the singlet vev in $\overline{\mathbf{126}}$ is written as

$$\overline{\Delta} \equiv \langle (\mathbf{1},\mathbf{1},0)\rangle \subseteq \langle \mathbf{1}(10)\rangle \subseteq \langle \overline{\mathbf{126}}\rangle\,. \tag{6.9}$$

All the states H^u_i, H^d_i and the vev $\overline{\Delta}$ are canonically normalized analogous to Eq. (6.6).

In order to get Yukawa relations which differ from the renormalizable case, i.e. $m = n = 0$, the GUT scale factors should contract in a non-trivial way with the EW Higgs representation $\mathbf{H}$ and the fermionic representations $\mathbf{16}_{I,J}$. This is most easily achieved by writing the $\mathbf{H}$, $\mathbf{45}$ and $\mathbf{210}$ as 32×32 matrices in spinor space (cf. Eq. (3.31)). Furthermore, the $\mathbf{16}$ is embedded into a 32-dimensional vector according to Eq. (3.26). Actually, we limit ourselves to invariants of this form, i.e. where the contractions happen in a "spinorial way". A general superpotential operator of this form is then written as

$$W \supset \Big(\prod_{i=1}^{n}\prod_{j=1}^{m}\mathbf{45}_{\alpha_i}\mathbf{210}_{\beta_j}\Big)^{A}{}_{D}\,(\mathbf{16}_I)^D\,C_{AB}\,\mathbf{H}^B{}_{E}\,\Big(\prod_{k=1}^{n'}\prod_{l=1}^{m'}\mathbf{45}_{\alpha'_k}\mathbf{210}_{\beta'_l}\Big)^{E}{}_{F}\,(\mathbf{16}_J)^F\,, \qquad (6.10)$$

with the spinor indices $A, B, C, D, E, F \in \{1, ..., 32\}$ and the charge conjugation matrix C_{AB} specified in Eq. (3.23). The products over i, j, k, l in parentheses represent ordinary matrix multiplications. Since the SM singlet vevs $\langle\mathbf{45}\rangle$ and $\langle\mathbf{210}\rangle$ form diagonal matrices, they commute among each other, but they do not commute with the doublets/antidoublets in $\mathbf{H}$. Thus, in Eq. (6.10) we distinguish whether a $\mathbf{45}$ or $\mathbf{210}$ acts on $\mathbf{16}_I$ or $\mathbf{16}_J$, which is also indicated by primed and unprimed labels.

The $n + n'$ factors of the representation $\mathbf{45}$ have an index α_i or α'_k, since they may correspond to different fields. Thus, the SM singlet vevs of these factors may point in different directions. Analogously the $m + m'$ factors of the representation $\mathbf{210}$ carry an index β_j or β'_l. The more complicated labels, e.g. α_i instead of i, are used later to indicate specific alignments of the vevs.

The type of operators as in Eq. (6.10) can be generated from a renormalizable theory by integrating out heavy mediators of the type $\mathbf{16}$ and $\overline{\mathbf{16}}$, which is investigated in detail in Section 6.3.

Broadly speaking, there are two approaches how to generate Yukawa terms from a non-renormalizable operator as in Eq. (6.10):

- The GUT scale vevs in the $\mathbf{45}$ and $\mathbf{210}$ are in the well aligned "discrete" directions of the maximal subgroups G_{51} and G_{422} from Eq. (6.3) and (6.4). These directions can be generated, for example, by a suitable set of invariants in the superpotential of the Higgs sector.

- The GUT scale vevs are not restricted to the discrete directions from the previous point, but they can have "arbitrary" (continuous) directions in the SM singlet spaces of the representations $\mathbf{45}$ and $\mathbf{210}$. This approach is suitable if the Higgs sector of a model does not fix the alignments, or if one assumes that the Higgs sector is rich enough to generate such an alignment, without explicitly constructing it.

The results for the two cases are discussed in Section 6.2.1 and 6.2.2, respectively. In principle, there is also the "mixed" case, where some GUT scale vevs point in discrete and some in arbitrary directions. We briefly comment on that case at the end of Section 6.2.2.

6.2.1 Discrete directions

It is assumed that the GUT scale vev of each factor $\mathbf{45}_{\alpha_i}$ and $\mathbf{45}_{\alpha'_k}$ in Eq. (6.10) lies in one of the four well aligned directions X_1, X_2, $\widetilde{X}_1$ or $\widetilde{X}_2$ defined in Eq. (6.3) and (6.4),

which specifies the labelling, e.g. $\alpha_1 = X_1$ or $\alpha_1 = \widetilde{X}_2$. Analogously, it is assumed that the vevs of each $\mathbf{210}_{\beta_j}$ and $\mathbf{210}_{\beta'_l}$ has one of the six alignments Z_1, Z_2, Z_3, $\widetilde{Z}_1$, $\widetilde{Z}_2$ and $\widetilde{Z}_3$. However, we do not specify how these vev alignments can be constructed from a GUT Higgs superpotential.

This setup is an extension of the studies in [138], where they only considered the factors **45** in the case $\mathbf{H} = \mathbf{10}$. Since discrete vev alignments do not introduce additional parameters into the Yukawa sector, this approach of constructing Yukawa terms is the analogue of the predictive approach with Clebsch-Gordan coefficients in SU(5) GUTs, as for example in Chapter 5. However, in SO(10) there may be additional freedom in the Yukawa predictions, because of the possible non-alignment of the light MSSM Higgs doublets with the doublets in the GUT representations, as discussed later in this section (cf. also Section 3.3).

As stated above, in spinor notation the GUT scale vevs $\langle \mathbf{45} \rangle^A{}_B$ and $\langle \mathbf{210} \rangle^A{}_B$, which are aligned in one of the discrete directions, form diagonal 32×32 matrices. Furthermore, the $\mathbf{16}^A$, which contains the SM fermions of one family, and the conjugate representation $\overline{\mathbf{16}}^A$ are embedded into a 32-dimensional vector according to Eq. (3.26). Thus, each entry on the diagonal of $\langle \mathbf{45} \rangle^A{}_B$ and $\langle \mathbf{210} \rangle^A{}_B$ corresponds to an SM particle p or its conjugate $\bar{p}$ and is labelled by $q(p)$ or $q(\bar{p})$, referred to as "charge". The charges are normalized such that $q(Q) = 1$ for the quark doublet (or $q(u^c) = 1$ if $q(Q) = 0$). Note that $q(\bar{p}) = -q(p)$. A list of the charges and the corresponding normalization factors $\mathcal{N}$ of the vevs, regarding the normalizations in Eq. (6.6), is provided in Table 6.1 and 6.2. Knowing these quantities is sufficient to reconstruct the vev matrices $\langle \mathbf{45} \rangle^A{}_B$ and $\langle \mathbf{210} \rangle^A{}_B$.

Table 6.1: The charges q for the SM fermions for the different vev alignments X of the **45** listed in Eq. (6.3) and (6.4), including the corresponding normalization factors $\mathcal{N}$.

Particle	X_1	X_2	$\widetilde{X}_1$	$\widetilde{X}_2$
Q	1	1	0	1
u^c	1	-4	1	-1
d^c	-3	2	-1	-1
L	-3	-3	0	-3
e^c	1	6	-1	3
ν^c	5	0	1	3
$\mathcal{N}$	$-\sqrt{2/5}$	$-2/\sqrt{15}$	2	$-\sqrt{2/3}$

Using these charges to express the GUT scale vevs of the **45** and **210**, the general Yukawa operator from Eq. (6.10) for fixed family indices I and J takes the following form

Table 6.2: The charges q for the SM fermions for the different vev alignments Z of the **210** listed in Eq. (6.3) and (6.4), including the corresponding normalization factors $\mathcal{N}$.

Particle	Z_1	Z_2	Z_3	$\widetilde{Z}_1$	$\widetilde{Z}_2$	$\widetilde{Z}_3$
Q	1	1	1	1	1	0
u^c	1	-4	-1	-1	1	1
d^c	-1	-6	0	-1	1	-1
L	-1	9	0	1	-3	0
e^c	1	6	-3	-1	-3	3
ν^c	-5	0	0	-1	-3	-3
$\mathcal{N}$	$4\sqrt{3/5}$	$-4/\sqrt{15}$	$8\sqrt{3}$	$2\sqrt{6}$	$2\sqrt{2}$	4

at the MSSM level:

$$
\begin{aligned}
W \supset \frac{C}{\Lambda^{n+n'+m+m'}} \Bigg(\prod_{i,j,k,l} \mathcal{N}_{\alpha_i} \mathcal{N}_{\beta_j} \mathcal{N}_{\alpha'_k} \mathcal{N}_{\beta'_l} X_{\alpha_i} X_{\alpha'_k} Z_{\beta_j} Z_{\beta'_l} \Bigg) \Bigg(& \\
Q_I \, u^c_J \, H^{\mathbf{H}}_u \Bigg[& \; C^{\mathbf{H}}_{ud} \prod_{i,j,k,l} q_{\alpha_i}(Q) \, q_{\beta_j}(Q) \, q_{\alpha'_k}(u^c) \, q_{\beta'_l}(u^c) \Bigg] \\
+ Q_J \, u^c_I \, H^{\mathbf{H}}_u \Bigg[& s^{\mathbf{H}} \, C^{\mathbf{H}}_{ud} \prod_{i,j,k,l} q_{\alpha_i}(u^c) \, q_{\beta_j}(u^c) \, q_{\alpha'_k}(Q) \, q_{\beta'_l}(Q) \Bigg] \\
+ Q_I \, d^c_J \, H^{\mathbf{H}}_d \Bigg[& \; C^{\mathbf{H}}_{ud} \prod_{i,j,k,l} q_{\alpha_i}(Q) \, q_{\beta_j}(Q) \, q_{\alpha'_k}(d^c) \, q_{\beta'_l}(d^c) \Bigg] \\
+ Q_J \, d^c_I \, H^{\mathbf{H}}_d \Bigg[& s^{\mathbf{H}} \, C^{\mathbf{H}}_{ud} \prod_{i,j,k,l} q_{\alpha_i}(d^c) \, q_{\beta_j}(d^c) \, q_{\alpha'_k}(Q) \, q_{\beta'_l}(Q) \Bigg] \\
+ L_I \, e^c_J \, H^{\mathbf{H}}_e \Bigg[& \; C^{\mathbf{H}}_{e\nu} \prod_{i,j,k,l} q_{\alpha_i}(L) \, q_{\beta_j}(L) \, q_{\alpha'_k}(e^c) \, q_{\beta'_l}(e^c) \Bigg] \\
+ L_J \, e^c_I \, H^{\mathbf{H}}_e \Bigg[& s^{\mathbf{H}} \, C^{\mathbf{H}}_{e\nu} \prod_{i,j,k,l} q_{\alpha_i}(e^c) \, q_{\beta_j}(e^c) \, q_{\alpha'_k}(L) \, q_{\beta'_l}(L) \Bigg] \\
+ L_I \, \nu^c_J \, H^{\mathbf{H}}_\nu \Bigg[& \; C^{\mathbf{H}}_{e\nu} \prod_{i,j,k,l} q_{\alpha_i}(L) \, q_{\beta_j}(L) \, q_{\alpha'_k}(\nu^c) \, q_{\beta'_l}(\nu^c) \Bigg] \\
+ L_J \, \nu^c_I \, H^{\mathbf{H}}_\nu \Bigg[& s^{\mathbf{H}} \, C^{\mathbf{H}}_{e\nu} \prod_{i,j,k,l} q_{\alpha_i}(\nu^c) \, q_{\beta_j}(\nu^c) \, q_{\alpha'_k}(L) \, q_{\beta'_l}(L) \Bigg] \\
+ \nu^c_I \, \nu^c_J \, \overline{\Delta} \Bigg[& \; C^{\mathbf{H}}_{\Delta} \prod_{i,j,k,l} q_{\alpha_i}(\nu^c) \, q_{\beta_j}(\nu^c) \, q_{\alpha'_k}(\nu^c) \, q_{\beta'_l}(\nu^c) \Bigg] \Bigg) .
\end{aligned}
\tag{6.11}
$$

The $\mathcal{N}_{\alpha_i}$ and q_{α_i} label the normalization factors and the charges from Table 6.1 for the alignments $X_{\alpha_i} \in \{X_1, X_2, \widetilde{X}_1, \widetilde{X}_2\}$ of the factors $\langle \mathbf{45}_{\alpha_i} \rangle$. The same definitions hold for $\mathcal{N}_{\alpha'_k}$ and $q_{\alpha'_k}$. Moreover, the normalization factors and charges corresponding to the factors $\langle \mathbf{210}_{\beta_j} \rangle$ and $\langle \mathbf{210}_{\beta'_l} \rangle$ can be read off from Table 6.2. The **H**-dependent constants $s^{\mathbf{H}}$ and

$C^{\mathbf{H}}$ are given in Table 6.3, where in addition the fields $H^{\mathbf{H}}_{u,d,e,\nu}$ in terms of the doublets H^u_i and antidoublets H^d_i from Eq. (6.7) and (6.8), respectively, are defined. Finally, the non-renormalizable operator is suppressed by the mass scale Λ, e.g. the mass scale of mediators, to the power $n + n' + m + m'$, and C is a dimensionless constant. Note that the product of normalizations $\mathcal{N}$ and the product of vev sizes X or Z can be absorbed into the overall operator coefficient $C/\Lambda^{n+n'+m+m'}$.

Table 6.3: The **H**-dependent quantities which are present in Eq. (6.11), where **H** represents either a **10**, a $\overline{\mathbf{126}}$ or a **120**.

H	**10**	$\overline{\mathbf{126}}$	**120**
$s^{\mathbf{H}}$	1	1	-1
$C^{\mathbf{H}}_{ud}$	$\sqrt{2}$	$4\sqrt{10}$	4
$C^{\mathbf{H}}_{e\nu}$	$\sqrt{2}$	$-12\sqrt{10}$	$-4\sqrt{3}$
$C^{\mathbf{H}}_{\Delta}$	0	$-16\sqrt{15}$	0
$H^{\mathbf{H}}_u$	H^u_1	H^u_2	H^u_4
$H^{\mathbf{H}}_d$	H^d_1	H^d_2	$\frac{\sqrt{3}}{2}H^d_3 - \frac{1}{2}H^d_4$
$H^{\mathbf{H}}_e$	H^d_1	H^d_2	$\frac{1}{2}H^d_3 + \frac{\sqrt{3}}{2}H^d_4$
$H^{\mathbf{H}}_\nu$	H^u_1	H^u_2	H^u_3

Since both $\mathbf{16}_I$ and $\mathbf{16}_J$ contain all SM fermions of one generation, including a right-handed neutrino, for each of the four fermion sectors there are always two Yukawa operators in Eq. (6.11). For example, in the up-sector the field Q either originates from $\mathbf{16}_I$ and u^c from $\mathbf{16}_J$ or vice versa, leading to the two Yukawa terms. The last term in Eq. (6.11), which contains the SM singlet vev $\overline{\Delta}$, forms a Majorana mass term of the right-handed neutrinos. This term is only present if $\mathbf{H} = \overline{\mathbf{126}}$, since **10** and **120** do not contain an SM singlet.

The doublet and antidoublet states H^u_i and H^d_i of **H**, which are connected to the fields $H^{\mathbf{H}}_{u,d,e,\nu}$ in Eq. (6.11) via the relations in Table 6.3, may not be well aligned with the light MSSM doublets H_u and H_d, if there are multiple doublet-antidoublet pairs in a specific model. The alignment depends on the form of the doublet mass matrix M_D, which in turn depends on the form of the Higgs sector of the model. Since only the EW doublets H_u and H_d acquire a vev, the masses of the SM fermions may depend on Higgs sector parameters which enter M_D, as discussed in Section 3.3. Moreover, because in GUTs the doublet and triplet mass matrices are associated, the dependence on the Higgs sector parameters is directly related to doublet-triplet splitting. Although the construction of a complete Higgs sector is beyond the scope of this chapter, in Section 6.4 we provide some examples of simple Higgs sector scenarios, which are predictive in the Yukawa sector, i.e. they do not introduce additional parameters in the Yukawa sector.

A GUT operator with family indices (I, J) contributes to the entries (I, J), but also to the entries (J, I) of the Yukawa matrices at the MSSM level. Thus, if one wants to implement single operator dominance in all the Yukawa entries, i.e. every Yukawa entry is dominantly generated by only one operator, in order to obtain maximal predictivity,

there can be at most six (dominant) Yukawa operators at the GUT level. It is well known, that for renormalizable operators, i.e. $n = n' = 0$ and $m = m' = 0$, the Yukawa matrices are symmetric in case of $\mathbf{H}$ is equal to $\mathbf{10}$ or $\overline{\mathbf{126}}$, and antisymmetric for the $\mathbf{120}$, which is reproduced by the factor $s^{\mathbf{H}}$ in Eq. (6.11). However, for non-renormalizable operators these symmetry properties are lost, because the product over α_i, β_j of the charges acting on $\mathbf{16}_I$ is not the same as the product over α'_k, β'_l of charges acting on $\mathbf{16}_J$.

Of particular importance for flavour GUT model building are predictions for ratios of the diagonal Yukawa entries between the different sectors. The Yukawa ratios for the case $I = J$ read

$$\begin{aligned}
\frac{(\mathbf{Y}_e)_{II}}{(\mathbf{Y}_d)_{II}} &= \chi^{\mathbf{H}}_{ed} \frac{C^{\mathbf{H}}_{e\nu}}{C^{\mathbf{H}}_{ud}} \frac{\prod\limits_{i,j,k,l} q_{\alpha_i}(L)\, q_{\beta_j}(L)\, q_{\alpha'_k}(e^c)\, q_{\beta'_l}(e^c) + s^{\mathbf{H}} \prod\limits_{i,j,k,l} q_{\alpha_i}(e^c)\, q_{\beta_j}(e^c)\, q_{\alpha'_k}(L)\, q_{\beta'_l}(L)}{\prod\limits_{i,j,k,l} q_{\alpha_i}(Q)\, q_{\beta_j}(Q)\, q_{\alpha'_k}(d^c)\, q_{\beta'_l}(d^c) + s^{\mathbf{H}} \prod\limits_{i,j,k,l} q_{\alpha_i}(d^c)\, q_{\beta_j}(d^c)\, q_{\alpha'_k}(Q)\, q_{\beta'_l}(Q)}\,, \\
\frac{(\mathbf{Y}_u)_{II}}{(\mathbf{Y}_d)_{II}} &= \chi^{\mathbf{H}}_{ud} \frac{\prod\limits_{i,j,k,l} q_{\alpha_i}(Q)\, q_{\beta_j}(Q)\, q_{\alpha'_k}(u^c)\, q_{\beta'_l}(u^c) + s^{\mathbf{H}} \prod\limits_{i,j,k,l} q_{\alpha_i}(u^c)\, q_{\beta_j}(u^c)\, q_{\alpha'_k}(Q)\, q_{\beta'_l}(Q)}{\prod\limits_{i,j,k,l} q_{\alpha_i}(Q)\, q_{\beta_j}(Q)\, q_{\alpha'_k}(d^c)\, q_{\beta'_l}(d^c) + s^{\mathbf{H}} \prod\limits_{i,j,k,l} q_{\alpha_i}(d^c)\, q_{\beta_j}(d^c)\, q_{\alpha'_k}(Q)\, q_{\beta'_l}(Q)}\,, \\
\frac{(\mathbf{Y}_\nu)_{II}}{(\mathbf{Y}_d)_{II}} &= \chi^{\mathbf{H}}_{\nu d} \frac{C^{\mathbf{H}}_{e\nu}}{C^{\mathbf{H}}_{ud}} \frac{\prod\limits_{i,j,k,l} q_{\alpha_i}(L)\, q_{\beta_j}(L)\, q_{\alpha'_k}(\nu^c)\, q_{\beta'_l}(\nu^c) + s^{\mathbf{H}} \prod\limits_{i,j,k,l} q_{\alpha_i}(\nu^c)\, q_{\beta_j}(\nu^c)\, q_{\alpha'_k}(L)\, q_{\beta'_l}(L)}{\prod\limits_{i,j,k,l} q_{\alpha_i}(Q)\, q_{\beta_j}(Q)\, q_{\alpha'_k}(d^c)\, q_{\beta'_l}(d^c) + s^{\mathbf{H}} \prod\limits_{i,j,k,l} q_{\alpha_i}(d^c)\, q_{\beta_j}(d^c)\, q_{\alpha'_k}(Q)\, q_{\beta'_l}(Q)}\,,
\end{aligned} \tag{6.12}$$

where the factors $\chi^{\mathbf{H}}$ are defined by

$$\chi^{\mathbf{H}}_{ed} := \frac{H^{\mathbf{H}}_e}{H^{\mathbf{H}}_d}\,, \qquad \chi^{\mathbf{H}}_{ud} := \frac{H^{\mathbf{H}}_u}{H^{\mathbf{H}}_d}\frac{H_d}{H_u}\,, \qquad \chi^{\mathbf{H}}_{\nu d} := \frac{H^{\mathbf{H}}_\nu}{H^{\mathbf{H}}_d}\frac{H_d}{H_u}\,. \tag{6.13}$$

These factors may depend on parameters of the Higgs sector due to the presence of the fields $H^{\mathbf{H}}_{u,d,e,\nu}$ in the definitions, as discussed above. Though, there are simple scenarios of Higgs sectors, as shown in Section 6.4, for which the $\chi^{\mathbf{H}}$ are fixed numbers. For each of these scenarios the values for the $\chi^{\mathbf{H}}$ factors are listed in Table 6.4, where the numbering # of the scenarios corresponds to the one in Table 6.7. Furthermore, for each scenario the available Higgs representations $\mathbf{H}$ are listed. Usually $\mathbf{H}$ corresponds to a particular representation, however in scenario #5 and 6 two different $\mathbf{H}$-representations are available. Finally, a general observation is, that $\chi^{\mathbf{H}}_{ed} = 1$ if $\mathbf{H} = \mathbf{10}$ or $\mathbf{H} = \overline{\mathbf{126}}$, independent of the form of the Higgs sector, because $H^{\mathbf{H}}_d = H^{\mathbf{H}}_e$ in this case (cf. Table 6.3).

Although SU(5) is a subgroup of SO(10), Clebsch-Gordan ratios between the down-quark and the charged lepton sector from SU(5) operators are not necessarily reproduced in SO(10), since each SO(10) Yukawa operator actually combines two operators at the SU(5) level in a given sector, thus modifying the singe operator SU(5) predictions (cf. Eq. (6.11) and (6.12)). However, since at the renormalizable level the products over i, j, k, l in Eq. (6.12) are just equal to 1, and also $\chi^{\mathbf{H}}_{ed} = 1$ in case of $\mathbf{H} \in \{\mathbf{10}, \overline{\mathbf{126}}\}$, the ratio between the down-quark and the charged lepton Yukawa coupling is simply given by $C^{\mathbf{H}}_{e\nu}/C^{\mathbf{H}}_{ud}$. For the two choices of $\mathbf{H}$ we then get the Yukawa ratios 1 and -3, respectively, which correspond to b-τ unification and the Georgi-Jarlskog factor [132], respectively, in the context of SU(5).

An application of the general formula for the calculation of Yukawa ratios in Eq. (6.12) is given in Table 6.5, where the Yukawa ratios for all superpotential operators up to

Table 6.4: Examples of scenarios where the $\chi^{\mathbf{H}}$ factors have fixed numerical values. The scenarios correspond to the predictive Higgs sectors listed in Table 6.7 with the same numbering #. For each case the available representation(s) **H** and the values of the $\chi^{\mathbf{H}}$ factors are listed.

#	**H**	$\chi^{\mathbf{H}}_{ed}$	$\chi^{\mathbf{H}}_{ud}$	$\chi^{\mathbf{H}}_{\nu d}$
1	**10**	1	1	1
2	**120**	$-1/\sqrt{3}$	-1	$1/\sqrt{3}$
3	**120**	$\sqrt{3}$	1	$\sqrt{3}$
4	$\overline{\mathbf{126}}$	1	1	1
5	**10**	1	-1	-1
	120	$-1/\sqrt{3}$	-1	$1/\sqrt{3}$
6	**10**	1	-1	-1
	120	$\sqrt{3}$	1	$\sqrt{3}$

dimension 5, i.e. $n + n' + m + m' \leq 2$, and for all possible combinations of discrete vev alignments which provide $|(\mathbf{Y}_e)_{II}/(\mathbf{Y}_d)_{II}| \leq 8$ are calculated, in the predictive scenario #1 from Table 6.4. In this scenario $\mathbf{H} = \mathbf{10}$, with $H_1^u = H_u$ and $H_1^d = H_d$, and all $\chi^{\mathbf{H}} = 1$. Table 6.5 shows, that different GUT operators or different vev alignments may predict the same Yukawa ratios, thus they are listed under the same number. The predicted Clebsch-Gordan coefficients are also graphically illustrated in Figure 6.1, using the same numbering. The purpose of the figure is that one can quickly find suitable Yukawa ratios for model building, where the corresponding GUT operators can then be read off from the table.

6.2.2 Arbitrary directions

It is assumed that the GUT scale vevs of the **45** and **210** can point in an arbitrary directions in the singlet spaces $\mathbb{C}^2$ and $\mathbb{C}^3$, respectively. For simplicity, we restrict ourselves to the case, where a Yukawa operator as in Eq. (6.10) only contains one single copy of a **45** and **210**, i.e. all the $n + n'$ vevs associated with α_i and α'_k point in the same direction, and analogous for the $m + m'$ vevs corresponding to β_j and β'_l. Since there is at most one copy of each representation, a minimal set of new parameters from the vev alignments is introduced, which provides maximal predictivity. Note that this approach of constructing Yukawa terms has no good analogue in SU(5), since low dimensional irreducible representations of SU(5) contain at most one SM singlet state, thus there is no freedom in the alignment of the GUT scale vevs.

Since only the directions of the GUT scale vevs, but not their size (which can be absorbed into the overall operator coefficient), have an impact on the predicted Yukawa relations between the different sectors, we define the following complex ratios:

$$\kappa := X_2/X_1\,, \qquad \kappa_1 := Z_2/Z_1\,, \qquad \kappa_2 := Z_3/Z_1\,, \tag{6.14}$$

using the G_{51} adapted bases. The discrete alignments from Eq. (6.3) and (6.4) used in Section 6.2.1 correspond to special values of these ratios, which are determined by applying

Eq. (6.5) and (6.14), and are listed in Table 6.6.

In order to reconstruct the entries in the diagonal matrices $\langle \mathbf{45} \rangle^A{}_B$ and $\langle \mathbf{210} \rangle^A{}_B$, we consider the combined charge of a particle $p \in \{Q, u^c, d^c, L, e^c, \nu^c\}$ with respect to a vev alignment specified by the ratios κ, κ_1 and κ_2. These combined charges concerning the **45** and **210** are given by the order one polynomials $P_p(\kappa)$ and $R_p(\kappa_1, \kappa_2)$, respectively:

$$\begin{aligned} P_p(\kappa) &:= \frac{1}{X_1} \sum_{i=1}^{2} \mathcal{N}_{X_i}\, q_{X_i}(p)\, X_i \\ &= \mathcal{N}_{X_1}\, q_{X_1}(p) + \mathcal{N}_{X_2}\, q_{X_2}(p)\, \kappa\,, \end{aligned} \tag{6.15}$$

$$\begin{aligned} R_p(\kappa_1, \kappa_2) &:= \frac{1}{Z_1} \sum_{i=1}^{3} \mathcal{N}_{Z_i}\, q_{Z_i}(p)\, Z_i \\ &= \mathcal{N}_{Z_1}\, q_{Z_1}(p) + \mathcal{N}_{Z_2}\, q_{Z_2}(p)\, \kappa_1 + \mathcal{N}_{Z_3}\, q_{Z_3}(p)\, \kappa_2\,. \end{aligned} \tag{6.16}$$

In these definitions, again the G_{51} adapted bases X_i ($i \in \{1, 2\}$) and Z_i ($i \in \{1, 2, 3\}$) for the GUT scale vevs are used. Furthermore, the normalization factors $\mathcal{N}_{X_i}$ and $\mathcal{N}_{Z_i}$, as well as the charges $q_{X_i}(p)$ and $q_{Z_i}(p)$ are listed in Table 6.1 and 6.2.

Having specified the combined charges for an arbitrary vev alignment in Eq. (6.15) and (6.16), the general Yukawa operator from Eq. (6.10) for fixed family indices I and J and one single copy of a **45** and **210** takes the following form at the MSSM level:

$$\begin{aligned} W \supset\, & \frac{C}{\Lambda^{n+n'+m+m'}}\, X_1^{n+n'}\, Z_1^{m+m'} \Bigg(\\ & Q_I\, u_J^c\, H_u^{\mathbf{H}} \left[\quad C_{ud}^{\mathbf{H}}\, P_Q(\kappa)^n\, R_Q(\kappa_1, \kappa_2)^m\, P_{u^c}(\kappa)^{n'}\, R_{u^c}(\kappa_1, \kappa_2)^{m'} \right] \\ & + Q_J\, u_I^c\, H_u^{\mathbf{H}} \left[s^{\mathbf{H}}\, C_{ud}^{\mathbf{H}}\, P_{u^c}(\kappa)^n\, R_{u^c}(\kappa_1, \kappa_2)^m\, P_Q(\kappa)^{n'}\, R_Q(\kappa_1, \kappa_2)^{m'} \right] \\ & + Q_I\, d_J^c\, H_d^{\mathbf{H}} \left[\quad C_{ud}^{\mathbf{H}}\, P_Q(\kappa)^n\, R_Q(\kappa_1, \kappa_2)^m\, P_{d^c}(\kappa)^{n'}\, R_{d^c}(\kappa_1, \kappa_2)^{m'} \right] \\ & + Q_J\, d_I^c\, H_d^{\mathbf{H}} \left[s^{\mathbf{H}}\, C_{ud}^{\mathbf{H}}\, P_{d^c}(\kappa)^n\, R_{d^c}(\kappa_1, \kappa_2)^m\, P_Q(\kappa)^{n'}\, R_Q(\kappa_1, \kappa_2)^{m'} \right] \\ & + L_I\, e_J^c\, H_e^{\mathbf{H}} \left[\quad C_{e\nu}^{\mathbf{H}}\, P_L(\kappa)^n\, R_L(\kappa_1, \kappa_2)^m\, P_{e^c}(\kappa)^{n'}\, R_{e^c}(\kappa_1, \kappa_2)^{m'} \right] \\ & + L_J\, e_I^c\, H_e^{\mathbf{H}} \left[s^{\mathbf{H}}\, C_{e\nu}^{\mathbf{H}}\, P_{e^c}(\kappa)^n\, R_{e^c}(\kappa_1, \kappa_2)^m\, P_L(\kappa)^{n'}\, R_L(\kappa_1, \kappa_2)^{m'} \right] \\ & + L_I\, \nu_J^c\, H_\nu^{\mathbf{H}} \left[\quad C_{e\nu}^{\mathbf{H}}\, P_L(\kappa)^n\, R_L(\kappa_1, \kappa_2)^m\, P_{\nu^c}(\kappa)^{n'}\, R_{\nu^c}(\kappa_1, \kappa_2)^{m'} \right] \\ & + L_J\, \nu_I^c\, H_\nu^{\mathbf{H}} \left[s^{\mathbf{H}}\, C_{e\nu}^{\mathbf{H}}\, P_{\nu^c}(\kappa)^n\, R_{\nu^c}(\kappa_1, \kappa_2)^m\, P_L(\kappa)^{n'}\, R_L(\kappa_1, \kappa_2)^{m'} \right] \\ & + \nu_I^c\, \nu_J^c\, \overline{\Delta} \left[\, C_\Delta^{\mathbf{H}}\, P_{\nu^c}(\kappa)^{n+n'}\, R_{\nu^c}(\kappa_1, \kappa_2)^{m+m'} \right] \Bigg). \end{aligned} \tag{6.17}$$

The Yukawa operator has a similar form as the one in Eq. (6.11) in the case of discrete alignments, where the products over i, j, k, l are replaced by powers n, n', m, m' of the polynomials P_p and R_p. Note that the normalization factors $\mathcal{N}$ of the vevs are integrated in the polynomials, thus they can not be absorbed by the coefficient in front of the operator. Again, the **H**-dependent quantities are listed in Table 6.3, and for each of the four sectors there are two Yukawa terms in Eq. (6.17).

The most general approach to generate Yukawa terms from a non-renormalizable operator as in Eq. (6.10) can be treated by a straight forward extension of the result in Eq. (6.17). In particular, this approach describes the case of multiple **45** and **210** where each GUT scale vev points in its own (arbitrary) direction. The corresponding Yukawa terms are then calculated by replacing the powers of the polynomials P and R in Eq. (6.17) by a product, where each polynomial correspond to one GUT scale vev, thus having its own κ-variable(s). Discrete alignments in SU(5) or Pati-Salam directions are described by using the special κ-values from Table 6.6.

Table 6.5: List of Yukawa ratios from Eq. (6.12) for $\mathbf{H} = \mathbf{10}$ and the predictive scenario #1 from Table 6.4. All ratios for superpotential operators up to dimension five (i.e. $n + n' + m + m' \leq 2$) using the discrete SU(5) and Pati-Salam vev alignments of the **45** and **210** from Eq. (6.3) and (6.4) are presented, which feature $|(\mathbf{Y}_e)_{II}/(\mathbf{Y}_d)_{II}| \leq 8$. For each tuple of Yukawa ratios, all suitable combinations of vev alignments are listed, where the fields $\{\mathbf{45}_{\alpha_i}, \mathbf{210}_{\beta_j}\}$ on the left- and the fields $\{\mathbf{45}_{\alpha'_k}, \mathbf{210}_{\beta'_l}\}$ on the right-hand side of the **10** are separated by a vertical bar. A dot indicates that there is no field.

Nr	$\left(\frac{(\mathbf{Y}_e)_{II}}{(\mathbf{Y}_d)_{II}}, \frac{(\mathbf{Y}_u)_{II}}{(\mathbf{Y}_d)_{II}}, \frac{(\mathbf{Y}_\nu)_{II}}{(\mathbf{Y}_d)_{II}}\right)$	$\left(\{\mathbf{45}_{\alpha_i}, \mathbf{210}_{\beta_j}\}\|\{\mathbf{45}_{\alpha'_k}, \mathbf{210}_{\beta'_l}\}\right)$
1	$(-3,-1,3)$	$(\widetilde{Z}_3\|\cdot)$, $(\widetilde{X}_1,\widetilde{X}_2\|\cdot)$, $(X_1,\widetilde{Z}_2\|\cdot)$, $(X_2,\widetilde{Z}_2\|\cdot)$, $(\widetilde{X}_1,\widetilde{Z}_2\|\cdot)$, $(\widetilde{Z}_1,\widetilde{Z}_3\|\cdot)$, $(X_1\|\widetilde{X}_1)$, $(X_2\|\widetilde{X}_1)$, $(\widetilde{X}_1\|\widetilde{X}_2)$, $(X_1\|\widetilde{Z}_2)$, $(X_2\|\widetilde{Z}_2)$, $(\widetilde{X}_1\|\widetilde{Z}_2)$, $(\widetilde{Z}_1\|\widetilde{Z}_3)$
2	$(-3,0,0)$	$(Z_3\|\cdot)$, $(X_1,Z_3\|\cdot)$, $(Z_1,Z_3\|\cdot)$, $(X_1\|Z_3)$, $(Z_1\|Z_3)$
3	$(-3,\frac{3}{5},-\frac{9}{5})$	$(Z_2\|\cdot)$, $(X_1,X_2\|\cdot)$
4	$(-3,1,-3)$	$(\widetilde{Z}_2\|\cdot)$, $(\widetilde{X}_1,\widetilde{Z}_3\|\cdot)$, $(\widetilde{X}_2,\widetilde{Z}_1\|\cdot)$, $(\widetilde{X}_2\|\widetilde{Z}_1)$
5	$(-\frac{9}{7},\frac{5}{7},-\frac{27}{7})$	$(\widetilde{X}_2,Z_2\|\cdot)$, $(\widetilde{X}_2\|Z_2)$
6	$(-\frac{21}{19},-\frac{3}{19},-\frac{27}{19})$	$(X_1,Z_2\|\cdot)$
7	$(-1,-1,1)$	$(\widetilde{X}_1\|Z_1)$
8	$(-1,-\frac{2}{3},0)$	$(\widetilde{X}_1,Z_2\|\cdot)$
9	$(-1,0,-2)$	$(X_1,\widetilde{Z}_1\|\cdot)$, $(X_1\|\widetilde{Z}_1)$
10	$(-1,0,2)$	$(Z_1,\widetilde{Z}_1\|\cdot)$, $(Z_1\|\widetilde{Z}_1)$
11	$(-1,1,-5)$	$(\widetilde{X}_1,Z_1\|\cdot)$
12	$(-\frac{9}{11},-\frac{17}{11},\frac{27}{11})$	$(X_2,Z_2\|\cdot)$
13	$(-\frac{3}{7},-\frac{3}{7},-\frac{9}{7})$	$(Z_1,Z_2\|\cdot)$
14	$(-\frac{3}{7},\frac{3}{7},\frac{45}{7})$	$(Z_1\|Z_2)$
15	$(-\frac{1}{3},\frac{1}{3},\frac{5}{3})$	$(X_1,\widetilde{X}_1\|\cdot)$
16	$(0,-1,0)$	$(\widetilde{X}_1\|Z_3)$, $(Z_3\|\widetilde{Z}_3)$
17	$(\frac{3}{7},\frac{5}{7},\frac{9}{7})$	$(Z_2,\widetilde{Z}_1\|\cdot)$, $(Z_2\|\widetilde{Z}_1)$
18	$(1,-1,-5)$	$(Z_1\|Z_1)$
19	$(1,-1,-1)$	$(X_1\|\cdot)$, $(X_2\|\cdot)$, $(\widetilde{X}_1\|\cdot)$, $(\widetilde{X}_1,\widetilde{Z}_1\|\cdot)$, $(\widetilde{X}_1\|\widetilde{Z}_1)$
20	$(1,-\frac{1}{2},-\frac{5}{2})$	$(X_1\|Z_1)$
21	$(1,-\frac{1}{3},5)$	$(X_1\|X_1)$
22	$(1,\frac{1}{5},\frac{17}{5})$	$(X_1,X_1\|\cdot)$
23	$(1,\frac{1}{3},-5)$	$(X_1,\widetilde{Z}_3\|\cdot)$, $(X_1\|Z_2)$
24	$(1,\frac{1}{2},-\frac{11}{2})$	$(X_1,Z_1\|\cdot)$
25	$(1,1,1)$	$(\cdot\|\cdot)$, $(\widetilde{X}_1,\widetilde{X}_1\|\cdot)$, $(\widetilde{Z}_1,\widetilde{Z}_1\|\cdot)$, $(\widetilde{Z}_1\|\widetilde{Z}_1)$
26	$(1,1,13)$	$(Z_1,Z_1\|\cdot)$
27	$(3,-1,-3)$	$(Z_1\|\widetilde{Z}_3)$
28	$(3,-\frac{2}{3},0)$	$(Z_2,\widetilde{Z}_3\|\cdot)$
29	$(3,0,-6)$	$(\widetilde{X}_2,Z_1\|\cdot)$, $(\widetilde{X}_2\|Z_1)$
30	$(3,0,6)$	$(X_1,\widetilde{X}_2\|\cdot)$, $(X_1\|\widetilde{X}_2)$
31	$(3,1,15)$	$(Z_1,\widetilde{Z}_3\|\cdot)$
32	$(3,2,0)$	$(X_2,\widetilde{X}_1\|\cdot)$, $(Z_3,\widetilde{Z}_1\|\cdot)$, $(Z_3\|\widetilde{Z}_1)$
33	$(\frac{117}{37},\frac{17}{37},\frac{81}{37})$	$(Z_2,Z_2\|\cdot)$
34	$(\frac{9}{2},-\frac{5}{2},0)$	$(X_2\|Z_3)$
35	$(\frac{9}{2},\frac{5}{6},0)$	$(Z_2\|Z_3)$

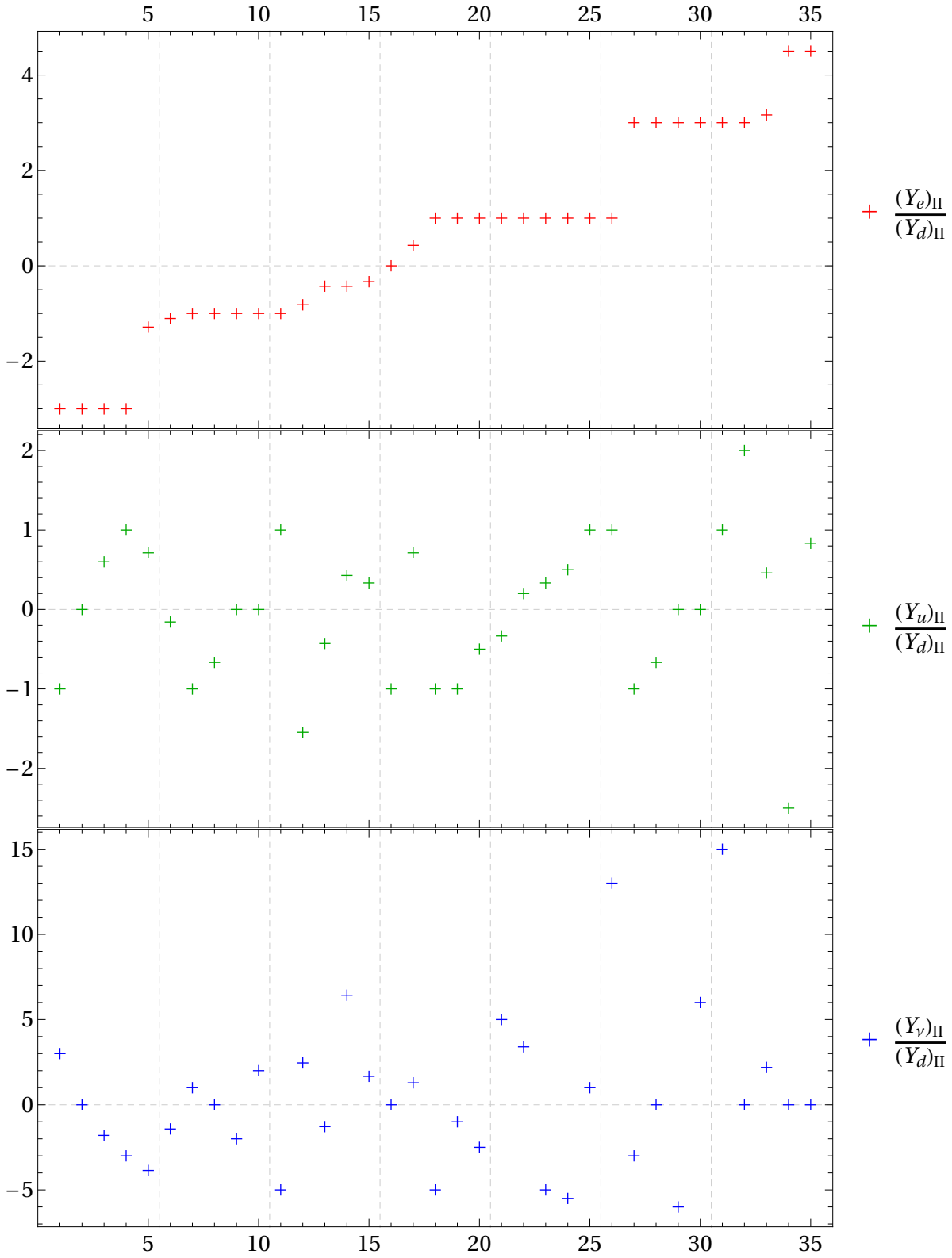

Figure 6.1: Graphical illustration of the Yukawa ratios that are listed in Table 6.5 with the same numbering, which is specified on the x-axis. The tuples of Yukawa ratios are ordered lexicographically with respect to the values of the three ratios.

Table 6.6: List of the special values of the ratios κ, κ_1 and κ_2 which reproduce the discrete vev alignments in the representations **45** and **210** from Eq. (6.3) and (6.4).

alignment	κ	alignment	κ_1	κ_2
X_1	0	Z_1	0	0
X_2	∞	Z_2	∞	0
		Z_3	0	∞
$\widetilde{X}_1$	$-\sqrt{3/2}$	$\widetilde{Z}_1$	-2	$\sqrt{5}$
$\widetilde{X}_2$	$\sqrt{2/3}$	$\widetilde{Z}_2$	$4/3$	$\sqrt{5/9}$
		$\widetilde{Z}_3$	$-1/3$	$-\sqrt{5/9}$

6.3 Construction of the Yukawa operators via mediators

A non-renormalizable superpotential operator of the schematic form as in Eq. (6.1) generates Yukawa terms at the MSSM level, once the **45** and **210** acquired SM singlet vevs at the GUT scale. Apart from the choice of the Higgs representation **H**, the GUT scale vev alignments and the powers n and m, also the particular contraction of the SO(10) representations to form a gauge singlet impacts the shape of the MSSM Yukawa terms. For example, in the case of $\mathbf{H} = \mathbf{10}$, $n = 1$ and $m = 0$, there are two possible independent ways of contracting the indices, namely

$$W \supset \mathbf{45}^A{}_D \, (\mathbf{16}_I)^D \, C_{AB} \, \mathbf{10}^B{}_E \, (\mathbf{16}_J)^E \,, \tag{6.18}$$

$$W \supset (\mathbf{16}_I)^A \, C_{AB} \, (\mathbf{45} \cdot \mathbf{10})^B{}_E \, (\mathbf{16}_J)^E \,, \tag{6.19}$$

where

$$(\mathbf{45} \cdot \mathbf{10})^B{}_E = \mathbf{45}^{ij} \, P_{jk} \, \mathbf{10}^k \, (\Gamma_i)^B{}_E \,, \tag{6.20}$$

using the conventions from Section 3.2. The difference between the two invariants is, whether the **10** and the **45** are contracted via a spinor index, as in Eq. (6.18), or via a fundamental index, as in Eq. (6.19). Since both operators contain the same set of fields, also additional global U(1) or $\mathbb{Z}_k$ symmetries can not distinguish between the two invariants. Thus, from the point of view of symmetries always both operators are present for a specific tuple of family indices (I, J). However, this is in contradiction with the concept of single operator dominance.

A way to resolve this shortcoming in model building, apart from artificially setting one operator to zero, is, to generate the non-renormalizable operators as effective operators from a renormalizable theory by integrating out heavy mediator fields, which have masses above the GUT scale. For example, the operator in Eq. (6.18) is obtained from a renormalizable superpotential by integrating out mediators in the representations **16** and $\overline{\mathbf{16}}$ (embedded into 32-dimensional vectors as in Eq. (3.26)). On the other hand, the operator in Eq. (6.19) is generated via a mediator **10**. In principle, we could also choose a mediator **120** instead of the **10**, however the resulting operator is not linearly independent from the other two. The two cases are graphically illustrated in Figure 6.2. This shows, that for a particular set of mediators only one of the two operators in Eq. (6.18) and (6.19) is generated.

The above considerations also apply to general operators as in Eq. (6.1). In Figure 6.3 it is shown, how a non-renormalizable operator with $\mathbf{H} = \mathbf{10}$ and an arbitrary number of **45** is generated by using mediators of the type **16** and $\overline{\mathbf{16}}$. In general, each GUT scale vev $\langle \mathbf{45} \rangle$ can point in a different direction. Optionally, a **45** can be replaced by a **210**, and the **10** by a $\overline{\mathbf{126}}$ or $\overline{\mathbf{120}}$, in order to describe the general case. Because of the mediators **16** and $\overline{\mathbf{16}}$, in the effective operator the contractions between the **45** and the **10** happen via a spinor index. Thus, the effective operator in Figure 6.3 corresponds to a non-renormalizable operator as in Eq. (6.10). As already discussed, because the matrices $\langle \mathbf{45} \rangle^A{}_B$ and $\langle \mathbf{210} \rangle^A{}_B$ are diagonal, they commute among each other, but they do not commute with the EW doublets in $\mathbf{H}^A{}_B$. Thus, the relative order of the GUT-scale

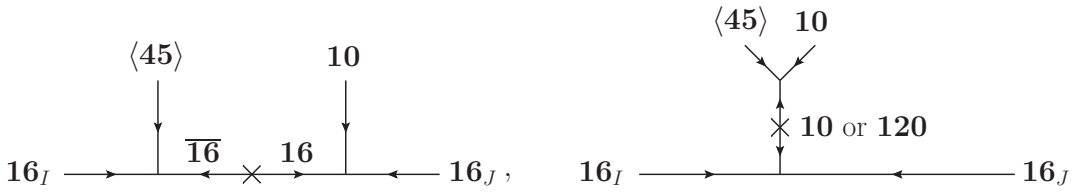

Figure 6.2: Examples of non-renormalizable superpotential operators which are constructed from renormalizable operators by use of mass insertions of heavy mediator fields, indicated by a $\times$. The two diagrams have the same external fields, but different mediators, and represent the two different non-renormalizable operators in Eq. (6.18) and (6.19). The angle brackets denote a GUT scale vev, such that Yukawa terms at the MSSM level are formed.

vevs on each side of $\mathbf{H}$ has no impact on the Yukawa terms at the MSSM level, but it is important whether a vev is located on the left- or on the right-hand side of $\mathbf{H}$.

The operator in Eq. (6.10) represents the most general effective operator, which we can get from a renormalizable superpotential using mediators $\mathbf{16}$ and $\overline{\mathbf{16}}$. In principle, an external leg with a $\mathbf{45}$ or $\mathbf{10}$ in Figure 6.3 can have a more complicated tree structure, if additional mediators of a different type are present. Two examples of how an external leg can look like in such a case are given in Figure 6.4. However, in the following we restrict ourselves to the cases where the mediators have the representations $\mathbf{16}$ and $\overline{\mathbf{16}}$.

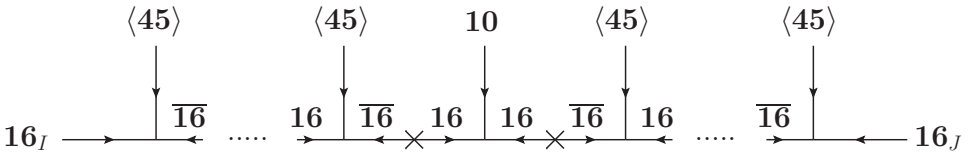

Figure 6.3: A generic non-renormalizable superpotential operator of the form $\mathbf{16}_I \cdot \mathbf{16}_J \cdot \mathbf{10} \cdot \mathbf{45}^n$, which is constructed from renormalizable interactions by using mass insertions of mediators of the type $\mathbf{16}$ and $\overline{\mathbf{16}}$, indicated by a $\times$. The GUT scale vevs, which are denoted by angle brackets, commute among each other, but not with the EW doublets of the Higgs field representation. Hence, it is important whether a $\langle\mathbf{45}\rangle$ is located on the left- or on the right-hand side of the $\mathbf{10}$.

Even if we use only $\mathbf{16}$ and $\overline{\mathbf{16}}$ mediators, there are still multiple possibilities to form effective operators of the form as in Eq. (6.10), because the external legs with a $\mathbf{45}$ or $\mathbf{10}$ in Figure 6.3 can be permuted. In order to distinguish between these cases, we introduce a global U(1) symmetry (or alternatively a discrete subgroup $\mathbb{Z}_k$) in the renormalizable theory. The charge assignments to the fields are defined in Figure 6.5. We assume that there are M legs with a $\mathbf{45}$ or $\mathbf{210}$ on the left-hand side of $\mathbf{H}$, and N of these legs on the right-hand side, i.e. $n + m = M$ and $n' + m' = N$. Once the mediators are integrated out in Figure 6.5, we get the following effective operator

$$W \supset \left((\mathbf{X}_M)^{A_M}{}_{A_{M-1}} \dots (\mathbf{X}_1)^{A_1}{}_D \, (\mathbf{16}_I)^D \right) C_{A_M B} \, \mathbf{H}^B{}_{E_N} \left((\mathbf{Y}_N)^{E_N}{}_{E_{N-1}} \dots (\mathbf{Y}_1)^{E_1}{}_F \, (\mathbf{16}_J)^F \right), \tag{6.21}$$

where each $\mathbf{X}_i$ and $\mathbf{Y}_j$ represents either a $\mathbf{45}$ or a $\mathbf{210}$. Note that up to a possible overall minus sign, the placement of the charge conjugation matrix C does not affect the form

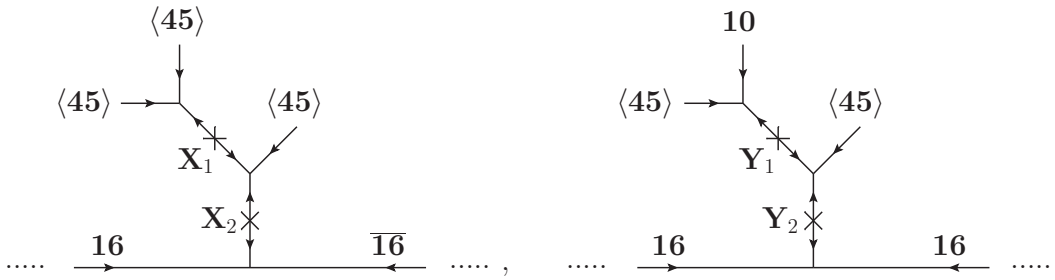

Figure 6.4: Examples of external legs with a complicated tree structure, which may be present in the diagram of Figure 6.3, if in addition to the **16** and $\overline{\mathbf{16}}$ also other types of mediators are considered. An external leg which contains only GUT scale vevs $\langle\mathbf{45}\rangle$ is shown on the left-hand side, whereas an external leg with a Higgs representation **10** is shown on the right-hand side. An incomplete list of possible mediators in the two diagrams is given by: $(\mathbf{X}_1, \mathbf{X}_2) \in \{(\mathbf{45},\mathbf{45}), (\mathbf{45},\mathbf{210}), (\mathbf{54},\mathbf{45})\}$, and $(\mathbf{Y}_1, \mathbf{Y}_2) \in \{(\mathbf{10},\mathbf{10}), (\mathbf{120},\overline{\mathbf{126}}), (\mathbf{10},\mathbf{120}))\}$.

of the operator. The charges of the mediators **16** on the left and on the right of **H** are labelled by γ_i and δ_j, respectively (the $\overline{\mathbf{16}}$ have charges $-\gamma_i$ and $-\delta_j$). Furthermore, the fields $\mathbf{X}_i$ and $\mathbf{Y}_j$ carry charges x_i and y_j, and the charges of the fermionic $\mathbf{16}_{I,J}$ and the Higgs representation **H** are denoted by $f_{I,J}$ and h, respectively.

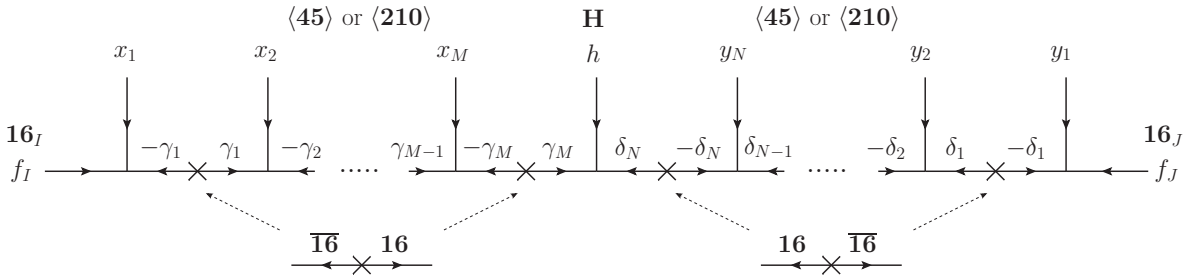

Figure 6.5: The charges of the fields in Figure 6.3 concerning a global U(1) symmetry. The fields **H** and $\mathbf{16}_{I,J}$ carry the charges h and $f_{I,J}$, respectively. Furthermore, on the left-hand side of **H** the charges of the **45** and **210** are labelled by x_i, and the ones of the mediators **16**, $\overline{\mathbf{16}}$ by γ_i, $-\gamma_i$. The replacements $x_i \mapsto y_j$ and $\gamma_i \mapsto \delta_j$ then provide charges of the corresponding fields on the right-hand side of **H**.

Since the total charge of each operator at the renormalizable level has to be zero, the charges of the mediators are completely determined by the ones of the $\mathbf{16}_{I,J}$ and of the $\mathbf{X}_i$ and $\mathbf{Y}_j$, namely

$$\gamma_i = f_I + \sum_{s=1}^{i} x_s \quad (i = 1, ..., M)\,, \tag{6.22}$$

$$\delta_j = f_J + \sum_{t=1}^{j} y_t \quad (j = 1, ..., N)\,. \tag{6.23}$$

For $i = M$ and $j = N$ the two equations imply that the charge of the $\mathbf{H}$ is given by

$$h = -\big(f_I + f_J + \sum_{s=1}^{M} x_s + \sum_{t=1}^{N} y_t\big)\,, \tag{6.24}$$

which is exactly the condition, that the total charge of the effective operator is equal to zero. If we choose a discrete global symmetry $\mathbb{Z}_k$, the identities in Eqs. (6.22)–(6.24) hold modulo k.

For a given diagram as in Figure 6.5 with a suitable set of charges, it has to be checked whether a different diagram with the same external legs, but in a permuted order, can be constructed by using the same set (or a subset) of mediators. If that is not the case, we say that the diagram is "protected". Since the form of the Yukawa terms at the MSSM level depends only on the location of the GUT scale vevs $\langle\mathbf{45}\rangle$ and $\langle\mathbf{210}\rangle$ relative to the $\mathbf{H}$, but not on the specific order of the vevs on each side of $\mathbf{H}$, the protection of a diagram is a sufficient, but not a necessary condition for single operator dominance.

We discuss whether a diagram can be protected or not with a suitable set of charges for the following two cases:

- $I \neq J$:
  In this case, a diagram can always be protected, i.e. the external legs are in a unique order. For example, choose $x_s > 0$, $y_t > 0$ and $q_J = q_I + \sum_{s=1}^{m} x_s + \sum_{t=1}^{n} y_t$, where different **45** or **210** are assumed to have different charges x_s and y_t, such that no single charge is the sum of other charges.

- $I = J$:

  – If all $\mathbf{X}_i$ and $\mathbf{Y}_j$ are the same field, i.e. the operator contains just one field **45** or one field **210**, the diagram can only be protected in case of $|M - N| \leq 1$, which means that the diagram is as symmetric as possible. If this condition is not fulfilled, a given diagram always comes along with a more symmetric diagram, which may give different contributions to the MSSM Yukawa terms. An example of that case is shown in Figure 6.6.

  – If not all $\mathbf{X}_i$ and $\mathbf{Y}_j$ are the same field, a specific order of the external legs may not be possible to protect. However, the predictions for the Yukawa terms at the MSSM level do not depend on the order of the GUT scale vevs on each side of $\mathbf{H}$. We checked numerically, that for a given diagram, there exists always an equivalent diagram concerning the predictions of the Yukawa terms, which can be protected. An example is shown in Figure 6.7.

The above discussion shows, that the class of non-renormalizable superpotential operators defined in Eq. (6.10), where the contractions happen in a "spinorial way", is well motivated, since they can be constructed from renormalizable interactions by integrating out heavy mediator fields of the type **16** and $\overline{\mathbf{16}}$. Furthermore, the assignment of global charges to the fields allows in most cases to choose a unique operator for given family indices (I, J) to generate the Yukawa terms at the MSSM level, which corresponds to the concept of single operator dominance. In a concrete model one has to be aware, that the charges f_I and f_J can not be chosen independently for each of the nine tuples of family indices, and that a chosen set of mediators for given indices (I, J) may allow to generate unwanted effective operators for other tuples of family indices.

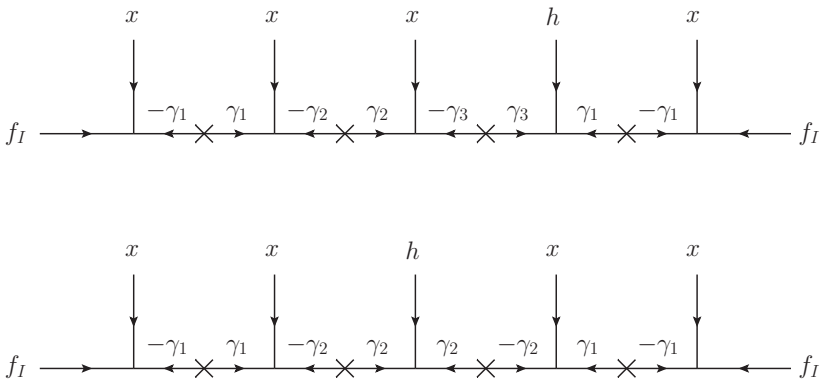

Figure 6.6: An example of a diagram in the case of $I = J$ and only one field **45** or **210** with charge x, which can not be protected. If the upper diagram is present, the lower, more symmetric diagram can be formed as well, by using a subset of the mediators.

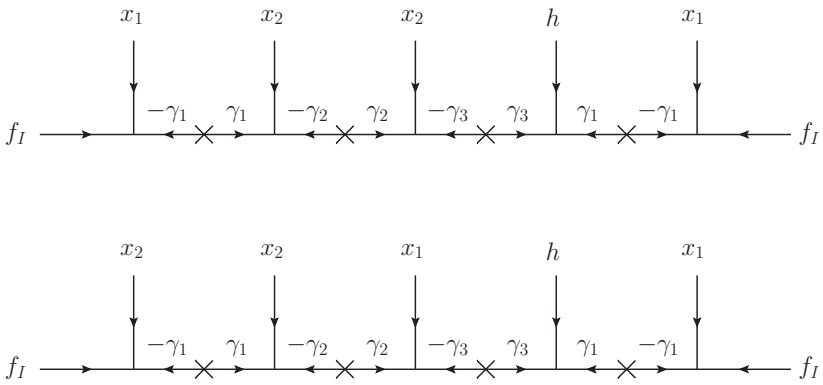

Figure 6.7: Example of two diagrams in the case of $I = J$ which lead to the same MSSM Yukawa terms, but where only one of them can be protected. Both diagrams contain two different fields **45** or **210** with charges x_1 and x_2. If the upper diagram is present, the symmetric diagram with the external leg structure x_1-x_2 and x_2-x_1 on the left- and on the right-hand side of h, respectively, can be constructed as well, for any choice of the global charges. On the other hand, the lower diagram, where the external legs on the left-hand side of h are permuted, can be protected by an appropriate choice of charges, e.g. $f_I = 0$, $x_1 = 3$ and $x_2 = 1$.

6.4 Examples of predictive Higgs sectors

In this section we consider simple scenarios of Higgs sectors which are predictive in the Yukawa sector. Predictive means that no additional parameters a_i and b_i in the Yukawa sector are introduced, due to non-alignment of the doublet states H_i^u and H_i^d in the GUT representations with the EW doublets H_u and H_d, respectively, as discussed in Section 3.3. In general, a_i and b_i are functions of Higgs sector parameters. In terms of mass eigenstates of the doublet mass matrix, H_i^u and H_i^d are written as

$$H_i^u = a_i^* \, H_u + \dots \,, \qquad\qquad H_i^d = b_i^* \, H_d + \dots \,, \tag{6.25}$$

where the dots indicate states with a vanishing vev. In order to be predictive in the Yukawa sector, the coefficients a_i and b_i corresponding to the same Higgs representation $\mathbf{H}$ must be identical up to a constant factor. This allows to absorb the Higgs parameter dependence into the Yukawa couplings. In such a case the $\chi^{\mathbf{H}}$ ratios from Eq. (6.13) have constant values (up to the factor H_d/H_u). The simplest case is, if a_i and b_i are just constants.

Each predictive scenario we consider in this section is based on one of the following four superpotentials in the Higgs sector:

$$W_{\text{(i)}} = \tfrac{1}{2}\, m_{10}\, \mathbf{10}_i\, \mathbf{10}^i - \sqrt{\tfrac{5}{3}}\, \lambda'_{112}\, \mathbf{10}_i\, \mathbf{10}_i\, \mathbf{54}^{ij} \,, \tag{6.26}$$

$$W_{\text{(ii)}} = \tfrac{1}{2}\, m_{120}\, \mathbf{120}_{ijk}\, \mathbf{120}^{ijk} - 2\sqrt{15}\, \lambda'_{233} \mathbf{120}^{ijk}\, \mathbf{120}_{ijl}\, \mathbf{54}_k{}^l \,, \tag{6.27}$$

$$\begin{aligned} W_{\text{(iii)}} = m_{126}\, \overline{\mathbf{126}}_{ijklm}\, \mathbf{126}^{ijklm} &+ \sqrt{15}\, \lambda'_{25\bar{5}}\, \mathbf{126}_{ijklm}\, \mathbf{126}^{ijkln}\, \mathbf{54}^m{}_n \\ &+ \sqrt{15}\, \lambda'_{2\bar{5}\bar{5}}\, \overline{\mathbf{126}}_{ijklm}\, \overline{\mathbf{126}}^{ijkln}\, \mathbf{54}^m{}_n \,, \end{aligned} \tag{6.28}$$

$$W_{\text{(iv)}} = \tfrac{1}{2}\, m_{10}\, \mathbf{10}_i\, \mathbf{10}^i + \tfrac{1}{2}\, m_{120}\, \mathbf{120}_{ijk}\, \mathbf{120}^{ijk} + \tfrac{\sqrt{15}}{2}\, \lambda_{123}\, \mathbf{120}_{ijk}\, \mathbf{10}^i\, \mathbf{45}^{jk} \,, \tag{6.29}$$

where the **45** and **54** acquire GUT scale singlet vevs. The **45** in the Higgs and in the Yukawa sector may be different fields. Moreover, the vev of **54** is labelled by W_{54}. Note that these superpotentials contain only operators which are relevant for the construction of the doublet and triplet mass matrices; we do not consider spontaneous symmetry breaking of the SO(10) gauge group. Furthermore, the doublet-triplet splitting is achieved by fine-tuning of one of the parameters in the Higgs sector, such that $\det M_D = 0$ and $\det M_T \neq 0$.

A list of the predictive scenarios is given in Table 6.7, where for each scenario the corresponding superpotential term from Eqs (6.26)–(6.29), the available representations $\mathbf{H}$ and the additional GUT representations are specified. Furthermore, the fine-tuning condition of the parameters for DT splitting and the location of the light mass eigenstates $H_{u,d}$ in the flavour eigenstates $H_i^{u,d}$ are stated.

In the following we briefly comment on the different predictive scenarios from Table 6.7:

- In the scenarios #1–3 the parameters a_i and b_i have fixed values. These are the simplest scenarios for $\mathbf{H} = \mathbf{10}$ and $\mathbf{H} = \mathbf{120}$. Since the **10** contains only one doublet pair $H_1^{u,d}$, the mass matrices M_D and M_T in scenario #1 are just 1×1-dimensional. Scenario #2 and 3 are based on the same Higgs superpotential $W_{\text{(ii)}}$, but different

Table 6.7: Examples of predictive Higgs sectors with DT splitting, where for each scenario the available representations **H**, the additional SO(10) representations in the Higgs sector, the Higgs superpotential, the fine-tuning condition for DT splitting, and the location of the MSSM Higgses $H_{u,d}$ in the flavor states $H_i^{u,d}$ are specified. If the predictions in the Yukawa sector are considered, the proportionality sign $\propto$ can be replaced by an equal sign $=$.

#	**H**	other reps	superpotential	fine-tuning	Higgs location
1	**10**	**54**	$W_{(\mathrm{i})}$	$\lambda'_{112} = -\frac{m_{10}}{W_{54}}$	$H_1^{u,d} = H_{u,d}$
2	**120**	**54**	$W_{(\mathrm{ii})}$	$\lambda'_{233} = -\frac{m_{120}}{6W_{54}}$	$H_3^{u,d} = -\frac{1}{2}H_{u,d}$ $H_4^{u,d} = \frac{\sqrt{3}}{2}H_{u,d}$
3	**120**	**54**	$W_{(\mathrm{ii})}$	$\lambda'_{233} = \frac{3m_{120}}{2W_{54}}$	$H_3^{u,d} = \frac{\sqrt{3}}{2}H_{u,d}$ $H_4^{u,d} = \frac{1}{2}H_{u,d}$
4	$\overline{\mathbf{126}}$	**126**, **54**	$W_{(\mathrm{iii})}$	$\lambda'_{255} = \frac{m_{126}^2}{W_{54}^2 \lambda'_{2\bar{5}\bar{5}}}$	$H_2^{u,d} \propto H_{u,d}$
5	**10**,**120**	$\langle \mathbf{45} \rangle = \widetilde{X}_1$	$W_{(\mathrm{iv})}$	$\lambda_{123} = \frac{2\sqrt{2}i}{\widetilde{X}_1\sqrt{5}}\sqrt{m_{10}m_{120}}$	$H_1^u \propto H_u$ $H_1^d \propto -H_d$ $H_3^{u,d} \propto -H_{u,d}$ $H_4^{u,d} \propto \sqrt{3}H_{u,d}$
6	**10**,**120**	$\langle \mathbf{45} \rangle = \widetilde{X}_2$	$W_{(\mathrm{iv})}$	$\lambda_{123} = \frac{2i}{\widetilde{X}_2\sqrt{5}}\sqrt{m_{10}m_{120}}$	$H_1^u \propto H_u$ $H_1^d \propto -H_d$ $H_3^{u,d} \propto \sqrt{3}H_{u,d}$ $H_4^{u,d} \propto H_{u,d}$

fine-tuning conditions for DT splitting are implemented. The **120** contains $H_3^{u,d}$ and $H_4^{u,d}$, thus the space of doublets and antidoublets in these scenarios is 2-dimensional.

- In scenario #4, the $\overline{\mathbf{126}}$ is used to construct the Yukawa operators. It contains the doublet pair $H_2^{u,d}$, however H_2^u and H_2^d are located in different SU(5) representations **5** and $\overline{\mathbf{45}}$ (cf. Eq. (6.7) and (6.8)). Moreover, $\overline{\mathbf{126}}$ is a complex representation, thus an additional representation **126**, which contains another doublet pair, has to be introduced in order to form a mass term in the superpotential. Because of these issues, it is more tricky than in #1–3 to find a predictive scenario. For the given fine-tuning condition we find $H_2^u = c\,H_u$ and $H_2^d = c\,H_d$ (i.e. $a_2 = b_2 = c$), where c is a function of the parameters of $W_{(\mathrm{iii})}$. Thus, the scenario is predictive in the Yukawa sector. Note, parts of the light states $H_{u,d}$ are contained in the (anti)doublets of **126**, which however are not present in the Yukawa operators. In Table 6.7, the factor c is simply indicated by the proportionality sign $\propto$. If one is only interested in the predictions for the Yukawa sector at the MSSM level, the $\propto$ sign can be replaced by the equal sign $=$.

- In each of the scenarios #5 and 6 there are two different **H**-representations available,

namely the **10** and the **120**. Thus, there are three doublet-antidoublet pairs. The difference between the two scenarios is the different alignment of the GUT scale vev $\langle \mathbf{45} \rangle$ in the Pati-Salam directions $\widetilde{X}_1$ and $\widetilde{X}_2$, respectively, defined in Eq. (6.4). Although in both scenarios the coefficients a_i and b_i are dependent on the Higgs potential parameters, as in scenario #4, both cases are predictive. For example, in #5 we have $H_1^u = c\, H_u$, $H_1^d = -c\, H_d$ and $H_3^{u,d} = -\tilde{c}\, H_{u,d}$, $H_4^{u,d} = \sqrt{3}\,\tilde{c}\, H_{u,d}$, where c and $\tilde{c}$ are functions of the parameters of $W_{(\mathrm{iv})}$, which means $a_1 = -b_1 = c$, $a_3 = b_3 = -\tilde{c}$ and $a_4 = b_4 = \sqrt{3}\,\tilde{c}$. Again, the sign $\propto$ in Table 6.7 can be replaced by $=$, if one is interested in the Yukawa sector at the MSSM level.

CHAPTER 7

Quantitative calculation of proton decay from dimension 5 operators in SUSY models

7.1 Motivation

In supersymmetric GUTs, the dominant contributions to proton decay are typically induced by dimension 5 operators, assuming that the theory respects matter parity such that baryon and lepton number violating dimension 4 operators are forbidden. The dimension 5 operators are generated by integrating out heavy color triplet and antitriplet states $(\mathbf{3}.\mathbf{1})(-\frac{1}{3})$ and $(\overline{\mathbf{3}}.\mathbf{1})(+\frac{1}{3})$, respectively, which are usually present in the same GUT representations as the EW doublet states. At the SUSY scale, where the superpartners of the SM particles are integrated out, the baryon and lepton number violating four-fermion operators, which cause proton decay, are constructed at 1-loop level by dressing the dimension 5 operators with gluino, chargino and neutralino exchange diagrams.

The currently most stringent bounds on proton decay are given by the Super-Kamiokande experiment [92], in particular for the channels which have a lepton and one of the mesons π^0, η^0, K^+ in the final state. It turns out, that in concrete SUSY GUT models with sparticle masses of $\mathcal{O}(10\,\text{TeV})$ or smaller (so called low-energy SUSY), the triplet mass scale which suppresses the dimension 5 operators must typically be at around $10^{17}\,\text{GeV}$ or even higher, in order that the predicted proton decay is compatible with the experimental data (see e.g. [95]). Depending on the form of the triplet mass matrix, which in turn depends on the implementation of doublet-triplet splitting, this mass scale is either in one-to-one correspondence with the masses of the triplet-antitriplet pairs, or it is given by some effective mass scale, as for example in the (double) missing partner mechanism (cf. Section 3.3 for references).

In general, the rough estimate of $\gtrsim 10^{17}\,\text{GeV}$ for the triplet mass scale shows, that even if all the triplet masses are located at the GUT scale, the prediction for proton decay may be in tension or even in contradiction with the experimental data. Thus, a quantitative calculation of the partial decay widths for the dominant decay channels of the proton is necessary, in order to determine whether the predictions for proton decay of a SUSY GUT model are compatible with the experimental bounds or not.

The purpose of this chapter is to specify the procedure and the relevant formulas to quantitatively calculate the partial decay widths of a proton or neutron with a meson and a lepton in the final state, in the context of nucleon decay from dimension 5 operators. The formulas are taken from various sources, but the main part of the calculation follows the considerations in [97]. The algorithm has been implemented in a Mathematica package, which forms an extension of SusyTC [106], but is also compatible with standard SLHA

output of SUSY spectrum generators.

This chapter is based on an ongoing project and is organized as follows: in Section 7.2 the numerical procedure, including all the relevant formulas, to calculate proton decay from dimension 5 operators is described. An example calculation is then presented in Section 7.3, by applying the algorithm to a toy model.

7.2 Numerical procedure

In this section we describe the procedure to numerically calculate various partial decay widths of the proton and the neutron. The considerations are limited to the case of nucleon decay from dimension 5 operators. The formulas for the dressing of the dimension 5 operators and the calculation of the decay amplitudes are taken from [97]. Thus, we adapt our notation in order to match the conventions used in that reference. In particular this means, that for the family indices we use small letters $i, j, k, l, ...$ instead of capital letters $I, J, K, L, ...$, and the dimension 5 operators from Section 3.4 are written as $C_{5L,R}^{ijkl} \equiv \mathbf{C}_{5L,R}^{IJKL}$.

For completeness, we state the effective superpotential of the dimension 5 operators from Eq. (3.46) again in the adapted notation:

$$\begin{aligned} W_5 = &-\tfrac{1}{2} C_{5L}^{ijkl}\, \epsilon_{\hat{a}\hat{b}\hat{c}}\, (Q_i^{\hat{a}} \cdot L_j)(Q_k^{\hat{b}} \cdot Q_l^{\hat{c}}) \\ &- C_{5R}^{ijkl}\, \epsilon^{\hat{a}\hat{b}\hat{c}}\, u_{i\hat{a}}^c\, d_{j\hat{b}}^c\, e_k^c\, u_{l\hat{c}}^c\,, \end{aligned} \tag{7.1}$$

where $\hat{a}, \hat{b}, \hat{c}$ are $\mathrm{SU}(3)_\mathrm{C}$ indices with $\epsilon_{123} = \epsilon^{123} = 1$, and the contraction of $\mathrm{SU}(2)_\mathrm{L}$ indices is given by $\Psi \cdot \Phi = \epsilon_{ab}\, \Psi^a\, \Phi^b$ with $\epsilon_{12} = 1$.

7.2.1 Running of the dimension 5 operators

In a supersymmetric GUT model, the dimension 5 operators are specified at the GUT scale by integrating out heavy triplet states. To calculate the dressing at the SUSY scale, the RG running has to be taken into account. The β-functions of the dimension 5 operators in the MSSM at 1-loop in the $\overline{\mathrm{DR}}$ scheme, by using the left-right convention for the Yukawa matrices (cf. Eq. (2.219)), are given by

$$\begin{aligned} \beta(C_{5L}^{ijkl}) = \;& C_{5L}^{mjkl} \big(\mathbf{Y}_d \mathbf{Y}_d^\dagger + \mathbf{Y}_u \mathbf{Y}_u^\dagger\big)^i{}_m + C_{5L}^{imkl} \big(\mathbf{Y}_e \mathbf{Y}_e^\dagger + \mathbf{Y}_\nu \mathbf{Y}_\nu^\dagger\big)^j{}_m \\ &+ C_{5L}^{ijml} \big(\mathbf{Y}_d \mathbf{Y}_d^\dagger + \mathbf{Y}_u \mathbf{Y}_u^\dagger\big)^k{}_m + C_{5L}^{ijkm} \big(\mathbf{Y}_d \mathbf{Y}_d^\dagger + \mathbf{Y}_u \mathbf{Y}_u^\dagger\big)^l{}_m \\ &+ C_{5L}^{ijkl} \big(-\tfrac{2}{5} g_1^2 - 6 g_2^2 - 8 g_3^2 \big)\,, \end{aligned} \tag{7.2}$$

$$\begin{aligned} \beta(C_{5R}^{ijkl}) = \;& C_{5R}^{mjkl} \big(2 \mathbf{Y}_u^\dagger \mathbf{Y}_u\big)_m{}^i + C_{5R}^{imkl} \big(2 \mathbf{Y}_d^\dagger \mathbf{Y}_d\big)_m{}^j \\ &+ C_{5R}^{ijml} \big(2 \mathbf{Y}_e^\dagger \mathbf{Y}_e\big)_m{}^k + C_{5R}^{ijkm} \big(2 \mathbf{Y}_u^\dagger \mathbf{Y}_u\big)_m{}^l \\ &+ C_{5R}^{ijkl} \big(-\tfrac{12}{5} g_1^2 - 8 g_3^2 \big)\,. \end{aligned} \tag{7.3}$$

The β-functions are computed by means of the general formulas in [135] for the 1-loop anomalous dimension matrix $\gamma_m{}^i$, and the non-renormalization theorem of the

superpotential [139–141]. We use the GUT normalization for the $\mathrm{U}(1)_\mathrm{Y}$ gauge coupling g_1; the SM normalization can be recovered by $g_1^{\mathrm{SM}} = \sqrt{3/5}\, g_1$. The RGEs are then given by

$$\frac{\mathrm{d}x}{\mathrm{d}\log\mu} = \frac{1}{16\pi^2}\beta(x)\,, \tag{7.4}$$

where $x \in \{C_{5L}^{ijkl}, C_{5R}^{ijkl}\}$ and μ is the renormalization scale. The β-functions for the gauge couplings and the Yukawa matrices can be found, for example, in [107, 135].

Note that the right-handed neutrinos are integrated out at their respective mass scales, and it is assumed that all these masses are above the SUSY scale. Thus, in the running from the GUT scale to the SUSY scale the number of columns of $\mathbf{Y}_\nu$ decreases, until $\mathbf{Y}_\nu$ is not present anymore.

7.2.2 Dressing of the dimension 5 operators

As discussed in Section 3.4, the dimension 6 operators are built at 1-loop level by dressing the dimension 5 operators with gluino, chargino and neutralino exchange diagrams, which takes place at the SUSY scale, where the superpartners of the SM particles are integrated out. To calculate the dressing of the dimension 5 operators we use the formulas from [97]. Beside the dimension 5 operators, the calculation involves the rotation matrices of the sfermions, charginos and neutralinos, as well as the mass eigenvalues of the sparticles. It is convenient to use the SLHA [142] and SLHA2 [143] conventions to specify these quantities. In Appendix C.1 the relevant formulas for the dressing, as well as the matching of the conventions used in [97] with the SLHA conventions are specified. Furthermore, in [96] all the relevant diagrams for nucleon decay from dimension 5 operators can be found.

Apart from integrating out the sparticles at the SUSY scale, we also switch to the EW symmetry broken phase of the SM. In the following u_i, d_i and e_i ($i \in \{1,2,3\}$) represent the mass eigenstates of the up-type quarks, the down-type quarks and the charged leptons. In contrast, the ν_i represent the neutrinos in the interaction basis. The additional label L or R indicates whether a state is a left- or a right-handed Weyl spinor.[1] The dimension 6 operators $\widetilde{C}$ (at the Lagrangian level), which are relevant for the calculation of proton decay, include only mass eigenstates of the fermions which are lighter than the nucleons and are given by

$$\begin{aligned}\mathcal{L}_{\not B} = \frac{1}{16\pi^2}\epsilon_{\hat{a}\hat{b}\hat{c}}\Big(&\widetilde{C}_{LL}(udue)^{ik}(u_L^{\hat{a}}d_{Li}^{\hat{b}})(u_L^{\hat{c}}e_{Lk}) + \widetilde{C}_{RL}(udue)^{ik}(u_R^{\hat{a}}d_{Ri}^{\hat{b}})(u_L^{\hat{c}}e_{Lk})\\ &+ \widetilde{C}_{LR}(udue)^{ik}(u_L^{\hat{a}}d_{Li}^{\hat{b}})(u_R^{\hat{c}}e_{Rk}) + \widetilde{C}_{RR}(udue)^{ik}(u_R^{\hat{a}}d_{Ri}^{\hat{b}})(u_R^{\hat{c}}e_{Rk})\\ &+ \widetilde{C}_{LL}(udd\nu)^{ijk}(u_L^{\hat{a}}d_{Li}^{\hat{b}})(d_{Lj}^{\hat{c}}\nu_{Lk}) + \widetilde{C}_{RL}(udd\nu)^{ijk}(u_R^{\hat{a}}d_{Ri}^{\hat{b}})(d_{Lj}^{\hat{c}}\nu_{Lk})\\ &+ \tfrac{1}{2}\widetilde{C}_{RL}(ddu\nu)^{ijk}(d_{Ri}^{\hat{a}}d_{Rj}^{\hat{b}})(u_L^{\hat{c}}\nu_{Lk})\Big) + c.c.\,.\end{aligned} \tag{7.5}$$

Since only the lightest up-type quark u_1 is lighter than the proton and the neutron, only this state is present in Eq. (7.5) and the label i is neglected. Analogously, the index i in d_i and e_i takes only the values $1, 2$, because the heaviest down-type quark and charged lepton ($i = 3$) are heavier than the two nucleons. In contrast, all three states ν_i are present.

[1] Note, in the notation of Section 1.1 the right-handed Weyl spinor u_R reads $u_R \equiv \bar{u}_R^\dagger$, and similar for d_R and e_R.

7.2.3 Running of the dimension 6 operators

In order to calculate the decay width of the proton and the neutron, the RG running of the dimension 6 operators from the SUSY scale to the mass scale of the nucleons has to be taken into account. Following [144], the main contribution to the running of the dimension 6 operators comes from the strong gauge coupling g_3. At 1-loop the β-functions in the $\overline{\text{MS}}$ scheme of the dimension 6 operators $\widetilde{C}$ from Eq. (7.5), written in the general form $\widetilde{C}^{ijkl}$, and of the gauge coupling g_3 are given by

$$\beta(\widetilde{C}^{ijkl}) = -4\, g_3^2\, \widetilde{C}^{ijkl}\,, \tag{7.6}$$

$$\beta(g_3) = \Big(-11 + \frac{2}{3} N_F \Big) g_3^3\,, \tag{7.7}$$

where N_F is the number of quarks whose masses are below the renormalization scale μ. The RGEs have the form as specified in Eq. (7.4). Note that the running of the dimension 6 operators just corresponds to an overall scaling factor, which is also referred to as the long range effect on the effective operators $\widetilde{C}$.

7.2.4 Partial decay widths

The formula for the calculation of the partial decay widths of a nucleon B_i with a meson M_j and a lepton l_k in the final state is taken from [97] and is given by

$$\Gamma(B_i \to M_j\, l_k) = \frac{m_i}{32\pi} \left(1 - \frac{m_j^2}{m_i^2}\right)^2 \frac{1}{f_\pi^2} \left(\left|A_L^{ijk}\right|^2 + \left|A_R^{ijk}\right|^2 \right), \tag{7.8}$$

where m_i and m_j are the masses of the nucleon and the meson, respectively. Moreover, $f_\pi = 0.130\,\text{GeV}$ (cf. PDG [13]) is the pion decay constant.

The amplitudes A_L^{ijk} and A_R^{ijk} for different decay channels are calculated by using the dimension 6 operators at the nucleon mass scale, and are specified in Table 7.1. In particular, the following decay channels for the proton p and the neutron n are listed in the table:

- proton: $p \to e_k^+ \pi^0$, $p \to e_k^+ \eta^0$, $p \to e_k^+ K^0$, $p \to \bar{\nu}_k \pi^+$, $p \to \bar{\nu}_k K^+$,
- neutron: $n \to e_k^+ \pi^-$, $n \to \bar{\nu}_k \pi^0$, $n \to \bar{\nu}_k \eta^0$, $n \to \bar{\nu}_k K^0$.

(7.9)

Note that $k \in \{1, 2\}$ for e_k^+, since the heaviest charged lepton is heavier than the nucleons, and $k \in \{1, 2, 3\}$ for $\bar{\nu}_k$.

Table 7.1: Formulas for the amplitudes A_L^{ijk} and A_R^{ijk} of different decay channels of the proton p and the neutron n. In particular, B_i labels the nucleon, and l_k and M_j label the lepton and the meson, respectively, in the final state. The nucleon mass m_N is taken as the average of the proton mass m_p and the neutron mass m_n, and the baryon mass $m_{B'}$ is given by the average of m_Λ and m_Σ. The additional constants with the corresponding (approximate) values are the constants from hyperon decay $F \approx 0.463$, $D \approx 0.804$ (cf. [91, 145]), and the parameters for the proton decay matrix element $\alpha \approx 0.0090\,\mathrm{GeV}^3$, $\beta \approx 0.0096\,\mathrm{GeV}^3$ (cf. [91, 146]).

B_i	l_k	M_j		A_L^{ijk} , A_R^{ijk}
p	e_k^+	π^0	L	$\frac{1}{\sqrt{2}}\big(1+F+D\big)\,\big(\alpha_p\widetilde{C}_{RL}(udue)^{1k}+\beta_p\widetilde{C}_{LL}(udue)^{1k}\big)$
			R	$-\frac{1}{\sqrt{2}}\big(1+F+D\big)\,\big(\alpha_p\widetilde{C}_{LR}(udue)^{1k}+\beta_p\widetilde{C}_{RR}(udue)^{1k}\big)$
		η_0	L	$\sqrt{\frac{3}{2}}\big(-\frac{1}{3}+F-\frac{1}{3}D\big)\,\alpha_p\widetilde{C}_{RL}(udue)^{1k}+\sqrt{\frac{3}{2}}\big(1+F-\frac{1}{3}D\big)\,\beta_p\widetilde{C}_{LL}(udue)^{1k}$
			R	$-\sqrt{\frac{3}{2}}\big(-\frac{1}{3}+F-\frac{1}{3}D\big)\,\alpha_p\widetilde{C}_{LR}(udue)^{1k}-\sqrt{\frac{3}{2}}\big(1+F-\frac{1}{3}D\big)\,\beta_p\widetilde{C}_{RR}(udue)^{1k}$
		K^0	L	$\big(-1+\frac{m_N}{m_{B'}}(F-D)\big)\,\alpha_p\widetilde{C}_{RL}(udue)^{2k}+\big(1+\frac{m_N}{m_{B'}}(F-D)\big)\,\beta_p\widetilde{C}_{LL}(udue)^{2k}$
			R	$-\big(-1+\frac{m_N}{m_{B'}}(F-D)\big)\,\alpha_p\widetilde{C}_{LR}(udue)^{2k}-\big(1+\frac{m_N}{m_{B'}}(F-D)\big)\,\beta_p\widetilde{C}_{RR}(udue)^{2k}$
	$\bar{\nu}_k$	π^+	L	$\big(1+F+D\big)\,\big(\alpha_p\widetilde{C}_{RL}(uddu)^{11k}+\beta_p\widetilde{C}_{LL}(uddu)^{11k}\big)$
		K^+	L	$\big(1-\frac{m_N}{m_{B'}}(F-\frac{1}{3}D)\big)\,\alpha_p\widetilde{C}_{RL}(ddu\nu)^{12k}+\big(1+\frac{m_N}{m_{B'}}(F+\frac{1}{3}D)\big)\,\alpha_p\widetilde{C}_{RL}(uddu)^{12k}$
				$+\big(\frac{m_N}{m_{B'}}\frac{2}{3}D\big)\,\alpha_p\widetilde{C}_{RL}(uddu)^{21k}+\big(1+\frac{m_N}{m_{B'}}(F+\frac{1}{3}D)\big)\,\beta_p\widetilde{C}_{LL}(uddu)^{12k}$
				$+\big(\frac{m_N}{m_{B'}}\frac{2}{3}D\big)\,\beta_p\widetilde{C}_{LL}(uddu)^{21k}$
n	e_k^+	π^-	L	$\big(1+F+D\big)\,\big(\alpha_p\widetilde{C}_{RL}(udue)^{1k}+\beta_p\widetilde{C}_{LL}(udue)^{1k}\big)$
			R	$-\big(1+F+D\big)\,\big(\alpha_p\widetilde{C}_{LR}(udue)^{1k}+\beta_p\widetilde{C}_{RR}(udue)^{1k}\big)$
	$\bar{\nu}_k$	π^0	L	$-\frac{1}{\sqrt{2}}\big(1+F+D\big)\,\big(\alpha_p\widetilde{C}_{RL}(uddu)^{11k}+\beta_p\widetilde{C}_{LL}(uddu)^{11k}\big)$
		η_0	L	$\sqrt{\frac{3}{2}}\big(-\frac{1}{3}+F-\frac{1}{3}D\big)\,\alpha_p\widetilde{C}_{RL}(uddu)^{11k}+\sqrt{\frac{3}{2}}\big(1+F-\frac{1}{3}D\big)\,\beta_p\widetilde{C}_{LL}(uddu)^{11k}$
		K_0	L	$\big(-\frac{m_N}{m_{B'}}\frac{2}{3}D\big)\,\alpha_p\widetilde{C}_{RL}(ddu\nu)^{12k}+\big(1+\frac{m_N}{m_{B'}}(F+\frac{1}{3}D)\big)\,\alpha_p\widetilde{C}_{RL}(uddu)^{12k}$
				$+\big(-1+\frac{m_N}{m_{B'}}(F-\frac{1}{3}D)\big)\,\alpha_p\widetilde{C}_{RL}(uddu)^{21k}+\big(1+\frac{m_N}{m_{B'}}(F+\frac{1}{3}D)\big)\,\beta_p\widetilde{C}_{LL}(uddu)^{12k}$
				$+\big(1+\frac{m_N}{m_{B'}}(F-\frac{1}{3}D)\big)\,\beta_p\widetilde{C}_{LL}(uddu)^{21k}$

7.3 Example calculation

To demonstrate the procedure described Section 7.2 to calculate nucleon decay from dimension 5 operators, we apply the algorithm to an example SU(5) model in this section. The texture of the Yukawa matrices in the quark and charged lepton sector is adopted from the class of models in Chapter 5, however the neutrino sector is not considered. In particular, we take the same Clebsch-Gordan coefficients, namely $(6, 6, -\frac{1}{2})$, for the first two families in the charged lepton sector as in model 8 listed Table 5.2, and a CG coefficient of $-\frac{3}{2}$ for the third family. An SU(5) model with this Yukawa texture has been constructed as a complete flavour model in [147], where the double missing partner mechanism has been implemented to solve the DT splitting problem. In order to determine the quasi-Yukawa matrices, which are used to construct the dimension 5 operators, for each non-zero entry in the down-quark Yukawa matrix a superpotential term at the SU(5) level according to [147] is specified, which features the corresponding CG coefficient in the charged lepton sector from above. Furthermore, we implement mSUGRA boundary conditions for the soft terms at the GUT scale.

7.3.1 Model setup

The implementation of the example model is specified at the GUT scale, by using the LR convention for the Yukawa matrices from Eq. (2.219). The Yukawa matrix in the up-quark sector is parametrized as follows

$$\mathbf{Y}_u = \mathbf{U}_{23}(\theta_{23}^{uL})\, \mathbf{U}_{12}(\theta_{12}^{uL})\, \mathrm{diag}(y_{11}^u, y_{22}^u, y_{33}^u)\, \mathbf{U}_{12}^{\mathsf{T}}(\theta_{12}^{uL})\, \mathbf{U}_{23}^{\mathsf{T}}(\theta_{23}^{uL})\,, \tag{7.10}$$

where the two unitary matrices have the form

$$\mathbf{U}_{23}(\theta_{23}^{uL}) = \begin{pmatrix} 1 & 0 & 0 \\ 0 & \cos\theta_{23}^{uL} & \sin\theta_{23}^{uL} \\ 0 & -\sin\theta_{23}^{uL} & \cos\theta_{23}^{uL} \end{pmatrix}, \quad \mathbf{U}_{12}(\theta_{12}^{uL}) = \begin{pmatrix} \cos\theta_{12}^{uL} & -i\sin\theta_{12}^{uL} & 0 \\ -i\sin\theta_{12}^{uL} & \cos\theta_{12}^{uL} & 0 \\ 0 & 0 & 1 \end{pmatrix}. \tag{7.11}$$

Furthermore, the Yukawa matrix in the down-quark sector is given by

$$\mathbf{Y}_d = \begin{pmatrix} 0 & y_{12}^d & 0 \\ y_{21}^d & y_{22}^d & 0 \\ 0 & 0 & y_{33}^d \end{pmatrix}, \tag{7.12}$$

where all parameters y_{IJ}^d are real and positive. Note, compared to the class of models in Chapter 5, there is no complex phase in the $(2,1)$-entry of $\mathbf{Y}_d$, since such a phase only impacts observables in the neutrino sector, which, however, is not considered in the present model.

To construct the superpotential operators at the SU(5) level in the Yukawa sector, which provide the correct CG coefficients in the charged lepton sector and determine the form of the quasi-Yukawa couplings, we use the standard embedding of the SM fermions into the F_I and T_I ($I \in \{1,2,3\}$), which form a $\overline{\mathbf{5}}$ and a $\mathbf{10}$ of SU(5), respectively. Moreover, the doublets H_u and H_d of the MSSM, as well as a heavy triplet-antitriplet pair, are embedded into the five-dimensional Higgs representations H_5 and $\overline{H}_5$, respectively, and the Higgs representation H_{24} is assumed to acquire an SM singlet vev at the GUT scale.

Following [147], for the Yukawa operators which contain $T_I\,T_J$, and basically generate the Yukawa terms in the up-quark sector, we choose the same minimal superpotential term for all tuples of family indices (I, J), namely

$$(\mathbf{Y}_u)_{IJ}: \quad W \supset T_I\,T_J\,H_5\,. \tag{7.13}$$

Moreover, the Yukawa operators which contain $T_I\,F_J$, and generate the non-zero Yukawa terms in the down-quark and charged lepton sector, correspond to the following superpotential terms:

$$(\mathbf{Y}_d)_{12}: \quad W \supset (T_1)_{\overline{\mathbf{45}}\otimes\overline{\mathbf{45}}}\left(\overline{H}_5\,H_{24}\right)_{\mathbf{45}}\left(F_2\,H_{24}\right)_{\mathbf{45}}, \tag{7.14a}$$

$$(\mathbf{Y}_d)_{21}: \quad W \supset \left(T_2\,H_{24}\right)_{\overline{\mathbf{10}}}\left(F_1\,\overline{H}_5\right)_{\mathbf{10}}, \tag{7.14b}$$

$$(\mathbf{Y}_d)_{22}: \quad W \supset \left(T_2\,H_{24}\right)_{\overline{\mathbf{10}}}\left(F_2\,\overline{H}_5\right)_{\mathbf{10}}, \tag{7.14c}$$

$$(\mathbf{Y}_d)_{33}: \quad W \supset \left(T_3\,\overline{H}_5\right)_{\overline{\mathbf{5}}}\left(F_3\,H_{24}\right)_{\mathbf{5}}. \tag{7.14d}$$

The lowered SU(5) representations indicate which type of mediators has been used to construct the effective operators from renormalizable interactions. The Yukawa and quasi-Yukawa terms at the MSSM level emerge from the SU(5) superpotential operators in Eq. (7.13) and (7.14) by substituting H_{24} with its GUT scale vev $\langle H_{24}\rangle$.

According to the embedding of the SM fermions into the representations F_I and T_I, and the doublet H_d into $\overline{H}_5$, the charged lepton Yukawa matrix is given by

$$\mathbf{Y}_e = \begin{pmatrix} 0 & 6 & 0 \\ -\frac{1}{2} & 6 & 0 \\ 0 & 0 & -\frac{3}{2} \end{pmatrix} \cdot \mathbf{Y}_d^{\mathsf{T}}\,, \tag{7.15}$$

where the explicitly written matrix states the CG coefficients concerning the down-quark Yukawa matrix from Eq. (7.12), and the dot $\cdot$ indicates the entrywise product of two matrices. Furthermore, in SU(5) the quasi-Yukawa matrices $\tilde{\mathbf{Y}}_{qq}, \tilde{\mathbf{Y}}_{eu}$ and $\tilde{\mathbf{Y}}_{ql}, \tilde{\mathbf{Y}}_{ud}$ are related to $\mathbf{Y}_u$ and $\mathbf{Y}_d$, respectively, due to the embedding of the heavy triplet and antitriplet into the H_5 and $\overline{H}_5$. Since in our model only one triplet-antitriplet pair couples to the SM fields, we neglect the "triplet index" i in the quasi-Yukawa matrices (cf. Eq. (3.42)), so they carry only family indices I, J. Using the same notation as in Eq. (7.15), the quasi-Yukawa matrices have the form

$$\begin{aligned} \tilde{\mathbf{Y}}_{qq} &= (-1)_{3\times3}\cdot\mathbf{Y}_u\,, & \tilde{\mathbf{Y}}_{eu} &= (+1)_{3\times3}\cdot\mathbf{Y}_u\,, \\ \tilde{\mathbf{Y}}_{ql} &= \begin{pmatrix} 0 & -1 & 0 \\ -1 & -1 & 0 \\ 0 & 0 & \frac{3}{2} \end{pmatrix}\cdot\mathbf{Y}_d\,, & \tilde{\mathbf{Y}}_{ud} &= \begin{pmatrix} 0 & \frac{2}{3} & 0 \\ -4 & -4 & 0 \\ 0 & 0 & 1 \end{pmatrix}\cdot\mathbf{Y}_d\,. \end{aligned} \tag{7.16}$$

The dimension 5 operators, which are relevant for proton decay, are then given by (cf. Eq. (3.44) and (3.45))

$$\mathbf{C}_{5L}^{IJKN} = \frac{1}{\tilde{M}_T}\,(\tilde{\mathbf{Y}}_{ql})_{IJ}\,(\tilde{\mathbf{Y}}_{qq})_{KN}\,, \tag{7.17}$$

$$\mathbf{C}_{5R}^{IJKN} = \frac{1}{\tilde{M}_T}\,(\tilde{\mathbf{Y}}_{ud})_{IJ}\,(\tilde{\mathbf{Y}}_{eu})_{KN}\,. \tag{7.18}$$

Although only the doublet and triplet pair from H_5 and $\overline{H}_5$ couples to the SM fields, in general there may be additional (anti)doublet and (anti)triplet states, so that the corresponding mass matrices $\mathbf{M}_D$ and $\mathbf{M}_T$ are extended. This is for example the case, if the missing partner mechanism or the double missing partner mechanism as in [147] is implemented. Assuming that the first row and column in $\mathbf{M}_T$ correspond to the triplet and antitriplet from H_5 and $\overline{H}_5$, the inverse of the effective triplet mass scale $\tilde{M}_T$ is then given by $\tilde{M}_T^{-1} = (\mathbf{M}_T^{-1})_{11}$, i.e. by the $(1,1)$-entry of the inverse triplet mass matrix. Note, depending on the form of $\mathbf{M}_T$ and the parameters in the Higgs sector, the effective mass scale $\tilde{M}_T$ can be much bigger than the actual masses of the triplets, as for example in the (double) missing partner mechanism.

The mSUGRA boundary conditions at the GUT scale imply, that the trilinear couplings are proportional to the Yukawa couplings, with a proportionality factor a_0. Moreover, there is one universal soft scalar mass m_0 and one gaugino mass $M_{1/2}$ (cf. Eq. (2.223)).

7.3.2 Numerical analysis

Having specified the model setup at the GUT scale in Section 7.3.1, we fit the parameters of the model to measured observables in the quark and charged lepton sector at low energies, as well as to the EW Higgs mass. In addition, following the procedure from Section 7.2, we calculate nucleon decay from dimension 5 operators, in particular the partial decay widths of the proton and the neutron listed in Eq. (7.9). The experimental bounds for the various decay channels are included in the fit as well.

To reduce the number of free parameters in the example model, we fix the gauge couplings at the GUT scale: $g_3 = 0.698$, $g_2 = 0.697$ and $g_1 = 0.704$, which is consistent with the experimental values at low energies. Furthermore, since the effective triplet mass scale $\tilde{M}_T$ depends on the particularities of the unspecified Higgs sector, and since $\tilde{M}_T$ only affects the nucleon decay widths by an overall scaling, i.e. $\Gamma \propto 1/\tilde{M}_T^2$, we fix the value of $\tilde{M}_T$ in the following analysis. Finally, we choose $\operatorname{sign}\mu = +1$.

- **Parameters:**
  In total our example model contains 13 real parameters at the GUT scale, namely the five parameters $y^u_{11}, y^u_{22}, y^u_{33}, \theta^{uL}_{12}, \theta^{uL}_{23}$ in the up-quark Yukawa matrix, the four parameters $y^d_{12}, y^d_{21}, y^d_{22}, y^d_{33}$ in the down-quark Yukawa matrix, the three mSUGRA parameters $a_0, m_0, M_{1/2}$ and the ratio $\tan\beta$ of the EW Higgs vevs in the MSSM. We take the following ranges for the parameters:

$$\begin{aligned}
&y^u_{11} \in [0,\, 1\cdot 10^{-5}]\,,\quad y^u_{22} \in [0,\, 5\cdot 10^{-3}]\,,\quad y^u_{33} \in [0,\, 1]\,,\quad \theta^{uL}_{12} \in [0,\, 0.2]\,,\quad \theta^{uL}_{23} \in [0,\, 0.1]\,,\\
&y^d_{12} \in [0,\, 5\cdot 10^{-3}]\,,\quad y^d_{21} \in [0,\, 5\cdot 10^{-3}]\,,\quad y^d_{22} \in [0,\, 0.01]\,,\quad y^d_{33} \in [0,\, 1]\,,\\
&a_0 \in [-200,\, +200]\,\text{TeV}\,,\quad m_0 \in [0,\, 100]\,\text{TeV}\,,\quad M_{1/2} \in [0,\, 100]\,\text{TeV}\,,\quad \tan\beta \in [5,\, 60]\,.
\end{aligned} \tag{7.19}$$

- **Observables:**
  The 13 parameters of the model are fitted to 14 measured observables at the Z boson mass scale: these are the Yukawa couplings in the up-quark sector y_u, y_c, y_t, in the down-quark sector y_d, y_s, y_b, and in the charged lepton sector y_e, y_ν, y_τ, as well

as the CKM parameters $\theta_{12}^{\mathrm{CKM}}, \theta_{13}^{\mathrm{CKM}}, \theta_{23}^{\mathrm{CKM}} \delta^{\mathrm{CKM}}$ and the EW Higgs mass m_h. The experimental values of the Yukawa couplings at M_Z are given in [94], where for the Yukawa couplings of the charged leptons we take a standard deviation of 1% of the central value, which roughly corresponds to the precision of the running. Moreover, the experimental value of m_h is given in PDG (2018) [13], where we take a standard deviation of 3 GeV, which roughly corresponds to the uncertainty in the theoretical calculation of the Higgs mass.

The experimental bounds for the decay channels of the proton, namely $p \to e_k^+ \pi^0$, $p \to e_k^+ \eta^0$, $p \to e_k^+ K^0$, $p \to \bar{\nu}_k \pi^+$, $p \to \bar{\nu}_k K^+$, and of the neutron, namely $n \to e_k^+ \pi^-$, $n \to \bar{\nu}_k \pi^0$, $n \to \bar{\nu}_k \eta^0$, $n \to \bar{\nu}_k K^0$, where $e_k^+ \in \{e^+, \mu^+\}$, are set by the Super-Kamiokande experiment [92], and they are listed in Table 7.2. In the model fit, for each partial decay width the experimental bound is considered as the standard deviation of a normal distribution centred at zero. Furthermore, for decay channels with a neutrino $\bar{\nu}_k$ ($k \in \{1, 2, 3\}$) in the final state, we compare the sum of the three partial decay widths with the experimental data.

Table 7.2: Experimental bounds for the partial decay widths Γ of various decay channels of the proton and neutron. The data is taken from Figure 5-3 in [93].

Decay channel	Experimental bound
Proton	
$p \to e^+ \pi^0$	$\Gamma < 1.3 \cdot 10^{-66}\,\mathrm{GeV}$
$p \to \mu^+ \pi^0$	$\Gamma < 2.7 \cdot 10^{-66}\,\mathrm{GeV}$
$p \to e^+ \eta^0$	$\Gamma < 5.1 \cdot 10^{-66}\,\mathrm{GeV}$
$p \to \mu^+ \eta^0$	$\Gamma < 1.7 \cdot 10^{-65}\,\mathrm{GeV}$
$p \to e^+ K^0$	$\Gamma < 1.9 \cdot 10^{-65}\,\mathrm{GeV}$
$p \to \mu^+ K^0$	$\Gamma < 1.3 \cdot 10^{-66}\,\mathrm{GeV}$
$p \to \bar{\nu} \pi^+$	$\Gamma < 7.4 \cdot 10^{-65}\,\mathrm{GeV}$
$p \to \bar{\nu} K^+$	$\Gamma < 3.2 \cdot 10^{-66}\,\mathrm{GeV}$
Neutron	
$n \to e^+ \pi^-$	$\Gamma < 1.0 \cdot 10^{-65}\,\mathrm{GeV}$
$n \to \mu^+ \pi^-$	$\Gamma < 2.1 \cdot 10^{-65}\,\mathrm{GeV}$
$n \to \bar{\nu} \pi^0$	$\Gamma < 2.1 \cdot 10^{-65}\,\mathrm{GeV}$
$n \to \bar{\nu} \eta^0$	$\Gamma < 3.7 \cdot 10^{-65}\,\mathrm{GeV}$
$n \to \bar{\nu} K^0$	$\Gamma < 1.7 \cdot 10^{-64}\,\mathrm{GeV}$

For given values of the parameters, the Yukawa matrices, the soft terms and the dimension 5 operators are implemented at the GUT scale $M_{\mathrm{GUT}} = 2 \cdot 10^{16}\,\mathrm{GeV}$ according

to Section 7.3.1. To perform the RG running in the MSSM, the RGEs of the dimension 5 operators from Eq. (7.2) and (7.3) are incorporated into the Mathematica package SusyTC [106]. The running of the Yukawa matrices, the soft terms and the gauge couplings is calculated at 2-loop, whereas the running of the dimension 5 operators is calculated at 1-loop. At the SUSY scale M_{SUSY}, which is determined dynamically in SusyTC, the dressing of the dimension 5 operators is performed, and the nucleon decay is calculated according to the procedure in Section 7.2. Furthermore, the EW Higgs mass is calculated by using FeynHiggs 2.14.0 [108–115]. In SusyTC, the MSSM is matched to SM by taking account of the SUSY threshold corrections, and the running from the SUSY scale to the Z boson mass scale $M_Z = 91.2\,\text{GeV}$ in the SM is performed at 2-loop. At M_Z the observables in the quark and charged lepton sector, namely the Yukawa couplings and the CKM parameters, are calculated.

We fit the model for two different values of the effective triplet mass scale, namely $\tilde{M}_T = 1.0 \cdot 10^{18}\,\text{GeV}$ and $\tilde{M}_T = 1.0 \cdot 10^{19}\,\text{GeV}$. As measure for the goodness of the fit we use the χ^2 function. Moreover, to calculate the posterior density of the parameters and the observables, we perform an MCMC analysis by using an adaptive Metropolis-Hastings algorithm [117]. All prior distributions for the parameters are chosen to be flat within the corresponding intervals given in Eq. (7.19).

We check EW vacuum stability by means of an interpolated grid, which provides the vacuum lifetime as a function of the mSUGRA parameters a_0, m_0, $M_{1/2}$ and $\tan\beta$. To compute that grid, we used Vevacious 1.2.03 [148], SPheno 4.0.3 [149, 150] and the predefined model from SARAH 4.14.1 [151, 152] with possible charge breaking via stau vevs. As threshold for the lifetime of the vacuum the age of the universe is taken.

7.3.3 Results

Applying the numerical procedure from above, we fit the example model for the two fixed values of the effective triplet mass scale $\tilde{M}_T = 1.0 \cdot 10^{18}\,\text{GeV}$ and $\tilde{M}_T = 1.0 \cdot 10^{19}\,\text{GeV}$. In Table 7.3, for both scenarios the values of the model parameters in the best fit points are listed. Furthermore, in Table 7.4 for each scenario, the total χ^2 (χ^2_{total}) of the best fit point is stated, as well as the partial sum over the contributions from the fit of the fermion sector and the EW Higgs mass (χ^2_{flavour}), and the partial sum over the contributions from nucleon decay (χ^2_{nucleon}). As expected, the total χ^2 is smaller for a bigger effective triplet mass scale $\tilde{M}_T$, because the nucleon decay is more suppressed in that case. Moreover, in both scenarios the main contribution to the χ^2 comes from the fit of the fermion sector and the EW Higgs mass, and in particular from the observable y_s.

The predicted 1σ HPD intervals of the SM superpartners and the extra MSSM Higgs states are shown in Figure 7.1 for the two scenarios. Furthermore, the masses of the sparticles in the two best fit points from Table 7.3 are shown as black lines.[2] Note that for the SM superpartners the running masses are used. We see that the mass spectrum for $\tilde{M}_T = 1.0 \cdot 10^{18}\,\text{GeV}$ (upper) is heavier than for $\tilde{M}_T = 1.0 \cdot 10^{19}\,\text{GeV}$ (lower). The bigger masses of the sparticles in case of a smaller effective triplet mass scale are necessary in order that the predictions for the nucleon decay are compatible with the experimental

[2]The determination of the best fit point and the calculation of the posterior density correspond to a frequentist and a Bayesian approach, respectively, for the model analysis. Thus, the sparticle masses in the best fit points are not necessarily contained in the corresponding 1σ HPD intervals.

bounds. The hierarchy between the mass spectra in the two scenarios is also reflected by the different values of the universal soft mass parameter m_0 and the gaugino mass parameter $M_{1/2}$ at the GUT scale for the two best fit points from Table 7.3.

The above analysis of the example model illustrates, that the quantitative calculation of proton and neutron decay from dimension 5 operators in flavour GUT models is necessary to account for the experimental bounds on the decay widths. In a realistic flavour GUT model, the effective triplet mass scale is determined by the implementation of the Higgs sector.

Table 7.3: List of the model parameters in the best points of the two senarios with differnt effective triplet mass scales $\tilde{M}_T$.

Parameter	$\tilde{M}_T = 1.0 \cdot 10^{18}\,\text{GeV}$	$\tilde{M}_T = 1.0 \cdot 10^{19}\,\text{GeV}$
y^u_{11}	$2.63 \cdot 10^{-6}$	$2.61 \cdot 10^{-6}$
y^u_{22}	$1.27 \cdot 10^{-3}$	$1.28 \cdot 10^{-3}$
y^u_{33}	$4.20 \cdot 10^{-1}$	$4.27 \cdot 10^{-1}$
θ^{uL}_{12}	$8.63 \cdot 10^{-2}$	$8.64 \cdot 10^{-2}$
θ^{uL}_{23}	$3.52 \cdot 10^{-2}$	$3.43 \cdot 10^{-2}$
y^d_{12}	$4.76 \cdot 10^{-4}$	$5.54 \cdot 10^{-4}$
y^d_{21}	$5.52 \cdot 10^{-4}$	$6.42 \cdot 10^{-4}$
y^d_{22}	$2.08 \cdot 10^{-3}$	$2.42 \cdot 10^{-3}$
y^d_{33}	$1.51 \cdot 10^{-1}$	$1.79 \cdot 10^{-1}$
a_0	$-75.4\,\text{TeV}$	$-64.4\,\text{TeV}$
m_0	$30.1\,\text{TeV}$	$26.3\,\text{TeV}$
$M_{1/2}$	$8.73\,\text{TeV}$	$6.79\,\text{TeV}$
$\tan\beta$	27.6	31.6

Table 7.4: List of the χ^2 values in the best fit points of the two scenarios with differnt effective triplet mass scales $\tilde{M}_T$. The total χ^2 of the fit is labelled as χ^2_{total}, whereas χ^2_{flavour} contains only the contributions from the fit of the fermion sector and the EW Higgs mass, and χ^2_{nucleon} contains the contributions from nucleon decay.

Scenario	χ^2_{total}	χ^2_{flavour}	χ^2_{nucleon}
$\tilde{M}_T = 1.0 \cdot 10^{18}\,\text{GeV}$	3.64	3.42	0.22
$\tilde{M}_T = 1.0 \cdot 10^{19}\,\text{GeV}$	3.21	3.21	< 0.01

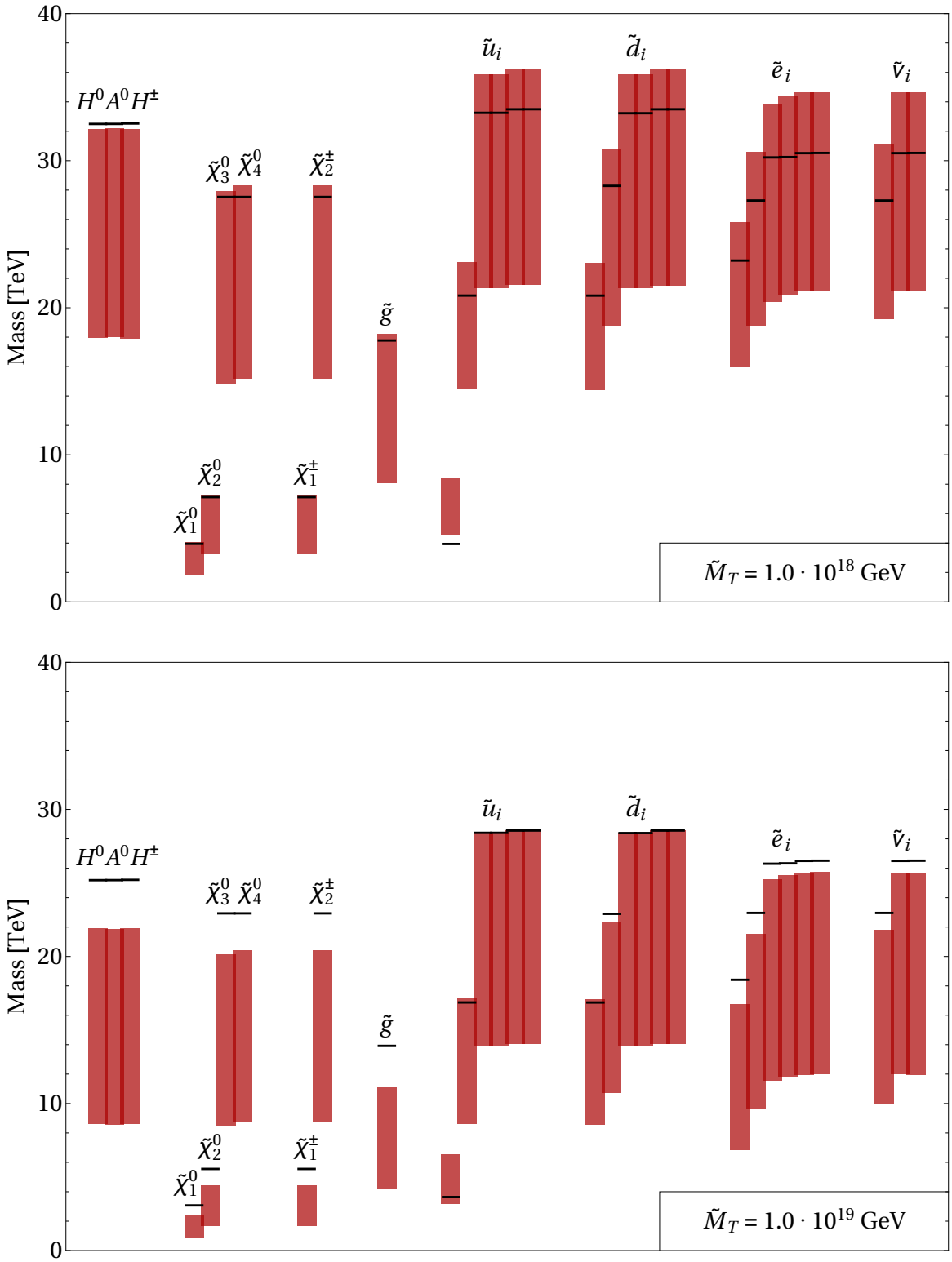

Figure 7.1: The 1σ HPD intervals, indicated as red bars, of the SM superpartners and of the extra MSSM Higgs states from the MCMC analysis for the two scenarios with effective triplet mass scales $\tilde{M}_T = 1.0 \cdot 10^{18}$ GeV (upper) and $\tilde{M}_T = 1.0 \cdot 10^{19}$ GeV (lower). Furthermore, for both scenarios the masses of the sparticles in the best fit points from Table 7.3 are shown as black lines.

PART IV

Summary and conclusions

Summary and conclusions

In this thesis, we studied several new aspects of flavour model building in the framework of supersymmetric Grand Unified Theories. We mainly focussed on GUT models with an SU(5) or SO(10) gauge group, and supersymmetry is considered in the context of supergravity. Apart from calculating concrete predictions in flavour GUT models and investigating the predictive power of certain model classes, we also showed how SUSY breaking can be incorporated in flavour model building in a consistent manner and we specified the numerical procedure to quantitatively calculate nucleon decay from dimension 5 operators in SUSY models. While in Part II the theoretical framework of supersymmetry and Grand Unification was set, we addressed the concrete implementation of flavour models in Part III. In the following, a summary of the prime results from the previous chapters is given.

- Starting from the general Lagrangian which describes the coupling of the supergravity multiplet to matter and gauge multiplets, we discussed spontaneous supersymmetry breaking, and in particular gravity mediated SUSY breaking from a hidden sector, in Chapter 2. A detailed calculation was performed, to show that in such a scenario under specified conditions all terms which contain fields of the observable sector and which are not suppressed by the Planck scale are either part of a globally supersymmetric Lagrangian or they break supersymmetry explicitly. We found that if the Kähler potential, the superpotential and the gauge kinetic function are renormalizable with respect to the observable sector fields, and in addition the Kähler potential contains no terms which are holomorphic in these fields, the SUSY breaking terms represent soft scalar mass terms, soft scalar linear terms and gaugino mass terms. Furthermore, we verified that the mass scale of the SUSY breaking terms is determined by the gravitino mass.

- In Chapter 4, we discussed how a typical flavon sector of a flavour model can be combined with a SUSY breaking sector in the context of supergravity. In particular, we considered flavour GUT models with $N_{\rm F}$ flavon fields and $N_{\rm D}$ driving fields ($N_{\rm D} > N_{\rm F}$), where the flavour structure is generated once the family symmetry is spontaneously broken by flavon vevs. It was shown, that after a suitable change of basis in the driving fields, $N_{\rm F}$ of these fields serve as driving fields for the flavon fields, whereas the remaining $N_{\rm D} - N_{\rm F}$ fields can be used to implement SUSY breaking. For the case of a single SUSY breaking field, we verified numerically that the simultaneous breaking of the flavour symmetry and supersymmetry is consistent, by implementing a simple SUSY breaking sector.

  In order to investigate the predictive power of flavour GUT models in the presence of a SUSY breaking sector, we considered as an example the flavour GUT model from [98] with slight modifications. In particular, the model is based on an SU(5) GUT symmetry and an A_4 family symmetry, in combination with a $\mathbb{Z}_4^{\rm R}$ R-symmetry

and the CSD2 setup in the neutrino sector. Following the general considerations from Chapter 2 concerning gravity mediated supersymmetry breaking, the structure of the soft SUSY breaking terms at the GUT scale were determined. In addition, a fit of the model was performed, where in addition to the observables in the fermion sectors, also the dark matter relic density, the EW Higgs mass and various flavour violating processes were taken into account. We found that the predicted mass spectrum of the sparticles, as well as the predicted WIMP-nucleon cross section are at the edge of the reach of future 100 TeV pp proton colliders and of the future XENONnT experiment, respectively.

- A systematic analysis of a novel class of supersymmetric SU(5) models was performed in Chapter 5, in order to determine promising model candidates for future model building, and to investigate the predictions of this class of models. The model setup at the level of the MSSM was guided by simplicity and predictivity, by taking SU(5) boundary conditions at the GUT scale into account. In particular, we followed the principle of single operator dominance, such that the relations between the down-quark and charged lepton Yukawa couplings at the GUT scale are fixed by Clebsch-Gordan coefficients, where we assumed that there is no mixing between the first two and the third family in these sectors. Viable combinations of CG coefficients for the model analysis were selected by considering the Yukawa double ratio $(y_\mu/y_e)(y_d/y_s)$, which is approximately stable under RG running and SUSY threshold corrections. Furthermore, we implemented a unitarity triangle angle $\alpha_{\mathrm{UT}} = 90^\circ$ in the quark sector to predict the CP violating phase of the CKM matrix. The mixing angles and phases in the lepton sector were predicted by the CSD2 scheme in the neutrino sector, as well as by contributions from the charged lepton sector, which are fixed by the fit of the charged fermion masses and the CKM parameters.

  For each viable tuple of CG coefficients and both CSD2 variants, we performed a fit to the experimentally measured observables in the fermion sector, and all model candidates which provide a $\chi^2 < 15$ were listed. A general feature of this class of models is, that the CP violating phase δ^{PMNS} in the lepton sector is predicted in the rough range $[230^\circ, 290^\circ]$. Moreover, we found that different model candidates predict different ranges for the mixing angle $\theta_{23}^{\mathrm{PMNS}}$ and for the Yukawa ratio y_d/y_s, where all the predicted ranges are smaller than the experimental uncertainty. Thus, more precise measurements of these quantities in future experiments can distinguish between model candidates or can even exclude the whole class of models.

- In the context of SO(10) Grand Unification, a class of non-renormalizable Yukawa operators of the schematic form $W \supset \mathbf{16}_I \cdot \mathbf{16}_J \cdot \mathbf{H} \cdot \mathbf{45}^n \cdot \mathbf{210}^m$ was investigated in Chapter 6, and the predictions for the Yukawa couplings in the up-quark, down-quark, charged lepton and neutrino sector were computed. The representation $\mathbf{H} \in \{\mathbf{10}, \mathbf{120}, \overline{\mathbf{126}}\}$ contains the EW doublets of the MSSM (or parts of them) and the SM fermions are embedded into the $\mathbf{16}_{I,J}$, with family indices I, J. In general, each **45** and **210** factor ($n, m \in \mathbb{N}$) corresponds to a separate field, and the Yukawa terms at the MSSM level are formed once these fields acquire SM singlet vevs at the GUT scale. Since the **45** and the **210** contain two and three SM singlet states, respectively, we distinguished between the case where the vevs point in well aligned

"discrete" directions of the SU(5) and Pati-Salam subgroups, and the case where the vevs can point in "arbitrary" directions in the singlet spaces. In addition, we focussed on the case where the contraction of the representations in the non-renormalizable operator happens via an SO(10) spinor index.

We provided general formulas to compute the Yukawa couplings in the different fermion sectors from the above class of SO(10) operators, which can be used for future model building. Since the relative order of the **45** and **210** factors with respect to the **H** impacts the predictions, we discussed in detail, how a unique operator can be built from renormalizable interactions by using mediators of the type $\mathbf{16}, \overline{\mathbf{16}}$, to achieve single operator dominance in the Yukawa sector. Furthermore, we found that in contrast to SU(5) GUTs, a possible non-alignment of the EW Higgs doublets $H_{u,d}$ with the doublet states in **H** may introduce additional parameters from the doublet mass matrix into the Yukawa sector of the MSSM. Thus, the exact implementation of doublet-triplet splitting is crucial to make predictions for the Yukawa ratios at the GUT scale.

- In Chapter 7, we described the procedure to quantitatively calculate nucleon decay from dimension 5 operators in SUSY models. Following [97], all formulas for the dressing of the dimension 5 operators and the calculation of the amplitudes of different decay channels, as well as for the running between the different energy scales were specified. In particular, partial decay widths of the proton and neutron with a meson and a lepton in the final state were considered. Furthermore, we specified the matching of the conventions in [97] with the standardized SLHA conventions, to get compatibility with the output of SUSY spectrum generators. The algorithm has been implemented in a Mathematica package, which is part of an ongoing project.

  As a demonstration, we applied the algorithm to an SU(5) toy model, which is based on one of the viable model candidates from Chapter 5. We specified suitable SU(5) Yukawa operators to calculate the dimension 5 operators at the GUT scale by integrating out the heavy triplet states. Due to the embedding of the doublet and triplet states into joint GUT representations, the dimension 5 operators are related to the Yukawa operators at the GUT scale. For two fixed values of the effective triplet mass scale, namely $\tilde{M}_T = 1.0 \cdot 10^{18}\,\text{GeV}$ and $\tilde{M}_T = 1.0 \cdot 10^{19}\,\text{GeV}$, we fitted the model parameters to the experimental data, including nucleon decay widths, and computed the predictions for the sparticle spectrum.

In summary, we gave several new insights into flavour model building in the framework of supersymmetric Grand Unified Theories. Apart from investigating the predictions of concrete flavour GUT models, we specified general procedures for future model building.

PART V

Appendices

APPENDIX A

Appendix to Chapter 4

A.1 The renormalizable superpotential

In this appendix we present the complete superpotential at the renormalizable level of the flavour GUT model (without the SUSY breaking and GUT symmetry breaking sector), which was introduced in Section 4.3, including all the flavon, driving and messenger fields. The model corresponds to the one in [98], with slight modifications. All superpotential operators of at most dimension three and which are allowed by the symmetries of the model are considered. The model contains a SU(5) GUT symmetry, a A_4 family symmetry and a $\mathbb{Z}_4^R$ R-symmetry, as well as two $\mathbb{Z}_4$ and four $\mathbb{Z}_3$ shaping symmetries. A list of the matter, the Higgs and the flavon fields, including the respective representations under the symmetries of the model, is given in Table A.1. In addition, the driving and the messenger fields are listed in Table A.2 and A.3, respectively. It is assumed that the masses of the messenger fields are above the GUT scale, such that effective operators as in Eq. (4.2) in the flavon sector are generated, after these fields are integrated out. In that equation, a generic messenger mass scale is written as Λ.

The part of the renormalizable superpotential which contains the mass terms of the messenger fields reads

$$W_\Lambda^{\text{ren}} = M_{\Gamma_i}\Gamma_i\overline{\Gamma}_i + M_{\Sigma_i}\Sigma_i\overline{\Sigma}_i + M_{\Omega_i}\Omega_i\overline{\Omega}_i + M_{\Xi_1}\Xi_1\overline{\Xi}_1\,, \tag{A.1}$$

and the superpotential of the flavon sector has the form

$$\begin{aligned} W_{\text{flavon}}^{\text{ren}} = {} & O_{1;2}\theta_1\theta_2 + O_{1;3}\theta_1\theta_3 + O_{2;3}\theta_2\theta_3 + O_{111;211}\theta_{111}\theta_{211} + O_{111;23}\theta_{111}\theta_{23} \\ & + O_{23;211}\theta_{23}\theta_{211} + O_{2;102}\theta_2\theta_{102} + O_{211;102}\theta_{211}\theta_{102} + O_{1;23}\theta_1\theta_{23} \\ & + A_1\theta_1^2 + A_2\theta_2^2 + A_3\theta_3^2 + A_{111}\big(\theta_{111}^2 + \theta_{111}\rho_{111} + \theta_{111}\tilde{\rho}_{111}\big) \\ & + P\Gamma_9\xi_u + \overline{\Gamma}_9\xi_u^2 + P\Gamma_8^2 + \overline{\Gamma}_8\theta_2^2 + \overline{\Gamma}_8\theta_2'^2 + P\Gamma_7^2 + \overline{\Gamma}_7\big(\theta_{111}^2 + \rho_{111}^2 + \tilde{\rho}_{111}^2\big) \\ & + P\theta_{211}\Gamma_6 + \theta_{211}^2\overline{\Gamma}_6 + P\xi_2\Gamma_5 + \xi_2^2\overline{\Gamma}_5 + P\xi_1\Gamma_4 + \xi_1^2\overline{\Gamma}_4 + P\rho_{23}\Gamma_3 + \big(\theta_{23}^2 + \rho_{23}^2\big)\overline{\Gamma}_3 \\ & + P\rho_{102}\Gamma_2 + \big(\theta_{102}^2 + \rho_{102}^2\big)\overline{\Gamma}_2 + P\theta'_{102}\Gamma_1 + \theta_{102}'^2\overline{\Gamma}_1 + P + P^3\,, \end{aligned} \tag{A.2}$$

where the coefficients in front of the operators are neglected. The terms which contain A_4 flavon triplets generate the flavon vev alignments from Eq. (4.22). The other terms fix the phases of the flavon singlet vevs after the messengers are integrated out (cf. the discussion in Section 4 of [98]).

The renormalizable superpotential of the matter sector consists of the three parts

$$\begin{aligned} W_d^{\text{ren}} &= T_3\overline{H}_5\overline{\Sigma}_3 + F\theta_3\Sigma_3 + F\theta_{23}\Sigma_1 + T_2\overline{\Sigma}_1\overline{\Xi}_1 + \overline{H}'_5 H_{24}\Xi_1 \\ &\quad + F\theta_{102}\Sigma_2 + T_2\overline{\Sigma}_2\overline{\Sigma}_6 + \theta_{102}\Sigma_6\overline{\Sigma}_4 + H_{24}\overline{H}_5\Sigma_4 \\ &\quad + T_1\theta_2\overline{\Omega}_4 + F\Omega_4\overline{\Sigma}_5 + \theta_2\Sigma_5\overline{\Sigma}_4\,, \\ W_u^{\text{ren}} &= T_1 H_5\Omega_3 + \xi_1\Omega_2\overline{\Omega}_3 + T_1\xi_u\overline{\Omega}_2 + \Omega_2\xi_u\overline{\Omega}_1 + T_2\Gamma_4\overline{\Omega}_1 \\ &\quad + \overline{\Gamma}_4\xi_1^2 + T_2 H_5\Omega_1 + T_3\xi_1\overline{\Omega}_1 + T_3^2 H_5\,, \\ W_\nu^{\text{ren}} &= \xi_1 N_1^2 + \xi_2 N_2^2 + N_1 H_5\overline{\Sigma}_1 + N_2 H_5\overline{\Sigma}_2\,, \end{aligned} \tag{A.3}$$

which, apart from flavon and messenger fields, contain the matter fields F, T_1, T_2, T_3, N_1 and N_2, as well as the Higgs fields H_5, $\overline{H}_5$, $\overline{H}'_5$ and H_{24}, where the first three Higgs representations contain the EW (anti)doublets and the last one gets an SM singlet GUT scale vev. Again, the coefficients in front of the operators are neglected. Once the messenger fields are integrated out, Eq. (A.3) results in the effective superpotential from Eq. (4.25).

There are additional renormalizable operators, which are not part of the superpotentials from Eqs. (A.1)–(A.3). These operators are given by

$$\begin{aligned} W_{\text{neg}}^{\text{ren}} &= T_1\Gamma_9\overline{\Omega}_1 + T_2\Gamma_9\overline{\Omega}_3 + \Gamma_9\Omega_1\overline{\Omega}_2 + \Gamma_4\overline{\Omega}_2\Omega_3 + \Gamma_1\Sigma_4\overline{\Sigma}_6 \\ &\quad + PA_2^2 + PA_{111}^2 + A_{111}\tilde{\rho}_{111}\theta_{111} + O_{211;211}^3 \\ &\quad + \overline{\Gamma}_1^3 + \overline{\Gamma}_2^3 + \overline{\Gamma}_3^3 + \overline{\Gamma}_4^3 + \overline{\Gamma}_5^3 + \overline{\Gamma}_6^3 + P\overline{\Gamma}_7^2 + \overline{\Gamma}_7\rho_{111}\tilde{\rho}_{111} + P\overline{\Gamma}_8^2 + \overline{\Gamma}_9^3\,. \end{aligned} \tag{A.4}$$

The first two operators lead to the effective operator $T_1T_2H_5\xi_u^2$, which also emerges from W_u^{ren}. All other operators induce effective operators of dimension seven or higher. Thus, they are subdominant compared to the effective operators from the other parts of the superpotential, which are of dimension six at most.

Table A.1: List of the matter, Higgs and flavon fields of the flavour GUT model. For each field the representation under the symmetries of the model is specified, where a dot indicates a singlet.

	SU(5)	A_4	$\mathbb{Z}_4^R$	$\mathbb{Z}_4^{(a)}$	$\mathbb{Z}_4^{(b)}$	$\mathbb{Z}_3^{(a)}$	$\mathbb{Z}_3^{(b)}$	$\mathbb{Z}_3^{(c)}$	$\mathbb{Z}_3^{(d)}$
Matter fields									
F	$\bar{\mathbf{5}}$	**3**	1	.	.	.	.	1	2
T_1	**10**	.	1	3	3	1	1	.	.
T_2	**10**	.	1	3	3	2	1	2	.
T_3	**10**	.	1	3	3	.	.	2	.
N_1	**1**	.	1	.	2	1	2	.	.
N_2	**1**	.	1	2	2	2	.	2	.
Higgs fields									
H_5	**5**	.	.	2	2	.	.	2	.
$\overline{H}_5$	$\bar{\mathbf{5}}$	.	.	.	.	.	.	.	.
$\overline{H}'_5$	$\bar{\mathbf{5}}$	.	.	2	.	.	2	1	2
H_{45}	**45**	.	.	.	2	.	1	1	1
H_{24}	**24**	.	.	1	1	2	2	2	1
S	.	.	2	2	2	.	.	1	.
Flavon fields									
θ_{102}	.	**3**	.	.	.	1	.	1	1
θ_{23}	.	**3**	.	2	.	2	1	.	1
θ_1	.	**3**	.	1	3	1	.	.	1
θ_2	.	**3**	.	.	3	.	.	.	.
θ_3	.	**3**	.	1	1	.	.	.	1
θ_{111}	.	**3**	.	3	3	.	.	.	.
θ_{211}	.	**3**	.	.	.	2	1	1	.
ξ_u	.	.	.	.	.	.	2	1	.
ξ_1	.	.	.	.	.	1	2	.	.
ξ_2	.	.	.	.	.	2	.	2	.
θ'_2	.	.	.	.	1	.	.	.	.
θ'_{102}	.	.	.	.	.	1	.	.	2
ρ_{111}	.	.	.	3	3	.	.	.	.
$\tilde{\rho}_{111}$	.	.	.	3	3	.	.	.	.
ρ_{23}	.	.	.	.	.	2	1	.	1
ρ_{102}	.	.	.	.	.	1	.	1	1

Table A.2: List of the driving fields of the flavour GUT model. For each field the representation under the symmetries of the model is specified, where a dot indicates a singlet. Note, for each operator in the flavon sector which contains the field P, a differnt copy of that field is introduced in order to fix the flavon vev alignments.

	SU(5)	A_4	$\mathbb{Z}_4^R$	$\mathbb{Z}_4^{(a)}$	$\mathbb{Z}_4^{(b)}$	$\mathbb{Z}_3^{(a)}$	$\mathbb{Z}_3^{(b)}$	$\mathbb{Z}_3^{(c)}$	$\mathbb{Z}_3^{(d)}$
Driving fields									
$O_{1;2}$	.	.	2	3	2	2	.	.	2
$O_{1;3}$	.	.	2	2	.	2	.	.	1
$O_{2;3}$	.	.	2	3	.	.	.	.	2
$O_{111;211}$	.	.	2	1	1	1	2	2	.
$O_{111;23}$	.	.	2	3	1	1	2	.	2
$O_{23;211}$	.	.	2	2	.	2	1	2	2
$O_{2;102}$	.	.	2	.	1	2	.	2	2
$O_{211;102}$	.	.	2	.	.	.	2	1	2
$O_{1;23}$	.	.	2	1	1	.	2	.	1
A_1	.	**3**	2	2	2	1	.	.	1
A_2	.	**3**	2	.	2	.	.	.	.
A_3	.	**3**	2	2	2	.	.	.	1
A_{111}	.	**3**	2	2	2	.	.	.	.
P	.	.	2	.	.	.	.	.	.

Table A.3: List of the messenger fields of the flavour GUT model. For each field the representation under the symmetries of the model is specified, where a dot indicates a singlet.

	SU(5)	A_4	$\mathbb{Z}_4^R$	$\mathbb{Z}_4^{(a)}$	$\mathbb{Z}_4^{(b)}$	$\mathbb{Z}_3^{(a)}$	$\mathbb{Z}_3^{(b)}$	$\mathbb{Z}_3^{(c)}$	$\mathbb{Z}_3^{(d)}$
Messenger fields									
Γ_1, $\overline{\Gamma}_1$	.	.	0, 2	.	.	2, 1	.	.	1, 2
Γ_2, $\overline{\Gamma}_2$	.	.	0, 2	.	.	2, 1	.	2, 1	2, 1
Γ_3, $\overline{\Gamma}_3$	.	.	0, 2	.	.	1, 2	2, 1	.	2, 1
Γ_4, $\overline{\Gamma}_4$	.	.	0, 2	.	.	2, 1	1, 2	.	.
Γ_5, $\overline{\Gamma}_5$	.	.	0, 2	.	.	1, 2	.	1, 2	.
Γ_6, $\overline{\Gamma}_6$	.	**3**, **3**	0, 2	.	.	1, 2	2, 1	2, 1	.
Γ_7, $\overline{\Gamma}_7$	.	.	0, 2	2, 2	2, 2	.	.	.	.
Γ_8, $\overline{\Gamma}_8$	.	.	0, 2	.	2, 2	.	.	.	.
Γ_9, $\overline{\Gamma}_9$	.	.	0, 2	.	.	.	1, 2	2, 1	.
Σ_1, $\overline{\Sigma}_1$	**5**, $\overline{\mathbf{5}}$	.	1, 1	2, 2	.	1, 2	2, 1	2, 1	.
Σ_2, $\overline{\Sigma}_2$	**5**, $\overline{\mathbf{5}}$	.	1, 1	.	.	2, 1	.	1, 2	.
Σ_3, $\overline{\Sigma}_3$	**5**, $\overline{\mathbf{5}}$	.	1, 1	3, 1	3, 1	.	.	2, 1	.
Σ_4, $\overline{\Sigma}_4$	**5**, $\overline{\mathbf{5}}$	.	2, 0	3, 1	3, 1	1, 2	1, 2	1, 2	2, 1
Σ_5, $\overline{\Sigma}_5$	**5**, $\overline{\mathbf{5}}$	.	2, 0	3, 1	2, 2	1, 2	1, 2	1, 2	2, 1
Σ_6, $\overline{\Sigma}_6$	**5**, $\overline{\mathbf{5}}$	.	2, 0	3, 1	3, 1	.	1, 2	1, 2	.
Ω_1, $\overline{\Omega}_1$	**10**, $\overline{\mathbf{10}}$	.	1, 1	3, 1	3, 1	1, 2	2, 1	2, 1	.
Ω_2, $\overline{\Omega}_2$	**10**, $\overline{\mathbf{10}}$	.	1, 1	3, 1	3, 1	1, 2	.	1, 2	.
Ω_3, $\overline{\Omega}_3$	**10**, $\overline{\mathbf{10}}$	.	1, 1	3, 1	3, 1	2, 1	2, 1	1, 2	.
Ω_4, $\overline{\Omega}_4$	**10**, $\overline{\mathbf{10}}$	**3**, **3**	1, 1	3, 1	2, 2	1, 2	1, 2	.	.
Ξ_1, $\overline{\Xi}_1$	**45**, $\overline{\mathbf{45}}$	.	2, 0	1, 3	3, 1	1, 2	2, 1	.	.

APPENDIX B

Appendix to Chapter 5

B.1 Approximate identities for the PMNS parameters

In this appendix we present approximate identities for the angles and the physical phases of the PMNS matrix in the context of the class of models considered in Section 5.2. For the PMNS matrix we use the definition from Eq. (1.23), which is given by

$$\mathbf{U}^{\text{PMNS}} = \mathbf{U}_e^L \, \mathbf{U}_\nu \,, \tag{B.1}$$

where the two unitary matrices on the right-hand side are present in the diagonalizations of the lepton mass matrices

$$\mathbf{M}_e^{\text{diag}} = (\mathbf{U}_e^L)^* \, \mathbf{M}_e \, (\mathbf{U}_e^R)^\mathsf{T} \,, \tag{B.2}$$

$$\mathbf{M}_\nu^{\text{diag}} = \mathbf{U}_\nu^\mathsf{T} \, \mathbf{M}_\nu \, \mathbf{U}_\nu \,, \tag{B.3}$$

as stated in Eq. (1.15) and (1.22), respectively. The matrices $\mathbf{U}_e^L$ and $\mathbf{U}_\nu$ are parametrized in the following general way:

$$\mathbf{U}_e^L = \mathbf{P}^{eL} \, \mathbf{U}_{23}^{eL} \, \mathbf{U}_{13}^{eL} \, \mathbf{U}_{12}^{eL} \,, \tag{B.4}$$

$$\mathbf{U}_\nu = \mathbf{U}_{23}^{\nu} \, \mathbf{U}_{13}^{\nu} \, \mathbf{U}_{12}^{\nu} \, \mathbf{P}^{\nu} \,, \tag{B.5}$$

with the rotation matrices

$$\begin{aligned} \mathbf{U}_{12} &= \begin{pmatrix} c_{12} & s_{12} e^{-i\delta_{12}} & 0 \\ -s_{12} e^{i\delta_{12}} & c_{12} & 0 \\ 0 & 0 & 1 \end{pmatrix} , \qquad \mathbf{U}_{13} = \begin{pmatrix} c_{13} & 0 & s_{13} e^{-i\delta_{13}} \\ 0 & 1 & 0 \\ -s_{13} e^{i\delta_{13}} & 0 & c_{13} \end{pmatrix} , \\ \mathbf{U}_{23} &= \begin{pmatrix} 1 & 0 & 0 \\ 0 & c_{23} & s_{23} e^{-i\delta_{23}} \\ 0 & -s_{23} e^{i\delta_{23}} & c_{23} \end{pmatrix} , \end{aligned} \tag{B.6}$$

where $c_{ij} \equiv \cos\theta_{ij}$ and $s_{ij} \equiv \sin\theta_{ij}$, and the diagonal matrix

$$\mathbf{P} = \text{diag}(e^{i\eta_1}, e^{i\eta_2}, e^{i\eta_3}) \,. \tag{B.7}$$

For the Yukawa matrix $\mathbf{Y}_e$ of the charged leptons we use the texture from Eq. (5.30). Since $\mathbf{Y}_e$ is block diagonal, there is no mixing between the first two and the third family, which implies $\theta_{13}^{eL} = \theta_{23}^{eL} = 0$. Moreover, the phases in $\mathbf{P}^{eL}$ are not fixed, thus we set them equal to zero in the following calculations, namely $\eta_i^{eL} = 0$. Since the class of models

has the feature that $c_y y \ll c_x x$ (and also $c_z z \ll c_x x$), the quantities θ_{12}^{eL} and δ_{12}^{eL} can be expanded in terms of the ratio $(c_y y)/(c_x x)$. Up to first order, this expansion reads

$$\theta_{12}^{eL} \approx \left|\frac{c_y}{c_x}\frac{y}{x}\right|, \qquad \delta_{12}^{eL} \approx \pi - \gamma\,. \tag{B.8}$$

For the left-handed neutrino mass matrix we use one of the two textures from Eq. (5.33), depending on the CSD2 scenario. The CSD2 setup has the feature that $\epsilon \ll 1$. Up to first order in ϵ the parameters in $\mathbf{U}_\nu$ have the following form in the CSD2 scenario $\mathbf{M}_\nu^{(102)}$:

$$\begin{aligned}
&\theta_{12}^\nu \approx \arcsin\left(\frac{1}{\sqrt{3}}\right), && \delta_{12}^\nu \approx \epsilon\sin\alpha\,, && \eta_1^\nu \approx -\frac{1}{2}\epsilon\sin\alpha\,,\\
&\theta_{13}^\nu \approx \frac{\epsilon}{\sqrt{2}}\,, && \delta_{13}^\nu \approx \alpha - \frac{7}{2}\epsilon\sin\alpha\,, && \eta_2^\nu \approx -\frac{\alpha}{2} + \frac{3}{2}\epsilon\sin\alpha\,,\\
&\theta_{23}^\nu \approx \frac{\pi}{4} - \epsilon\cos\alpha\,, && \delta_{23}^\nu \approx \pi - 2\epsilon\sin\alpha\,, && \eta_3^\nu \approx \pi - \frac{3}{2}\epsilon\sin\alpha\,,
\end{aligned} \tag{B.9}$$

whereas in the CSD2 scenario $\mathbf{M}_\nu^{(102)}$ the identities read

$$\begin{aligned}
&\theta_{12}^\nu \approx \arcsin\left(\frac{1}{\sqrt{3}}\right), && \delta_{12}^\nu \approx -\epsilon\sin\alpha\,, && \eta_1^\nu \approx -\frac{1}{2}\epsilon\sin\alpha\,,\\
&\theta_{13}^\nu \approx \frac{\epsilon}{\sqrt{2}}\,, && \delta_{13}^\nu \approx \pi + \alpha - \frac{3}{2}\epsilon\sin\alpha\,, && \eta_2^\nu \approx -\frac{\alpha}{2} - \frac{1}{2}\epsilon\sin\alpha\,,\\
&\theta_{23}^\nu \approx \frac{\pi}{4} + \epsilon\cos\alpha\,, && \delta_{23}^\nu \approx \pi + 2\epsilon\sin\alpha\,, && \eta_3^\nu \approx \pi + \frac{1}{2}\epsilon\sin\alpha\,.
\end{aligned} \tag{B.10}$$

In the following we present general formulas for the parameters in the PMNS matrix, by using the parametrization

$$\mathbf{U}^{\rm PMNS} = \mathbf{U}_{23}^{\rm PMNS}\,\mathbf{U}_{13}^{\rm PMNS}\,\mathbf{U}_{12}^{\rm PMNS}\,\mathbf{P}^{\rm PMNS}\,, \tag{B.11}$$

where the matrices on the right-hand side correspond to the ones in Eq. (B.6) and (B.7). The formulas are bases on the assumptions $\theta_{13}^{eL} = \theta_{23}^{eL} = 0$ and $\theta_{12}^{eL}, \theta_{13}^\nu \ll 1$, which are motivated by the above calculations. Up to first order in θ_{12}^{eL} and θ_{13}^ν the identities for the PMNS parameters read

$$\begin{aligned}
s_{12}^{\rm PMNS} e^{-i\delta_{12}^{\rm PMNS}} &\approx s_{12}^\nu e^{-i(\delta_{12}^\nu + \theta_{12}^{eL} t_{12}^\nu c_{23}^\nu \sin(\delta_{12}^\nu - \delta_{12}^{eL}))} + \theta_{12}^{eL} c_{12}^\nu c_{23}^\nu e^{-i\delta_{12}^{eL}}\,,\\
s_{13}^{\rm PMNS} e^{-i\delta_{13}^{\rm PMNS}} &\approx \theta_{13}^\nu e^{-i\delta_{13}^\nu} + \theta_{12}^{eL} s_{23}^\nu e^{-i(\delta_{23}^\nu + \delta_{12}^{eL})}\,,\\
s_{23}^{\rm PMNS} e^{-i\delta_{23}^{\rm PMNS}} &\approx s_{23}^\nu e^{-i\delta_{23}^\nu}\,,
\end{aligned} \tag{B.12}$$

where the abbreviations $c_{ij}^\nu \equiv \cos\theta_{ij}^\nu$, $s_{ij}^\nu \equiv \sin\theta_{ij}^\nu$ and $t_{ij}^\nu \equiv \tan\theta_{ij}^\nu$ are used. In addition, the identities for the phases in $\mathbf{P}^{\rm PMNS}$ are given by

$$\begin{aligned}
\eta_1^{\rm PMNS} &\approx \eta_1^\nu - \theta_{12}^{eL} t_{12}^\nu c_{23}^\nu \sin(\delta_{12}^\nu - \delta_{12}^{eL})\,,\\
\eta_2^{\rm PMNS} &\approx \eta_2^\nu + \theta_{12}^{eL} t_{12}^\nu c_{23}^\nu \sin(\delta_{12}^\nu - \delta_{12}^{eL})\,,\\
\eta_3^{\rm PMNS} &\approx \eta_3^\nu\,.
\end{aligned} \tag{B.13}$$

The CP violating phase and the two Majorana phases of the PMNS matrix are recovered by the formulas

$$\begin{aligned}
\delta^{\rm PMNS} &= \delta_{13}^{\rm PMNS} - \delta_{12}^{\rm PMNS} - \delta_{23}^{\rm PMNS}\,, \\
\varphi_1^{\rm PMNS} &= -2(\delta_{12}^{\rm PMNS} + \delta_{23}^{\rm PMNS} + \eta_1^{\rm PMNS} - \eta_3^{\rm PMNS})\,, \\
\varphi_2^{\rm PMNS} &= -2(\delta_{23}^{\rm PMNS} + \eta_2^{\rm PMNS} - \eta_3^{\rm PMNS})\,.
\end{aligned} \tag{B.14}$$

If the approximate identities from Eqs. (B.8)–(B.10), which are specific for the considered class of models, are plugged into the general formulas for the PMNS parameters in Eqs. (B.12)–(B.14), we can write the PMNS angles and phases as an expansion of θ_{12}^{eL} and ϵ. In the CSD2 scenario $\mathbf{M}_\nu^{(102)}$ the expansion reads

$$\theta_{12}^{\rm PMNS} \approx 35.3^\circ - \frac{\theta_{12}^{eL}}{\sqrt{2}}\cos\gamma\,, \tag{B.15}$$

$$\theta_{13}^{\rm PMNS} \approx \frac{1}{\sqrt{2}}\big(\epsilon^2 + {\theta_{12}^{eL}}^2 + 2\epsilon\theta_{12}^{eL}\cos(\alpha+\gamma)\big)^{1/2}\,, \tag{B.16}$$

$$\theta_{23}^{\rm PMNS} \approx 45^\circ - \epsilon\cos\alpha\,, \tag{B.17}$$

$$\delta^{\rm PMNS} \approx \arg\big(\epsilon e^{i(\pi+\alpha)} + \theta_{12}^{eL} e^{i(\pi-\gamma)}\big)\,, \tag{B.18}$$

$$\varphi_2^{\rm PMNS} \approx \alpha - 2\epsilon\sin\alpha + \theta_{12}^{eL}\sin\gamma\,, \tag{B.19}$$

whereas in the CSD2 scenario $\mathbf{M}_\nu^{(120)}$ the approximate identities are given by

$$\theta_{12}^{\rm PMNS} \approx 35.3^\circ - \frac{\theta_{12}^{eL}}{\sqrt{2}}\cos\gamma\,, \tag{B.20}$$

$$\theta_{13}^{\rm PMNS} \approx \frac{1}{\sqrt{2}}\big(\epsilon^2 + {\theta_{12}^{eL}}^2 - 2\epsilon\theta_{12}^{eL}\cos(\alpha+\gamma)\big)^{1/2}\,, \tag{B.21}$$

$$\theta_{23}^{\rm PMNS} \approx 45^\circ + \epsilon\cos\alpha\,, \tag{B.22}$$

$$\delta^{\rm PMNS} \approx \arg\big(\epsilon e^{i\alpha} + \theta_{12}^{eL} e^{i(\pi-\gamma)}\big)\,, \tag{B.23}$$

$$\varphi_2^{\rm PMNS} \approx \alpha - 2\epsilon\sin\alpha + \theta_{12}^{eL}\sin\gamma\,. \tag{B.24}$$

Because the CSD2 setup predicts the lightest neutrino mass to be zero, the Majorana phase $\varphi_1^{\rm PMNS}$ is not physical, and therefore not listed. Furthermore, for the CP violating phase $\delta^{\rm PMNS}$ only the zeroth order term is written, since in the PMNS matrix it appears in combination with the angle $\theta_{13}^{\rm PMNS}$, which is of the order of ϵ and θ_{12}^{eL}. In particular, we get the following identities

$$s_{13}^{\rm PMNS} e^{i\delta^{\rm PMNS}} \approx \frac{\epsilon}{\sqrt{2}} e^{i(\pi+\alpha)} + \frac{\theta_{12}^{eL}}{\sqrt{2}} e^{i(\pi-\gamma)}\,, \tag{B.25}$$

$$s_{13}^{\rm PMNS} e^{i\delta^{\rm PMNS}} \approx \frac{\epsilon}{\sqrt{2}} e^{i\alpha} + \frac{\theta_{12}^{eL}}{\sqrt{2}} e^{i(\pi-\gamma)}\,. \tag{B.26}$$

for the CSD2 scenarios $\mathbf{M}_\nu^{(102)}$ and $\mathbf{M}_\nu^{(120)}$, respectively.

APPENDIX C

Appendix to Chapter 7

C.1 Dressing of the dimension 5 operators

C.1.1 Matching with SLHA conventions

In the following we specify how the conventions in [97] (later referred to as GN), which are used in the dressing of the dimension 5 operators, are related to the standardized set of conventions in SLHA [142] and SLHA2 [143]. We use the same notations as in the respective references.

- The Yukawa matrices are related as follows:

GN	SLHA		
f_U	Y_U	$=$	f_U
f_D	Y_D	$=$	$-f_D$
f_L	Y_E	$=$	f_L^{T}

  where the Yukawa matrices are given in GN: Eq. (A.1.1), and SLHA: Eq. (3). In particular, GN uses LR convention in the up- and down-quark sector (f_U and f_D), and RL convention in the charged lepton sector (f_L). On the other hand, SLHA uses LR convention in all sectors.

- Both, GN and SLHA, use the SM normalization for the gauge coupling g_1 of $\mathrm{U}(1)_\mathrm{Y}$, and they also use the same convention for the μ-term.

- In the EW symmetry broken phase the mass matrices of the sfermions are written in a basis where the sfermions are aligned with their SM superpartners.
  - GN uses the basis where the mass matrices $M_U = M_U^{\mathrm{diag}}$ (up-quarks) and $M_L = M_L^{\mathrm{diag}}$ (charged leptons) are diagonal, and the mass matrices $M_D = V_{\mathrm{CKM}}^* M_D^{\mathrm{diag}}$ (down-quarks) and $M_\nu = V_{\mathrm{PMNS}}^* M_\nu^{\mathrm{diag}} V_{\mathrm{PMNS}}^{\mathsf{T}}$ (neutrinos) are rotated by the CKM and PMNS matrix, respectively (u_L and d_L as well as e_L and ν_L are assumed to form doublets under rotations).[1]
  - SLHA uses the basis where all fermion mass matrices are diagonal, which corresponds to the super-CKM/PMNS basis.

[1] The definitions of the CKM and PMNS matrix are in agreement with the ones from Eq. (1.16) and (1.23).

The relation between the sfermion, the chargino and the neutralino mass matrices in GN and SLHA are then the following:

GN	SLHA		
$\mathcal{M}^2_{\widetilde{u}}$	$(\mathcal{M}^2_{\widetilde{u}})_{\text{sCKM}}$	$=$	$(\mathcal{M}^2_{\widetilde{u}})^{\mathsf{T}}$
$\mathcal{M}^2_{\widetilde{d}}$	$(\mathcal{M}^2_{\widetilde{d}})_{\text{sCKM}}$	$=$	$U_d(\mathcal{M}^2_{\widetilde{d}})^{\mathsf{T}}U_d^\dagger$ with $U_d = \begin{pmatrix} V_{\text{CKM}}^\dagger & 0 \\ 0 & \mathbb{1} \end{pmatrix}$
$\mathcal{M}^2_{\widetilde{e}}$	$(\mathcal{M}^2_{\widetilde{e}})_{\text{sPMNS}}$	$=$	$\mathcal{M}^2_{\widetilde{e}}$
$\mathcal{M}^2_{\widetilde{\nu}}$	$(\mathcal{M}^2_{\widetilde{\nu}})_{\text{sPMNS}}$	$=$	$U_\nu(\mathcal{M}^2_{\widetilde{\nu}})^{\mathsf{T}}U_\nu^\dagger$ with $U_\nu = V_{\text{PMNS}}^\dagger$
$\mathcal{M}_C$	$\mathcal{M}_{\widetilde{\psi}^+}$	$=$	$-\mathcal{M}_C$
$\mathcal{M}_N$	$\mathcal{M}_{\widetilde{\psi}^0}$	$=$	$\mathcal{M}_N$

The mass matrices of the sfermions are given in GN: Eqs. (A.1.6)–(A.1.9), and SLHA2: Eq. (11), (12), (24) and (25). In addition, the mass matrices of the charginos and neutralinos are stated in GN: Eq. (A.1.11), and SLHA: Eq. (21) and (22).

The mass matrices of the squarks and charged sleptons $\widetilde{f}$ ($f \in \{u, d, e\}$) are 6×6-dimensional, written in the basis $(\widetilde{f}_{L1}, \widetilde{f}_{L2}, \widetilde{f}_{L3}, \widetilde{f}_{R1}, \widetilde{f}_{R2}, \widetilde{f}_{R3})$, where $\widetilde{f}_{L,Ri}$ is the superpartner of $f_{L,Ri}$, i.e.

$$\mathcal{M}^2_{\widetilde{f}} = \begin{pmatrix} \mathcal{M}^2_{LL} & \mathcal{M}^2_{LR} \\ \mathcal{M}^2_{RL} & \mathcal{M}^2_{RR} \end{pmatrix}, \tag{C.1}$$

where each entry represents a 3×3-block. In contrast, the mass matrix $\mathcal{M}^2_{\widetilde{\nu}} \equiv \mathcal{M}^2_{LL}$ of the sneutrinos is only 3×3-dimensional, since only left-handed neutrinos are present.

Moreover, the 2×2-dimensional mass matrix $\mathcal{M}_C$ of the charginos is written in the basis $(\widetilde{W}^\pm, \widetilde{H}_u^\pm)$, and for the 4×4-dimensional mass matrix $\mathcal{M}_N$ of the neutralinos the basis $(\widetilde{B}, \widetilde{W}^0, \widetilde{H}_d^0, \widetilde{H}_u^0)$ is used.

- The definitions and relations of the sparticle rotation matrices in GN and SLHA are given by:

GN	SLHA		Relation
$\widetilde{U}_U(\mathcal{M}^2_{\widetilde{u}})^{\mathsf{T}}\widetilde{U}_U^\dagger = \text{diag}$	$R_u(\mathcal{M}^2_{\widetilde{u}})_{\text{sCKM}}R_u^\dagger = \text{diag}$	$\Rightarrow$	$\widetilde{U}_U = R_u$
$\widetilde{U}_D(\mathcal{M}^2_{\widetilde{d}})^{\mathsf{T}}\widetilde{U}_D^\dagger = \text{diag}$	$R_d(\mathcal{M}^2_{\widetilde{d}})_{\text{sCKM}}R_d^\dagger = \text{diag}$	$\Rightarrow$	$\widetilde{U}_D = R_dU_d$
$\widetilde{U}_L^\dagger\mathcal{M}^2_{\widetilde{e}}\widetilde{U}_L = \text{diag}$	$R_e(\mathcal{M}^2_{\widetilde{e}})_{\text{sPMNS}}R_e^\dagger = \text{diag}$	$\Rightarrow$	$\widetilde{U}_L = R_e^\dagger$
$\widetilde{U}_N^\dagger\mathcal{M}^2_{\widetilde{\nu}}\widetilde{U}_N = \text{diag}$	$R_\nu(\mathcal{M}^2_{\widetilde{\nu}})_{\text{sPMNS}}R_\nu^\dagger = \text{diag}$	$\Rightarrow$	$\widetilde{U}_N = (R_\nu U_\nu)^\dagger$
$-U_-^\dagger\mathcal{M}_C U_+ = \text{diag}$	$U(\mathcal{M}_C)_{\text{SLHA}}V^{\mathsf{T}} = \text{diag}$	$\Rightarrow$	$U_- = U^\dagger$, $U_+ = V^{\mathsf{T}}$
$U_N^{\mathsf{T}}\mathcal{M}_N U_N = \text{diag}$	$N^*(\mathcal{M}_N)_{\text{SLHA}}N^\dagger = \text{diag}$	$\Rightarrow$	$U_N = N^\dagger$

where "diag" indicates a diagonal matrix with real, positive entries. The definitions for the sfermion rotation matrices are taken from GN: Eq. (A.1.10), and SLHA2: Eqs. (28)–(31), whereas the definitions for the chargino and neutralino rotation matrices are stated in GN: Eq. (A.1.12), and SLHA: Eq. (12) and (15).

C.1.2 Calculation of the dimension 6 operators

In the following, $\widetilde{u}_I$, $\widetilde{d}_I$, $\widetilde{e}_I$ and $\widetilde{\nu}_i$ denote the up-type squarks, down-type squarks, charged sleptons and sneutrinos, and $\widetilde{G}$, $\widetilde{\chi}^{\pm}_{\alpha}$ and $\widetilde{\chi}^{0}_{\bar{\alpha}}$ label the gluinos, charginos and neutralinos, respectively. All these states are in the mass eigenbasis. Moreover, u_i, d_i and e_i represent the mass eigenstates of the up-type quarks, down-type quarks and charged leptons, whereas ν_i represents the neutrinos in the interaction basis. The additional label L or R in later calculations indicates whether the Weyl spinor is left- or right-handed. The indices of the above mass eigenstates take the following values: squarks and charged sleptons $I, J, M, N \in \{1,2,3,4,5,6\}$, charginos $\alpha \in \{1,2\}$, neutralinos $\bar{\alpha} \in \{1,2,3,4\}$, SM fermions and sneutrinos $i, j, k, l \in \{1,2,3\}$.

The squared masses of the sfermions are denoted by $m^2_{\widetilde{u}_I}$, $m^2_{\widetilde{d}_I}$, $m^2_{\widetilde{e}_I}$ and $m^2_{\widetilde{\nu}_i}$. Furthermore, the masses of the gluinos, charginos and neutralinos are written as M_G, M_C^{α} and $M_N^{\bar{\alpha}}$, respectively, and the ones of the quarks and charged leptons as $m_i^{(u)}$, $m_i^{(d)}$ and $m_i^{(e)}$. Note that the neutrino masses are neglected in the following.

C.1.2.1 Interactions in the mass eigenbasis

The Lagrangian of the fermion-sfermion-gluino/chargino/neutralino interactions in the corresponding mass eigenbases is given by

$$\mathcal{L}_{\text{int}} = \mathcal{L}_{\text{int}}(\widetilde{G}) + \mathcal{L}_{\text{int}}(\widetilde{\chi}^{\pm}) + \mathcal{L}_{\text{int}}(\widetilde{\chi}^{0})\,, \tag{C.2a}$$

$$\begin{aligned}\mathcal{L}_{\text{int}}(\widetilde{G}) = &-i\sqrt{2}g_3\widetilde{d}^{*I}\overline{\widetilde{G}}\Big(\big(\Gamma^{(d)}_{GL}\big)^{j}{}_{I}\,d_{Lj} + \big(\Gamma^{(d)}_{GR}\big)^{j}{}_{I}\,d_{Rj}\Big)\\ &- i\sqrt{2}g_3\widetilde{u}^{*I}\overline{\widetilde{G}}\Big(\big(\Gamma^{(u)}_{GL}\big)^{j}{}_{I}\,u_{Lj} + \big(\Gamma^{(u)}_{GR}\big)^{j}{}_{I}\,u_{Rj}\Big)\\ &+ c.c.\,,\end{aligned} \tag{C.2b}$$

$$\begin{aligned}\mathcal{L}_{\text{int}}(\widetilde{\chi}^{\pm}) = &\,g_2\overline{\widetilde{\chi}}^{-}_{\alpha}\Big(\big(\Gamma^{(d)}_{CL}\big)^{j\alpha}{}_{I}\,d_{Lj} + \big(\Gamma^{(d)}_{CR}\big)^{j\alpha}{}_{I}\,d_{Rj}\Big)\widetilde{u}^{*I}\\ &\,g_2\overline{\widetilde{\chi}}^{+}_{\alpha}\Big(\big(\Gamma^{(u)}_{CL}\big)^{j\alpha}{}_{I}\,u_{Lj} + \big(\Gamma^{(u)}_{CR}\big)^{j\alpha}{}_{I}\,u_{Rj}\Big)\widetilde{d}^{*I}\\ &\,g_2\overline{\widetilde{\chi}}^{-}_{\alpha}\Big(\big(\Gamma^{(e)}_{CL}\big)^{j\alpha}{}_{i}\,e_{Lj} + \big(\Gamma^{(e)}_{CR}\big)^{j\alpha}{}_{i}\,e_{Rj}\Big)\widetilde{\nu}^{*i}\\ &\,g_2\overline{\widetilde{\chi}}^{+}_{\alpha}\big(\Gamma^{(\nu)}_{CL}\big)^{j\alpha}{}_{I}\,\nu_{Lj}\,\widetilde{e}^{*I}\\ &+ c.c.\,,\end{aligned} \tag{C.2c}$$

$$\begin{aligned}\mathcal{L}_{\text{int}}(\widetilde{\chi}^{0}) = &\,g_2\overline{\widetilde{\chi}}^{0}_{\bar{\alpha}}\Big(\big(\Gamma^{(d)}_{NL}\big)^{j\bar{\alpha}}{}_{I}\,d_{Lj} + \big(\Gamma^{(d)}_{NR}\big)^{j\bar{\alpha}}{}_{I}\,d_{Rj}\Big)\widetilde{d}^{*I}\\ &\,g_2\overline{\widetilde{\chi}}^{0}_{\bar{\alpha}}\Big(\big(\Gamma^{(u)}_{NL}\big)^{j\bar{\alpha}}{}_{I}\,u_{Lj} + \big(\Gamma^{(u)}_{NR}\big)^{j\bar{\alpha}}{}_{I}\,u_{Rj}\Big)\widetilde{u}^{*I}\\ &\,g_2\overline{\widetilde{\chi}}^{0}_{\bar{\alpha}}\Big(\big(\Gamma^{(e)}_{NL}\big)^{j\bar{\alpha}}{}_{I}\,e_{Lj} + \big(\Gamma^{(e)}_{NR}\big)^{j\bar{\alpha}}{}_{I}\,e_{Rj}\Big)\widetilde{e}^{*I}\\ &\,g_2\overline{\widetilde{\chi}}^{0}_{\bar{\alpha}}\big(\Gamma^{(\nu)}_{NL}\big)^{j\bar{\alpha}}{}_{i}\,\nu_{Lj}\,\widetilde{\nu}^{*i}\\ &+ c.c.\,.\end{aligned} \tag{C.2d}$$

The formulas for the mixing factors Γ are taken from [97], and are presented in the following, where $m_W = g_2 v/2$ (with $v \approx 246\,\text{GeV}$) is the W boson mass,

$t_W \equiv \tan\theta_W = g_1/g_2$ the tangent of the Weinberg angle, $c_\beta \equiv \cos\beta$ and $s_\beta \equiv \sin\beta$:

- **Gluinos**:

$$\left(\Gamma^{(d)}_{GL}\right)^{j}{}_{I} = \sum_{k=1}^{3} \left(\widetilde{U}_D\right)_I{}^{k} \left(V_{\mathrm{CKM}}\right)_k{}^{j}, \tag{C.3a}$$

$$\left(\Gamma^{(d)}_{GR}\right)^{j}{}_{I} = \left(\widetilde{U}_D\right)_I{}^{j+3}, \tag{C.3b}$$

$$\left(\Gamma^{(u)}_{GL}\right)^{j}{}_{I} = \left(\widetilde{U}_U\right)_I{}^{j}, \tag{C.3c}$$

$$\left(\Gamma^{(u)}_{GR}\right)^{j}{}_{I} = \left(\widetilde{U}_U\right)_I{}^{j+3}. \tag{C.3d}$$

- **Charginos**:

$$\left(\Gamma^{(d)}_{CL}\right)^{j\alpha}{}_{I} = \sum_{k=1}^{3} \left(\left(\widetilde{U}_U\right)_I{}^{k} \left(U_+\right)_1{}^{\alpha} + \left(\widetilde{U}_U\right)_I{}^{k+3} \frac{m_k^{(u)}}{\sqrt{2}\, m_W\, s_\beta} \left(U_+\right)_2{}^{\alpha} \right) \left(V_{\mathrm{CKM}}\right)_k{}^{j}, \tag{C.4a}$$

$$\left(\Gamma^{(d)}_{CR}\right)^{j\alpha}{}_{I} = -\sum_{k=1}^{3} \left(\widetilde{U}_U\right)_I{}^{k} \left(V_{\mathrm{CKM}}\right)_k{}^{j} \frac{m_j^{(d)}}{\sqrt{2}\, m_W\, c_\beta} \left(U_-\right)_2{}^{\alpha}, \tag{C.4b}$$

$$\left(\Gamma^{(u)}_{CL}\right)^{j\alpha}{}_{I} = \left(\widetilde{U}_D\right)_I{}^{j} \left(U_-^\dagger\right)_\alpha{}^{1} - \sum_{k=1}^{3} \left(\widetilde{U}_D\right)_I{}^{k+3} \frac{m_k^{(d)}}{\sqrt{2}\, m_W\, c_\beta} \left(V^\dagger_{\mathrm{CKM}}\right)_k{}^{j} \left(U_-^\dagger\right)_\alpha{}^{2}, \tag{C.4c}$$

$$\left(\Gamma^{(u)}_{CR}\right)^{j\alpha}{}_{I} = \left(\widetilde{U}_D\right)_I{}^{j} \frac{m_j^{(u)}}{\sqrt{2}\, m_W\, s_\beta} \left(U_+^\dagger\right)_\alpha{}^{2}, \tag{C.4d}$$

$$\left(\Gamma^{(e)}_{CL}\right)^{j\alpha}{}_{i} = -\left(\widetilde{U}^\dagger_N\right)_i{}^{j} \left(U_+\right)_1{}^{\alpha}, \tag{C.4e}$$

$$\left(\Gamma^{(e)}_{CR}\right)^{j\alpha}{}_{i} = \frac{m_j^{(e)}}{\sqrt{2}\, m_W\, c_\beta} \left(\widetilde{U}^\dagger_N\right)_i{}^{j} \left(U_-\right)_2{}^{\alpha}, \tag{C.4f}$$

$$\left(\Gamma^{(\nu)}_{CL}\right)^{j\alpha}{}_{I} = -\left(\widetilde{U}^\dagger_L\right)_I{}^{j} \left(U_-^\dagger\right)_\alpha{}^{1} + \frac{m_j^{(e)}}{\sqrt{2}\, m_W\, c_\beta} \left(\widetilde{U}^\dagger_L\right)_I{}^{j+3} \left(U_-^\dagger\right)_\alpha{}^{2}. \tag{C.4g}$$

- **Neutralinos**:

$$\begin{aligned} \left(\Gamma^{(d)}_{NL}\right)^{j\bar{\alpha}}{}_{I} = \sqrt{2} \Big(&+ \frac{1}{2} \left(U_N\right)_2{}^{\bar{\alpha}} - \frac{1}{6}\, t_W \left(U_N\right)_1{}^{\bar{\alpha}} \Big) \sum_{k=1}^{3} \left(\widetilde{U}_D\right)_I{}^{k} \left(V_{\mathrm{CKM}}\right)_k{}^{j} \\ &- \frac{m_j^{(d)}}{\sqrt{2}\, m_W\, c_\beta} \left(U_N\right)_3{}^{\bar{\alpha}} \left(\widetilde{U}_D\right)_I{}^{j+3}, \end{aligned} \tag{C.5a}$$

$$\left(\Gamma^{(d)}_{NR}\right)^{j\bar{\alpha}}{}_{I} = \sqrt{2}\left(-\frac{1}{3}\,t_W\left(U_N^\dagger\right)_{\bar{\alpha}}{}^{1}\right)\left(\widetilde{U}_D\right)_I{}^{j+3} - \frac{m_j^{(d)}}{\sqrt{2}\,m_W\,c_\beta}\left(U_N^\dagger\right)_{\bar{\alpha}}{}^{3}\sum_{k=1}^{3}\left(\widetilde{U}_D\right)_I{}^{k}\left(V_{\rm CKM}\right)_k{}^{j}, \tag{C.5b}$$

$$\left(\Gamma^{(u)}_{NL}\right)^{j\bar{\alpha}}{}_{I} = \sqrt{2}\left(-\frac{1}{2}\left(U_N\right)_2{}^{\bar{\alpha}} - \frac{1}{6}\,t_W\left(U_N\right)_1{}^{\bar{\alpha}}\right)\left(\widetilde{U}_U\right)_I{}^{j} - \frac{m_j^{(u)}}{\sqrt{2}\,m_W\,s_\beta}\left(U_N\right)_4{}^{\bar{\alpha}}\left(\widetilde{U}_U\right)_I{}^{j+3}, \tag{C.5c}$$

$$\left(\Gamma^{(u)}_{NR}\right)^{j\bar{\alpha}}{}_{I} = \sqrt{2}\left(+\frac{2}{3}\,t_W\left(U_N^\dagger\right)_{\bar{\alpha}}{}^{2}\right)\left(\widetilde{U}_U\right)_I{}^{j+3} - \frac{m_j^{(u)}}{\sqrt{2}\,m_W\,s_\beta}\left(U_N^\dagger\right)_{\bar{\alpha}}{}^{4}\left(\widetilde{U}_U\right)_I{}^{j}, \tag{C.5d}$$

$$\left(\Gamma^{(e)}_{NL}\right)^{j\bar{\alpha}}{}_{I} = \sqrt{2}\left(+\frac{1}{2}\left(U_N\right)_2{}^{\bar{\alpha}} + \frac{1}{2}\,t_W\left(U_N\right)_1{}^{\bar{\alpha}}\right)\left(\widetilde{U}_L^\dagger\right)_I{}^{j} - \frac{m_j^{(e)}}{\sqrt{2}\,m_W\,c_\beta}\left(U_N\right)_3{}^{\bar{\alpha}}\left(\widetilde{U}_L^\dagger\right)_I{}^{j+3}, \tag{C.5e}$$

$$\left(\Gamma^{(e)}_{NR}\right)^{j\bar{\alpha}}{}_{I} = \sqrt{2}\left(-t_W\left(U_N^\dagger\right)_{\bar{\alpha}}{}^{1}\right)\left(\widetilde{U}_L^\dagger\right)_I{}^{j+3} - \frac{m_j^{(e)}}{\sqrt{2}\,m_W\,c_\beta}\left(U_N^\dagger\right)_{\bar{\alpha}}{}^{3}\left(\widetilde{U}_L^\dagger\right)_I{}^{j}, \tag{C.5f}$$

$$\left(\Gamma^{(\nu)}_{NL}\right)^{j\bar{\alpha}}{}_{i} = \sqrt{2}\left(-\frac{1}{2}\left(U_N\right)_2{}^{\bar{\alpha}} + \frac{1}{2}\,t_W\left(U_N\right)_1{}^{\bar{\alpha}}\right)\left(\widetilde{U}_N^\dagger\right)_i{}^{j}. \tag{C.5g}$$

C.1.2.2 Dimension 5 operators in component form

In the EW symmetry broken phase, the dimension 5 operators from the superpotential in Eq. (7.1) have the following form at the Lagrangian level

$$\begin{aligned}\mathcal{L}_5 = \epsilon_{\hat{a}\hat{b}\hat{c}}\Big(&C(\widetilde{u}\widetilde{d}ue_L)^{MNij}\widetilde{u}_M^{\hat{a}}\widetilde{d}_N^{\hat{b}}(u_{Li}^{\hat{c}}e_{Lj}) + \tfrac{1}{2}C(\widetilde{u}\widetilde{u}de_L)^{MNij}\widetilde{u}_M^{\hat{a}}\widetilde{u}_N^{\hat{b}}(d_{Li}^{\hat{c}}e_{Lj})\\ &+ C(\widetilde{u}\widetilde{d}ue_R)^{MNij}\widetilde{u}_M^{\hat{a}}\widetilde{d}_N^{\hat{b}}(u_{Ri}^{\hat{c}}e_{Rj}) + \tfrac{1}{2}C(\widetilde{u}\widetilde{u}de_R)^{MNij}\widetilde{u}_M^{\hat{a}}\widetilde{u}_N^{\hat{b}}(d_{Ri}^{\hat{c}}e_{Rj})\\ &+ C(\widetilde{u}\widetilde{d}d\nu_L)^{MNij}\widetilde{u}_M^{\hat{a}}\widetilde{d}_N^{\hat{b}}(d_{Li}^{\hat{c}}\nu_{Lj}) + \tfrac{1}{2}C(\widetilde{d}\widetilde{d}u\nu_L)^{MNij}\widetilde{d}_M^{\hat{a}}\widetilde{d}_N^{\hat{b}}(u_{Li}^{\hat{c}}\nu_{Lj})\\ &+ C(\widetilde{u}\widetilde{e}ud_L)^{IJkl}\widetilde{u}_I^{\hat{a}}\widetilde{e}_J(u_{Lk}^{\hat{b}}d_{Ll}^{\hat{c}}) + \tfrac{1}{2}C(\widetilde{d}\widetilde{e}uu_L)^{IJkl}\widetilde{d}_I^{\hat{a}}\widetilde{e}_J(u_{Lk}^{\hat{b}}u_{Ll}^{\hat{c}})\\ &+ C(\widetilde{u}\widetilde{e}ud_R)^{IJkl}\widetilde{u}_I^{\hat{a}}\widetilde{e}_J(u_{Rk}^{\hat{b}}d_{Rl}^{\hat{c}}) + \tfrac{1}{2}C(\widetilde{d}\widetilde{e}uu_R)^{IJkl}\widetilde{d}_I^{\hat{a}}\widetilde{e}_J(u_{Rk}^{\hat{b}}u_{Rl}^{\hat{c}})\\ &+ C(\widetilde{d}\widetilde{\nu}ud_L)^{Ijkl}\widetilde{d}_I^{\hat{a}}\widetilde{\nu}_j(u_{Lk}^{\hat{b}}d_{Ll}^{\hat{c}}) + \tfrac{1}{2}C(\widetilde{u}\widetilde{\nu}dd_L)^{Ijkl}\widetilde{u}_I^{\hat{a}}\widetilde{\nu}_j(d_{Lk}^{\hat{b}}d_{Ll}^{\hat{c}})\Big),\end{aligned} \tag{C.6}$$

where $\hat{a},\hat{b},\hat{c}$ are $\mathrm{SU}(3)_\mathrm{C}$ indices and $\epsilon_{123}=1$. Furthermore, the mass eigenbasis for the fermions and sfermions is used, except for the neutrinos, which are in the interaction basis.

The expressions of the C coefficients are taken from [97]. They are calculated by using the $C_{5L,R}^{ijkl}$ coefficients in the basis of the superfields $Q_i, L_i, u_i^c, d_i^c, e_i^c$ where the Yukawa couplings f_U and f_L are diagonal, and $f_D = V_{\text{CKM}}^* f_D^{\text{diag}}$ and $M_\nu = V_{\text{PMNS}}^* M_\nu^{\text{diag}} V_{\text{PMNS}}^{\mathsf{T}}$. This is the same basis as used for the alignment of the sfermions in Section C.1.1. The C coefficients are then given by

$$C(\widetilde{u}\widetilde{d}ue_L)^{MNij} = \left(C_{5L}^{ijkl} - C_{5L}^{kjil}\right)\left(\widetilde{U}_U^\dagger\right)_k{}^M \left(\widetilde{U}_D^\dagger\right)_l{}^N, \tag{C.7a}$$

$$C(\widetilde{u}\widetilde{u}de_L)^{MNij} = \left(C_{5L}^{kjlm} - C_{5L}^{ljkm}\right)\left(\widetilde{U}_U^\dagger\right)_k{}^M \left(\widetilde{U}_U^\dagger\right)_l{}^N \left(V_{\text{CKM}}\right)_m{}^i, \tag{C.7b}$$

$$C(\widetilde{u}\widetilde{d}ue_R)^{MNij} = \left(C_{5R}^{*klji} - C_{5R}^{*iljk}\right)\left(\widetilde{U}_U^\dagger\right)_{k+3}{}^M \left(\widetilde{U}_D^\dagger\right)_{l+3}{}^N, \tag{C.7c}$$

$$C(\widetilde{u}\widetilde{u}de_R)^{MNij} = \left(C_{5R}^{*lijk} - C_{5R}^{*kijl}\right)\left(\widetilde{U}_U^\dagger\right)_{k+3}{}^M \left(\widetilde{U}_U^\dagger\right)_{l+3}{}^N, \tag{C.7d}$$

$$C(\widetilde{u}\widetilde{d}d\nu_L)^{MNij} = \left(C_{5L}^{mjkl} - C_{5L}^{ljkm}\right)\left(\widetilde{U}_U^\dagger\right)_k{}^M \left(\widetilde{U}_D^\dagger\right)_l{}^N \left(V_{\text{CKM}}\right)_m{}^i, \tag{C.7e}$$

$$C(\widetilde{d}\widetilde{d}u\nu_L)^{MNij} = \left(C_{5L}^{ljik} - C_{5L}^{kjil}\right)\left(\widetilde{U}_D^\dagger\right)_k{}^M \left(\widetilde{U}_D^\dagger\right)_l{}^N, \tag{C.7f}$$

$$C(\widetilde{u}\widetilde{e}ud_L)^{IJkl} = \left(C_{5L}^{ijkm} - C_{5L}^{kjim}\right)\left(\widetilde{U}_U^\dagger\right)_i{}^I \left(\widetilde{U}_L\right)_j{}^J \left(V_{\text{CKM}}\right)_m{}^l, \tag{C.7g}$$

$$C(\widetilde{d}\widetilde{e}uu_L)^{IJkl} = \left(C_{5L}^{kjli} - C_{5L}^{ljki}\right)\left(\widetilde{U}_D^\dagger\right)_i{}^I \left(\widetilde{U}_L\right)_j{}^J, \tag{C.7h}$$

$$C(\widetilde{u}\widetilde{e}ud_R)^{IJkl} = \left(C_{5R}^{*klji} - C_{5R}^{*iljk}\right)\left(\widetilde{U}_U^\dagger\right)_{i+3}{}^I \left(\widetilde{U}_L\right)_{j+3}{}^J, \tag{C.7i}$$

$$C(\widetilde{d}\widetilde{e}uu_R)^{IJkl} = \left(C_{5R}^{*lijk} - C_{5R}^{*kijl}\right)\left(\widetilde{U}_D^\dagger\right)_{i+3}{}^I \left(\widetilde{U}_L\right)_{j+3}{}^J, \tag{C.7j}$$

$$C(\widetilde{d}\widetilde{\nu}ud_L)^{Ijkl} = \left(C_{5L}^{inkm} - C_{5L}^{mnki}\right)\left(\widetilde{U}_D^\dagger\right)_i{}^I \left(\widetilde{U}_N\right)_n{}^j \left(V_{\text{CKM}}\right)_m{}^l, \tag{C.7k}$$

$$C(\widetilde{u}\widetilde{\nu}dd_L)^{Ijkl} = \left(C_{5L}^{qnip} - C_{5L}^{pniq}\right)\left(\widetilde{U}_U^\dagger\right)_i{}^I \left(\widetilde{U}_N\right)_n{}^j \left(V_{\text{CKM}}\right)_p{}^k \left(V_{\text{CKM}}\right)_q{}^l, \tag{C.7l}$$

where $*$ indicates complex conjugation.

C.1.2.3 Dressing

The Lagrangian of the dimension 6 operators $\widetilde{C}$, which are relevant for proton decay, contains only mass eigenstates of the fermions which are lighter than the nucleons. Thus, only the lightest up-type quark u_1 is considered and the index i is neglected. Furthermore, in the mass eigenstates d_i and e_i the index is limited to the values $i \in \{1, 2\}$, whereas all

three states ν_i in the interaction basis are considered. The Lagrangian is then given by

$$\begin{aligned}\mathcal{L}_{\not B} = \frac{1}{16\pi^2}\epsilon_{\hat{a}\hat{b}\hat{c}}\Big(&\widetilde{C}_{LL}(udue)^{ik}(u_L^{\hat{a}}d_{Li}^{\hat{b}})(u_L^{\hat{c}}e_{Lk}) + \widetilde{C}_{RL}(udue)^{ik}(u_R^{\hat{a}}d_{Ri}^{\hat{b}})(u_L^{\hat{c}}e_{Lk})\\ &+ \widetilde{C}_{LR}(udue)^{ik}(u_L^{\hat{a}}d_{Li}^{\hat{b}})(u_R^{\hat{c}}e_{Rk}) + \widetilde{C}_{RR}(udue)^{ik}(u_R^{\hat{a}}d_{Ri}^{\hat{b}})(u_R^{\hat{c}}e_{Rk})\\ &+ \widetilde{C}_{LL}(udd\nu)^{ijk}(u_L^{\hat{a}}d_{Li}^{\hat{b}})(d_{Lj}^{\hat{c}}\nu_{Lk}) + \widetilde{C}_{RL}(udd\nu)^{ijk}(u_R^{\hat{a}}d_{Ri}^{\hat{b}})(d_{Lj}^{\hat{c}}\nu_{Lk})\\ &+ \tfrac{1}{2}\widetilde{C}_{RL}(ddu\nu)^{ijk}(d_{Ri}^{\hat{a}}d_{Rj}^{\hat{b}})(u_L^{\hat{c}}\nu_{Lk})\Big)\,.\end{aligned} \tag{C.8}$$

These operators are built at 1-loop level by dressing the dimension 5 operators from Section C.1.2.2, where the interactions specified in Section C.1.2.1 are used. Following [97], the dimension 6 operators are calculated as

$$\widetilde{C}_{LL}(udue)^{ik} = \widetilde{C}_{LL}(udue)^{ik}_{G} + \widetilde{C}_{LL}(udue)^{ik}_{\chi^\pm} + \widetilde{C}_{LL}(udue)^{ik}_{\chi^0}\,, \tag{C.9a}$$

$$\widetilde{C}_{LL}(udue)^{ik}_{G} = \frac{4}{3}\frac{g_3^2}{M_G}C(\widetilde{u}\widetilde{d}ue_L)^{MN1k}\left(\Gamma^{(u)}_{GL}\right)^{1}{}_{M}\left(\Gamma^{(d)}_{GL}\right)^{i}{}_{N}H(u^G_M, x^G_N)\,, \tag{C.9b}$$

$$\begin{aligned}\widetilde{C}_{LL}(udue)^{ik}_{\chi^\pm} = \frac{g_2^2}{M_C^\alpha}\Big(&- C(\widetilde{u}\widetilde{d}ue_L)^{MN1k}\left(\Gamma^{(u)}_{CL}\right)^{1\alpha}{}_{N}\left(\Gamma^{(d)}_{CL}\right)^{i\alpha}{}_{M}H(x^\alpha_M, u^\alpha_N)\\ &+ C(\widetilde{d}\widetilde{\nu}ud_L)^{Nm1i}\left(\Gamma^{(u)}_{CL}\right)^{1\alpha}{}_{N}\left(\Gamma^{(e)}_{CL}\right)^{k\alpha}{}_{m}H(u^\alpha_N, z^\alpha_m)\Big)\,,\end{aligned} \tag{C.9c}$$

$$\begin{aligned}\widetilde{C}_{LL}(udue)^{ik}_{\chi^0} = \frac{g_2^2}{M_N^{\bar\alpha}}\Big(&C(\widetilde{u}\widetilde{d}ue_L)^{MN1k}\left(\Gamma^{(u)}_{NL}\right)^{1\bar\alpha}{}_{M}\left(\Gamma^{(d)}_{NL}\right)^{i\bar\alpha}{}_{N}H(v^{\bar\alpha}_M, y^{\bar\alpha}_N)\\ &+ C(\widetilde{u}\widetilde{e}ud_L)^{MN1i}\left(\Gamma^{(u)}_{NL}\right)^{1\bar\alpha}{}_{M}\left(\Gamma^{(e)}_{NL}\right)^{k\bar\alpha}{}_{N}H(v^{\bar\alpha}_M, z^{\bar\alpha}_N)\Big)\,,\end{aligned} \tag{C.9d}$$

$$\widetilde{C}_{RL}(udue)^{ik} = \widetilde{C}^{(6)}_{RL}(udue)^{ik} + \widetilde{C}_{RL}(udue)^{ik}_{G} + \widetilde{C}_{RL}(udue)^{ik}_{\chi^\pm} + \widetilde{C}_{RL}(udue)^{ik}_{\chi^0}\,, \tag{C.9e}$$

$$\widetilde{C}_{RL}(udue)^{ik}_{G} = \frac{4}{3}\frac{g_3^2}{M_G}C(\widetilde{u}\widetilde{d}ue_L)^{MN1k}\left(\Gamma^{(u)}_{GR}\right)^{1}{}_{M}\left(\Gamma^{(d)}_{GR}\right)^{i}{}_{N}H(u^G_M, x^G_N)\,, \tag{C.9f}$$

$$\widetilde{C}_{RL}(udue)^{ik}_{\chi^\pm} = -\frac{g_2^2}{M_C^\alpha}C(\widetilde{u}\widetilde{d}ue_L)^{MN1k}\left(\Gamma^{(u)}_{CR}\right)^{1\alpha}{}_{N}\left(\Gamma^{(d)}_{CR}\right)^{i\alpha}{}_{M}H(x^\alpha_M, u^\alpha_N)\,, \tag{C.9g}$$

$$\begin{aligned}\widetilde{C}_{RL}(udue)^{ik}_{\chi^0} = \frac{g_2^2}{M_N^{\bar\alpha}}\Big(&C(\widetilde{u}\widetilde{d}ue_L)^{MN1k}\left(\Gamma^{(u)}_{NR}\right)^{1\bar\alpha}{}_{M}\left(\Gamma^{(d)}_{NR}\right)^{i\bar\alpha}{}_{N}H(v^{\bar\alpha}_M, y^{\bar\alpha}_N)\\ &+ C(\widetilde{u}\widetilde{e}ud_R)^{MN1i}\left(\Gamma^{(u)}_{NL}\right)^{1\bar\alpha}{}_{M}\left(\Gamma^{(e)}_{NL}\right)^{k\bar\alpha}{}_{N}H(v^{\bar\alpha}_M, z^{\bar\alpha}_N)\Big)\,,\end{aligned} \tag{C.9h}$$

$$\widetilde{C}_{LR}(udue)^{ik} = \widetilde{C}^{(6)}_{LR}(udue)^{ik} + \widetilde{C}_{LR}(udue)^{ik}_{G} + \widetilde{C}_{LR}(udue)^{ik}_{\chi^\pm} + \widetilde{C}_{LR}(udue)^{ik}_{\chi^0}\,, \tag{C.9i}$$

$$\widetilde{C}_{LR}(udue)^{ik}_{G} = \frac{4}{3}\frac{g_3^2}{M_G}C(\widetilde{u}\widetilde{d}ue_R)^{MN1k}\left(\Gamma^{(u)}_{GL}\right)^{1}{}_{M}\left(\Gamma^{(d)}_{GL}\right)^{i}{}_{N}H(u^G_M, x^G_N)\,, \tag{C.9j}$$

$$\widetilde{C}_{LR}(udue)^{ik}_{\chi^\pm} = \frac{g_2^2}{M_C^\alpha}\Big(- C(\widetilde{u}\widetilde{d}ue_R)^{MN1k}\left(\Gamma^{(u)}_{CL}\right)^{1\alpha}{}_N\left(\Gamma^{(d)}_{CL}\right)^{i\alpha}{}_M H(x^\alpha_M, u^\alpha_N) + C(\widetilde{d}\widetilde{\nu}ud_L)^{Nm1i}\left(\Gamma^{(u)}_{CR}\right)^{1\alpha}{}_N\left(\Gamma^{(e)}_{CR}\right)^{k\alpha}{}_m H(u^\alpha_N, z^\alpha_m)\Big)\,, \tag{C.9k}$$

$$\widetilde{C}_{LR}(udue)^{ik}_{\chi^0} = \frac{g_2^2}{M_N^{\bar\alpha}}\Big(C(\widetilde{u}\widetilde{d}ue_R)^{MN1k}\left(\Gamma^{(u)}_{NL}\right)^{1\bar\alpha}{}_M\left(\Gamma^{(d)}_{NL}\right)^{i\bar\alpha}{}_N H(v^{\bar\alpha}_M, y^{\bar\alpha}_N) + C(\widetilde{u}\widetilde{e}ud_L)^{MN1i}\left(\Gamma^{(u)}_{NR}\right)^{1\bar\alpha}{}_M\left(\Gamma^{(e)}_{NR}\right)^{k\bar\alpha}{}_N H(v^{\bar\alpha}_M, z^{\bar\alpha}_N)\Big)\,, \tag{C.9l}$$

$$\widetilde{C}_{RR}(udue)^{ik} = \widetilde{C}_{RR}(udue)^{ik}_G + \widetilde{C}_{RR}(udue)^{ik}_{\chi^\pm} + \widetilde{C}_{RR}(udue)^{ik}_{\chi^0}\,, \tag{C.9m}$$

$$\widetilde{C}_{RR}(udue)^{ik}_G = \frac{4}{3}\frac{g_3^2}{M_G}C(\widetilde{u}\widetilde{d}ue_R)^{MN1k}\left(\Gamma^{(u)}_{GR}\right)^1{}_M\left(\Gamma^{(d)}_{GR}\right)^i{}_N H(u^G_M, x^G_N)\,, \tag{C.9n}$$

$$\widetilde{C}_{RR}(udue)^{ik}_{\chi^\pm} = -\frac{g_2^2}{M_C^\alpha}C(\widetilde{u}\widetilde{d}ue_R)^{MN1k}\left(\Gamma^{(u)}_{CR}\right)^{1\alpha}{}_N\left(\Gamma^{(d)}_{CR}\right)^{i\alpha}{}_M H(x^\alpha_M, u^\alpha_N)\,, \tag{C.9o}$$

$$\widetilde{C}_{RR}(udue)^{ik}_{\chi^0} = \frac{g_2^2}{M_N^{\bar\alpha}}\Big(C(\widetilde{u}\widetilde{d}ue_R)^{MN1k}\left(\Gamma^{(u)}_{NR}\right)^{1\bar\alpha}{}_M\left(\Gamma^{(d)}_{NR}\right)^{i\bar\alpha}{}_N H(v^{\bar\alpha}_M, y^{\bar\alpha}_N) + C(\widetilde{u}\widetilde{e}ud_R)^{MN1i}\left(\Gamma^{(u)}_{NR}\right)^{1\bar\alpha}{}_M\left(\Gamma^{(e)}_{NR}\right)^{k\bar\alpha}{}_N H(v^{\bar\alpha}_M, z^{\bar\alpha}_N)\Big)\,, \tag{C.9p}$$

$$\widetilde{C}_{LL}(uddv)^{ijk} = \widetilde{C}_{LL}(uddv)^{ijk}_G + \widetilde{C}_{LL}(uddv)^{ijk}_{\chi^\pm} + \widetilde{C}_{LL}(uddv)^{ijk}_{\chi^0}\,, \tag{C.10a}$$

$$\widetilde{C}_{LL}(uddv)^{ijk}_G = \frac{4}{3}\frac{g_3^2}{M_G}\Big(C(\widetilde{u}\widetilde{d}d\nu_L)^{MNjk}\left(\Gamma^{(u)}_{GL}\right)^1{}_M\left(\Gamma^{(d)}_{GL}\right)^i{}_N H(u^G_M, x^G_N) + C(\widetilde{d}\widetilde{d}u\nu_L)^{MN1k}\left(\Gamma^{(d)}_{GL}\right)^j{}_M\left(\Gamma^{(d)}_{GL}\right)^i{}_N H(x^G_M, x^G_N)\Big)\,, \tag{C.10b}$$

$$\widetilde{C}_{LL}(uddv)^{ijk}_{\chi^\pm} = \frac{g_2^2}{M_C^\alpha}\Big(- C(\widetilde{u}\widetilde{d}d\nu_L)^{MNjk}\left(\Gamma^{(u)}_{CL}\right)^{1\alpha}{}_N\left(\Gamma^{(d)}_{CL}\right)^{i\alpha}{}_M H(x^\alpha_M, u^\alpha_N) + C(\widetilde{u}\widetilde{e}ud_L)^{MN1i}\left(\Gamma^{(d)}_{CL}\right)^{j\alpha}{}_M\left(\Gamma^{(\nu)}_{CL}\right)^{k\alpha}{}_N H(x^\alpha_M, w^\alpha_N)\Big)\,, \tag{C.10c}$$

$$\widetilde{C}_{LL}(uddv)^{ijk}_{\chi^0} = \frac{g_2^2}{M_N^{\bar\alpha}}\Big(C(\widetilde{u}\widetilde{d}d\nu_L)^{MNjk}\left(\Gamma^{(u)}_{NL}\right)^{1\bar\alpha}{}_M\left(\Gamma^{(d)}_{NL}\right)^{i\bar\alpha}{}_N H(v^{\bar\alpha}_M, y^{\bar\alpha}_N) + C(\widetilde{d}\widetilde{d}u\nu_L)^{MN1k}\left(\Gamma^{(d)}_{NL}\right)^{j\bar\alpha}{}_M\left(\Gamma^{(d)}_{NL}\right)^{i\bar\alpha}{}_N H(y^{\bar\alpha}_M, y^{\bar\alpha}_N) + C(\widetilde{d}\widetilde{\nu}ud_L)^{Mn1i}\left(\Gamma^{(d)}_{NL}\right)^{j\bar\alpha}{}_M\left(\Gamma^{(\nu)}_{NL}\right)^{k\bar\alpha}{}_n H(y^{\bar\alpha}_M, w^{\bar\alpha}_n) + C(\widetilde{u}\widetilde{\nu}dd_L)^{Mnji}\left(\Gamma^{(u)}_{NL}\right)^{1\bar\alpha}{}_M\left(\Gamma^{(\nu)}_{NL}\right)^{k\bar\alpha}{}_n H(v^{\bar\alpha}_M, w^{\bar\alpha}_n)\Big)\,, \tag{C.10d}$$

$$\widetilde{C}_{RL}(uddv)^{ijk} = \widetilde{C}^{(6)}_{RL}(uddv)^{ijk} + \widetilde{C}_{RL}(uddv)^{ijk}_G + \widetilde{C}_{RL}(uddv)^{ijk}_{\chi^\pm} + \widetilde{C}_{RL}(uddv)^{ijk}_{\chi^0}\,, \tag{C.10e}$$

$$\widetilde{C}_{RL}(uddv)_G^{ijk} = \frac{4}{3}\frac{g_3^2}{M_G} C(\widetilde{u}\widetilde{d}d\nu_L)^{MNjk} \left(\Gamma_{GR}^{(u)}\right)^1{}_M \left(\Gamma_{GR}^{(d)}\right)^i{}_N H(u_M^G, x_N^G)\,, \tag{C.10f}$$

$$\begin{aligned}\widetilde{C}_{RL}(uddv)_{\chi^\pm}^{ijk} = \frac{g_2^2}{M_C^\alpha}\Big(&- C(\widetilde{u}\widetilde{d}d\nu_L)^{MNjk} \left(\Gamma_{CR}^{(u)}\right)^{1\alpha}{}_N \left(\Gamma_{CR}^{(d)}\right)^{i\alpha}{}_M H(x_M^\alpha, u_N^\alpha) \\ &+ C(\widetilde{u}\widetilde{e}ud_R)^{MN1i} \left(\Gamma_{CL}^{(d)}\right)^{j\alpha}{}_M \left(\Gamma_{CL}^{(\nu)}\right)^{k\alpha}{}_N H(x_M^\alpha, w_N^\alpha)\Big)\,,\end{aligned} \tag{C.10g}$$

$$\widetilde{C}_{RL}(uddv)_{\chi^0}^{ijk} = \frac{g_2^2}{M_N^{\bar\alpha}} C(\widetilde{u}\widetilde{d}d\nu_L)^{MNjk} \left(\Gamma_{NR}^{(u)}\right)^{1\bar\alpha}{}_M \left(\Gamma_{NR}^{(d)}\right)^{i\bar\alpha}{}_N H(v_M^{\bar\alpha}, y_N^{\bar\alpha})\,, \tag{C.10h}$$

$$\widetilde{C}_{RL}(dd u\nu)^{ijk} = \widetilde{C}_{RL}(dd u\nu)_G^{ijk} + \widetilde{C}_{RL}(dd u\nu)_{\chi^0}^{ijk}\,, \tag{C.11a}$$

$$\widetilde{C}_{RL}(dd u\nu)_G^{ijk} = \frac{4}{3}\frac{g_3^2}{M_G} C(\widetilde{d}\widetilde{d}u\nu_L)^{MN1k} \left(\Gamma_{GR}^{(d)}\right)^i{}_M \left(\Gamma_{GR}^{(d)}\right)^j{}_N H(x_M^G, x_N^G)\,, \tag{C.11b}$$

$$\widetilde{C}_{RL}(dd u\nu)_{\chi^0}^{ijk} = \frac{g_2^2}{M_N^{\bar\alpha}} C(\widetilde{d}\widetilde{d}u\nu_L)^{MN1k} \left(\Gamma_{NR}^{(d)}\right)^{i\bar\alpha}{}_M \left(\Gamma_{NR}^{(d)}\right)^{j\bar\alpha}{}_N H(y_M^{\bar\alpha}, y_N^{\bar\alpha})\,. \tag{C.11c}$$

The coefficients $\widetilde{C}^{(6)}_{RL,LR}$ indicate potential contributions to the dimension 6 operators, which originate by integrating out heavy scalar or vector leptoquarks. These contributions are typically small compared to the ones from the dimension 5 operators. The loop function H is defined as follows

$$H(x,y) = \frac{1}{x-y}\left(\frac{x\log x}{x-1} - \frac{y\log y}{y-1}\right), \tag{C.12}$$

where the arguments are squared mass ratios of sfermions and gluinos, charginos or neutralinos:

$$x_M^G = \frac{m^2_{\widetilde{d}_M}}{M_G^2}\,, \qquad u_M^G = \frac{m^2_{\widetilde{u}_M}}{M_G^2}\,, \tag{C.13a}$$

$$x_M^\alpha = \frac{m^2_{\widetilde{u}_M}}{M_C^{\alpha 2}}\,, \qquad u_M^\alpha = \frac{m^2_{\widetilde{d}_M}}{M_C^{\alpha 2}}\,, \qquad z_m^\alpha = \frac{m^2_{\widetilde{\nu}_m}}{M_C^{\alpha 2}}\,, \qquad w_M^\alpha = \frac{m^2_{\widetilde{e}_M}}{M_C^{\alpha 2}}\,, \tag{C.13b}$$

$$v_M^{\bar\alpha} = \frac{m^2_{\widetilde{u}_M}}{M_N^{\bar\alpha 2}}\,, \qquad y_M^{\bar\alpha} = \frac{m^2_{\widetilde{d}_M}}{M_N^{\bar\alpha 2}}\,, \qquad z_M^{\bar\alpha} = \frac{m^2_{\widetilde{e}_M}}{M_N^{\bar\alpha 2}}\,, \qquad w_m^{\bar\alpha} = \frac{m^2_{\widetilde{\nu}_m}}{M_N^{\bar\alpha 2}}\,. \tag{C.13c}$$

Bibliography

[1] S. Antusch and C. Hohl, "Predictions from a flavour GUT model combined with a SUSY breaking sector," JHEP **1710** (2017) 155 [arXiv:1706.04274 [hep-ph]].

[2] S. Antusch, C. Hohl, C. K. Khosa and V. Susic, "Predicting $\delta^{\rm PMNS}$, $\theta_{23}^{\rm PMNS}$ and fermion mass ratios from flavour GUTs with CSD2," JHEP **1812** (2018) 025 [arXiv:1808.09364 [hep-ph]].

[3] S. Antusch, C. Hohl and V. Susic, "Yukawa ratio predictions in non-renormalizable SO(10) GUT models," JHEP **2002** (2020) 086 [arXiv:1911.12807 [hep-ph]].

[4] S. Antusch, C. Hohl, S. F. King and V. Susic, "Non-universal Z' from SO(10) GUTs with vector-like family and the origin of neutrino masses," Nucl. Phys. B **934** (2018) 578 [arXiv:1712.05366 [hep-ph]].

[5] S. Antusch, C. Hohl and V. Susic, "Comparatively Light Extra Higgs States as Signature of SUSY SO(10) GUTs with 3rd Family Yukawa Unification," arXiv:1910.05191 [hep-ph].

[6] C. Hohl, "Notes on the derivation of the general supergravity/matter/Yang-Mills Lagrangian for $N = 1$ supersymmetry in $d = 4$ dimensions using superspace techniques," [arXiv:2005.09504 [hep-th]].

[7] S. L. Glashow, "Partial Symmetries of Weak Interactions," Nucl. Phys. **22** (1961) 579.

[8] S. Weinberg, "A Model of Leptons," Phys. Rev. Lett. **19** (1967) 1264.

[9] A. Salam, "Weak and Electromagnetic Interactions," Conf. Proc. C **680519** (1968) 367.

[10] S. L. Glashow, J. Iliopoulos and L. Maiani, "Weak Interactions with Lepton-Hadron Symmetry," Phys. Rev. D **2** (1970) 1285.

[11] D. J. Gross and F. Wilczek, "Ultraviolet Behavior of Nonabelian Gauge Theories," Phys. Rev. Lett. **30** (1973) 1343.

[12] H. D. Politzer, "Reliable Perturbative Results for Strong Interactions?," Phys. Rev. Lett. **30** (1973) 1346.

[13] M. Tanabashi *et al.* [Particle Data Group], "Review of Particle Physics," Phys. Rev. D **98** (2018) no.3, 030001.

[14] C. N. Yang and R. L. Mills, "Conservation of Isotopic Spin and Isotopic Gauge Invariance," Phys. Rev. **96** (1954) 191.

[15] P. W. Anderson, "Plasmons, Gauge Invariance, and Mass," Phys. Rev. **130** (1963) 439.

[16] F. Englert and R. Brout, "Broken Symmetry and the Mass of Gauge Vector Mesons," Phys. Rev. Lett. **13** (1964) 321.

[17] P. W. Higgs, "Broken Symmetries and the Masses of Gauge Bosons," Phys. Rev. Lett. **13** (1964) 508.

[18] G. S. Guralnik, C. R. Hagen and T. W. B. Kibble, "Global Conservation Laws and Massless Particles," Phys. Rev. Lett. **13** (1964) 585.

[19] N. Cabibbo, "Unitary Symmetry and Leptonic Decays," Phys. Rev. Lett. **10** (1963) 531.

[20] M. Kobayashi and T. Maskawa, "CP Violation in the Renormalizable Theory of Weak Interaction," Prog. Theor. Phys. **49** (1973) 652.

[21] R. Davis, Jr., D. S. Harmer and K. C. Hoffman, "Search for neutrinos from the sun," Phys. Rev. Lett. **20** (1968) 1205.

[22] Y. Fukuda *et al.* [Kamiokande Collaboration], "Solar neutrino data covering solar cycle 22," Phys. Rev. Lett. **77** (1996) 1683.

[23] Y. Fukuda *et al.* [Super-Kamiokande Collaboration], "Evidence for oscillation of atmospheric neutrinos," Phys. Rev. Lett. **81** (1998) 1562 [hep-ex/9807003].

[24] Y. Abe *et al.* [Double Chooz Collaboration], "Indication of Reactor $\bar{\nu}_e$ Disappearance in the Double Chooz Experiment," Phys. Rev. Lett. **108** (2012) 131801 [arXiv:1112.6353 [hep-ex]].

[25] F. P. An *et al.* [Daya Bay Collaboration], "Observation of electron-antineutrino disappearance at Daya Bay," Phys. Rev. Lett. **108** (2012) 171803 [arXiv:1203.1669 [hep-ex]].

[26] D. G. Michael *et al.* [MINOS Collaboration], "Observation of muon neutrino disappearance with the MINOS detectors and the NuMI neutrino beam," Phys. Rev. Lett. **97** (2006) 191801 [hep-ex/0607088].

[27] M. H. Ahn *et al.* [K2K Collaboration], "Measurement of Neutrino Oscillation by the K2K Experiment," Phys. Rev. D **74** (2006) 072003 [hep-ex/0606032].

[28] N. Agafonova *et al.* [OPERA Collaboration], "Observation of a first ν_τ candidate in the OPERA experiment in the CNGS beam," Phys. Lett. B **691** (2010) 138 [arXiv:1006.1623 [hep-ex]].

[29] V. A. Kudryavtsev [DUNE Collaboration], "Underground physics with DUNE," J. Phys. Conf. Ser. **718** (2016) no.6, 062032 [arXiv:1601.03496 [physics.ins-det]].

[30] F. Zwicky, "Die Rotverschiebung von extragalaktischen Nebeln," Helv. Phys. Acta **6** (1933) 110 [Gen. Rel. Grav. **41** (2009) 207].

[31] S. Smith, "The Mass of the Virgo Cluster," Astrophys. J. **83** (1936) 23.

[32] V. C. Rubin and W. K. Ford, Jr., "Rotation of the Andromeda Nebula from a Spectroscopic Survey of Emission Regions," Astrophys. J. **159** (1970) 379.

[33] M. S. Roberts and R. N. Whitehurst, "The rotation curve and geometry of M31 at large galactocentric distances," Astrophysical Journal, Vol. 201, p. 327-346

[34] F. Zwicky, "On the Masses of Nebulae and of Clusters of Nebulae," Astrophys. J. **86** (1937) 217.

[35] D. Walsh, R. F. Carswell and R. J. Weymann, "0957 + 561 A, B - Twin quasistellar objects or gravitational lens," Nature **279** (1979) 381.

[36] M. Markevitch, A. H. Gonzalez, L. David, A. Vikhlinin, S. Murray, W. Forman, C. Jones and W. Tucker, "A Textbook example of a bow shock in the merging galaxy cluster 1E0657-56," Astrophys. J. Lett. **567** (2002) L27 [astro-ph/0110468].

[37] D. Clowe, M. Bradac, A. H. Gonzalez, M. Markevitch, S. W. Randall, C. Jones and D. Zaritsky, "A direct empirical proof of the existence of dark matter," Astrophys. J. Lett. **648** (2006) L109 [astro-ph/0608407].

[38] S. Weinberg, "Implications of Dynamical Symmetry Breaking," Phys. Rev. D **13** (1976) 974 Addendum: [Phys. Rev. D **19** (1979) 1277].

[39] E. Gildener, "Gauge Symmetry Hierarchies," Phys. Rev. D **14** (1976) 1667.

[40] L. Susskind, "Dynamics of Spontaneous Symmetry Breaking in the Weinberg-Salam Theory," Phys. Rev. D **20** (1979) 2619.

[41] G. 't Hooft, C. Itzykson, A. Jaffe, H. Lehmann, P. K. Mitter, I. M. Singer and R. Stora, "Recent Developments in Gauge Theories. Proceedings, Nato Advanced Study Institute, Cargese, France, August 26 - September 8, 1979," NATO Sci. Ser. B **59** (1980) pp.1.

[42] M. J. G. Veltman, "The Infrared - Ultraviolet Connection," Acta Phys. Polon. B **12** (1981) 437.

[43] N. Sakai, "Naturalness in Supersymmetric Guts," Z. Phys. C **11** (1981) 153.

[44] L. Girardello and M. T. Grisaru, "Soft Breaking of Supersymmetry," Nucl. Phys. B **194** (1982) 65.

[45] S. P. Martin, "A Supersymmetry primer," Adv. Ser. Direct. High Energy Phys. **21** (2010) 1 [Adv. Ser. Direct. High Energy Phys. **18** (1998) 1] [hep-ph/9709356].

[46] S. Weinberg, "Baryon and Lepton Nonconserving Processes," Phys. Rev. Lett. **43** (1979) 1566.

[47] P. Minkowski, "$\mu \to e\gamma$ at a Rate of One Out of 10^9 Muon Decays?," Phys. Lett. **67B** (1977) 421.

[48] M. Gell-Mann, P. Ramond and R. Slansky, "Complex Spinors and Unified Theories," Conf. Proc. C **790927** (1979) 315 [arXiv:1306.4669 [hep-th]].

[49] T. Yanagida, "Horizontal gauge symmetry and masses of neutrinos," Conf. Proc. C **7902131** (1979) 95.

[50] R. N. Mohapatra and G. Senjanovic, "Neutrino Mass and Spontaneous Parity Nonconservation," Phys. Rev. Lett. **44** (1980) 912.

[51] B. Pontecorvo, "Mesonium and anti-mesonium," Sov. Phys. JETP **6** (1957) 429 [Zh. Eksp. Teor. Fiz. **33** (1957) 549].

[52] B. Pontecorvo, "Inverse beta processes and nonconservation of lepton charge," Sov. Phys. JETP **7** (1958) 172 [Zh. Eksp. Teor. Fiz. **34** (1957) 247].

[53] Z. Maki, M. Nakagawa and S. Sakata, "Remarks on the unified model of elementary particles," Prog. Theor. Phys. **28** (1962) 870.

[54] I. Esteban, M. C. Gonzalez-Garcia, A. Hernandez-Cabezudo, M. Maltoni and T. Schwetz, "Global analysis of three-flavour neutrino oscillations: synergies and tensions in the determination of θ_{23}, δ_{CP}, and the mass ordering," JHEP **1901** (2019) 106 [arXiv:1811.05487 [hep-ph]].

[55] H. Miyazawa, "Baryon Number Changing Currents," Prog. Theor. Phys. **36** (1966) no.6, 1266.

[56] J. L. Gervais and B. Sakita, "Field Theory Interpretation of Supergauges in Dual Models," Nucl. Phys. B **34** (1971) 632.

[57] D. V. Volkov and V. P. Akulov, "Is the Neutrino a Goldstone Particle?," Phys. Lett. **46B** (1973) 109.

[58] P. Ramond, "Dual Theory for Free Fermions," Phys. Rev. D **3** (1971) 2415.

[59] D. V. Volkov and V. A. Soroka, "Higgs Effect for Goldstone Particles with Spin 1/2," JETP Lett. **18** (1973) 312 [Pisma Zh. Eksp. Teor. Fiz. **18** (1973) 529].

[60] D. Z. Freedman, P. van Nieuwenhuizen and S. Ferrara, "Progress Toward a Theory of Supergravity," Phys. Rev. D **13** (1976) 3214.

[61] S. Deser and B. Zumino, "Consistent Supergravity," Phys. Lett. **62B** (1976) 335.

[62] J. Wess and J. Bagger, "Supersymmetry and supergravity,"

[63] P. Binetruy, G. Girardi and R. Grimm, "Supergravity couplings: A Geometric formulation," Phys. Rept. **343** (2001) 255 [hep-th/0005225].

[64] R. Percacci and E. Sezgin, "Properties of gauged sigma models," hep-th/9810183.

[65] E. Abdalla and M. Forger, "Integrable Nonlinear σ Models With Fermions," Commun. Math. Phys. **104** (1986) 123.

[66] J. Bagger, D. Nemeschansky and S. Yankielowicz, "Anomaly Constraints On Nonlinear Sigma Models," Nucl. Phys. B **262** (1985) 478.

[67] A. Moroianu, "Lectures on Kähler Geometry," Cambridge University Press (2007)

[68] D. Z. Freedman and A. Van Proeyen, "Supergravity,"

[69] P. Fre, "Lectures on special Kahler geometry and electric - magnetic duality rotations," Nucl. Phys. Proc. Suppl. **45BC** (1996) 59 [hep-th/9512043].

[70] I. L. Buchbinder and S. M. Kuzenko, "Ideas and methods of supersymmetry and supergravity: Or a walk through superspace," Bristol, UK: IOP (1998) 656 p

[71] H. P. Nilles, "Dynamically Broken Supergravity and the Hierarchy Problem," Phys. Lett. **115B** (1982) 193.

[72] S. Deser and B. Zumino, "Broken Supersymmetry and Supergravity," Phys. Rev. Lett. **38** (1977) 1433.

[73] E. Cremmer, B. Julia, J. Scherk, S. Ferrara, L. Girardello and P. van Nieuwenhuizen, "Spontaneous Symmetry Breaking and Higgs Effect in Supergravity Without Cosmological Constant," Nucl. Phys. B **147** (1979) 105.

[74] P. Fayet, "Mixing Between Gravitational and Weak Interactions Through the Massive Gravitino," Phys. Lett. **70B** (1977) 461.

[75] G. Moultaka, M. Rausch de Traubenberg and D. Tant, "Low Energy Supergravity Revisited (I)," Int. J. Mod. Phys. A **34** (2019) no.01, 1950004 [arXiv:1611.10327 [hep-th]].

[76] S. K. Soni and H. A. Weldon, "Analysis of the Supersymmetry Breaking Induced by N=1 Supergravity Theories," Phys. Lett. **126B** (1983) 215.

[77] S. Dimopoulos and H. Georgi, "Softly Broken Supersymmetry and SU(5)," Nucl. Phys. B **193** (1981) 150.

[78] H. P. Nilles, "Supersymmetry, Supergravity and Particle Physics," Phys. Rept. **110** (1984) 1.

[79] H. E. Haber and G. L. Kane, "The Search for Supersymmetry: Probing Physics Beyond the Standard Model," Phys. Rept. **117** (1985) 75.

[80] H. Georgi and S. L. Glashow, "Unity of All Elementary Particle Forces," Phys. Rev. Lett. **32** (1974) 438.

[81] J. C. Pati and A. Salam, "Lepton Number as the Fourth Color," Phys. Rev. D **10** (1974) 275 Erratum: [Phys. Rev. D **11** (1975) 703].

[82] H. Fritzsch and P. Minkowski, "Unified Interactions of Leptons and Hadrons," Annals Phys. **93** (1975) 193.

[83] R. Slansky, "Group Theory for Unified Model Building," Phys. Rept. **79** (1981) 1.

[84] A. Masiero, D. V. Nanopoulos, K. Tamvakis and T. Yanagida, "Naturally Massless Higgs Doublets in Supersymmetric SU(5)," Phys. Lett. **115B** (1982) 380.

[85] B. Grinstein, "A Supersymmetric SU(5) Gauge Theory with No Gauge Hierarchy Problem," Nucl. Phys. B **206** (1982) 387.

[86] J. Hisano, T. Moroi, K. Tobe and T. Yanagida, "Suppression of proton decay in the missing partner model for supersymmetric SU(5) GUT," Phys. Lett. B **342** (1995) 138 [hep-ph/9406417].

[87] K. S. Babu, I. Gogoladze and Z. Tavartkiladze, "Missing Partner Mechanism in SO(10) Grand Unification," Phys. Lett. B **650** (2007) 49 [hep-ph/0612315].

[88] K. S. Babu, I. Gogoladze, P. Nath and R. M. Syed, "Variety of SO(10) GUTs with Natural Doublet-Triplet Splitting via the Missing Partner Mechanism," Phys. Rev. D **85** (2012) 075002 [arXiv:1112.5387 [hep-ph]].

[89] S. Dimopoulos and F. Wilczek, "Incomplete Multiplets in Supersymmetric Unified Models," Print-81-0600 (SANTA BARBARA), NSF-ITP-82-07.

[90] K. S. Babu and S. M. Barr, "Natural suppression of Higgsino mediated proton decay in supersymmetric SO(10)," Phys. Rev. D **48** (1993) 5354 [hep-ph/9306242].

[91] P. Nath and P. Fileviez Perez, "Proton stability in grand unified theories, in strings and in branes," Phys. Rept. **441** (2007) 191 [hep-ph/0601023].

[92] M. L. Marshak, "The Soudan Mine Experiment: A Dense Detector For Baryon Decay.,"

[93] R. Brock *et al.*, "Proton Decay,"

[94] S. Antusch and V. Maurer, "Running quark and lepton parameters at various scales," JHEP **1311** (2013) 115 [arXiv:1306.6879 [hep-ph]].

[95] B. Bajc, S. Lavignac and T. Mede, "Challenging the minimal supersymmetric SU(5) model," AIP Conf. Proc. **1604** (2015) no.1, 297-304 [arXiv:1310.3093 [hep-ph]].

[96] B. Bajc, P. Fileviez Perez and G. Senjanovic, "Proton decay in minimal supersymmetric SU(5)," Phys. Rev. D **66** (2002) 075005 [hep-ph/0204311].

[97] T. Goto and T. Nihei, "Effect of RRRR dimension five operator on the proton decay in the minimal SU(5) SUGRA GUT model," Phys. Rev. D **59** (1999) 115009 [hep-ph/9808255].

[98] S. Antusch, S. F. King and M. Spinrath, "Spontaneous CP violation in $A_4 \times SU(5)$ with Constrained Sequential Dominance 2," Phys. Rev. D **87** (2013) no.9, 096018 [arXiv:1301.6764 [hep-ph]].

[99] S. Antusch, S. F. King, C. Luhn and M. Spinrath, "Right Unitarity Triangles and Tri-Bimaximal Mixing from Discrete Symmetries and Unification," Nucl. Phys. B **850** (2011) 477 [arXiv:1103.5930 [hep-ph]].

[100] S. Antusch, S. F. King, M. Malinsky and M. Spinrath, "Quark mixing sum rules and the right unitarity triangle," Phys. Rev. D **81** (2010) 033008 [arXiv:0910.5127 [hep-ph]].

[101] S. Antusch, S. F. King, C. Luhn and M. Spinrath, "Trimaximal mixing with predicted θ_{13} from a new type of constrained sequential dominance," Nucl. Phys. B **856** (2012) 328 [arXiv:1108.4278 [hep-ph]].

[102] C. Patrignani *et al.* [Particle Data Group], "Review of Particle Physics," Chin. Phys. C **40** (2016) no.10, 100001.

[103] J. Rosiek, "SUSY FLAVOR v2.5: a computational tool for FCNC and CP-violating processes in the MSSM," Comput. Phys. Commun. **188** (2015) 208 [arXiv:1410.0606 [hep-ph]].

[104] A. Crivellin, J. Rosiek, P. H. Chankowski, A. Dedes, S. Jaeger and P. Tanedo, "SUSY_FLAVOR v2: A Computational tool for FCNC and CP-violating processes in the MSSM," Comput. Phys. Commun. **184** (2013) 1004 [arXiv:1203.5023 [hep-ph]].

[105] J. Rosiek, P. Chankowski, A. Dedes, S. Jager and P. Tanedo, "SUSY_FLAVOR: A Computational Tool for FCNC and CP-violating Processes in the MSSM," Comput. Phys. Commun. **181** (2010) 2180 [arXiv:1003.4260 [hep-ph]].

[106] S. Antusch and C. Sluka, "Predicting the Sparticle Spectrum from GUTs via SUSY Threshold Corrections with SusyTC," JHEP **1607** (2016) 108 [arXiv:1512.06727 [hep-ph]].

[107] S. Antusch, J. Kersten, M. Lindner, M. Ratz and M. A. Schmidt, "Running neutrino mass parameters in see-saw scenarios," JHEP **0503** (2005) 024 [hep-ph/0501272].

[108] H. Bahl, T. Hahn, S. Heinemeyer, W. Hollik, S. Paßehr, H. Rzehak and G. Weiglein, "Precision calculations in the MSSM Higgs-boson sector with FeynHiggs 2.14," Comput. Phys. Commun. **249** (2020) 107099 [arXiv:1811.09073 [hep-ph]].

[109] H. Bahl, S. Heinemeyer, W. Hollik and G. Weiglein, "Reconciling EFT and hybrid calculations of the light MSSM Higgs-boson mass," Eur. Phys. J. C **78** (2018) no.1, 57 [arXiv:1706.00346 [hep-ph]].

[110] H. Bahl and W. Hollik, "Precise prediction for the light MSSM Higgs boson mass combining effective field theory and fixed-order calculations," Eur. Phys. J. C **76** (2016) no.9, 499 [arXiv:1608.01880 [hep-ph]].

[111] T. Hahn, S. Heinemeyer, W. Hollik, H. Rzehak and G. Weiglein, "High-Precision Predictions for the Light CP -Even Higgs Boson Mass of the Minimal Supersymmetric Standard Model," Phys. Rev. Lett. **112** (2014) no.14, 141801 [arXiv:1312.4937 [hep-ph]].

[112] M. Frank, T. Hahn, S. Heinemeyer, W. Hollik, H. Rzehak and G. Weiglein, "The Higgs Boson Masses and Mixings of the Complex MSSM in the Feynman-Diagrammatic Approach," JHEP **0702** (2007) 047 [hep-ph/0611326].

[113] G. Degrassi, S. Heinemeyer, W. Hollik, P. Slavich and G. Weiglein, "Towards high precision predictions for the MSSM Higgs sector," Eur. Phys. J. C **28** (2003) 133 [hep-ph/0212020].

[114] S. Heinemeyer, W. Hollik and G. Weiglein, "The Masses of the neutral CP - even Higgs bosons in the MSSM: Accurate analysis at the two loop level," Eur. Phys. J. C **9** (1999) 343 [hep-ph/9812472].

[115] S. Heinemeyer, W. Hollik and G. Weiglein, "FeynHiggs: A Program for the calculation of the masses of the neutral CP even Higgs bosons in the MSSM," Comput. Phys. Commun. **124** (2000) 76 [hep-ph/9812320].

[116] G. Belanger, F. Boudjema, A. Pukhov and A. Semenov, "micrOMEGAs: A Tool for dark matter studies," Nuovo Cim. C **033N2** (2010) 111 [arXiv:1005.4133 [hep-ph]].

[117] G. O. Roberts and J. S. Rosenthal, "Examples of adaptive MCMC" Journal of Computational and Graphical Statistics, Vol. 18, pp. 349-367

[118] J. A. Casas, A. Lleyda and C. Munoz, "Strong constraints on the parameter space of the MSSM from charge and color breaking minima," Nucl. Phys. B **471** (1996) 3 [hep-ph/9507294].

[119] B. Bajc, S. Lavignac and T. Mede, "Resurrecting the minimal renormalizable supersymmetric SU(5) model," JHEP **1601** (2016) 044 [arXiv:1509.06680 [hep-ph]].

[120] U. Sarid, "Tools for tunneling," Phys. Rev. D **58** (1998) 085017 [hep-ph/9804308].

[121] S. R. Coleman, "The Fate of the False Vacuum. 1. Semiclassical Theory," Phys. Rev. D **15** (1977) 2929 Erratum: [Phys. Rev. D **16** (1977) 1248].

[122] T. Golling *et al.*, "Physics at a 100 TeV pp collider: beyond the Standard Model phenomena," CERN Yellow Rep. (2017) no.3, 441 [arXiv:1606.00947 [hep-ph]].

[123] E. Aprile *et al.* [XENON Collaboration], "Physics reach of the XENON1T dark matter experiment," JCAP **1604** (2016) 027 [arXiv:1512.07501 [physics.ins-det]].

[124] P. F. Harrison, D. H. Perkins and W. G. Scott, "Tri-bimaximal mixing and the neutrino oscillation data," Phys. Lett. B **530** (2002) 167 [hep-ph/0202074].

[125] Z. z. Xing, "Nearly tri bimaximal neutrino mixing and CP violation," Phys. Lett. B **533** (2002) 85 [hep-ph/0204049].

[126] S. F. King, "Predicting neutrino parameters from SO(3) family symmetry and quark-lepton unification," JHEP **0508** (2005) 105 [hep-ph/0506297].

[127] R. Hempfling, "Yukawa coupling unification with supersymmetric threshold corrections," Phys. Rev. D **49** (1994) 6168.

[128] L. J. Hall, R. Rattazzi and U. Sarid, "The Top quark mass in supersymmetric SO(10) unification," Phys. Rev. D **50** (1994) 7048 [hep-ph/9306309].

[129] M. Carena, M. Olechowski, S. Pokorski and C. E. M. Wagner, "Electroweak symmetry breaking and bottom - top Yukawa unification," Nucl. Phys. B **426** (1994) 269 [hep-ph/9402253].

[130] T. Blazek, S. Raby and S. Pokorski, "Finite supersymmetric threshold corrections to CKM matrix elements in the large tan Beta regime," Phys. Rev. D **52** (1995) 4151 [hep-ph/9504364].

[131] S. Antusch and M. Spinrath, "Quark and lepton masses at the GUT scale including SUSY threshold corrections," Phys. Rev. D **78** (2008) 075020 [arXiv:0804.0717 [hep-ph]].

[132] H. Georgi and C. Jarlskog, "A New Lepton - Quark Mass Relation in a Unified Theory," Phys. Lett. **86B** (1979) 297.

[133] S. Antusch and M. Spinrath, "New GUT predictions for quark and lepton mass ratios confronted with phenomenology," Phys. Rev. D **79** (2009) 095004 [arXiv:0902.4644 [hep-ph]].

[134] S. Antusch, S. F. King and M. Spinrath, "GUT predictions for quark-lepton Yukawa coupling ratios with messenger masses from non-singlets," Phys. Rev. D **89** (2014) no.5, 055027 [arXiv:1311.0877 [hep-ph]].

[135] S. P. Martin and M. T. Vaughn, "Two loop renormalization group equations for soft supersymmetry breaking couplings," Phys. Rev. D **50** (1994) 2282 Erratum: [Phys. Rev. D **78** (2008) 039903] [hep-ph/9311340].

[136] S. Antusch, M. Drees, J. Kersten, M. Lindner and M. Ratz, "Neutrino mass operator renormalization revisited," Phys. Lett. B **519** (2001) 238 [hep-ph/0108005].

[137] M. Agostini *et al.* [GERDA Collaboration], "Improved Limit on Neutrinoless Double-β Decay of ^{76}Ge from GERDA Phase II," Phys. Rev. Lett. **120** (2018) no.13, 132503 [arXiv:1803.11100 [nucl-ex]].

[138] G. Anderson, S. Raby, S. Dimopoulos, L. J. Hall and G. D. Starkman, "A Systematic SO(10) operator analysis for fermion masses," Phys. Rev. D **49** (1994) 3660 [hep-ph/9308333].

[139] J. Wess and B. Zumino, "A Lagrangian Model Invariant Under Supergauge Transformations," Phys. Lett. **49B** (1974) 52.

[140] J. Iliopoulos and B. Zumino, "Broken Supergauge Symmetry and Renormalization," Nucl. Phys. B **76** (1974) 310.

[141] M. T. Grisaru, W. Siegel and M. Rocek, "Improved Methods for Supergraphs," Nucl. Phys. B **159** (1979) 429.

[142] P. Z. Skands *et al.*, "SUSY Les Houches accord: Interfacing SUSY spectrum calculators, decay packages, and event generators," JHEP **0407** (2004) 036 [hep-ph/0311123].

[143] B. C. Allanach *et al.*, "SUSY Les Houches Accord 2," Comput. Phys. Commun. **180** (2009) 8 [arXiv:0801.0045 [hep-ph]].

[144] T. Nihei and J. Arafune, "The Two loop long range effect on the proton decay effective Lagrangian," Prog. Theor. Phys. **93** (1995) 665 [hep-ph/9412325].

[145] N. Cabibbo, E. C. Swallow and R. Winston, "Semileptonic hyperon decays," Ann. Rev. Nucl. Part. Sci. **53** (2003) 39 [hep-ph/0307298].

[146] N. Tsutsui *et al.* [CP-PACS and JLQCD Collaborations], "Lattice QCD calculation of the proton decay matrix element in the continuum limit," Phys. Rev. D **70** (2004) 111501 [hep-lat/0402026].

[147] S. Antusch, I. de Medeiros Varzielas, V. Maurer, C. Sluka and M. Spinrath, "Towards predictive flavour models in SUSY SU(5) GUTs with doublet-triplet splitting," JHEP **1409** (2014) 141 [arXiv:1405.6962 [hep-ph]].

[148] J. Camargo-Molina, B. O'Leary, W. Porod and F. Staub, "**Vevacious**: A Tool For Finding The Global Minima Of One-Loop Effective Potentials With Many Scalars," Eur. Phys. J. C **73** (2013) no.10, 2588 [arXiv:1307.1477 [hep-ph]].

[149] W. Porod, "SPheno, a program for calculating supersymmetric spectra, SUSY particle decays and SUSY particle production at e+ e- colliders," Comput. Phys. Commun. **153** (2003), 275-315 [arXiv:hep-ph/0301101 [hep-ph]].

[150] W. Porod and F. Staub, "SPheno 3.1: Extensions including flavour, CP-phases and models beyond the MSSM," Comput. Phys. Commun. **183** (2012), 2458-2469 [arXiv:1104.1573 [hep-ph]].

[151] F. Staub, "SARAH," [arXiv:0806.0538 [hep-ph]].

[152] F. Staub, "SARAH 4 : A tool for (not only SUSY) model builders," Comput. Phys. Commun. **185** (2014), 1773-1790 [arXiv:1309.7223 [hep-ph]].